ON CONVECTION AND FLOW IN POROUS MEDIA WITH CROSS-DIFFUSION

A THESIS SUBMITTED IN FULFILMENT OF THE ACADEMIC
REQUIREMENTS FOR THE DEGREE OF
DOCTOR OF PHILOSOPHY

By

Ahmed A. Khidir

School of Mathematics, Statistics and Computer Science
College of Agriculture, Engineering and Science
University of KwaZulu-Natal

August 2012

Contents

Abstract

In this thesis we studied convection and cross-diffusion effects in porous media. Fluid flow in different flow geometries was investigated and the equations for momentum, heat and mass transfer transformed into a system of ordinary differential equations using suitable dimensionless variables. The equations were solved using a recent successive linearization method. The accuracy, validity and convergence of the solutions obtained using this method were tested by comparing the calculated results with those in the published literature, and results obtained using other numerical methods such as the Runge-Kutta and shooting methods, the inbuilt Matlab `bvp4c` numerical routine and a local non-similarity method.

We investigated the effects of different fluid and physical parameters. These include the Soret, Dufour, magnetic field, viscous dissipation and thermal radiation parameters on the fluid properties and heat and mass transfer characteristics.

The study sought to (i) investigate cross-diffusion effects on momentum, heat and mass transport from a vertical flat plate immersed in a non-Darcy porous medium saturated with a non-Newtonian power-law fluid with viscous dissipation and thermal radiation effects, (ii) study cross-diffusion effects on vertical an exponentially stretching surface in porous medium and (iii) apply a recent hybrid linearization-spectral technique to solve the highly nonlinear and coupled governing equations. We further sought to show that this method is accurate, efficient and robust by comparing it

with established methods in the literature.

In this study the non-Newtonian behaviour of the fluid is characterized using the Ostwald-de Waele power-law model. Cross-diffusion effects arise in a broad range of fluid flow situations in many areas of science and engineering. We showed that cross-diffusion has a significant effect on heat and mass-transfer processes and cannot be neglected.

Declaration

The work described in this dissertation was carried out under the supervision and direction of Professor P. Sibanda, School of Mathematics, Statistics and Computer Science, University of KwaZulu-Natal, Pietermaritzburg, South Africa.
I, Ahmed A. Khidir, declare that this thesis under title

On Convection and Flow in Porous Media with Cross-Diffusion

is my own work and it has not been previously submitted to this or any other academic institution for a degree or diploma, or any other qualification. All published and unpublished material used in this thesis has been given full acknowledgement.

Signatures:

.....
Mr. Ahmed A. Khidir (Student)

.....
Prof. Precious Sibanda (Supervisor)

Dedication

To

my mother . . . . . Hawaa

my father . . . . . Abdalmgid

my wife . . . . . Aalya

and my son . . . . . Adel

Acknowledgements

My first and foremost gratitude goes to my PhD supervisor, Professor P. Sibanda for his support, advice and for the effort given in these three years in the development of my skills and the writting of this thesis. Without his help and support, this project would never have been possible.

Also, I would like to thank Dr. Faiz G. Awad for many interesting discussions, support, continuous and invaluable suggestions throughout my work. Thanks are also due to Dr. M. Narayana who gave many useful comments. The three years in the school has been fruitful, thanks to all the colleagues and members of the school. I feel fortunate to have made so many good Sudanese friends in Pietermaritzburg (South Africa), many thanks to all for supporting me and my family. Also, I wish to thank the Sudan government for providing the required financial support. I would like to extend my deepest gratitude to my father, brothers, sisters and friends. They always have provided unwavering love and encouragement. Thank you for believing in me.

Lastly, but certainly not least, thanks to my family, my wife Aalya and my son Adel for their love, tolerance and enduring support. Without their help and encouragement, I would have been finished well before I got started. I thank you from the bottom of my heart, I dedicate this thesis with love, to you and to our new family member.

Chapter 1

Introduction

1.1 Background and motivation

The transfer of heat and mass through porous media plays an important role in fluid mechanics and arises in many areas of natural and applied sciences. This includes such areas as petroleum engineering, geosciences (hydrogeology and geophysics), mechanics (acoustics, soil and rock mechanics) and biology, Chen and Ewing (2002).

A porous medium is defined as a material containing interconnected voids (pores), Bear and Bachmat (1972) and Ingham and Pop (1998). The material is usually called the matrix and the pores are typically filled by a fluid. In single-phase flow, the pores are saturated by a single fluid while in two-phase flow the void space is often shared by a liquid and a gas. The interconnectedness of the pores allows fluid flow through the material. In natural porous medium such as wood, sand, limestone rock and the human lung, the pores are distributed in an irregular manner with respect to size and shape and with irregular connections between the pores, Nield and Bejan (1999). A porous media is characterized by the porosity ϕ which is defined as the fraction of the

total volume of the medium that is occupied by void space (Kaviany 1995, Nield and Bejan 1999, Lehr and Lehr 2000 and Bridge and Demicco 2008). Mathematically, this is given by the ratio

$$\phi = \frac{V_V}{V_T}, \tag{1.1}$$

where V_V is the volume of void space and V_T is the total volume of the material.

Porosity is a fraction between 0 and 1 so that $1-\phi$ is the fraction that is occupied by a solid. The porosity does not normally exceed 0.6 for natural porous media and can vary between 0.2595 and 0.4764 for artificial beds of solid spheres of uniform diameter, Nield and Bejan (1999). The porosity of the soil, sand and coal lies in the range $0.43 - 0.54$, $0.37 - 0.50$ and $0.02 - 0.12$, respectively, Kaviany (1995). A porous media is also characterized by its permeability which controls the movement and storage of fluids in the porous media. Permeability is determined as part of the proportionality constant in Darcy's law (Darcy 1856) which relates discharge and fluid physical properties to the pressure gradient in the porous media. This law further relates the flow rate and the applied pressure difference in the hydrology of water supply. This proportionality has been expressed in one-dimension in the form (Bear 1972 and Nield and Bejan 1999)

$$u = -\frac{K}{\mu}\frac{\partial P}{\partial x}, \tag{1.2}$$

where $\partial P/\partial x$ is the pressure gradient in the direction of the flow, μ is the dynamic viscosity of the fluid and K is the permeability of the porous medium. The value of K depends on the geometry of the medium and is independent of the nature of the fluid, Nield and Bejan (1999). Equation (1.2) can be generalized in three-dimensions as

$$\nabla P = -\frac{\mu}{\mathbf{K}}\mathbf{v}, \tag{1.3}$$

where the permeability $\mathbf{K}$ is a second-order tensor, Bruschke and Advani (1990).

Darcy's law has been tested and verified experimentally by, among others, Nakayama and Koyama (1987b), Singh and Sharma (1990), Lage (1998) and Altevogt et al. (2003).

Since this law depends on the balance between the pressure gradient and the viscous force, it breaks down for high velocity, when the effect of flow inertia is no longer negligible, Nakayama (1995). The fluid inertia effect becomes important when the flow rate is high. The Darcy model is thus valid under conditions of low velocities and small porosity, Hong et al. (1987). It is therefore necessary in many real flows to modify the Darcy model to include non-Darcian effects in the analysis of transport in a porous medium. The inertia effects can be accounted for through the use of a Forchheimer model. Forchheimer (1901) added an extra term to equation (1.3) leading to a new model,

$$\nabla P = -\frac{\mu}{\mathbf{K}}\mathbf{v} - \frac{c_F}{\sqrt{\mathbf{K}}}\,\rho_f|\mathbf{v}|\mathbf{v}, \tag{1.4}$$

where c_F is a dimensionless form-drag constant and ρ_f is the fluid density. In addition, Forchheimer (1901) found that Darcy's law was not valid for flows through porous media with high permeability. Darcy's law also cannot account for the no-slip boundary condition at the interface between the solid wall and the porous medium, Chen and Horng (1999). The Darcian model is also only applicable when the Reynolds number is sufficiently small. For moderate to large Reynolds numbers one has to consider non-Darcian models. Several non-Darcy flow models have been proposed to include inertia effects on the pressure drop. Poulikakos and Bejan (1985) and Prasad and Tuntomo (1987) used the Forchheimer- extended Darcy equation to investigate the effects of inertia for flow through porous media. Brinkman (1947a,b) modified Darcy's law in order to model boundary frictional effects and to incorporate a viscous shear stress term and the no-slip condition at the wall by adding a Brinkman term

to equation (1.3). The new equations takes the form

$$\nabla P = -\frac{\mu}{\mathbf{K}}\mathbf{v} + \tilde{\mu}\nabla^2\mathbf{v}, \tag{1.5}$$

where $\tilde{\mu}$ is the effective viscosity. Brinkman assumed $\tilde{\mu}$ to be equal to the fluid viscosity μ.

The Brinkman model reduces to the momentum equation for viscous fluid flows without porosity as $\mathbf{K} \to \infty$ and to the Darcy equation as $\mathbf{K} \to \mathbf{0}$, Nakayama (1995) and Nield and Bejan (1999). The studies by Tong and Subramanian (1985), Sen (1987) and Laurait and Prasad (1987) used the Brinkman Darcy model to investigate the boundary effects on free convection in a vertical cavity. A combination of Brinkman and Forchheimer models is called the Brinkman-Forchheimer-Darcy model and has been extensively used by, for example, Marpu and Manipal (1995) who studied the effects of the Forchheimer inertial term and the Brinkman viscous term on natural convection and heat transfer in vertical cylindrical annuli filled with a fluid. They indicated that the Brinkman viscous term has a more significant effect on the average Nusselt number compared to the Forchheimer inertial terms.

The simplest fluid flow model is the Newtonian flow model. This model however does not fully describe observed flow characteristics due to deformation, viscosity time dependence and thinning effects. A non-Newtonian model generally fulfills most of the observation flow characterstics for real fluids. A fluid in which the shear rate varies with viscosity is called a non-Newtonian fluid. There are three types of non-Newtonian fluids, (i) pseudoplastics where the shear rate increases with decreasing viscosity. Examples of such fluids include real fluids such as glass and polymer melt, (ii) dilatant fluid where the shear rate increases with increasing viscosity and (iii) Bingham plastics where the relationship between the shear stress and shear rate is linear when a certain yield stress is exceeded. In the case of the flow of non-Newtonian fluids in a porous media, Darcy's law was modified by Shenoy (1993) who investigated

the following scenarios:

(1) The effect of replacing the Darcy term by $(\mu^*/\mathbf{K}^*)v^{n-1}\mathbf{v}$.

(2) The effect of replacing the Brinkman term by $(\mu^*/\varphi^n)\nabla\{|[0.5\Delta:\Delta]^{1/2}|^{n-1}\Delta\}$ for an Ostwald-de-Waele fluid.

(3) Retaining the Forchheimer term unchanged since it is independent of the viscosity.

Here μ^* is the consistency of the fluid, $\mathbf{K}$ is a modified permeability, Δ is the deformation tensor and n is the power-law index.

More extensions of Darcy's law can be found in Irmay (1958) and Wooding (1957). Most research in the last few decades has been based on the Brinkman-Forchheimer-extended Darcy model which is also known as the generalized model, Vafai (2005). Bhadauria (2007) used Brinkman-Forchheimer extended Darcy model to study the effect of temperature modulation on double diffusive convection in porous medium by making linear stability analysis. He found that the critical value of Rayleigh number decreases with decreases in the Darcy number. A detailed review of convection studies in a non-Darcy porous medium can be found in Nield and Bejan (1984).

Studies on heat and mass transfer in non-Newtonian fluids in porous media have been carried out by many researchers since heat and mass transfer plays an important role in engineering processes such as, for example, in food processing (Cheng 2008) and oil reservoir engineering (Shenoy 1993). Rastogi and Poulikakos (1995) studied the problem of double-diffusion from a vertical surface in a fluid saturated porous medium in a non-Newtonian power law fluid. They showed that for dilatant fluids, the velocity boundary layer is thinner than the thermal and concentration boundary layers, and that the opposite is true for pseudoplastic fluids. The problem of free convection heat and mass transfer over a vertical flat plate in a fluid-saturated

porous medium for non-Newtonian power-law fluids with yield stress has been investigated numerically by Jumah and Mujumdar (2000). They reported that the velocity, temperature and concentration distributions are significantly affected by the fluid rheology. Cheng (2008) investigated free convection over a vertical plate in a porous medium saturated with a non-Newtonian power-law fluid subject to Soret and Dufour effects. He concluded that the power-law exponent has the effect of reducing the temperature and concentration within the boundary layer.

This research is concerned with the convective transport of momentum, heat and mass in boundary layer flows. Heat is transferred from point to point due to temperature gradients. Three types or modes of heat transfer processes can be distinguished, Baehr and Stephan (1998) and Thirumaleshwar (2006). The first mode of heat transfer is heat conduction which refers to the transfer of energy between neighbouring molecules due to temperature gradients. The transfer of heat by conduction is described by Fourier's law which states that the rate of heat transfer in a given direction is linearly proportional to the negative temperature gradient. The proportionality constant in this relation is the thermal conductivity of the material, Rudramoorthy and Mayilsamy (2004). Heat conduction in gases is generally a slow process due to the large mean free path between molecules. Heat transfer due to a flowing fluid or convection is the second type of mechanism for heat transfer. Heat is transmitted from one place to another by the fluid's movement. The heat transport depends only on the fluid properties and is independent of the properties of the surface material, Kothandaraman (2006). Convection may be classified according to the nature of the flow as either, (i) natural or free convection, or (ii) forced convection. In natural convection, the movement of molecules is induced by buoyancy forces which arise from different densities caused by temperature variations in the fluid. Heat is transferred from the hot fluid to a cooler surface or from a hot surface to the cold fluid, Jaluria (1980), Kothandaraman (2006) and Rathore and Kapuno (2010). Forced convection is induced by external forces such as a pump or fan. A

combination of natural and forced natural convection is known as mixed convection. The third mode of heat transfer is thermal radiation. In this mode, the mechanism of heat transfer is electromagnetic waves between two surfaces with different temperatures, Kothandaraman (2006). Radiation heat transfer does not require orientation and colour.

Similar to heat transfer, mass may be transferred from one point to another by the movement of the fluid. The transfer of mass may take place due to potentials other than concentration differences, Kothandaraman (2006), or if there is a temperature gradient between two fluids, Thirumaleshwar (2006). Mass transfer is important in physical sciences, for example chemical engineering and biology. Mass transfer may be classified into three modes. The first mode is diffusive mass transfer. Mass transfer takes place from higher to lower concentration regions when the fluid is at rest. This mode is similar to conduction in heat transfer, Thirumaleshwar (2006). The second mode is convective mass transfer. This occurs when two fluids are moving together over a surface and the mass transfer in this case depends on the nature of the fluid flow, Sawhney (2010). The third mode of mass transfer is a combination of diffusion and convection effects known as a change of phase mode, Venkanna (2010). Mass transfer processes are similar to heat transfer processes in many other aspects. For example;

(1) Heat is transferred in the direction of lower temperatures and mass is also transferred in the direction of decreasing concentration.

(2) Both heat and mass transfer rates depend on the driving potentials.

(3) Heat and mass transfer stop when thermal equilibrium and concentration equilibrium is attained.

Many researchers studying the phenomena of momentum, heat and mass through

a porous media have investigated the influence of different fluid and physical parameters such as a chemical reaction, thermal radiation, viscous dissipation, Soret and Dufour parameters. Free convection through a porous medium using the Darcy model was first studied by Horton and Roger (1945) and Lapwood (1948). Brinkman (1947a) gave a calculation of the viscous force exerted by a flowing fluid on a dense swarm of particles. He used the model of spherical particles embedded in a porous mass to show that there is a relation between permeability, particle size and density. Experimental and numerical investigations of convection in porous layers was first proposed by Wooding (1957, 1963). Elder (1966) studied the steady free convection in a porous medium heated from below. He showed that the heat transferred across the layer is independent of the thermal conductivity of the medium and is proportional to the square of the temperature difference across the layer for the Rayleigh-type flow. McNabb (1965) analyzed boundary layer problem due to the cooling of a circular plate situated in the bottom plane boundary of a semi-infinite region. Lloyd and Sparrow (1970) studied natural and forced convection from a vertical flat plate by using a local similarity method to solve the governing equations. They showed that the validity of their numerical solutions ranged from pure forced convection to mixed convection. Cheng and Minkowycz (1977a) presented similarity solutions for free convective heat transfer about a vertical flat plate embedded in a porous medium for high Rayleigh numbers. Gupta and Gupta (1977) studied the temperature distribution for the problem of heat and mass transfer on a stretching sheet subject to suction and injection. They extended the study by Erickson et al. (1966) to the case of linear velocity movement of the stretched surface. Cheng (1977b) investigated combined free and forced convection buoyancy flow past bodies immersed in porous medium. Rajagopal et al. (1984) studied the flow of an incompressible second-order fluid past a stretching sheet. They showed that the cross-viscosity coefficient does not affect the velocity profile of two-dimensional flow and effects only the pressure distribution. Ranganathan and Viskanta (1984) studied inertial viscous effects in mixed convection flow along a vertical wall in porous medium They showed that

the effects of boundary friction and inertia are significant and cannot be neglected. Nakayama and Pop (1991) gave different similarity solutions for mixed convection in Darcy and non-Darcy porous media embedded in non-Newtonian fluid. Combined heat and mass transfer on natural convection in a porous medium was studied by Bejan and Khair (1985), Singh and Queeny (1997) and Trevisan and Bejan (1990). Rees and Pop (1994) discussed the natural convection flow over a vertical wavy surface in porous media saturated with Newtonian fluids, with a constant wall temperature being examined. Rees and Pop (1998) studied the free convection boundary layer flow from a vertical isothermal flat plate immersed in a micropolar fluid. Magyari and Keller (1999) found similarity solutions to the problem of heat and mass transfer in the boundary layers due to an exponentially stretching continuous surface. Murthy et al. (2004) reported on the influence of double stratification on free convection in a Darcy porous medium. They presented similarity solutions for the case of uniform wall heat and mass flux conditions by assuming the thermal and solutal stratification of the medium to vary as $x^{1/3}$ where x is the stream wise coordinate axis. An investigation of the effects of surface flexibility on the inviscid instability in fluid flow over a horizontal flat plate with heat transfer was studied by Motsa and Sibanda (2005). They considered large fluid buoyancy and showed that the effect of plate flexibility is important for small wave numbers and that the flow structure is indistinguishable from that obtained with rigid surfaces in the case of large compliancy parameters. Jayanthi and Kumari (2007) studied free and mixed convection in a porous medium. They considered variable viscosity in non-Newtonian fluid. Their results showed that heat transfer is more significant for liquids with variable viscosity than in the case of constant viscosity, while the opposite is true for gases. They also showed that variable viscosity has a significant effect on the velocity and the heat transfer rate. Makinde (2009) studied mixed convective flow from a vertical porous plate in porous medium with a constant heat flux and mass transfer with magnetic field effect. He found that both magnetic field and Eckert numbers have increasing effects on the skin friction for positive values of the buoyancy parameter. Narayana et al. (2009) studied free

convective heat and mass transfer in a doubly stratified porous medium saturated with a power-law fluid. By considering linear stratification for both temperature and concentration they obtained a series approximation for the stream function, temperature and concentration in terms of the thermal stratification parameter. Magyari et al. (2006) studied unsteady free convection over an infinite vertical flat plate embedded in a stable, thermally porous medium subject to sudden change in the plate temperature. Narayana and Murthy (2006) studied combined thermal convection and mass transfer in a doubly stratified non-Darcy porous medium adjacent to a vertical plate. They assumed linear stratification in the vertical direction with respect to both temperature and saute concentration. Laminar free convection from a continuously moving vertical surface in thermally-stratified, non-Darcy porous media was investigated by Bég et al. (2008). They extended the work of Takhar et al. (2001) and considered the effects of Darcy and Forchheimer numbers on the flow dynamics and heat transfer characteristic.

Heat transfer with thermal radiation has many industrial applications such as in power generation and in solar power technology. Investigations of thermal radiation on flow, heat and mass transfer were made by, among others, Raptis (1998) who investigated thermal radiation and free convection in flow through a porous medium. Hayat et al. (2007b) studied the effect of thermal radiation on MHD flow of an incompressible second grade fluid. Sajid and Hayat (2008) studied the effect of radiation of a viscous fluid over an exponentially stretching sheet. They found that the radiation and the Prandtl parameter have an opposite effect on the temperature and that the radiation parameter controls the thickness of the thermal boundary layer. This problem has also been solved numerically by Bidin and Nazar (2009). Mahmoud (2009) studied the effect of radiation on unsteady MHD flow and heat transfer subject to viscous dissipation effect and temperature dependent viscosity. He showed that the thermal boundary thickness decreases with thermal radiation. Recently, radiation and melting effects on mixed convection from a vertical surface embedded in a porous

medium for aiding and opposing eternal flows was investigated by Chamkha et al. (2010). Makinde (2011a)investigated hydromagnetic mixed convection heat and mass transfer flow of an incompressible Boussinesq fluid with constant heat flux in porous medium considering radiative heat transfer, viscous dissipation, and an nth order homogeneous chemical reaction. Anjalidevi and Devi (2011) investigated thermal radiation effects on MHD convective flow over a porous rotating disk with cross-diffusion effects. They showed that the thermal radiation and the thermo diffusion effects has significant effects on the thermal boundary layer.

Gebhart (1962) studied natural convection in fluids with viscous dissipation. He showed that viscous dissipation plays an important role in various devices. The study by Gebhart (1962) was extended by Gebhart and Mollendorf (1969) who obtained a similarity solution for exponential variation of the wall temperature. Nakayama and Pop (1989) studied free convection over a non-isothermal body of arbitrary shape in a porous medium with viscous dissipation. They showed that that viscous dissipation lowers the rate of heat transfer. Murthy and Singh (1997) studied the effect of viscous dissipation on a non-Darcy natural convection regime. They noted that a significant decrease in heat transfer can be observed with the inclusion of the viscous dissipation effect. Sibanda and Makinde (2010) investigated the heat transfer characteristics of steady MHD flow in a viscous electrically conducting incompressible fluid with Hall current past a rotating disk with ohmic heating and viscous dissipation. They found that the magnetic field retards the fluid motion due to the opposing Lorentz force generated by the magnetic field. Bhadauria and Srivastava (2010) discussed thermal instability in an electrically conducting two component fluid in porous medium consider the effect of modulation of the boundaries temperature on the onset of stationary convection. The magnetic field has been applied has been applied to a solute gradient between the boundaries. They showed that the effect of modulation may be zero when modulation frequency is zero and modulation disappears altogether at modulation frequency tends to infinity. Kairi and Murthy (2011b) studied the effect

of viscous dissipation on natural convection heat and mass transfer in a non-Darcy porous media. The study investigated free convection flow and chemical reaction with variable thermal conductivity and viscosity. They showed that there is a significant difference between the results pertaining to variable and constant fluid properties.

Recent advances in heat and mass transfer technology have allowed for the development of a new category of fluids called nanofluids, Choi (1995). Nanofluids are fluids created by dispersing solid nanoparticles in traditional heat transfer fluids. The average size of the particles may lie in the range 1-100 nm, Choi (2009). One of the important nanofluid features is its stability because the particles are low weight, small and have less chance of sedimentation, Das et al. (2006). Compared to the base fluids like oil or water, nanofluids have been shown to enhance thermophysical properties such as the heat transfer rate, thermal conductivity, thermal diffusivity and viscosity. Nanofluids therefore can be considered to be the next generation of heat transfer fluids, Lee et al. (1999) and Wang and Mujumdar (2007). Many experimental studies have been carried out to investigate heat and mass transfer in nanofluids in the last decade by, among others, Putra et al. (2003). Wen and Ding (2006) discussed uncertainties about using nanofluids in practical applications. Wang and Majumdar (2007) presented an overview of the recent developments on convection heat transfer characteristics in nanofluids. They showed that researchers have given more importance to the thermal conductivity, than the heat transfer characteristics, and there is a general lack of of physical understanding of convection in nanofluids. Singh et al. (2011) investigated the heat transfer behaviour of nanofluids in microchannels. They also showed that better heat transfer characteristics can be obtained with high concentration and low viscous base fluids of nanofluids.

1.2 The cross-diffusion effect

The relation between fluxes and the driving potentials is complex when heat and mass transfer occur together in a fluid, Pop and Ingham (2001). The energy flux induced by the temperature gradient is called the thermal-diffusion or Soret effect. On the other hand, the energy flux created by the concentration gradient is called the diffusion-thermo or Dufour effect. The effects of Soret and Dufour are known as cross-diffusion effects.

The cross-diffusion effects are often considered as second order phenomena although it is now known that they may become significant in porous media flows such as in geosciences, petrology, hydrology, etc. Indeed in many studies of heat and mass transfer processes, thermal-diffusion and the diffusion thermo effects are often neglected on the basis that they are of a smaller order of magnitude than the effects produced by Fourier and Fick laws, Mojtabi and Charrier-Mojtabi (2005). The diffusion-thermo effect has been found to be of considerable magnitude in some flows such that it cannot always be neglected, Eckert and Drake (1972). Dursunkaya and Worek (1992) analyzed the effects of Soret and Dufour numbers in transient and steady natural convection from a vertical surface while Kafoussias and Williams (1995) investigated the effects of Soret and Dufour numbers on mixed free-forced convective heat and mass transfer on steady laminar boundary layer flow along a heated vertical plate surface. They assumed that the viscosity of the fluid varied with temperature and showed that the Soret and Dufour effects have to be taken into consideration in heat and mass transfer studies. The Soret effect has been used for isotope separation and mixtures of gases with light and medium molecular weights such as hydrogen, hellium, nitrogen and air, Postelnicu (2004). Postelnicu (2004) studied the influence of a magnetic field on natural convection from vertical surfaces in porous media taking into account the Soret and Dufour effects. Alam and Rahman (2006b) investigated the problem of mixed convection flow past a vertical porous flat plate

for a hydrogen-air mixture with Soret and Dufour effects and variable suction. They used the Nachtsheim-Swigert shooting iteration technique together with a sixth order Runge-Kutta integration scheme to solve the problem. They reported that the Soret and Dufour effects should not be neglected for fluids with medium molecular weight (such as H_2, air). Li et al. (2006) studied the Soret and Dufour effects on heat and mass transfer in fluid flow with a strongly endothermic chemical reaction in a porous medium. Their results indicated that Soret and Dufour effects can not be ignored when the convectional velocity is lower or when the initial temperature of the feeding gas is high. Postelnicu (2007) investigated the effects of cross-diffusion on heat and mass transfer characteristics of natural convection from a vertical surface in a porous medium with chemical reaction. Abreu et al. (2007) studied both forced and natural heat and mass transfer in laminar boundary layer flows with Soret and Dufour effects. Kim et al. (2007) investigated cross-diffusion effects on the convective instabilities in nanofluids. They showed that Soret and Dufour effects make nanofluids unstable and heat transfer increases by the Soret effect in the binary nanofluids, is more significant than that in the normal nanofluids. Narayana and Murthy (2008) analyzed the effect of Soret and Dufour parameters on free convection from a horizontal flat plate in a Darcian fluid saturated porous medium. Motsa (2008) investigated Soret and Dufour effects on the onset of convection in a fluid-saturated porous medium. He showed that the Soret effect had a stabilizing effect in the case of stationary instability whereas the Dufour effect was destabilizing. Afify (2009) carried out an analysis of the effects of Soret and Dufour numbers on free convective heat and mass transfer over a stretching surface in the presence of suction and injection. His study showed that for fluids with medium molecular weight (H_2, air), thermal diffusion and diffusion-thermo effects should not be neglected. This study thus confirmed the earlier findings by Alam and Rahman (2006b). Kairi and Murthy (2009b) discussed the melting phenomena and the effect of Soret numbers on natural convection heat and mass transfer from a vertical flat plate with constant wall temperature and concentration in a non-Newtonian fluid saturated non-Darcy porous medium. They considered aiding and

opposing buoyancies in the study and found that the Soret number has a significant effect on the temperature and concentration profiles as well as the heat and mass transfer rates.

Recently, cross-diffusion effects on heat and mass transfer along a vertical wavy surface in a Newtonian fluid saturated Darcy porous medium have been investigated by Narayana and Sibanda (2010). They showed that increasing the Soret parameter leads to an increase in the axial mass transfer coefficient. They also showed that the heat transfer rate increases at the surface when a diffusion-thermo effect increases. Awad and Sibanda (2010a) investigated Soret and Dufour effects on heat and mass transfer in a micropolar fluid in a horizontal channel. They reported that Soret and Dufour effects have a significant influence on the thermal and concentration boundary layer profiles. Shateyi et al. (2010b) considered the influence of cross-diffusion on mixed convection over vertical surfaces in the presence of radiation and Hall effects. They showed that the Soret number has a decreasing effect on the temperature profile and an increasing effect on the concentration profile, while the effect of Soret and Dufour on the concentration and temperature distributions is opposite. They also noted that thermal-diffusion and diffusion-thermo effects have a significant influence on the velocity, temperature and concentration and thus have to be considered in the study of heat and mass transfer problems. The work of Parand et al. (2010a) has been extended by Awad et al. (2011a) to include the effects of the Soret mass flux and Dufour energy flux. They used a linearization technique to find solutions to the governing equations and assumed the thermal-diffusion and diffusion-thermo effects to be significant. Huang et al. (2011) studied the natural convection along an inclined stretching surface in a porous medium with thermal-diffusion and diffusion-thermo effects in the presence of a chemical reaction. They reported that the flow, thermal, and diffusion fields are influenced appreciably by the effects of Soret and Dufour numbers. They also observed for large Dufour numbers and small Soret numbers coincide with increasing concentration differences and decreasing temperature

differences. Awad et al. (2011b) studied the Soret and Dufour effects in flow over a wavy smooth cone. They noted that the thermal thickness decreases as the Dufour number increases. Pal and Mondal (2011) investigated the combined effects of Soret and Dufour numbers on unsteady MHD non-Darcy mixed convection over a stretching sheet embedded in a saturated porous medium in the presence of viscous dissipation, thermal radiation and a chemical reaction of first-order. They noted that the temperature profiles are strongly influenced by the Dufour effect. Makinde (2011b) analyzed the mixed convection flow of an incompressible Boussinesq fluid under the simultaneous action of buoyancy and transverse magnetic field with Soret and Dufour effects over a vertical porous plate with constant heat flux embedded in a porous medium. Makinde and Olanrewaju (2011c) studied the unsteady mixed convection flow past a vertical porous flat plate moving through a binary mixture in the presence of radiative heat transfer and nth-order Arrhenius type of irreversible chemical reaction by taking into account Dufour and Soret effects. Olanrewaju and Makinde (2011) carried out to study free convective of an incompressible, electrically conducting fluid past a moving vertical plate in the presence of suction and injection with cross-diffusion effects. they noted that Dufour and Soret effects should not be neglected for fluids with medium molecular weight (H2, air).

From previous studies it is clear that, (i) cross-diffusion has a significant effect on heat and mass transfer processes, and (ii) the Soret and Dufour numbers have opposite effects on the temperature and concentration profiles. The present study investigated the effects of cross-diffusion on heat and mass transfer in porous media

1.3 Analytical and numerical studies

A wide variety of problems in science and engineering can be described by coupled linear or non-linear systems of partial or ordinary differential equations. Compared to

nonlinear equations, linear equations can easily be solved. Finding analytical solutions to nonlinear problems on finite or infinite domains is one of the most challenging problems. Such problems do not usually admit closed from analytic solutions and in most cases we resort to finding approximate solutions using numerical approximation techniques. Common numerical methods used for solving nonlinear boundary value problems include Runge-Kutta methods, Keller-box method, finite difference method, finite element method and shooting method.

These methods have been used to solve many types of fluid flow models by many researchers. Rees and Pop (1998) used the Keller-box method to solve the problem of free convection from a vertical flat plate for a range of values of micropolar fluid parameters. The finite difference method has been used by Jumah and Mujumdar (2001) to study the Darcy-Forchheimer mixed convection from a vertical flat plate in a porous medium, under the coupled effects of thermal and mass diffusion. Using a Runge-Kutta scheme with the shooting method, Afify (2004) studied free convective flow and mass transfer over a stretching sheet with chemical reaction and magnetic field effects. Alam et al. (2006a) used a sixth order Runge-Kutta method, together with the shooting technique, to solve the problem of free convection in a fluid with temperature dependent viscosity along an inclined plate. The flow past a semi-infinite vertical plate with MHD with heat and mass transfer was investigated by Palani and Srikanth (2009) and the dimensionless governing equations were solved by an implicit finite difference scheme of Crank-Nicolson type. The Keller-box method has been used by Srinivasacharya and RamReddy (2010) to solve natural convection heat and mass transfer along a vertical plate embedded in a doubly stratified micropolar fluid in a non-Darcy porous medium. The finite element method has been used by Reddy and Reddy (2010) to investigate unsteady magnetohydrodynamic convective and dissipative fluid flow from a vertical porous plate with radiation effect. Sulochana et al. (2011) analyzed the Soret effect on convective heat and mass transfer through a porous medium in circular annulus using Galerkin finite element analysis

with quadratic polynomials.

A recent numerical technique, the fitted operator finite difference method (FOFDM), was proposed by Patidar (2005). He showed that the FOFDM is second order accurate for very small values of the perturbation parameter ε and fourth order accurate for moderate values of this parameter. He also showed this method is advantageous over the conventional methods such as finite difference methods and finite element methods. The technique has been used to find solutions of a class of self-adjoint singularly perturbed two-point boundary value problems, Lubuma and Patidar (2006) and Bashier and Patidar (2011a,b,c). Munyakazi and Patidar (2008) extended the work of Patidar (2005) and Lubuma and Patidar (2006) to the investigation of the performance of the Richardson extrapolation on some fitted operator finite difference methods. The studies by Bashier and Patidar (2011a,b) used the method to solve a singularly perturbed delay parabolic partial differential equation and a system of partial delay differential equations. The FOFDM has been extended by Munyakazi and Patidar (2010) to elliptic singular perturbation problems.

The main disadvantage of numerical methods in general however is that they often give very little insight into the structure of the solutions or the effects of the various parameters embedded in the governing equations.

Non-numerical approaches include the classical power-series method and its variants for systems of nonlinear differential equations with small or large embedded parameters such as the homotopy perturbation method, He (1999, 2003a,b, 2004, 2005, 2006) and the Hermite-Pade approximations, Guttamann (1989) and Tourigny and Drazin (2000). Other common non-perturbation methods in general use are Adomian decomposition method (ADM), Adomian (1989, 1990, 1992, 1994), and the δ-expansion method, Lyapunov (1992) and Awrejcewicz et al. (1998). However, it is well-known that most of these perturbation solutions are not valid in the whole physical region. These methods do not guarantee the convergence of the series solu-

tion, and the perturbation approximations may be only valid for weakly non-linear problems, Liao (2007).

Further disadvantages of perturbation methods are that, (i) they require the presence of a large or small parameter in the problem while non-perturbation methods require a careful selection of initial approximations and linear operators, and (ii) linearization usually leads to difficulties in the integration of higher order deformation equations.

A recent analytical method that has been used with great success is the homotopy analysis method (HAM) proposed by Liao (1992) in his PhD research. This method provides us with greater freedom in the selection of the initial guess and auxiliary linear operators than the other non-perturbation methods, Liao (2007, 2009). The method transforms the nonlinear differential equation to a system of ordinary differential equations that can easily be solved. The HAM contains a convergence-controlling parameter $\hbar$ which controls both the region of convergence and the convergence rate, and this is the most important innovation of this method. The HAM is thus a more general non-perturbation method and overcomes the restrictions of other methods because it suggests a way of ensuring the convergence of the solution. The HAM has been used to solve different types of non-linear heat and mass transfer problems. Abbasbandy (2006, 2007) used the HAM to solve heat transfer problems with high nonlinearity order. He compared his results with the homotopy perturbation method and showed that the homotopy perturbation method is valid only for small parameters. Hayat and Sajid (2007a) solved the MHD boundary layer flow of an upper-convected Maxwell fluid problem. Domairry et al. (2009) used the HAM to solve the nonlinear differential equation governing Jeffery-Hamel flow. Dinarvand and Rashidi (2010) used the HAM to solve the problem of laminar, isothermal, incompressible, and viscous flow in a rectangular domain bounded by two moving porous walls. Shateyi et al. (2010c) used the HAM in their investigation of natural convection and heat and

mass transfer when considering chemical reaction and heat generation. Awad and Sibanda (2010b) studying the cross-diffusion effects on free convection of heat and mass in micropolar fluid, found approximate analytical series solutions for the system of nonlinear differential equations. The HAM has also been successfully used to find solutions of several other types of nonlinear problems by, among others, Yang and Liao (2006), Liao (2006), Lipscombe (2010) and Liu (2010). In the HAM, an auxiliary function is used to avoid the appearance of secular terms in the solution. This is called the rule of coefficient ergodicity. The HAM represents the required solution of a differential equation as a sum of predetermined base functions that provide the so-called rule of solution expression.

The HAM does, however, suffer from a number of restrictive limitations as admitted by Liao (2003) and explained by Motsa et al. (2010b,c). Included in some of these restrictions are that:

(1) The HAM may not work, or its accuracy may be impaired for large values of the governing parameters.

(2) One has to carefully select an initial approximation and linear operator that will make the integration of the higher order deformation equations possible. That is because a complicated initial approximation and linear operator may result in higher order deformation equations that are difficult to integrate.

(3) The HAM solution must conform to the rule of solution expression and rule of coefficient ergodicity.

The spectral homotopy analysis method (SHAM) was proposed by Motsa et al. (2010b,c) in order to address these restrictions. In the SHAM the auxiliary linear operator and the higher order deformation equations are defined in terms of the Chebyshev spectral collocation differentiation matrix, Don and Solomonoff (1995).

Some advantages of this approach as pointed out by Motsa et al. (2010b) are that:

(i) We can use any initial guess as long as it satisfies the boundary conditions, while with the HAM one is restricted to selecting an initial guess that would allow for the easy integration of the higher order deformation equations.

(ii) The SHAM is more flexible than the HAM as one is not restricted to using the method of higher order deformation.

(iii) The SHAM leads to faster convergence in comparison with the standard HAM.

Comparisons between the HAM and the SHAM have been made by Motsa et al. (2010b). They solved the Darcy-Brinkman-Forchheimer equation for steady fully developed channel flow in a porous medium. They found among other things that:

(i) The SHAM converges much faster than the HAM. For example, they showed that the fourth order SHAM approximation gave good agreement with the numerical results.

(ii) The range of the auxiliary parameter $\hbar$ values is much wider in the SHAM than in HAM.

(iii) The optimal value of $\hbar$ in the SHAM is the maximum of the second order $\hbar$ curves. This finding is in line with the findings in Sibanda and Motsa (2012).

Motsa and Shateyi (2010d) used the SHAM to solve the problem of MHD rotating flow over a shrinking sheet. They showed that the SHAM rapidly converges to the numerical results. Motsa and Sibanda (2011b) solved the Falkner-Skan equation using the SHAM and compared the results with the HAM. They concluded that the SHAM required only two or three terms to achieve the accuracy of the numerical method. Makukula et al. (2010d) used the SHAM for the problem of fluid flow between two

moving porous walls. Sibanda et al. (2012) solved the problem of heat transfer in a third grade fluid between parallel plates. The SHAM has been improved and modified by, among others, Motsa et al. (2011a) who proposed an improved spectral homotopy analysis method (ISHAM). They applied the method to the Falkner-Skan and MHD boundary layer problems. Sibanda et al. (2012) proposed a modified spectral homotopy analysis method (MSHAM). They applied the method to the problem of the steady laminar flow of a pressure driven third-grade fluid with heat transfer. The main difference between the MSHAM and SHAM is that the MSHAM is applied to a transformed version of the governing equations, while the SHAM algorithm is applied to the original governing equations. They also showed that the MSHAM is more efficient than the SHAM. The use of spectral methods also provided greater flexibility in the choice of basis functions.

The challenge of finding more accurate, robust and computationally efficient solution techniques for nonlinear problems in engineering and science still remains. The method used in this study that remains to be generalized and whose robustness remains to be tested in the case of highly nonlinear equations with a strong coupling, is the successive linearisation method (SLM), Makukula et al. (2010b) and Motsa and Sibanda (2010a). This technique has been successfully used in a limited number of studies. Makukula et al. (2010c) solved the classical Von Karman equations for the boundary layer flow induced by a rotating disk using both the spectral homotopy analysis method and the SLM. They showed that the SLM gives better accuracy at lower orders than the spectral homotopy analysis method. Other studies such as Makukula et al. (2010a,d), Shateyi and Motsa (2010a) and Awad et al. (2011b) used the SLM to solve different boundary value problems in heat and mass transfer studies and showed by comparison with numerical techniques that the SLM is accurate, gives rapid convergence and is thus superior to some existing semi-analytical methods such as the Adomian decomposition method, the Laplace transform decomposition technique, the variational iteration method and the homotopy perturbation method. The

SLM is a non-perturbation method requiring neither the presence of an embedded perturbation parameter nor the addition of an artificial parameter. The method is therefore free of the major limitations associated with other perturbation methods.

However since this method is a linearization method, it is worth first discussing the earlier method of quasilinearization.

1.4 Method of quasilinearization

The quasilinearization method (QLM) was proposed by Bellman and Kalaba (1965) as a generalization of the Newton-Raphson method, Conte and Boor (1981) and Ralston and Rabinowitz (1988). The QLM method approximates the solution by treating the nonlinear terms as a perturbation about the linear ones and does not require the existence of a small parameter, Mandelzweig (1999). The method was developed and applied to a wide range of problems in different fields of science. Mandelzweig and Tabakin (2001) used the method to solve nonlinear ordinary differential equations such as the Duffing and Blasius equations. They showed that this method gives excellent results. Parand et al. (2010b) solved Volterra's model for the growth of a species population within a closed system using the QLM technique.

The convergence of this technique has been proven in the original works of Bellman and Kalaba (1965). They proved the convergence only under rather restrictive conditions of small intervals. Mandelzweig (1999) removed some unnecessary restrictive conditions by reformulating the proof of convergence of the method to be applicable to real physical applications.

To demonstrate the general idea of the QLM method, we consider the following second order nonlinear ordinary differential equation in one variable defined on the

interval $[a, b]$;

$$\frac{d^2u(x)}{dx^2} = F(u(x), u'(x), x), \tag{1.6}$$

with boundary conditions

$$u(a) = a_0, \qquad u(b) = b_0, \tag{1.7}$$

where F is an unknown nonlinear function of $u(x)$ and its derivatives and $x \in [a, b]$. The QLM method determines the solution of (1.6) after transforming this equation as follows (Bellman and Kalaba 1965 , Mandelzweig 1999 and Parand et al. 2010b);

$$\begin{aligned}\frac{d^2u_{i+1}}{dx^2} = F(u_i(x), u_i'(x), x) + (u_{i+1}(x) - u_i(x))\frac{\partial F}{\partial u}(u_i(x), u_i'(x), x) \\ +(u_{i+1}'(x) - u_i'(x))\frac{\partial F}{\partial u'}(u_i(x), u_i'(x), x),\end{aligned} \tag{1.8}$$

with boundary conditions

$$u_{i+1}(a) = a_0, \qquad u_{i+1}(b) = b_0, \qquad i = 0, 1, 2, ...m. \tag{1.9}$$

The initial guess $u_0(x)$ is chosen to satisfy boundary conditions at zero and $u_i(x)$ is known from the previous iteration. Starting from the initial guess we can calculate the mth order approximations successively using the formula (1.8).

1.5 The SLM technique

The SLM procedure linearizes the governing nonlinear equations which are then solved using spectral methods. To fully describe the SLM algorithm, let us consider the following boundary value problem of order n in the form

$$\mathcal{L}[u(x), u'(x), u''(x), ..., u^{(n)}] + \mathcal{N}[u(x), u'(x), u''(x), ..., u^{(n)}] = g(x), \tag{1.10}$$

where $\mathcal{L}$ and $\mathcal{N}$ are linear and nonlinear operators, $u(x)$ is an unknown function to be determined and $g(x)$ is a known function. We assume that equation (1.10) is to be solved for $x \in [a, b]$ subject to the boundary conditions

$$u(a) = a_0, \qquad u(b) = b_0. \tag{1.11}$$

We represent the vertical difference between the function $u(x)$ and the initial guess $u_0(x)$ by a function $U_1(x)$ as (see Figure 1.1)

$$U_1(x) = u(x) - u_0(x), \tag{1.12}$$

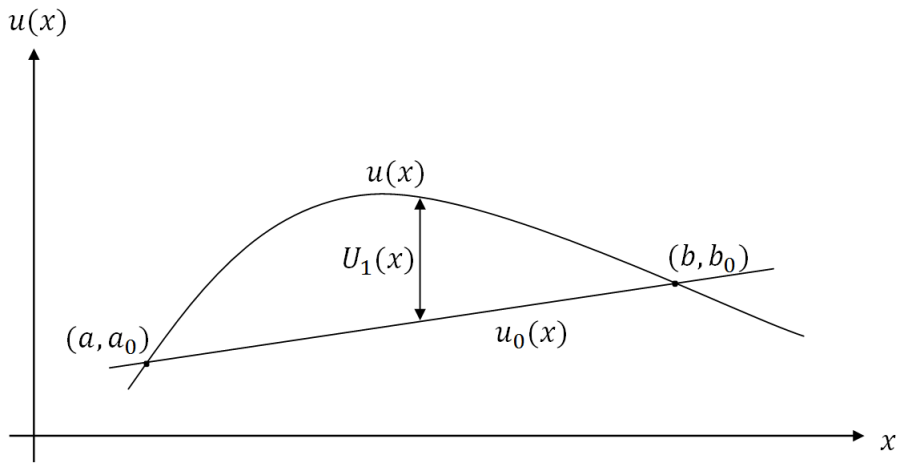

Figure 1.1: Geometric representation of the function $U_1(x)$

where $U_1(x)$ is an unknown functions and $u_0(x)$ is the initial guess which is chosen to satisfy boundary conditions (1.11). It is reasonable to assume, for example, that the initial approximation $u_0(x)$ is a linear function in case of second order problems defined on a finite domain and an exponential function for problems defined on an

infinite or a semi-infinite domain. Substituting (1.12) into (1.10), yields

$$\begin{aligned}&\mathcal{L}[U_1(x), U_1'(x), U_1''(x), ..., U_1^{(n)}] + \mathcal{L}[u_0(x), u_0'(x), u_0''(x), ..., u_0^{(n)}]\\&+\mathcal{N}[U_1(x) + u_0(x), U_1'(x) + u_0'(x), U_1''(x) + u_0''(x), ..., U_1^{(n)}(x) + u_0^{(n)}(x)]\\&\qquad\qquad = g(x)\ , \qquad (1.13)\end{aligned}$$

This equation is non-linear in $U_1(x)$, so it may not be possible to find an exact solution. We therefore look for a solution which is obtained by solving the linear part of the equation and neglecting the non-linear terms containing $U_1(x)$ and its derivatives. We further assume that $U_1(x)$ and its derivatives are very small, and denote the solution of the linearized equation (1.13) by $U_1(x)$, that is $U_1(x) \approx u_1(x)$. Equation (1.13) can be written as

$$\begin{aligned}\mathcal{L}[u_1(x), u_1'(x), u_1''(x), \cdots, u_1^{(n)}(x)] + f_{0,0}u_1(x) + f_{1,0}u_1'(x) + f_{2,0}u_1''(x)\\ + \cdots + f_{n,0}u_1^{(n)}(x) = \mathbf{R}_1(x), \qquad (1.14)\end{aligned}$$

where

$$\begin{aligned}f_{0,0} &= \frac{\partial N}{\partial u_1(x)}\left(u_0(x), u_0'(x), u_0''(x), \cdots, u_0^{(n)}(x)\right),\\ f_{1,0} &= \frac{\partial N}{\partial u_1'(x)}\left(u_0(x), u_0'(x), u_0''(x), \cdots, u_0^{(n)}(x)\right),\\ f_{2,0} &= \frac{\partial N}{\partial u_1''(x)}\left(u_0(x), u_0'(x), u_0''(x), \cdots, u_0^{(n)}(x)\right),\\ &\vdots\\ f_{n,0} &= \frac{\partial N}{\partial u_1^{(n)}(x)}\left(u_0(x), u_0'(x), u_0''(x), \cdots, u_0^{(n)}(x)\right),\end{aligned}$$

and

$$\mathbf{R}_1(x) = g(x) - \mathcal{L}[u_0(x), u_0'(x), u_0''(x), \cdots, u_0^{(n)}(x)] - \mathcal{N}[u_0(x), u_0'(x), u_0''(x), \cdots, u_o(x)^{(n)}].$$

Since the left hand side of equation (1.14) is linear and the right hand side is known, the equation can be solved for $u_1(x)$ subject to the boundary conditions

$$u(a) = 0, \qquad u(b) = 0. \tag{1.15}$$

Assuming that the solution of the linear equation (1.14) is close to the solution of the nonlinear equation (1.13), then the first approximation of the solution (order 1) is

$$u(x) \approx u_0(x) + u_1(x) \tag{1.16}$$

To improve this solution, we define the vertical difference between the functions $U_1(x)$ and $u_1(x)$ by a function $U_2(x)$ as (see Figure 1.2)

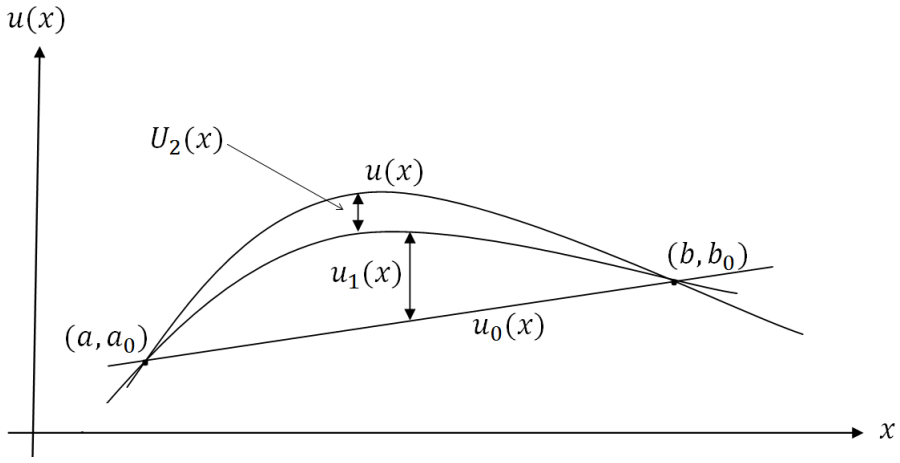

Figure 1.2: Geometric representation of the function $U_2(x)$

$$U_2(x) = U_1(x) - u_1(x), \tag{1.17}$$

Substitute (1.17) into equation (1.13) to give

$$\begin{aligned}
&\mathcal{L}[U_2(x), U_2'(x), U_2''(x), ..., U_2^{(n)}] \\
&+\mathcal{L}[u_0(x) + u_1(x), u_0'(x) + u_1'(x), u_0''(x) + u_1''(x), ..., u_0^{(n)} + u_1^{(n)}(x)] \\
&+\mathcal{N}[U_2(x) + u_0(x) + u_1(x), U_2'(x) + u_0'(x) + u_1'(x), U_2''(x) + u_0''(x) + u_1''(x) \\
&, ..., U_2^{(n)}(x) + u_0^{(n)})(x) + u_1^{(n)}(x)] = g(x), \qquad (1.18)
\end{aligned}$$

Since $u_0(x)$ and $u_1(x)$ are known and this equation is non-linear in $U_2(x)$, we solve the linearized equation after neglecting the non-linear terms containing $U_2(x)$ and its derivatives. We further assume that $U_2(x)$ and its derivatives are very small and denote the solution of the linearized equation (1.18) by $U_2(x)$, that is $U_2(x) \approx u_2(x)$. Equation (1.18) can be written as

$$\begin{aligned}
\mathcal{L}[u_2(x), u_2'(x), u_2''(x), \cdots, u_2^{(n)}(x)] + f_{0,0}u_2(x) + f_{1,0}u_2'(x) + f_{2,0}u_2''(x) \\
+ \cdots + f_{n,0}u_2^{(n)}(x) = \mathbf{R}_2(x), \qquad (1.19)
\end{aligned}$$

where

$$f_{0,0} = \frac{\partial N}{\partial u_2(x)} \left(u_0(x) + u_1(x), u_0'(x) + u_1'(x), u_0''(x) + u_1''(x), \cdots, u_0^{(n)}(x) + u_1^{(n)}(x)\right),$$

$$f_{1,0} = \frac{\partial N}{\partial u_2'(x)} \left(u_0(x) + u_1(x), u_0'(x) + u_1'(x), u_0''(x) + u_1''(x), \cdots, u_0^{(n)}(x) + u_1^{(n)}(x)\right),$$

$$f_{2,0} = \frac{\partial N}{\partial u_1''(x)} \left(u_0(x) + u_1(x), u_0'(x) + u_1'(x), u_0''(x) + u_1''(x), \cdots, u_0^{(n)}(x) + u_1^{(n)}(x)\right),$$

$$\vdots$$

$$f_{n,0} = \frac{\partial N}{\partial u_1^{(n)}(x)} \left(u_0(x) + u_1(x), u_0'(x) + u_1'(x), u_0''(x) + u_1''(x), \cdots, u_0^{(n)}(x) + u_1^{(n)}(x)\right),$$

and

$$\mathbf{R}_2(x) = g(x) - \mathcal{L}[u_0(x) + u_1(x), u_0'(x) + u_1'(x), \cdots, u_0^{(n)}(x) + u_1^{(n)}(x)] \\ -\mathcal{N}[u_0(x) + u_1(x), u_0'(x) + u_1'(x), \cdots, u_0^{(n)}(x) + u_1^{(n)}(x)].$$

After solving the equation (1.19), the second order approximation of $u(x)$ is given by

$$u(x) \approx u_0(x) + u_1(x) + u_2(x). \tag{1.20}$$

This process is repeated for $m = 2, 3, \cdots, i$. Thus, $u(x)$ is given by

$$\begin{aligned} u(x) &= U_1(x) + u_0(x), \\ &= U_2(x) + u_0(x) + u_1(x), \\ &= U_3(x) + u_0(x) + u_1(x) + u_2(x), \\ &\vdots \\ &= U_{i+1}(x) + u_0(x) + u_1(x) + u_2(x) + \cdots + u_i(x), \\ &= U_{i+1}(x) + \sum_{m=0}^{i} u_m(x). \end{aligned}$$

Thus, for large i, we can approximate the ith order solution $u(x)$ by

$$u(x) = \sum_{m=0}^{i} u_m(x). \tag{1.21}$$

The solution $u_i(x)$ can be determined from the linearized original equation (1.10) starting from the initial guess $u_0(x)$ and solving the linear equations for $u_i(x)$. In general, the form of the linearized equation for $u_i(x)$ is given by

$$\mathcal{L}[u_i(x), u_i'(x), u_i''(x), \cdots, u_i^{(n)}] + f_{0,i-1}u_i(x) + f_{1,i-1}u_i'(x) + f_{2,i-1}u_i''(x) \\ + \cdots + f_{n,i-1}u_i^{(n)}(x) = \mathbf{R}_{i-1}(x), \qquad i = 1, 2, \cdots, M, \tag{1.22}$$

subject to the boundary conditions

$$u_i(a) = 0, \qquad u_i(b) = 0, \tag{1.23}$$

where M is termed the order of the SLM.

$$f_{0,i-1} = \frac{\partial N}{\partial u_i(x)} \left(\sum_{m=0}^{i-1} u_m, \sum_{m=0}^{i-1} u'_m, \sum_{m=0}^{i-1} u''_m, ..., \sum_{m=0}^{i-1} u_m^{(n)} \right),$$

,

$$f_{1,i-1} = \frac{\partial N}{\partial u'_i(x)} \left(\sum_{m=0}^{i-1} u_m, \sum_{m=0}^{i-1} u'_m, \sum_{m=0}^{i-1} u''_m, ..., \sum_{m=0}^{i-1} u_m^{(n)} \right),$$

$$f_{2,i-1} = \frac{\partial N}{\partial u''_i(x)} \left(\sum_{m=0}^{i-1} u_m, \sum_{m=0}^{i-1} u'_m, \sum_{m=0}^{i-1} u''_m, ..., \sum_{m=0}^{i-1} u_m^{(n)} \right),$$

$$\vdots$$

$$f_{n,i-1} = \frac{\partial N}{\partial u_i^{(n)}(x)} \left(\sum_{m=0}^{i-1} u_m, \sum_{m=0}^{i-1} u'_m, \sum_{m=0}^{i-1} u''_m, ..., \sum_{m=0}^{i-1} u_m^{(n)} \right),$$

and

$$\mathbf{R}_{i-1}(x) = g(x) - \mathcal{L} \left(\sum_{m=0}^{i-1} u_m, \sum_{m=0}^{i-1} u'_m, \sum_{m=0}^{i-1} u''_m, ..., \sum_{m=0}^{i-1} u_m^{(n)} \right)$$

$$-\mathcal{N} \left(\sum_{m=0}^{i-1} u_m, \sum_{m=0}^{i-1} u'_m, \sum_{m=0}^{i-1} u''_m, ..., \sum_{m=0}^{i-1} u_m^{(n)} \right).$$

The ordinary differential equation(1.22) is linear and can easily be solved using any analytical or numerical method. In this study we used the Chebyshev spectral collocation method (Canuto 1988, Don and Solomonoff 1995, Trefethen 2000) to solve equation (1.22). The method is based on the Chebyshev polynomials defined on the interval $[-1, 1]$. We first transform the domain $[a, b]$ to the domain $[-1, 1]$ where the

Chebyshev spectral collocation method can be applied by using the transformation

$$(b-a)\xi = 2x - (a+b), \qquad -1 \leq \xi \leq 1. \tag{1.24}$$

Most problems in fluid mechanics are defined on the domain $[0, \infty)$. For this case we can use the domain truncation technique where the problem is solved in the interval $[0, L]$ instead of $[0, \infty)$ where L is the scaling parameter used to invoke the boundary condition at infinity. By using the mapping

$$\frac{\xi + 1}{2} = \frac{x}{L}, \qquad -1 \leq \xi \leq 1, \tag{1.25}$$

the problem is solved in the spectral domain $[-1, 1]$. We discretize the domain $[-1, 1]$ using the Gauss-Lobatto collocation points given by

$$\xi = \cos\frac{\pi j}{N}, \qquad j = 0, 1, 2, \ldots, N, \tag{1.26}$$

where N is the number of collocation points used. The function u_i is approximated at the collocation points as follows

$$u_i(\xi) \approx \sum_{k=0}^{N} u_i(\xi_k) T_k(\xi_j) \tag{1.27}$$

where T_k is the k^{th} Chebyshev polynomial given by

$$T_k(\xi) = \cos\left[k \cos^{-1}(\xi)\right]. \tag{1.28}$$

The derivatives of the variables at the collocation points are represented as

$$\frac{d^{(r)}u_i}{dx^{(r)}} = \sum_{k=0}^{N} \left[\frac{2}{b-a}\mathcal{D}_{kj}\right]^r u_i(\xi_k) \tag{1.29}$$

where r is the order of differentiation and $\mathcal{D}$ being the Chebyshev spectral differen-

tiation matrix whose entries are defined as (Canuto 1988, Don and Solomonoff 1995, Trefethen 2000)

$$\left.\begin{aligned} \mathcal{D}_{00} &= \frac{2N^2+1}{6}, \\ \mathcal{D}_{jk} &= \frac{c_j}{c_k}\frac{(-1)^{j+k}}{\xi_j-\xi_k}, \qquad j \neq k; \qquad j,k = 0,1,\ldots,N, \\ \mathcal{D}_{kk} &= -\frac{\xi_k}{2(1-\xi_k^2)}, \qquad k = 1,2,\ldots,N-1, \\ \mathcal{D}_{NN} &= -\frac{2N^2+1}{6}. \end{aligned}\right\} \tag{1.30}$$

Substituting equations (1.25)-(1.31) into equation (1.22) leads to the following system of matrix equation

$$\mathbf{A}_{i-1}\mathbf{X}_i = \mathbf{R}_{i-1}, \tag{1.31}$$

in which $\mathbf{A}_{i-1}$ is a $(N+1)\times(N+1)$ square matrix while $\mathbf{X}_i$ and $\mathbf{R}_{i-1}$ are $(N+1)\times 1$. After modifying the matrix system (1.31) to incorporate the modified the boundary conditions, the solution of (1.10) is obtained by

$$\mathbf{X}_i = \mathbf{A}_{i-1}^{-1}\mathbf{R}_{i-1} \tag{1.32}$$

1.6 Comparison of the QLM and SLM

In this section, we illustrate the use of the QLM and the SLM by solving a nonlinear second order differential equation. To demonstrate the convergence rates of the QLM and the SLM, the solutions of the problem are compared with the numerical solution at different orders of approximation. Consider the following nonlinear Bratu's boundary value problem, (Aris 1975, Boyd 2003, Wazwaz 2005)

$$u''(x) + \lambda e^{u(x)} = 0, \tag{1.33}$$

with boundary conditions

$$u(0) = 0 \qquad \text{and} \qquad u(1) = 0, \tag{1.34}$$

where $\lambda > 0$. The exact solution of (1.33) and (1.34) is given by

$$u(x) = -2 \ln \left[\frac{\cosh\left[(x - \frac{1}{2})\frac{\theta}{2}\right]}{\cosh\left(\frac{\theta}{4}\right)} \right], \tag{1.35}$$

where θ satisfies $\theta = \sqrt{2\lambda}\cosh(\theta/4)$. To apply the QLM to this test problem, we first linearize the equation using the form (1.8) to get the following mth approximation linear differential equation

$$u''_{i+1}(x) + \lambda e^{u_i(x)} u_{i+1}(x) = \lambda(u_i(x) - 1)e^{u_i(x)}, \;\; i = 0, 1, 2, .., m = 0, \tag{1.36}$$

subject to boundary conditions

$$u_{i+1}(0) = 0, \qquad u_{i+1}(1) = 0. \tag{1.37}$$

The initial guess $u_0(t)$ must be chosen in such a way that it satisfies the conditions (1.34). To apply the SLM technique to find a solution to equation (1.33), we start by assuming that the solution may be obtained in the form

$$u = u_0(t) + \sum_{m=1}^{M} u_m(t), \tag{1.38}$$

where M is the order of the method and u_0 is an initial approximation. Substituting (1.38) into equation (1.33) we get the linearized form

$$u''_{i+1}(x) + \lambda e^{u_i(x)} u_{i+1}(x) = -\left(u''_i(x) + \lambda e^{u_i(x)}\right), \tag{1.39}$$

subject to initial conditions

$$u_{i+1}(0) = 0, \qquad u_{i+1}(1) = 0. \tag{1.40}$$

Equations (1.36) and (1.39) were linearized and can be easily solved using any numerical methods. We observe from the linearized equations (1.36) and (1.39), that the boundary condition is not changed even for higher approximations for QLM solution but in the SLM solution the initial guess must be chosen to satisfy the boundary conditions (1.34) and for higher approximations to be zero. For the QLM and SLM solutions we selected the initial guess $u_0(x) = 0$. Tables 1.1 and 1.2 give a comparison of the convergence rates of the QLM and SLM solution at different orders of approximation with the exact solution at selected nodes when $\lambda = 1$ and $\lambda = 2$ for same initial approximation. A striking feature of the SLM is that a high level of accuracy is achieved at very low orders of approximation. For example, from Tables 1.1 and 1.2, convergence of the SLM is achieved at the second order and the third order of the solution when $\lambda = 1$ and $\lambda = 2$, respectively, while convergence of the QLM is not achieved even at the higher order of approximations. We can conclude that the SLM appears to be more efficient and converges more rapidly than the QLM for this particular problem. We note some similarities and differences between the QLM and SLM as follows:

(i) In the QLM the linearized equation is constructed as a generalization of the Newton-Raphson method whereas in the SLM this is constructed by first assuming that the solution may be obtained in the form $u = u_i + \sum u_m$ and neglecting the non-linear terms after substituting this into the given equation.

(ii) The QLM method treats only the nonlinear terms as a perturbation about the linear ones, Parand et al. (2010b).

(iii) The initial guess is chosen to satisfy the boundary conditions in both methods.

Table 1.1: Comparison of the absolute convergence rates of the QLM and SLM approximate solutions with the exact solution u(x) for when $\lambda = 1$.

x	Order	QLM	SLM	|QLM$-u(x)$|	|SLM$-u(x)$|
0.1	1st order	0.049555	0.049543	0.000292	0.000304
	2nd orer	0.049859	0.049847	0.000012	0.000000
	3rd order	0.049859	0.049847	0.000012	0.00000
0.2	1st order	0.088621	0.088600	0.000569	0.000590
	2nd orer	0.089212	0.089190	0.000022	0.000000
	3rd order	0.089212	0.089190	0.000022	0.000000
0.3	1st order	0.116807	0.116780	0.000802	0.000829
	2nd orer	0.117638	0.117609	0.000029	0.000000
	3rd order	0.117638	0.117609	0.000029	0.000000
0.4	1st order	0.133832	0.133801	0.000958	0.000989
	2nd orer	0.134824	0.134790	0.000034	0.000000
	3rd order	0.134824	0.134790	0.000034	0.000000
0.5	1st order	0.139526	0.139494	0.001013	0.001045
	2nd orer	0.140575	0.140539	0.000036	0.000000
	3rd order	0.140575	0.140539	0.000036	0.000000

(iv) The linearized equations by the SLM and QLM have the same linear terms and different source terms.

(v) The SLM converges more rapidly than the QLM.

The SLM is a recent method that remains to be generalized and whose robustness remains to be tested in the case of highly nonlinear equations with a strong coupling. We can summarize some of advantages of the SLM as follows;

(1) It is efficient for most non-linear equations and rapidly converges to the exact solution.

Table 1.2: Comparison of the convergence rates of the QLM and SLM approximate solutions with the exact solution u(x) for when $\lambda = 2$.

x	Order	QLM	SLM	|QLM$-u(x)$|	|SLM$-u(x)$|
0.1	2nd order	0.114471	0.114402	0.000060	0.000009
	3rd order	0.114480	0.114411	0.000069	0.000000
	4th order	0.114480	0.114411	0.000069	0.000000
0.2	2nd order	0.206534	0.206403	0.000115	0.000016
	3rd order	0.206550	0.206419	0.000131	0.000000
	4th order	0.206550	0.206419	0.000131	0.000000
0.3	2nd order	0.274036	0.273856	0.000157	0.000023
	3rd order	0.274059	0.273879	0.000180	0.000000
	4th order	0.274059	0.273879	0.000180	0.000000
0.4	2nd order	0.315274	0.315061	0.000186	0.000027
	3rd order	0.315301	0.315088	0.000213	0.000000
	4th order	0.315301	0.315088	0.000213	0.000000
0.5	2nd order	0.329146	0.328924	0.000194	0.000010
	3rd order	0.329175	0.328952	0.000223	0.000000
	4th order	0.329175	0.328952	0.000223	0.000000

(2) It does not require any parameter to control the convergence rate of the solution.

(3) It gives high accuracy with only a few iterations.

(4) It requires shorter times to run the code compared with some non-perturbation techniques.

The SLM is a very useful tool for solving strongly nonlinear equations arising from any area of science and engineering. It can be used in place of the traditional numerical methods such as finite differences, Runge-Kutta shooting methods, finite elements in solving non-linear boundary value problems.

1.7 Research objectives

The objectives of this study are:

(1) To investigate the Soret and viscous dissipation effects on natural convection from a vertical plate in a non-Darcy porous medium.

(2) To characterize the Soret effect on natural convection from a vertical plate in stratified porous medium saturated with a non-Newtonian fluid.

(3) To investigate mixed convection from a vertical plate in a non-Darcy porous medium in the presence of thermal radiation and viscous dissipation effects

(4) To investigate MHD and cross-diffusion effects on fluid flow over a vertical flat plate.

(5) To study cross-diffusion and radiation effects on the flow along an exponentially stretching sheet in porous media.

1.8 Structure of the thesis

The main body of the thesis consists of five chapters and the conclusion. In each chapter a specific problem is investigated. The chapters focus firstly on the effect of cross-diffusion on fluid flow in porous media, and secondly on the application of the linearization method to the solution of systems of differential equations. The chapters are;

- Chapter 2:

  In this chapter we investigated natural convection from a vertical plate in a

non-Darcy porous medium. We transformed the governing equations into a system of ordinary differential equations using a local non-similar method. The equations were solved using the SLM technique and the shooting method. The effects of Soret and viscous dissipation were determined and discussed.

- Chapter 3:

  The effect of the Soret parameter on flow, due to a vertical plate in a porous medium with variable viscosity was investigated. The Ostwald -de Waele power-law model was used to characterize the non-Newtonian behaviour of the fluid. The effect of various physical parameters such as power-law index, variable viscosity and thermal stratification parameters on the dynamics of the fluid are analyzed through computed results.

- Chapter 4:

  In this chapter we presented an investigation of mixed convective flow due to a vertical plate immersed in a non-Darcy porous medium saturated with a non-Newtonian power-law fluid with variable viscosity. The Rosseland approximation was used to describe the radiative heat flux accounted in the energy equation. The effects of thermal radiation and viscous dissipation were determined and discussed.

- Chapter 5:

  In this chapter we used a non-perturbation linearisation method to solve a coupled highly nonlinear boundary value problem, due to flow over a vertical surface in the presence of cross-diffusion effects subject to a magnetic field. The accuracy of the solutions has been tested using a local nonsimilarity method.

- Chapter 6:

  This chapter considered the cross-diffusion effect on convection from an exponentially stretching surface in a porous medium subject to viscous dissipation and radiation effects. The transformed ordinary differential equations were

solved using a linearization method. The accuracy and rate of convergence of the solution was tested using the Matlab `bvp4c` solver.

Chapter 2

Natural convection from a vertical plate immersed in a power-law fluid saturated non-Darcy porous medium with viscous dissipation and Soret effects*

Abstract

We investigate viscous dissipation and thermal-diffusion effects on natural convection from a vertical plate embedded in a fluid saturated non-Darcy porous medium. The non-Newtonian behavior of fluid is characterized by the Ostwald -de Waele power-law model. The governing partial differential equations are transformed into a system of

[0]* Submitted to the Journal of Fluid mechanics Research, (July 2011).

ordinary differential equations using a local non-similar method and the resulting boundary value problem is solved using a novel SLM. The accuracy of the SLM has been established by comparing the results with the shooting technique. The effects of physical parameters for the convective motion of the power-law liquid are presented both qualitatively and quantitatively. Heat and mass transfer coefficients are presented qualitatively for different values of the said parameters.

2.1 Introduction

Recent years have seen a spike in the number of studies devoted to the study of natural convection in fluid flows through porous media. This is an interesting and important subject in the area of heat transfer with wide applications in various fields such as geophysics, aerodynamic extrusion of polymer sheets, food processing and the manufacture of plastic films. The problem of natural convection and heat transfer in porous media have been carried out on vertical, inclined and horizontal surfaces by, among others, Chamkha and Khaled (1999) who investigated the heat and mass transfer through mixed convection from a vertical plate embedded in a porous medium.

The problem of natural convection in a non-Newtonian fluid over a vertical surface in porous media was studied by Chen and Chen (1988b). This was extended to a horizontal cylinder and a sphere in Chen and Chen (1988a). Cheng (2006) studied heat and mass transfer from a vertical plate with variable wall heat and mass fluxes in a porous medium saturated with a non-Newtonian power-law fluid. El-Hakiem (2001) investigated the problem of mixed convective heat transfer from a horizontal surface with variable wall heat flux. The horizontal surface was embedded in a porous medium saturated with an Ostwald-de-Waele type non-Newtonian fluid. Grosan et al. (2001) investigated free convection from a vertical flat plate saturated with a power-low Newtonian fluid. Nakayama et al. (1991) discussed the problem of natural

convection over a non-isothermal body of arbitrary shape embedded in a porous medium filled with a non-Newtonian fluid. Similarity and integral solutions were obtained by Nakayama and Koyama (1987a,b) for free convection along a vertical plate which was immersed in a thermally stratified, fluid-saturated porous medium with variable wall temperature. Review of the extensive work in this area is available in books by Nield and Bejan (1999), Ingham and Pop (1998), Pop and Igham (2001).

The effect of Soret and/or Dufour numbers on heat and mass transfer in porous medium with variable properties has been investigated by many researchers. Tsai and Huang (2009) obtained the solutions for heat and mass transfer coefficients for natural convection along a vertical surface with variable heat fluxes embedded in a porous medium. Thermal-diffusion (Soret) and diffusion-thermo (Dufour) effects were assumed to be significant. The effect of Soret and Dufour on free convection from a vertical plate with variable wall heat and mass fluxes in a porous medium saturated with a non-Newtonian power-law fluid was investigated by Ching (2011). Partha et al. (2006) studied the Soret and Dufour effects in a non-Darcy porous medium. Narayana and Murthy (2007, 2008) investigated the Soret and Dufour effects on free convection from a horizontal flat plate in doubly stratified Darcy porous media. Cheng (2009) investigated the effect of Soret and Dufour on heat and mass transfer from a vertical cone in a porous medium with a constant wall temperature and concentration. Cheng (2008) investigated the effect of Soret and Dufour on free convection boundary layer flow over a vertical cylinder in a porous medium with constant wall temperature and concentration.

In this chapter we investigate viscous dissipation and the Soret effect on natural convection from a vertical plate immersed in a non-Darcy porous medium saturated with a non-Newtonian power-law fluid. The viscosity variation is modelled using Reynolds' law, (Massoudi and Phuoc 2004 and Seddeek 2007), which assumes that the viscosity decreases exponentially with temperature. The governing equations were

solved using a novel SLM.

2.2 Mathematical formulation

Consider two-dimensional steady boundary layer flow over a vertical plate embedded in a non-Darcy porous medium saturated with a non-Newtonian power-law fluid with variable viscosity. The x-coordinate is measured along the plate from its leading edge and the y-coordinate normal to the plate. The plate is maintained at a constant temperature T_w and concentration C_w. The ambient fluid temperature is T_∞ and the concentration is C_∞. Figure 2.1 shows the physical configuration of the problem under consideration. The governing equations of continuity, momentum, energy and

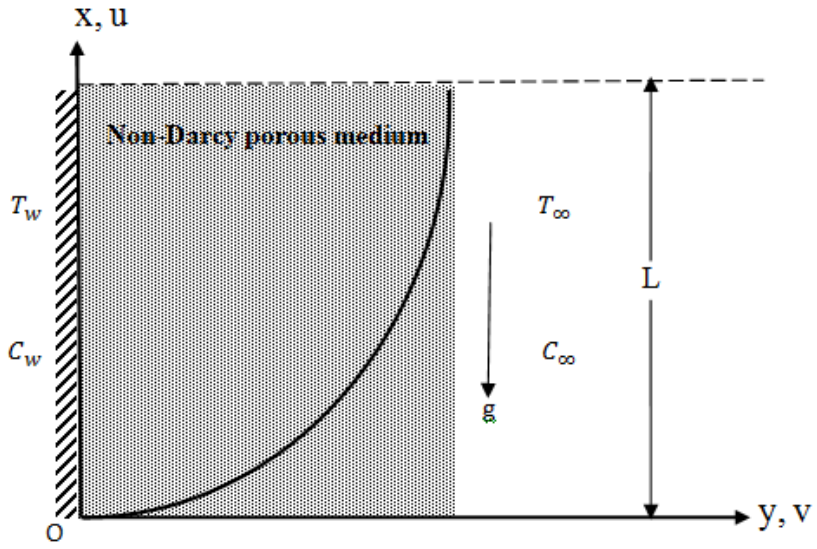

Figure 2.1: Physical model and coordinate system.

concentration under the Boussinesq approximations may be written as (see Shenoy

1993)

$$\frac{\partial u}{\partial x}+\frac{\partial v}{\partial y}=0, \tag{2.1}$$

$$\frac{\partial u^n}{\partial y}+\frac{\partial}{\partial y}\left(\frac{\rho_\infty b K^*}{\mu}u^2\right)=\frac{\partial}{\partial y}\left(\frac{\rho_\infty K^* \mathrm{g}}{\mu}[\beta_T(T-T_\infty)+\beta_C(C-C_\infty)]\right), \tag{2.2}$$

$$u\frac{\partial T}{\partial x}+v\frac{\partial T}{\partial y}=\alpha\frac{\partial^2 T}{\partial y^2}+\frac{\mu}{\rho_\infty K^* c_p}u\left(u^n+\frac{b\rho_\infty K^*}{\mu}u^2\right), \tag{2.3}$$

$$u\frac{\partial C}{\partial x}+v\frac{\partial C}{\partial y}=D\frac{\partial^2 C}{\partial y^2}+D_1\frac{\partial^2 T}{\partial y^2}, \tag{2.4}$$

where u and v are the velocity components along the x and y-directions respectively, n is the power-law index such that $n<1$ describes a pseudoplastic, $n=1$ represents a Newtonian fluid and $n>1$ is dilatant fluid, T and C are the fluid temperature and the concentration respectively, ρ_∞ is the reference density, g is the acceleration due to gravity, α is the effective thermal diffusivity, D is the effective solutal diffusivity, β_T and β_C are the thermal and concentration expansion coefficients, respectively, c_p is the specific heat at constant pressure, D_1 quantifies the contribution to the mass flux due to temperature gradient, b is the empirical constant associated with the Forchheimer porous inertia term, μ is the consistency index of power-law fluid and K^* is the modified permeability of the flow of the non-Newtonian power-law fluid. The modified permeability K^* is defined (see Christopher and Middleman 1965 and Dharmadhikari and Kale 1985) as;

$$K^*=\frac{1}{c_t}\left(\frac{n\varphi}{3n+1}\right)^n\left(\frac{50K}{3\varphi}\right)^{\frac{n+1}{2}} \qquad \text{with} \qquad K=\frac{\varphi^3 d^2}{150(1-\varphi)^2}$$

where φ is the porosity of the medium, d is the particle size and the constant c_t is given by

$$c_t=\begin{cases}\frac{25}{12} \quad (\text{for } n=1) & \text{Christopher and Middleman (1965)}\\ \frac{3}{2}\left(\frac{8n}{9n+3}\right)^n\left(\frac{10n-3}{6n+1}\right)\left(\frac{75}{16}\right)^{\frac{3(10n-3)}{10n+11}} & \text{Dharmadhikari and Kale (1985)}\end{cases}$$

for $n = 1$, $c_t = \dfrac{25}{12}$. The boundary conditions are

$$\left.\begin{array}{llll} v = 0, & T = T_w, & C = C_w & \text{at} \quad y = 0, \\ u \to 0, & T \to T_\infty, & C \to C_\infty & \text{as} \quad y \to \infty. \end{array}\right\} \tag{2.5}$$

The system of non-similar partial differential equations can be simplified by using the stream function ψ where

$$u = \frac{\partial \psi}{\partial y} \qquad \text{and} \qquad v = -\frac{\partial \psi}{\partial x}, \tag{2.6}$$

together with the following transformations

$$\left.\begin{array}{ll} \eta = \dfrac{y}{x} Ra_x^{1/2}, & \psi(V_d, \eta) = \alpha Ra_x^{1/2} f(V_d, \eta), \\ \theta(V_d, \eta) = \dfrac{T - T_\infty}{T_w - T_\infty}, & \phi(V_d, \eta) = \dfrac{C - C_\infty}{C_w - C_\infty}, \end{array}\right\} \tag{2.7}$$

where $Ra_x = \left(\dfrac{x}{\alpha}\right)\left[\dfrac{\rho_\infty K^* \mathrm{g} \beta_T (T_w - T_\infty)}{\mu_\infty}\right]^{1/n}$ is the local Rayleigh number and $V_d = \dfrac{g\beta_T x}{c_p}$ is the viscous dissipation parameter. The variation of viscosity with the dimensionless temperature is written in the form (see Elbashbeshy 2000 and Massoudi 2004):

$$\mu(\theta) = \mu_\infty e^{-\gamma\theta}, \tag{2.8}$$

where γ is a non-dimensional viscosity parameter that depends on the nature of the fluid, and μ_∞ is the ambient viscosity of the fluid. Using (2.7), the momentum, energy and concentration equations (2.2) - (2.4) reduce to the following system of equations;

$$nf'^{n-1}f'' + Gre^{\gamma\theta}\left(2f'f'' + \gamma\theta' f'^2\right) = e^{\gamma\theta}\left[\theta'(\gamma\theta + 1) + \Lambda(\gamma\theta'\phi + \phi')\right], \tag{2.9}$$

$$\theta'' + \frac{1}{2}f\theta' + V_d e^{-\gamma\theta} f'\left(f'^n + Gre^{\gamma\theta} f'^2\right) = V_d\left(f'\frac{\partial\theta}{\partial V_d} - \theta'\frac{\partial f}{\partial V_d}\right), \tag{2.10}$$

$$Le^{-1}\phi'' + \frac{1}{2}f\phi' + Sr\theta'' = V_d\left(f'\frac{\partial\phi}{\partial V_d} - \phi'\frac{\partial f}{\partial V_d}\right). \tag{2.11}$$

The transformed boundary conditions are

$$\left.\begin{aligned} &f(V_d,\eta)+2V_d\frac{\partial f(V_d,\eta)}{\partial V_d}=0,\ \theta(V_d,\eta)=1,\ \phi(V_d,\eta)=1 \qquad \text{at} \qquad \eta=0\\ &f'(V_d,\eta)\to 0,\ \theta(V_d,\eta)\to 0,\ \phi(V_d,\eta)\to 0 \qquad \text{as} \qquad \eta\to\infty \end{aligned}\right\} \tag{2.12}$$

where $Gr^* = b\left(\dfrac{K^{*2}\rho_\infty^2[g\beta_T(T_w-T_\infty)]^{2-n}}{\mu_\infty^2}\right)^{1/n}$ is the modified Grashof number, $Le = \dfrac{\alpha}{D}$ is the Lewis number, $Sr = \dfrac{D_1(T_w-T_\infty)}{\alpha(C_w-C_\infty)}$ is the Soret number and $\Lambda = \dfrac{\beta_C(C_w-C_\infty)}{\beta_T(T_w-T_\infty)}$ is the buoyancy term (where $\Lambda > 0$ represents aiding buoyancy and $\Lambda < 0$ represents opposing buoyancy). The primes in equations (2.9) - (2.11) represent differentiation with respect to the variable η. Integrating equation (2.9) once and using the boundary conditions (2.12) gives

$$f'^n + Gre^{\gamma\theta}f'^2 = (\theta+\Lambda\phi)e^{\gamma\theta}. \tag{2.13}$$

Substituting (2.13) in (2.9) and (2.10) we obtain

$$\left(nf'^{n-1}+2Gr^*e^{\gamma\theta}f'\right)f'' = \left(\theta'+\Lambda\phi'\right)e^{\gamma\theta}+\gamma\theta'f'^n, \tag{2.14}$$

$$\theta''+\frac{1}{2}f\theta'+V_df'(\theta+\Lambda\phi) = V_d\left(f'\frac{\partial\theta}{\partial V_d}-\theta'\frac{\partial f}{\partial V_d}\right). \tag{2.15}$$

The local skin-friction, heat and mass transfer coefficients can be respectively obtained from

$$\left.\begin{aligned} C_fPe_x^2 &= 2P_rRa_x^{3/2}f''(V_d,0)\\ Nu_x/Ra_x^{1/2} &= -\theta'(V_d,0)\\ Sh_x/Ra_x^{1/2} &= -\phi'(V_d,0) \end{aligned}\right\}. \tag{2.16}$$

where $P_r = \dfrac{\nu_\infty}{\alpha}$ and $Pe_x = \dfrac{U_\infty x}{\alpha}$.

2.3 Method of solution

Equations (2.11), (2.14) and (2.15) are solved subject to the boundary conditions (2.12). We first apply a local similarity and local non-similarity method (see Minkowycz and Sparrow 1974 and Sparrow and Yu 1971) and for the first level of truncation, we neglect the terms multiplied by $V_d\dfrac{\partial}{\partial V_d}$. This is particularly appropriate when $V_d \ll 1$. Thus the system of equations obtained is given by:

$$\left(nf'^{n-1} + 2Gr^* e^{\gamma\theta} f'\right) f'' = \left(\theta' + \Lambda\phi'\right) e^{\gamma\theta} + \gamma\theta' f'^n, \tag{2.17}$$

$$\theta'' + \frac{1}{2} f\theta' + V_d f'(\theta + \Lambda\phi) = 0, \tag{2.18}$$

$$Le^{-1}\phi'' + \frac{1}{2} f\phi' + Sr\theta'' = 0. \tag{2.19}$$

The corresponding boundary conditions are

$$\left.\begin{array}{llll} f(V_d,\eta) = 0, & \theta(V_d,\eta) = 1, & \phi(V_d,\eta) = 1 & \text{at} \quad \eta = 0, \\ f'(V_d,\eta) \to 0, & \theta(V_d,\eta) \to 0, & \phi(V_d,\eta) \to 0 & \text{as} \quad \eta \to \infty, \end{array}\right\} \tag{2.20}$$

For the second level of truncations, we introduce the following auxiliary variables $g = \dfrac{\partial f}{\partial V_d}$, $h = \dfrac{\partial \theta}{\partial V_d}$ and $k = \dfrac{\partial \phi}{\partial V_d}$ and recover the neglected terms at the first level of truncation. Thus, the governing equations at the second level are given by

$$\left(nf'^{n-1} + 2Gr^* e^{\gamma\theta} f'\right) f'' = \left(\theta' + \Lambda\phi'\right) e^{\gamma\theta} + \gamma\theta' f'^n, \tag{2.21}$$

$$\theta'' + \frac{1}{2} f\theta' + V_d f'(\theta + \Lambda\phi) = V_d(f'h - \theta' g), \tag{2.22}$$

$$Le^{-1}\phi'' + \frac{1}{2} f\phi' + Sr\theta'' = V_d(f'k - \phi' g), \tag{2.23}$$

and the corresponding boundary conditions are

$$\left.\begin{array}{llll} f(V_d,\eta) + 2V_d\dfrac{\partial f(V_d,\eta)}{\partial V_d} = 0, \ \theta(V_d,\eta) = 1, \ \phi(V_d,\eta) = 1 & \text{at} \quad \eta = 0 \\ f'(V_d,\eta) \to 0, \ \theta(V_d,\eta) \to 0, \ \phi(V_d,\eta) \to 0 & \text{as} \quad \eta \to \infty \end{array}\right\}. \tag{2.24}$$

The third level can be obtained by differentiating equations (2.21)-(2.23) with respect to V_d and neglecting the terms $\frac{\partial g}{\partial V_d}$, $\frac{\partial h}{\partial V_d}$ and $\frac{\partial k}{\partial V_d}$ to get the set of equations

$$\begin{aligned}
&\left(nf'^{n-1} + 2Gr^* e^{\gamma\theta} f'\right) g'' + \left[n(n-1)f'^{n-2} g' + 2Gr^* e^{\gamma\theta}(g' + \gamma h f')\right] f'' \\
&- \left[\gamma h(\theta' + \Lambda\phi') + h' + \Lambda k'\right] e^{\gamma\theta} - \gamma\left(n\theta' g' f'^{n-1} + f'^{n} h'\right) = 0, \qquad (2.25) \\
&h'' + \frac{1}{2}(fh' + 3g\theta') - f'h + V_d f'(h + \Lambda k) + (\theta + \Lambda\phi)(V_d g' + f') \\
&+ V_d(h'g - g'h) = 0, \qquad (2.26) \\
&Le^{-1}k'' + \frac{1}{2}(fk' + 3g\phi') - f'k + Srh'' + V_d(k'g - g'k) = 0, \qquad (2.27)
\end{aligned}$$

The corresponding boundary conditions are

$$\left.\begin{aligned}
&g(V_d,\eta) = 0, \quad h(V_d,\eta) = 0, \quad k(V_d,\eta) = 0 \quad \text{at} \quad \eta = 0 \\
&g'(V_d,\eta) \to 0, \quad h(V_d,\eta) \to 0, \quad k(V_d,\eta) \to 0 \quad \text{as} \quad \eta \to \infty
\end{aligned}\right\}. \qquad (2.28)$$

The set of differential equations (2.21)-(2.23) and (2.25)-(2.27) together with the boundary conditions (2.24) and (2.28) were solved by means of the SLM. The SLM algorithm starts with the assumption that the variables $f(\eta), \theta(\eta), \phi(\eta), g(\eta), h(\eta)$ and $k(\eta)$ can be expressed as

$$\left.\begin{aligned}
f(\eta) &= f_i(\eta) + \sum_{m=0}^{i-1} F_m(\eta), & \theta(\eta) &= \theta_i(\eta) + \sum_{m=0}^{i-1} \Theta_m(\eta), \\
\phi(\eta) &= \phi_i(\eta) + \sum_{m=0}^{i-1} \Phi_m(\eta), & g(\eta) &= g_i(\eta) + \sum_{m=0}^{i-1} G_m(\eta), \\
h(\eta) &= h_i(\eta) + \sum_{m=0}^{i-1} H_m(\eta), & k(\eta) &= k_i(\eta) + \sum_{m=0}^{i-1} K_m(\eta)
\end{aligned}\right\} \qquad (2.29)$$

where $f_i, \theta_i, \phi_i, g_i, h_i$ and k_i are unknown functions and $F_m, \Theta_m, \Phi_m, G_m, H_m$ and K_m, $(m \geq 1)$ are successive approximations which are obtained by recursively solving the linear part of the equation system that results from substituting firstly equation (2.29) in equations (2.21)-(2.23) and (2.25)-(2.27). The main assumption of the SLM is that $f_i, \theta_i, \phi_i, g_i, h_i$ and k_i become increasingly smaller when i becomes large, that

is

$$\lim_{i\to\infty} f_i = \lim_{i\to\infty} \theta_i = \lim_{i\to\infty} \phi_i = \lim_{i\to\infty} g_i = \lim_{i\to\infty} h_i = \lim_{i\to\infty} k_i = 0. \tag{2.30}$$

The initial guesses $F_0(\eta), \Theta_0(\eta), \Phi_0(\eta), G_0(\eta), H_0(\eta)$ and $K_0(\eta)$ which are chosen to satisfy the boundary conditions (2.24) and (2.28) which are taken to be

$$\left.\begin{aligned} F_0(\eta) = 1 - e^{-\eta}, \quad \Theta_0(\eta) = e^{-\eta}, \quad \Phi_0(\eta) = e^{-\eta} \\ G_0(\eta) = 1 - e^{-\eta}, \quad H_0(\eta) = \eta e^{-\eta}, \quad K_0(\eta) = \eta e^{-\eta} \end{aligned}\right\}. \tag{2.31}$$

Thus, starting from the initial guesses, the subsequent solutions $F_i, \Theta_i, \Phi_i, G_i, H_i$ and K_i $(i \geq 1)$ are obtained by successively solving the linearised form of the equations which are obtained by substituting equation (2.29) in the governing equations (2.21)-(2.23) and (2.25)-(2.27). The linearized equations to be solved are

$$a_{1,i-1}F_i'' + a_{2,i-1}F_i' + a_{3,i-1}\Theta_i' + a_{4,i-1}\Theta_i + a_{5,i-1}\Phi_i' = r_{1,i-1}, \tag{2.32}$$

$$\begin{aligned} b_{1,i-1}\Theta_i'' \quad &+b_{2,i-1}\Theta_i' + b_{3,i-1}\Theta_i + b_{4,i-1}F_i' + b_{5,i-1}F_i + b_{6,i-1}\Phi_i + b_{7,i-1}G_i \\ +b_{8,i-1}H_i \quad &= r_{2,i-1}, \end{aligned} \tag{2.33}$$

$$\begin{aligned} c_{1,i-1}\Phi_i'' \quad &+c_{2,i-1}\Phi_i' + c_{3,i-1}F_i' + c_{4,i-1}F_i + c_{5,i-1}\Theta_i'' + c_{6,i-1}G_i + c_{7,i-1}K_i \\ &= r_{3,i-1}, \end{aligned} \tag{2.34}$$

$$\begin{aligned} d_{1,i-1}G_i'' \quad &+d_{2,i-1}G_i' + d_{3,i-1}F_i'' + d_{4,i-1}F_i' + d_{6,i-1}\Theta_i' + d_{7,i-1}\Theta_i + d_{8,i-1}\Phi_i \\ +d_{9,i-1}H_i' \quad &+d_{10,i-1}H_i + d_{11,i-1}K_i' = r_{4,i-1}, \end{aligned} \tag{2.35}$$

$$\begin{aligned} e_{1,i-1}H_i'' \quad &+e_{2,i-1}H_i' + e_{3,i-1}H_i + e_{4,i-1}F_i' + e_{6,i-1}F_i + e_{7,i-1}\Theta_i' + e_{8,i-1}\Theta_i \\ +e_{9,i-1}\Phi_i \quad &+e_{10,i-1}G_i' + e_{11,i-1}G_i + e_{11,i-1}K_i = r_{5,i-1}, \end{aligned} \tag{2.36}$$

$$\begin{aligned} q_{1,i-1}K_i'' \quad &+q_{2,i-1}K_i' + q_{3,i-1}K_i + q_{4,i-1}F_i' + q_{6,i-1}F_i + q_{7,i-1}\Phi_i' + q_{8,i-1}G_i' \\ +q_{9,i-1}G_i \quad &+q_{10,i-1}H_i'' = r_{6,i-1}, \end{aligned} \tag{2.37}$$

subject to the boundary conditions

$$\left.\begin{aligned} F_i(0) = F_i'(\infty) = \Theta_i(0) = \Theta_i(\infty) = \Phi_i(0) = \Phi_i(\infty) \\ G_i(0) = G_i'(\infty) = H_i(0) = H_i(\infty) = K_i(0) = K_i(\infty) = 0 \end{aligned}\right\}, \tag{2.38}$$

where the coefficients parameters $a_{k,i-1}, b_{k,i-1}, c_{k,i-1}, d_{k,i-1}, e_{k,i-1}, q_{k,i-1}$ and $r_{k,i-1}$ depend on $F_0(\eta)$, $\Theta_0(\eta)$, $\Phi_0(\eta)$, $G_0(\eta)$, $H_0(\eta)$ and $K_0(\eta)$ and on their derivatives. The solution for F_i, Θ_i,Φ_i, G_i, H_i and K_i for $i \geq 1$ has been found by iteratively solving equations (2.32)-(2.38) and finally after M iterations the solutions $f(\eta)$, $\theta(\eta)$, $g(\eta)$ and $h(\eta)$ can be written as

$$\left.\begin{aligned} f(\eta) \approx \sum_{m=0}^{M} F_m(\eta), \qquad \theta(\eta) \approx \sum_{m=0}^{M} \Theta_m(\eta), \qquad \phi(\eta) \approx \sum_{m=0}^{M} \Phi_m(\eta) \\ g(\eta) \approx \sum_{m=0}^{M} G_m(\eta), \qquad h(\eta) \approx \sum_{m=0}^{M} H_m(\eta), \qquad k(\eta) \approx \sum_{m=0}^{M} K_m(\eta) \end{aligned}\right\}, \tag{2.39}$$

where M is termed the order of SLM approximations. Now we apply the Chebyshev spectral collocation method to equations (2.32)-(2.38). We apply the mapping

$$\frac{\eta}{L} = \frac{\xi + 1}{2}, \qquad -1 \leq \xi \leq 1, \tag{2.40}$$

to transform the domain $[0, \infty)$ to $[-1, 1]$ where L is used to invoke the boundary condition at infinity. We discretize the domain $[-1, 1]$ using the Gauss-Lobatto collocation points defined by

$$\xi = \cos\frac{\pi j}{N}, \qquad j = 0, 1, 2, \ldots, N, \tag{2.41}$$

where N is the number of collocation points. The functions F_i, Θ_i, G_i and H_i for $i \geq 1$ are approximated at the collocation points as follows

$$\left.\begin{aligned} F_i(\xi) &\approx \sum_{k=0}^{N} F_i(\xi_k)T_k(\xi_j), \qquad \Theta_i(\xi) \approx \sum_{k=0}^{N} \Theta_i(\xi_k)T_k(\xi_j), \\ \Phi_i(\xi) &\approx \sum_{k=0}^{N} \Phi_i(\xi_k)T_k(\xi_j), \qquad G_i(\xi) \approx \sum_{k=0}^{N} G_i(\xi_k)T_k(\xi_j), \\ H_i(\xi) &\approx \sum_{k=0}^{N} H_i(\xi_k)T_k(\xi_j), \qquad K_i(\xi) \approx \sum_{k=0}^{N} K_i(\xi_k)T_k(\xi_j) \end{aligned}\right\} \quad j = 0, 1, ..., N, \tag{2.42}$$

where T_k is the k^{th} Chebyshev polynomial given by

$$T_k(\xi) = \cos\left[k \cos^{-1}(\xi)\right]. \tag{2.43}$$

The derivatives of the variables at the collocation points are

$$\left.\begin{aligned} \frac{d^r F_i}{d\eta^r} &= \sum_{k=0}^{N} \mathcal{D}_{kj}^r F_i(\xi_k), \qquad \frac{d^r \Theta_i}{d\eta^r} = \sum_{k=0}^{N} \mathcal{D}_{kj}^r \Theta_i(\xi_k), \\ \frac{d^r \Phi_i}{d\eta^r} &= \sum_{k=0}^{N} \mathcal{D}_{kj}^r \Phi_i(\xi_k), \qquad \frac{d^r G_i}{d\eta^r} = \sum_{k=0}^{N} \mathcal{D}_{kj}^r G_i(\xi_k) \\ \frac{d^r H_i}{d\eta^r} &= \sum_{k=0}^{N} \mathcal{D}_{kj}^r H_i(\xi_k), \qquad \frac{d^r K_i}{d\eta^r} = \sum_{k=0}^{N} \mathcal{D}_{kj}^r K_i(\xi_k) \end{aligned}\right\} \qquad j = 0, 1, \ldots, N, \tag{2.44}$$

where r is the order of differentiation and $\mathcal{D}$ is the Chebyshev spectral differentiation matrix whose entries are defined in (1.30). After applying the Chebyshev spectral method to (2.32)-(2.37) we get the matrix system of equations

$$\mathbf{A}_{i-1}\mathbf{X}_i = \mathbf{R}_{i-1}. \tag{2.45}$$

subject to

$$\left.\begin{array}{ll} F_i(\xi_N) = \sum_{k=0}^{N} \mathbf{D}_{0k} F_i(\xi_k) = 0 \quad , & \Theta_i(\xi_N) = \Theta_i(\xi_0) = 0, \\ \Phi_i(\xi_N) = \Phi_i(\xi_0) = 0, & G_i(\xi_N) = \sum_{k=0}^{N} \mathbf{D}_{0k} G_i(\xi_k) = 0, \\ H_i(\xi_N) = H_i(\xi_0) = 0, & K_i(\xi_N) = K_i(\xi_0) = 0 \end{array}\right\} \tag{2.46}$$

In equation (2.45), $\mathbf{A}_{i-1}$ is a $(6N+6) \times (6N+6)$ square matrix and $\mathbf{X}_i$ and $\mathbf{R}_{i-1}$ are $(6N+6) \times 1$ column vectors and $\mathbf{D} = \frac{2}{L}\mathcal{D}$. Finally the solution is obtained as

$$\mathbf{X}_i = \mathbf{A}_{i-1}^{-1} \mathbf{R}_{i-1}. \tag{2.47}$$

2.4 Results and discussion

The non-linear differential equations (2.11), (2.14) and (2.15) with the boundary conditions (2.12) were solved by means of SLM together with local non-similarity method. The value of L was suitably chosen so that the boundary conditions at the outer edge of the boundary layer are satisfied. The results obtained here are accurate up to the 5th decimal place. In order to assess the accuracy of the solution, we made a comparison between the present results and the shooting technique. The comparison is given in Tables. 2.1 - 2.2 for aiding and opposing buoyancy respectively. The results are in good agreement. In addition, a comparison between the present results and Cheng (2000) for various buoyancy values Λ and the Lewis number Le is given in Table 2.3. The comparison shows that the present results are in excellent agreement with the similarity solutions reported by Cheng (2000). The effect of selected parameters on the temperature, concentration, heat and mass transfer coefficients is given in Figures 2.3 - 2.15.

Table 2.1: A comparison of $f'(\eta)$, $\theta(\eta)$ and $\phi(\eta)$ using the SLM and the shooting method for different values of n with $Gr^* = 1$, $\gamma = 1$, $Sr = 0.1$, $Le = 1$, $V_d = 0.2$ and $\Lambda = 0.1$

Profile	η	$n = 0.5$		$n = 1$		$n = 1.5$	
		SLM	Shooting	SLM	Shooting	SLM	Shooting
$f'(\eta)$	0.0	0.873428	0.873428	0.880874	0.880874	0.889552	0.889552
	0.1	0.849364	0.849364	0.857830	0.857830	0.867668	0.867668
	0.5	0.737032	0.737031	0.753227	0.753226	0.769738	0.769737
	1.0	0.571454	0.571452	0.607662	0.607660	0.636666	0.636664
	3.0	0.060470	0.060467	0.163331	0.163329	0.228299	0.228296
	5.0	0.003483	0.003478	0.031220	0.031216	0.069212	0.069207
$\theta(\eta)$	0.0	1.000000	1.000000	1.000000	1.000000	1.000000	1.000000
	0.1	0.968618	0.968618	0.966471	0.966471	0.965157	0.965157
	0.5	0.830564	0.830563	0.820001	0.820000	0.813463	0.813462
	1.0	0.651715	0.651713	0.631992	0.631990	0.619698	0.619696
	3.0	0.182389	0.182386	0.151355	0.151352	0.133811	0.133808
	5.0	0.044543	0.044538	0.028006	0.028002	0.020251	0.020246
$\phi(\eta)$	0.0	1.000000	1.000000	1.000000	1.000000	1.000000	1.000000
	0.1	0.959835	0.959835	0.957614	0.957614	0.956246	0.956246
	0.5	0.803541	0.803540	0.792688	0.792687	0.786026	0.786025
	1.0	0.625532	0.625530	0.605186	0.605184	0.592815	0.592813
	3.0	0.190722	0.190719	0.157410	0.157407	0.139087	0.139084
	5.0	0.052304	0.052299	0.033314	0.033310	0.024326	0.024321

2.4.1 Aiding buoyancy

Non-dimensional velocity profile in the non-Darcy medium is plotted for fixed value of γ, Gr^*, Le and Λ for various values of power-law index n, viscous dissipation parameter V_d and Soret number Sr in Fig. 2.2. It is interesting to note that the value of velocity $f'(\eta)$ increases with the viscous dissipation parameter. And at the same time,

Table 2.2: A comparison of $f'(\eta)$, $\theta(\eta)$ and $\phi(\eta)$ using the SLM and shooting method for different values of n with $Gr^* = 1$, $\gamma = 1$, $Sr = 0.1$, $Le = 1$, $V_d = 0.2$ and $\Lambda = -0.1$

Profile	η	$n = 0.5$		$n = 1$		$n = 1.5$	
		SLM	Shooting	SLM	Shooting	SLM	Shooting
$f'(\eta)$	0.0	0.764833	0.764833	0.782413	0.782413	0.798435	0.798435
	0.1	0.743531	0.743531	0.762209	0.762209	0.779301	0.779301
	0.5	0.645119	0.645120	0.671441	0.671442	0.694426	0.694427
	1.0	0.501380	0.501382	0.546064	0.546065	0.579579	0.579581
	3.0	0.059274	0.059277	0.156714	0.156717	0.218972	0.218975
	5.0	0.004132	0.004137	0.032827	0.032831	0.070303	0.070308
$\theta(\eta)$	0.0	1.000000	1.000000	1.000000	1.000000	1.000000	1.000000
	0.1	0.969520	0.969520	0.966868	0.966868	0.965272	0.965272
	0.5	0.838804	0.838805	0.825639	0.825640	0.817649	0.817650
	1.0	0.672016	0.672018	0.647144	0.647146	0.632019	0.632021
	3.0	0.215386	0.215389	0.174526	0.174529	0.152120	0.152124
	5.0	0.060882	0.060888	0.037109	0.037114	0.026308	0.026314
$\phi(\eta)$	0.0	1.000000	1.000000	1.000000	1.000000	1.000000	1.000000
	0.1	0.963281	0.963281	0.960520	0.960520	0.958848	0.958848
	0.5	0.819788	0.819789	0.806293	0.806294	0.798146	0.798147
	1.0	0.654319	0.654321	0.628954	0.628956	0.613793	0.613795
	3.0	0.226430	0.226434	0.183431	0.183435	0.160206	0.160210
	5.0	0.070796	0.070802	0.044052	0.044056	0.031686	0.031693

an increase in the value of Soret number increases the velocity distribution inside the boundary layer for all values of power-law index n. Figures 2.3(a)-2.3(b) show the variation of the non-dimensional temperature $\theta(\eta)$ and concentration $\phi(\eta)$ distributions for $n = 0.5$, $n = 1$ and $n = 1.5$ and two different values of viscous dissipation V_d and for fixed values of γ, Gr^*, Sr, Le and Λ. We observed that the increasing in viscous dissipation and power-low index decrease the dimensionless temperature and concentration distributions. This is because there would be a decrease of the thermal

Table 2.3: Comparison of the local Nusselt and Sherwood numbers between the current results and Cheng (2000) for various values of Λ and Le when $n = 1$,$Gr^* = 0$, $\gamma = 0$, $Sr = 0$, and $V_d = 0$.

		$\theta'(0)$		$\phi'(0)$	
Λ	Le	Cheng (2000)	Present	Cheng (2000)	Present
4	1	0.9923	0.9923	0.9923	0.9923
4	4	0.7976	0.7976	2.055	2.0549
4	10	0.6811	0.681	3.2899	3.2897
4	100	0.5209	0.521	10.521	10.5222
1	4	0.5585	0.5585	1.3575	1.3575
2	4	0.6494	0.6495	1.6243	1.6244
3	4	0.7278	0.7277	1.8525	1.8524

and concentration boundary layer thicknesses with the decrease of values of viscous dissipation and n. The effect of Soret parameter Sr on temperature and concentration profiles is shown in Figure 2.4. It is noted that the Soret parameter reduces the temperature distribution while enhancing the concentration distribution. This is because there would be a decrease in the thermal and increase in the concentration boundary layer thicknesses with the increase of values of Sr. In Fig. 2.5 variation of the skin-friction coefficient as a function of power-law index n is shown for different values of Sr, V_d and γ with fixed value of Gr^*, Le and Λ. From this figure, a decrease in $f''(0)$ is evident with increasing values of Sr and V_d for all values n. In other hand the skin-friction coefficient increases with increasing the non-dimensional viscosity parameter γ. The effect of the viscous dissipation parameter V_d on the Nusselt and Sherwood numbers varying n for different values of Sr and γ are shown in Figure 2.6 and Figure 2.7 respectively. An increasing of the viscous dissipation and the power-law index enhancing the heat and mass transfer coefficients for all Sr and γ.

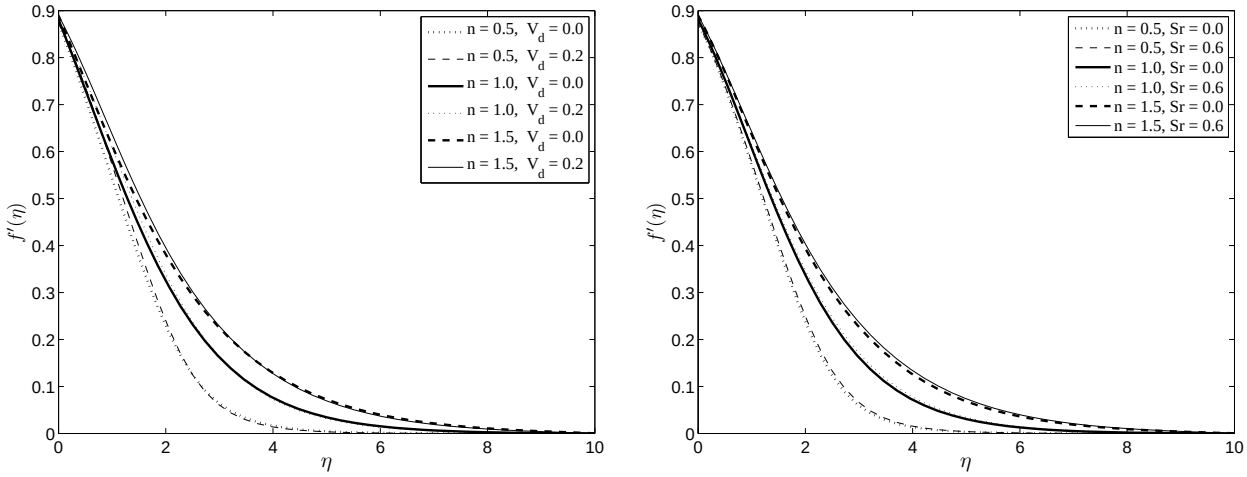

(a) (b)

Figure 2.2: Variation of (a) V_d and (b) Sr on $f'(\eta)$ against η varying n when $\gamma = 1, Gr^* = 1, Le = 1$ and $\Lambda = 0.1$.

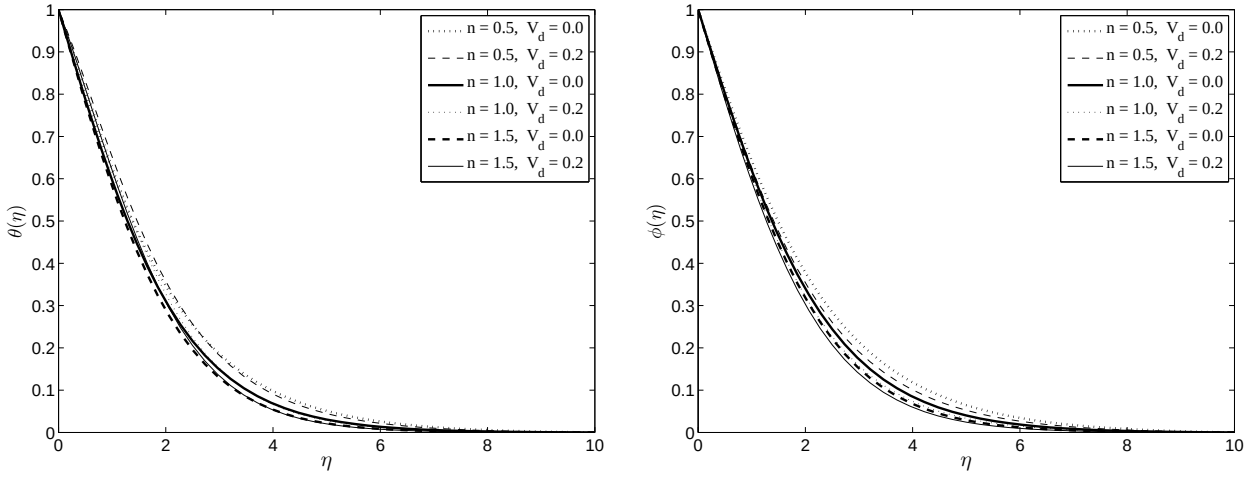

(a) (b)

Figure 2.3: Variation of (a) $\theta(\eta)$ and (b) $\phi(\eta)$ against η varying V_d and n when $\gamma = 1, Gr^* = 1, Sr = 0.1, Le = 1$ and $\Lambda = 0.1$.

The variation of the Nusselt and Sherwood numbers as a function of Sr are given in Figure 2.8 for different values of n and viscous dissipation parameter V_d. Increasing the Soret number increases the heat transfer rate for all power-law indices while reducing the mass transfer rate. This is because, either a decrease in concentration difference or an increases in temperature difference leads to an increase in the value

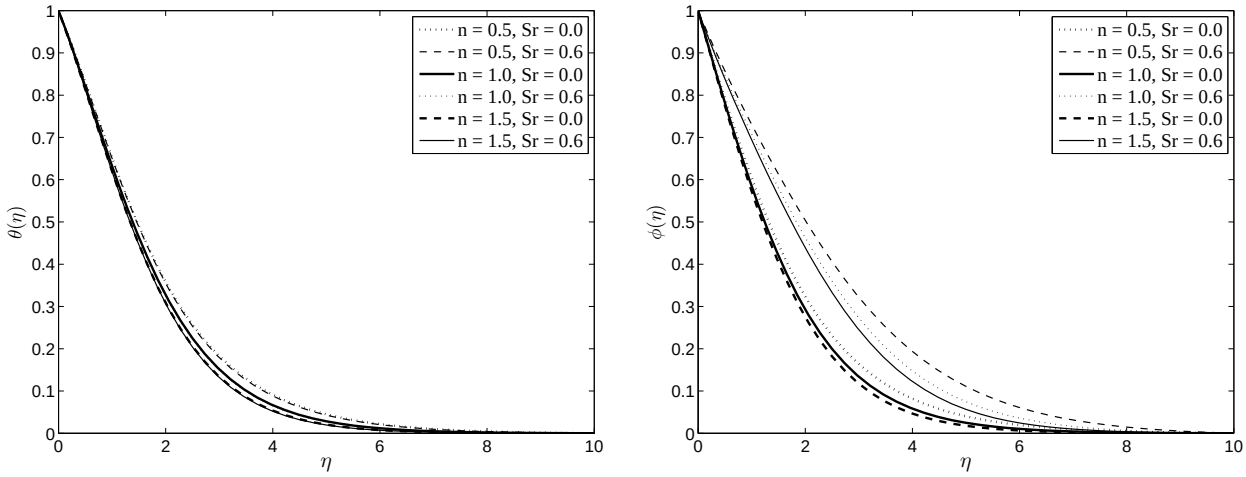

(a) (b)

Figure 2.4: Variation of (a) $\theta(\eta)$ and (b) $\phi(\eta)$ against η varying Sr and n when $\gamma = 1, Gr^* = 1, V_d = 0.2, Le = 1$ and $\Lambda = 0.1$.

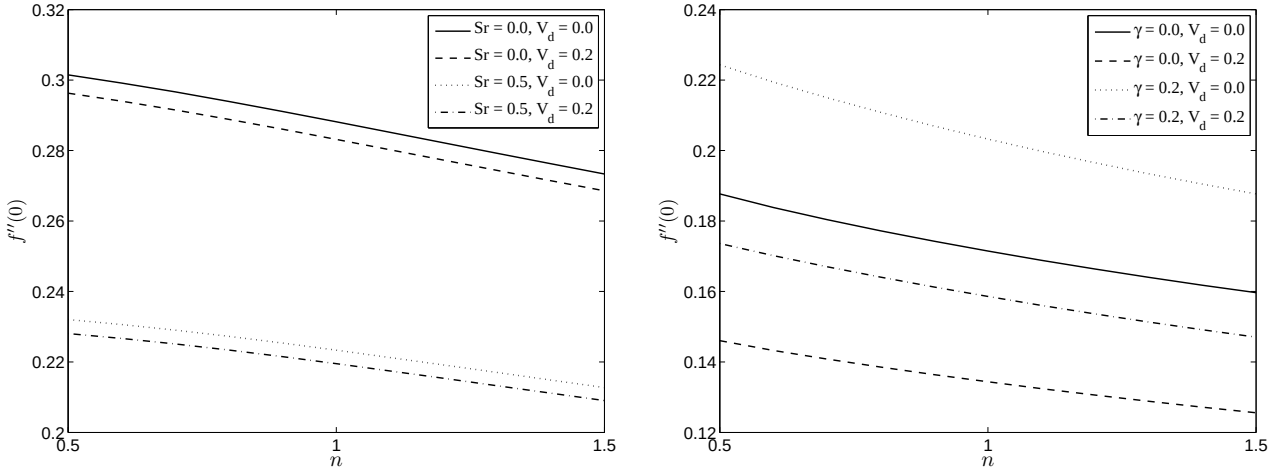

(a) (b)

Figure 2.5: Variation of $f''(0)$ against n varying (a) V_d and (b) Sr when $\gamma = 1, Gr^* = 1, Le = 1$ and $\Lambda = 0.1$.

of the Soret parameter

Figure 2.9 shows the variation of the Nusselt and Sherwood numbers with the viscosity parameter γ. Increasing the viscosity parameter increases the rates of heat and mass transfer for all values of V_d and power-low index n. Similar results were obtained by Jayanthi et al. (2007) and Kairi et al. (2011b).

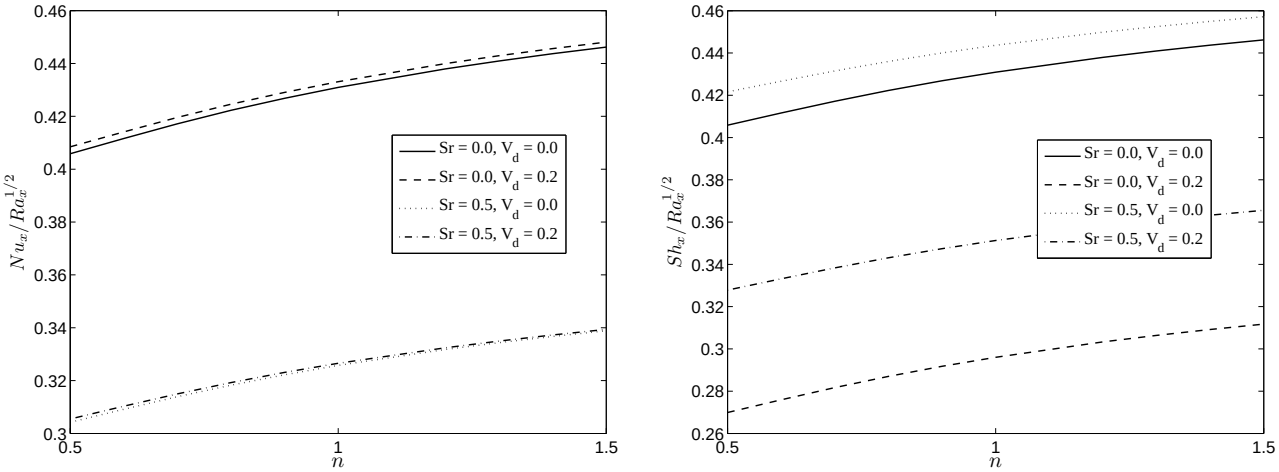

(a) (b)

Figure 2.6: Variation of (a) heat transfer and (b) mass transfer coefficients against V_d varying Sr and n when $\gamma = 1, Gr^* = 1, Le = 1$ and $\Lambda = 0.1$

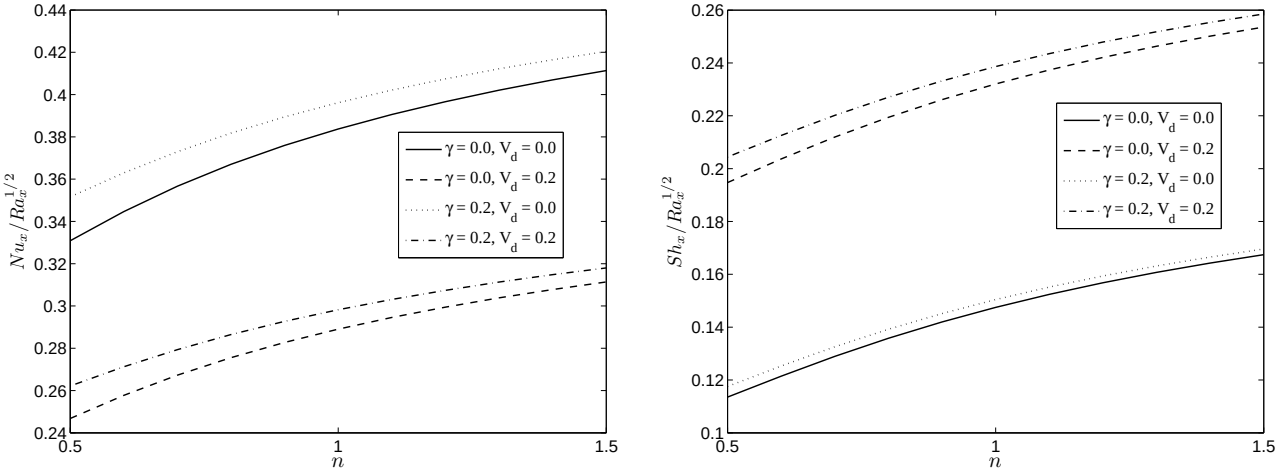

(a) (b)

Figure 2.7: Variation of (a) heat transfer and (b) mass transfer coefficients against V_d varying γ and n when $Sr = 1, Gr^* = 1, Le = 1$ and $\Lambda = 0.1$

2.4.2 Opposing buoyancy

Figure 2.10 shows the temperature and concentration distributions when $n = 0.5$, $n = 1$ and $n = 1.5$ for $V_d = 0$ and 0.2. We observed that, the increasing of V_d reduced the thermal and concentration disruptions for all values of n. The reason for this,

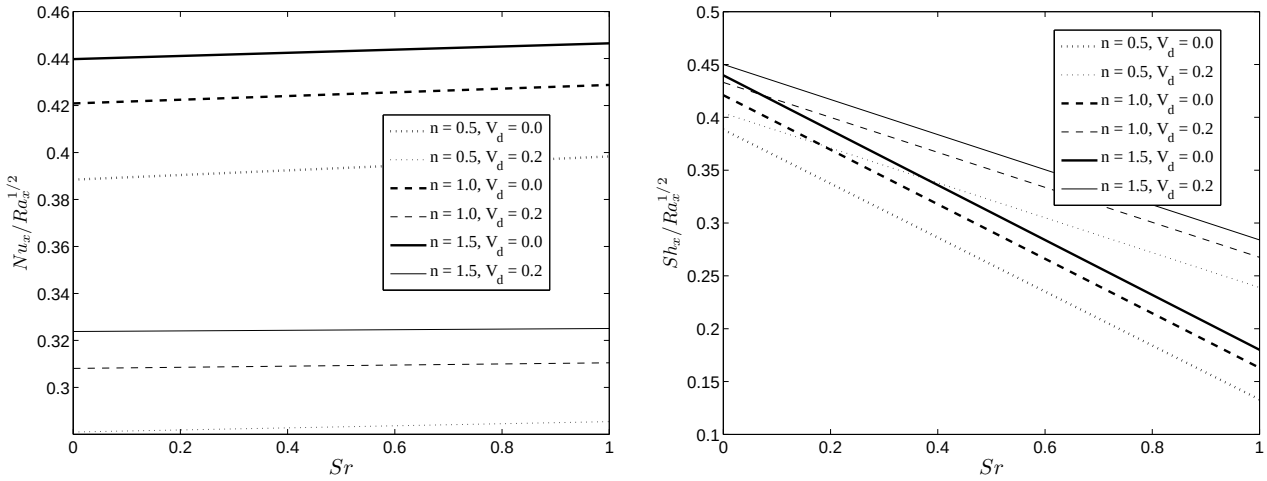

(a) (b)

Figure 2.8: Variation of (a) heat transfer and (b) mass transfer coefficients against Sr varying V_d and n when $\gamma = 0.5, Gr^* = 1, Le = 1$ and $\Lambda = 0.2$

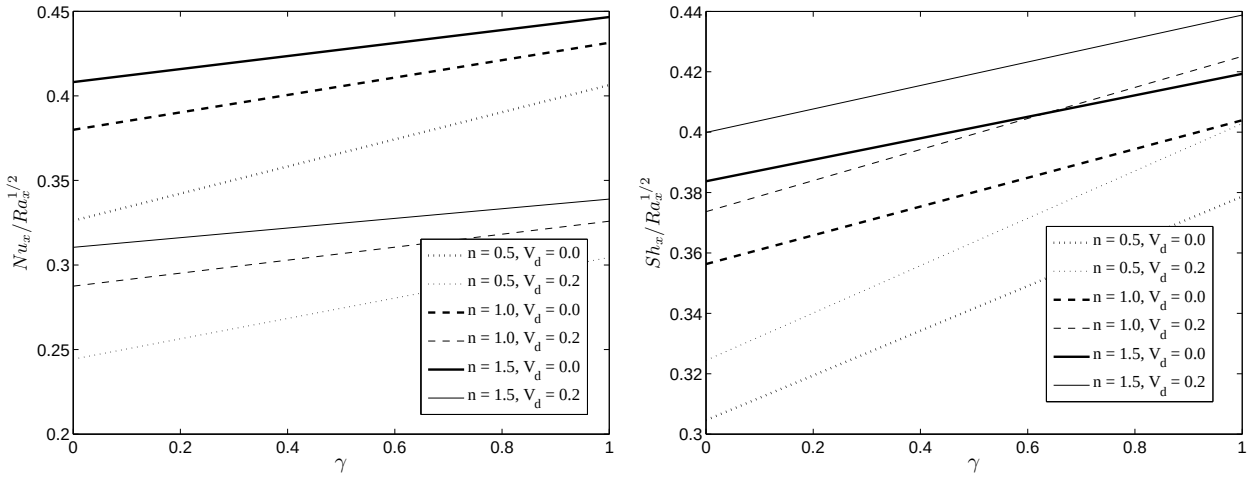

(a) (b)

Figure 2.9: Variation of (a) heat transfer and (b) mass transfer coefficients against γ varying V_d and n when $Sr = 0.1, Gr^* = 1, Le = 1$ and $\Lambda = 0.1$

because there would be a decrease of the thermal and concentration boundary layer thicknesses with the decrease of values of viscous dissipation.

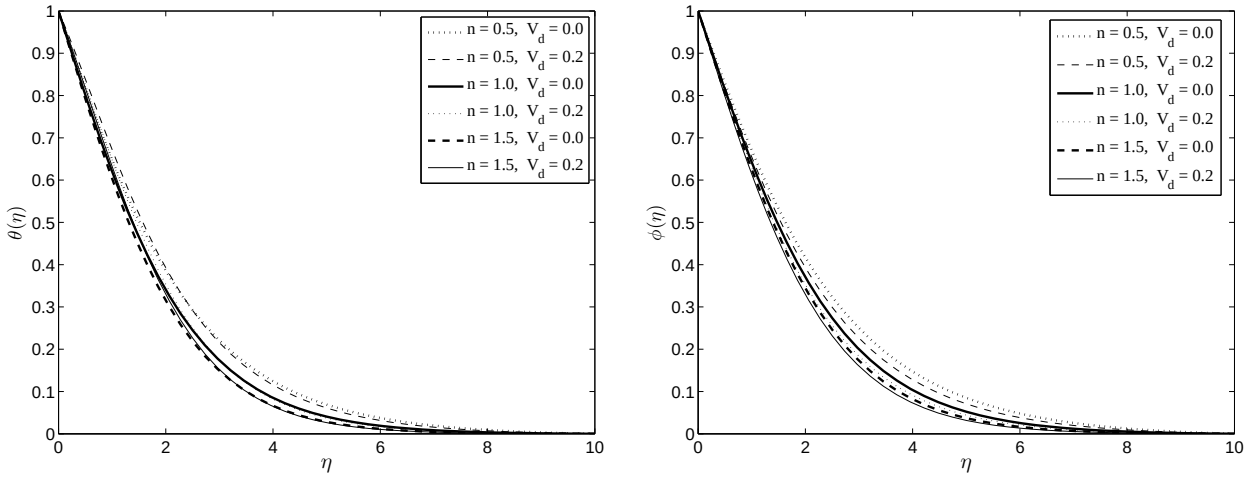

(a) (b)

Figure 2.10: Variation of (a) $\theta(\eta)$ and (b) $\phi(\eta)$ against η varying V_d and n when $\gamma = 1, Gr^* = 1, Sr = 0.1, Le = 1$ and $\Lambda = -0.1$.

The effect of the Soret parameter on the temperature and concentration distributions in Figures 2.11(a) - 2.11(b) for different values on the power-law index n. Soret number has increasing effects on the temperature and concentration distributions. This is because there would be a decrease of the thermal and concentration boundary layer thicknesses with the increase of values of Sr.

In Figure 2.12 - 2.13, the variation of $Nu_x/Ra_x^{1/2}$ and $Sh_x/Ra_x^{1/2}$ (respectively) as a function of V_d are shown for different types of power-law fluids and two values of Sr and γ while the other parameters are fixed. We note that an increasing V_d increases $Nu_x/Ra_x^{1/2}$ and $Sh_x/Ra_x^{1/2}$ in the presence or absence of Sr or γ.

The variation of the Nusselt and Sherwood numbers as a functions of Sr is displayed in Figure 2.14 for different values of n and V_d. We observed that both Nusselt and Sherwood numbers decreased with increasing in the Soret number.

Increasing the viscosity parameter γ enhances the rates of heat and mass transfer

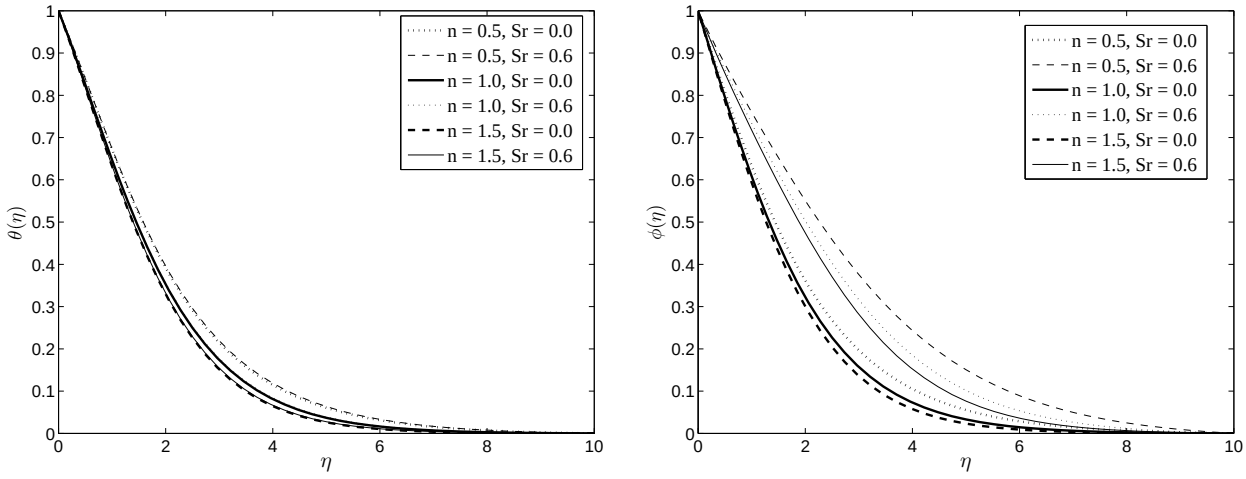

(a) (b)

Figure 2.11: Variation of (a) $\theta(\eta)$ and (b) $\phi(\eta)$ against η varying Sr and n when $\gamma = 1, Gr^* = 1, V_d = 0.2, Le = 1$ and $\Lambda = -0.1$.

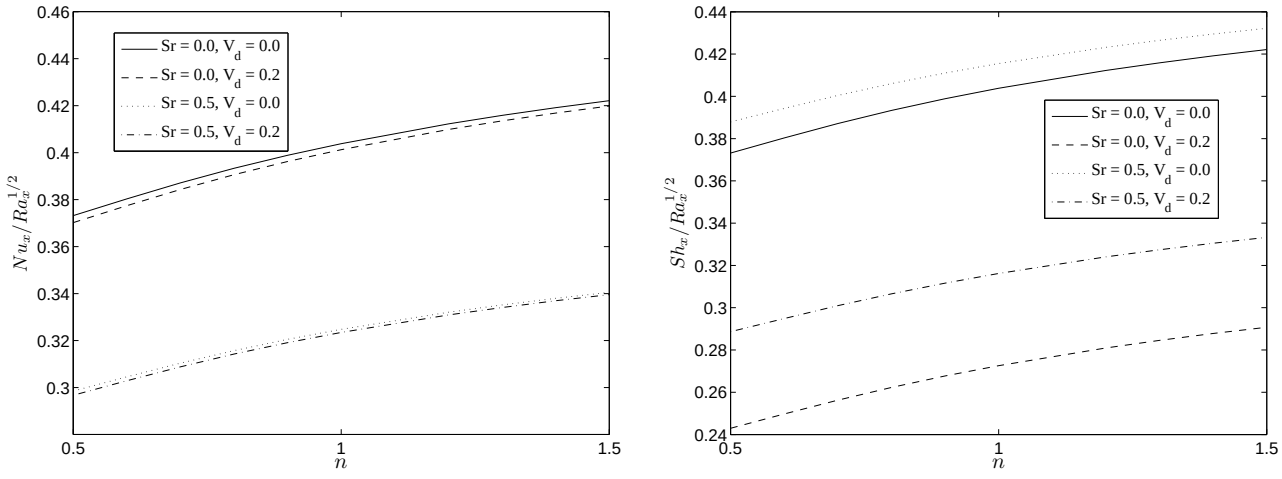

(a) (b)

Figure 2.12: Variation of (a) heat transfer and (b) mass transfer coefficients against V_d varying Sr and n when $\gamma = 1, Gr^* = 1, Le = 1$ and $\Lambda = -0.1$

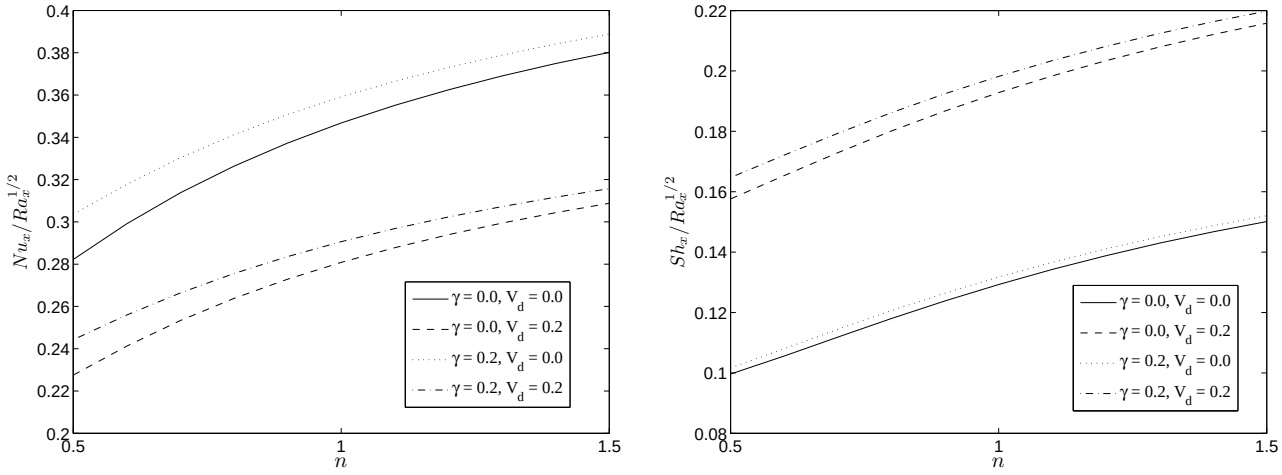

(a) (b)

Figure 2.13: Variation of (a) heat transfer and (b) mass transfer coefficients against V_d varying γ and n when $Sr = 1, Gr^* = 1, Le = 1$ and $\Lambda = -0.1$

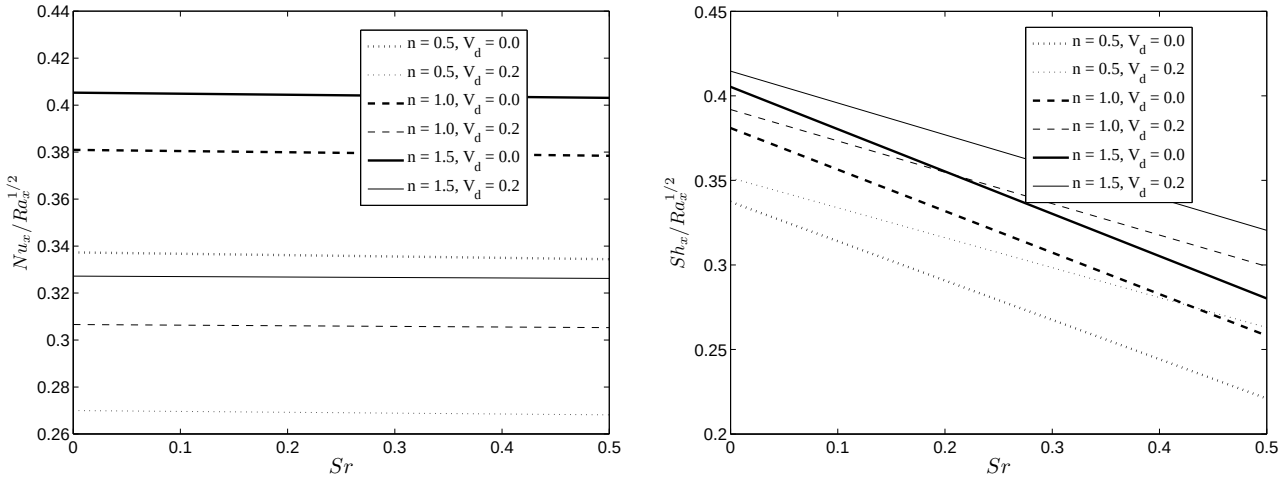

(a) (b)

Figure 2.14: Variation of (a) heat transfer and (b) mass transfer coefficients against Sr varying V_d and n when $\gamma = 0.5, Gr^* = 1, Le = 1$ and $\Lambda = -0.2$

coefficients for two values of V_d and all types of power-law fluids n as shown in Figure 2.15. This is also in line with the findings by Jayanthi et al. (2007) and Kairi et al. (2011b).

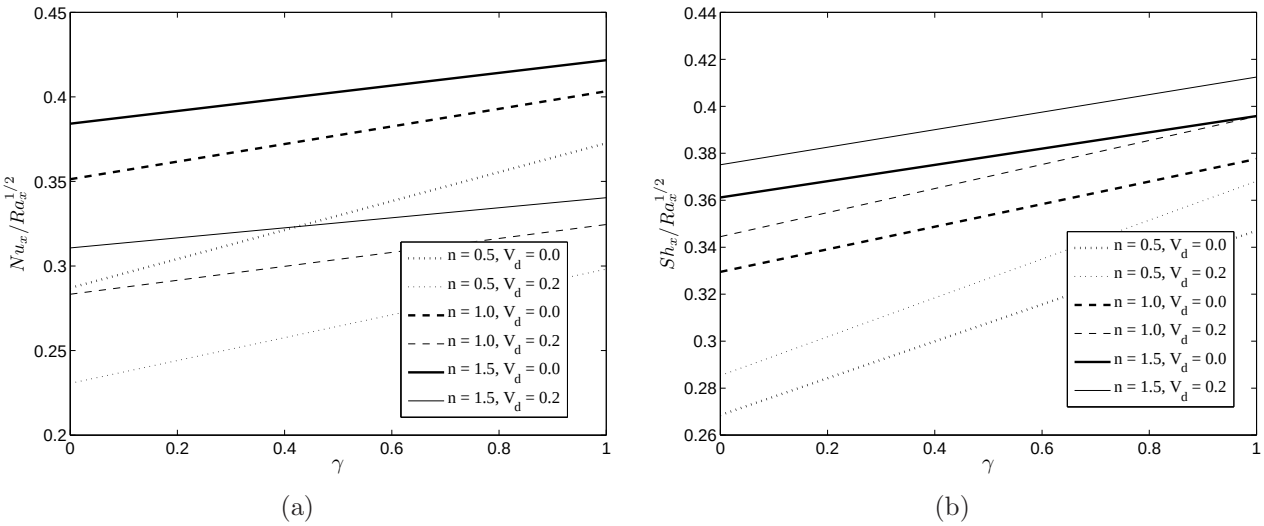

(a) (b)

Figure 2.15: Variation of (a) heat transfer and (b) mass transfer coefficients against γ varying V_d and n when $Sr = 0.1, Gr^* = 1, Le = 1$ and $\Lambda = -0.1$

2.5 Conclusions

We have investigated viscous dissipation and the Soret effects on natural convection from a vertical plate immersed in a power-law fluid saturated non-Darcy porous medium. The governing equations are transformed into ordinary differential equations and solved using the SLM. Qualitative results were presented showing the effects of various physical parameters on the fluid properties and the rates of heat and mass transfer. Velocity and temperature profiles are significantly affected by viscous dissipation, Soret number and variable viscosity parameters. The Nusselt and Sherwood numbers are enhanced by viscous dissipation for both cases $\Lambda > 0$ and $\Lambda < 0$. The Nusselt number increased by Soret number for aiding buoyancy case and decreased for opposing buoyancy case. The Sherwood number decreased by Soret number for $\Lambda > 0$

and $\Lambda < 0$. The viscosity parameter γ enhances heat and mass transfer coefficients in both cases of aiding buoyancy and opposing buoyancy.

Chapter 3

Soret effect on the natural convection from a vertical plate in a thermally stratified porous medium saturated with non-Newtonian liquid*

Abstract

The chapter analyzes the Soret effect on the free convection flow due to a vertical plate embedded in a non-Darcy thermally stratified porous medium saturated with a non-Newtonian power-law with variable viscosity. The Ostwald -de Waele power-law model is used to characterize the non-Newtonian behavior of the fluid. The governing

[0]* Under review; Journal of Heat Transfer-Transactions of ASME (March 2012).

partial differential equations are transformed into a system of ordinary differential equations and solved numerically using the SLM. The accuracy of the SLM has been tested by comparing the results with those obtained using the shooting technique. The effect of various physical parameters such as power-law index, Soret number, variable viscosity parameter and thermal stratification parameter on the dynamics of the fluid are analyzed through computed results. Heat and mass transfer coefficients are also shown graphically for different values of the parameters.

3.1 Introduction

The problem of natural convection heat and mass transfer from bodies immersed in thermally stratified fluid saturated porous medium arises in many important applications. Free convection in an enclosed rectangular cell filled with some fluid saturated porous medium with one wall heated and the other cooled gives rise to an important engineering application of thermal stratification. In such an application a stratified environment is created inside the cell by the heated fluid rising from the hot wall and the cool fluid falling from the cold wall. This process repeats and the hot fluid layer at the top of the cell always overlay the cold one at the bottom creating a stable stratified environment. A stratified environment can also be observed in nature in the form of atmospheric and lake stratification where different layers exhibit different temperatures. Other applications include thermal insulation, the enhanced recovery of petroleum resource, power production from geothermal resources and the design of nuclear reactors.

Early studies by Bejan (1984), Nakayama and Koyama (1987b) and Takhar and Pop (1987) deal with thermal stratification in a Darcian porous medium. The study of convective heat transfer in a porous medium in non-Newtonian fluids is of particular relevance as a number of industrially important fluids such as molten plastics, poly-

mers, pulps and slurries display non-Newtonian fluid behaviour. Tewari and Singh (1992) and Singh and Tewari (1993) investigated natural convection in a thermally stratified fluid saturated Darcy/non-Darcy porous media. They used a model proposed by Ergun (1952) in the study to include the inertia effect. They found that the heat transfer is significantly affected by the modified Grashof number and the stratification parameter. Shenoy (1994) presented many interesting applications of non-Newtonian power-law fluids with yield stress on convective heat transport in fluid saturated porous media such as in geothermal and oil reservoir engineering applications.

Natural convection from bodies of different geometrical shapes immersed in a non-Newtonian fluid saturated porous medium have been investigated by Chen and Chen (1988a,b) and Nakayama and Koyama (1991). Chamka (1997a,b) investigated hydromagnetic natural convection from a vertical/inclined surface adjacent to a thermally stratified porous medium. Non-Darcy free convection along a non-isothermal vertical surface in a thermally stratified porous medium with/with out heat flux was considered by Hung and Chen (1997) and Hung and Chen (1999), they showed in their studied cases, that the Darcy model always over-predicted the heat transfer rate with or without consideration of the thermal stratification effects. The non-Darcy free convection from a vertical cylinder embedded in a thermally stratified porous medium has been discussed by Chen and Horng (1999). They showed that the non-Darcy flow phenomena alters the flow and heat transfer characteristics significantly and also the thermal dispersion tends to enhance the heat transfer. The study of natural convection flow on a vertical isothermal thin cylinder embedded in a thermally stratified high porosity porous medium has been considered by Takhar et al. (2002). They showed that for certain values of the thermal stratification parameter, the wall of the cylinder gets heated instead of being cooled (i.e., the direction of the heat transfer changes). Ishak et al. (2008) theoretically studied the similarity solutions of the mixed convection boundary layer flow over a vertical surface embed-

ded in a thermally stratified porous medium. They assumed the external velocity and surface temperature to vary as x^m and found dual solutions in case of opposing flow ($m = 0$) and assisting flow ($m = 1$) regimes. Heat and mass transfer by natural convection along a vertical plate in a micropolar fluid saturated non-Darcy porous medium has been investigated by Srinivasacharya and RamReddy (2010). They observed that higher values of the coupling number result in lower velocity distribution but higher temperature, concentration distributions in the boundary layer compared to the Newtonian fluid case.

The problem of double diffusion from a vertical frustum of a wavy cone in porous media saturated with non-Newtonian power-law fluids with thermal and mass stratification has been discussed by Cheng (2008). His results show that the streamwise distributions of the local Nusselt number and the local Sherwood number are harmonic curves with a wave number twice the wave number of the surface of the vertical wavy truncated cone. Further, a smaller power-law index of the non-Newtonian fluid leads to a greater fluctuation of the local Nusselt and Sherwood numbers. Unsteady free convection along an infinite vertical flat plate embedded in a stably stratified fluid-saturated porous medium has been investigated by Magyari et al. (2006). They arrived at analytical solutions of the Darcy and energy equations by reducing the corresponding boundary value problem to a well-known Fourier heat conduction problem.

Kairi and Murthy (2009a) considered free convection in a thermally stratified non-Darcy porous medium saturated with a non-Newtonian fluid. They have arrived at similarity solution of the problem by assuming a specific power function form for the wall temperature and medium stratification. Free convective heat and mass transfer in a doubly stratified non-Darcy porous medium has been investigate by Narayana and Murthy (2006). As an important result of their investigation Narayana and Murthy (2006) have obtained the values of the governing parameters for which the

temperature and concentration profiles as well as the nondimensional heat and mass transfer coefficients behave abnormally. The analysis of the natural convective heat and mass transfer induced by a constant heat and mass fluxes vertical wavy wall in a non-Darcy double stratified porous medium has been discussed recently by Maria (2011). The results show that the greater influence on the natural convection process, on the temperature, concentration and stream function fields can be attributed to the thermal and mass stratification coefficients along with the buoyancy ratio.

Fluid properties such as viscosity and diffusivity are prone to vary with temperature, especially in the boundary layer region. So a model that incorporates variable fluid properties is often superior to one that assumes constant properties. In view of this many researchers have included variable fluid properties in the governing equations. Jayanthi and Kumari (2007) and Kairi et al. (2011b) considered the variable fluid properties to study the non-Newtonian natural convection from vertical surfaces embedded in porous medium. Jayanthi and Kumari (2007) used the reciprocal $\mu - T$ relation while Kairi et al. (2011b) used the exponential variation of viscosity with temperature and they both have showed that variable viscosity enhances the heat transfer. Effects of variable viscosity on non-Darcy MHD free convection along a non-isothermal vertical surface in a thermally stratified porous medium has been reported by Afify (2007). Using a reciprocal model for variable viscosity he showed that variable viscosity increases local Nusselt number. Makinde and Aziz (2010) investigated the effect of convective boundary condition on hydromagnetic mixed convection with heat and mass transfer from a vertical plate in a porous medium. They showed that the convective heat transfer parameter enhances both fluid velocity and temperature profile.

Though heat and mass transfer happen simultaneously in a moving fluid, the relations between the fluxes and the driving potentials are generally complicated. It should be noted that the energy flux can be generated by both temperature and

composition gradients. The energy flux caused by a composition gradient gives rise to the Dufour or diffusion-thermo effect. Mass fluxes created by temperature gradient lead to the Soret or thermal-diffusion effect. These effects are in collective known as cross-diffusion effects. In liquids the Dufour effect is negligibly small compared to the Soret effect. Kairi and Murthy (2011b) have investigated the Soret effects on the natural convection heat and mass transfer from vertical cone in a non-Newtonian fluid saturated non-Darcy porous medium in the presence of viscous dissipation. Their results show that in case of aiding buoyancy the Nusselt number is increased with Soret number up to some value of the dissipation parameter and decreased thereafter while in case of opposing buoyancy Nusselt number is decreased with Soret number for all values of dissipation parameter. Also, the Sherwood number is reduced with Soret number in both aiding and opposing buoyancy cases. Dufour effects on free convection heat and mass transfer in a doubly stratified Darcy porous medium was considered by Narayana and Murthy (2007). They reported similarity solutions for the case of constant heat and mass flux conditions when thermal and solutal stratification of the medium are assumed to vary in the power function as $x^{1/3}$. Further, they noted that for large differences between the values of cross-diffusion and double stratification parameters may lead to changes in the sign of the temperature and concentration fields. Mansour et al. (2008) investigated the effects of chemical reaction and thermal stratification on MHD free convective heat and mass transfer over a vertical stretching surface embedded in a porous media considering cross-diffusion effects. They observed reduction in the temperature and concentration distributions with decreases values of Soret number and increases values of Dufour number.

The present chapter aims to study the Soret effect on the free convection from a vertical plate in a thermally stratified non-Darcy porous medium saturated with non-Newtonian fluid possessing variable viscosity property. The viscosity variation is modeled using Reynolds' law, which assumes that viscosity decreases exponentially with temperature. We solve the nonlinear boundary value problem arising from the

non-dimensionalization and the application of a local non-similarity method using a novel SLM.

3.2 Governing equations

Consider the steady, laminar, two-dimensional natural convection boundary layer flow over a finite vertical flat plate embedded in a non-Darcy porous medium saturated with a non-Newtonian power-law fluid with variable viscosity. Figure 3.1 shows the physical configuration of the problem under consideration.

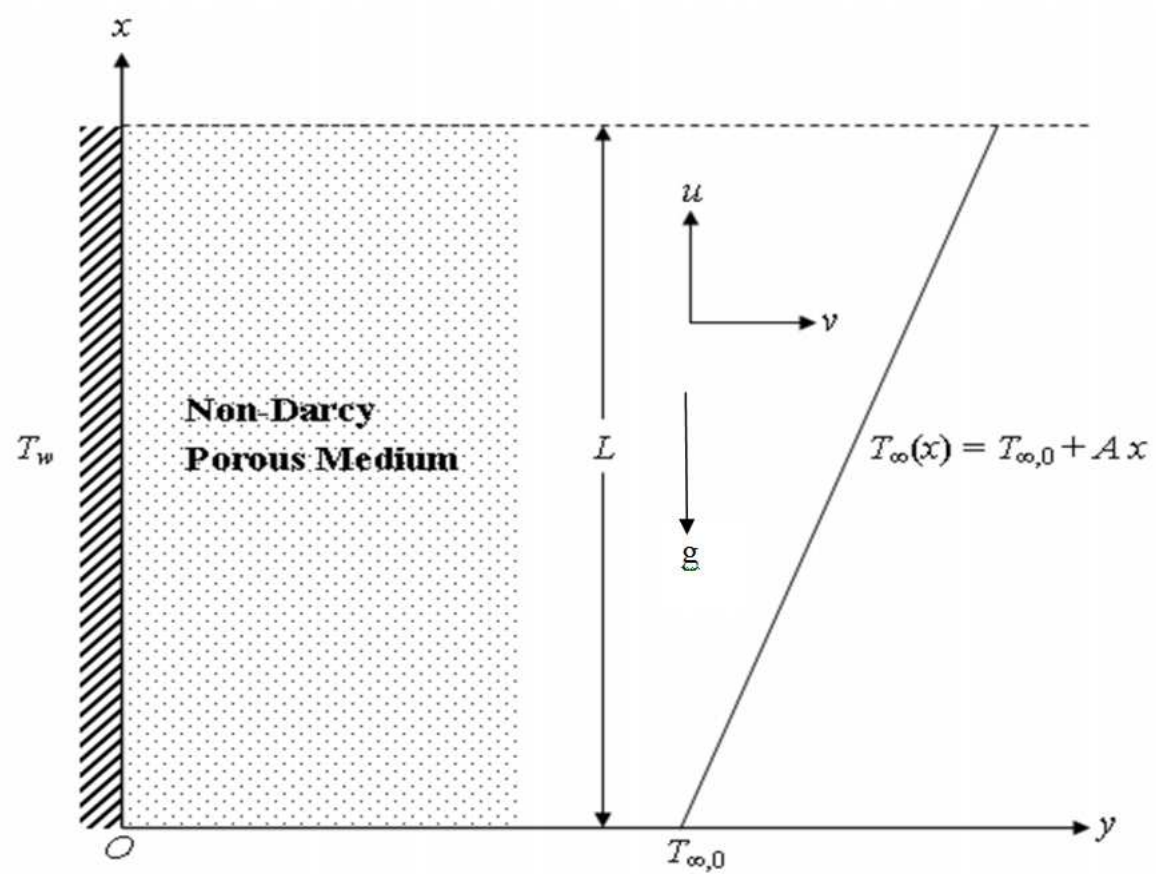

Figure 3.1: Physical configuration of the problem under study

The x-coordinate is measured along the plate from its leading edge and the y-

coordinate normal to the plate. The plate is at uniform temperature T_w and the ambient temperature T_∞ increases linearly with height. It is assumed to be of the form

$$T_\infty(x) = T_{\infty,0} + Ax \tag{3.1}$$

where $A = dT_\infty/dx$ is the slope of the ambient temperature profile and $T_{\infty,0}$ is the ambient temperature at $x = 0$. We restrict our analysis to only positive values of A corresponding to a stable, stratified ambient fluid. Assuming that; (i) the temperature of the plate at any point x exceeds the surrounding temperature, i.e., $T_w > T_\infty$, (ii) the convective fluid and the porous medium are everywhere in local thermodynamic equilibrium, (iii) the properties of the fluid (except the dynamic viscosity) and the porous medium are constant and following the usual boundary layer and Boussinesq approximations the governing equations may be written as (see Shenoy 1994);

$$\frac{\partial u}{\partial x} + \frac{\partial v}{\partial y} = 0, \tag{3.2}$$

$$\frac{\partial}{\partial y}\left(\frac{\mu}{\rho_\infty K^*}u^n\right) + \frac{\partial}{\partial y}\left(bu^2\right) = \mathrm{g}\left(\beta\frac{\partial T}{\partial y} + \beta^*\frac{\partial C}{\partial y}\right), \tag{3.3}$$

$$u\frac{\partial T}{\partial x} + v\frac{\partial T}{\partial y} = \alpha\frac{\partial^2 T}{\partial y^2}, \tag{3.4}$$

$$u\frac{\partial C}{\partial x} + v\frac{\partial C}{\partial y} = D\frac{\partial^2 C}{\partial y^2} + D_1\frac{\partial^2 T}{\partial y^2}, \tag{3.5}$$

where u and v are the average velocity components along the x and y directions, respectively, μ is the consistency index of the power-law fluid, ρ_∞ is the reference density, b is the empirical constant associated with the Forchheimer porous inertia term, g is the acceleration due to gravity, T is the fluid temperature, C is the solutal concentration, β and β^* are respectively the coefficients of thermal and solutal expansions, α is the effective thermal diffusivity, D is the solutal diffusivity, D_1 is the Soret coefficient that quantifies the contribution to the mass flux due to temperature gradient and n is the power-law index with $n < 1$ representing a pseudoplastic, $n = 1$ a Newtonian fluid and $n > 1$ a dilatant fluid respectively. Following Christopher and

Middleman (1965) and Dharmadhikari and Kale (1985), the modified permeability K^* of the non-Newtonian power-law fluid is defined as

$$K^* = \frac{1}{c_t}\left(\frac{n\varphi}{3n+1}\right)^n \left(\frac{50K}{3\varphi}\right)^{\frac{n+1}{2}} \qquad \text{where} \qquad K = \frac{\varphi^3 d^2}{150(1-\varphi)^2}$$

where φ is the porosity of the medium, d is the particle size and the constant c_t is given by

$$c_t = \begin{cases} \frac{25}{12} \quad (\text{for } n=1) & \text{Christopher and Middleman (1965)} \\ \frac{3}{2}\left(\frac{8n}{9n+3}\right)^n \left(\frac{10n-3}{6n+1}\right)\left(\frac{75}{16}\right)^{\frac{3(10n-3)}{10n+11}} & \text{Dharmadhikari and Kale (1985)} \end{cases}$$

The boundary conditions for solving equations (3.2) - (3.5) are taken to be

$$\left.\begin{array}{llll} v=0, & T=T_w, & C=C_w & \text{at} \quad y=0, \\ u\to 0, & T\to T_\infty(x), & C\to C_\infty & \text{as} \quad y\to\infty. \end{array}\right\} \tag{3.6}$$

The system of non-similar partial differential equations can be arrived at by using the stream function formulation where

$$u = \frac{\partial\psi}{\partial y} \qquad \text{and} \qquad v = -\frac{\partial\psi}{\partial x}, \tag{3.7}$$

together with the transformations

$$\left.\begin{array}{l} \eta = Ra_x^{1/2}\dfrac{y}{x}, \qquad \psi(\varepsilon,\eta) = \alpha Ra_x^{1/2} f(\varepsilon,\eta), \\ \theta(\varepsilon,\eta) = \dfrac{T-T_\infty(x)}{T_w - T_{\infty,0}} \qquad \text{and} \qquad \phi(\varepsilon,\eta) = \dfrac{C-C_\infty}{C_w - C_\infty} \end{array}\right\}, \tag{3.8}$$

where, $Ra_x = \left(\dfrac{x}{\alpha}\right)\left[\dfrac{\rho_\infty K^* \mathrm{g}\beta(T_w - T_{\infty,0})}{\mu_\infty}\right]^{1/n}$ is the local Rayleigh number and $\varepsilon = \dfrac{Ax}{T_w - T_{\infty,0}}$ is the local stratification parameter. The fluid viscosity obeying Reynolds viscosity model is given by

$$\mu(\theta) = \mu_\infty e^{-\gamma\theta}, \tag{3.9}$$

where γ is the non-dimensional viscosity parameter depending on the nature of the fluid and μ_∞ is the ambient viscosity of the fluid. With the introduction of stream function given in (3.7), the continuity equation (3.2) is automatically satisfied. Now, using the transformations (3.8) along with viscosity model given in (3.9), the momentum, energy and mass balance equations, (3.3) - (3.5) respectively, are reduced to the following partial differential equations:

$$\left[n(f')^{n-1} + 2Gr^* e^{\gamma\theta} f'\right] f'' = (\theta' + \Lambda\phi')e^{\gamma\theta} + \gamma(f')^n\theta', \tag{3.10}$$

$$\theta'' + \frac{1}{2}f\theta' - \varepsilon f' = \varepsilon\left(f'\frac{\partial\theta}{\partial\varepsilon} - \theta'\frac{\partial f}{\partial\varepsilon}\right), \tag{3.11}$$

$$\frac{1}{Le}\phi'' + \frac{1}{2}f\phi' + Sr\theta'' = \varepsilon\left(f'\frac{\partial\phi}{\partial\varepsilon} - \phi'\frac{\partial f}{\partial\varepsilon}\right), \tag{3.12}$$

The transformed boundary conditions are

$$\left.\begin{array}{llllll} f(\varepsilon,\eta) = 0, & \theta(\varepsilon,\eta) = 1-\varepsilon & \phi(\varepsilon,\eta) = 1 & \text{at} & \eta = 0 \\ f'(\varepsilon,\eta) \to 0, & \theta(\varepsilon,\eta) \to 0 & \phi(\varepsilon,\eta) \to 0 & \text{as} & \eta \to \infty \end{array}\right\}, \tag{3.13}$$

where $Gr^* = b\left[\dfrac{\rho_\infty^2 K^{*2}\left\{\mathbf{g}\beta(T_w - T_{\infty,0})\right\}^{2-n}}{\mu_\infty^2}\right]^{2/n}$ is the modified Reynolds number, $\Lambda = \dfrac{\beta^*}{\beta}\left(\dfrac{C_w - C_\infty}{T_w - T_{\infty,0}}\right)$ is the buoyancy ratio, $Le = \dfrac{\alpha}{D}$ is the Lewis number and $Sr = \dfrac{D_1}{\alpha}\left(\dfrac{T_w - T_{\infty,0}}{C_w - C_\infty}\right)$ is the Soret number. The primes in equations (3.10) - (3.13) represent the differentiation with respect to the variable η. The skin-friction, heat and mass transfer coefficients can be respectively obtained from

$$\left.\begin{array}{l} C_f Pe_x^2 = 2P_r Ra_x^{3/2} f''(\varepsilon,0) \\ Nu_x Ra_x^{-1/2} = -\theta'(\varepsilon,0) \\ Sh_x Ra_x^{-1/2} = -\phi'(\varepsilon,0) \end{array}\right\}. \tag{3.14}$$

where $P_r = \dfrac{\nu_\infty}{\alpha}$ and $Pe_x = \dfrac{U_\infty x}{\alpha}$.

3.3 Method of solution

We solve the system of equations (3.10) - (3.12) subject to the boundary conditions (3.13) by using a local similarity and local non-similarity method which has been widely used by many investigators (see Minkowycz and Sparrow 1974 and Sparrow and Yu 1971) to solve various problems possessing non-similar solutions. The boundary value problems resulting from this method are solved by the SLM and shooting techniques. For the first level of truncation, the terms involving $\varepsilon\dfrac{\partial}{\partial\varepsilon}$ are assumed to be small. This is particularly true when $\varepsilon \ll 1$. Thus the terms with $\varepsilon\dfrac{\partial}{\partial\varepsilon}$ in equations (3.10) - (3.12) can be neglected to get the following system of equations

$$\left[n(f')^{n-1} + 2Gr^* e^{\gamma\theta} f'\right] f'' = (\theta' + \Lambda\phi')e^{\gamma\theta} + \gamma(f')^n\theta', \tag{3.15}$$

$$\theta'' + \frac{1}{2}f\theta' - \varepsilon f' = 0, \tag{3.16}$$

$$\frac{1}{Le}\phi'' + \frac{1}{2}f\phi' + Sr\theta'' = 0. \tag{3.17}$$

The corresponding boundary conditions are

$$\left.\begin{array}{llll} f(\varepsilon,\eta) = 0, & \theta(\varepsilon,\eta) = 1, & \phi(\varepsilon,\eta) = 1 & \text{at} \quad \eta = 0 \\ f'(\varepsilon,\eta) \to 0, & \theta(\varepsilon,\eta) \to 0, & \phi(\varepsilon,\eta) \to 0 & \text{as} \quad \eta \to \infty \end{array}\right\}. \tag{3.18}$$

For the second level of truncations, we introduce the variables $g = \dfrac{\partial f}{\partial\varepsilon}$, $h = \dfrac{\partial\theta}{\partial\varepsilon}$ and $k = \dfrac{\partial\phi}{\partial\varepsilon}$ and recover the neglected terms at the first level of truncation. Thus, the governing equations at the second level are given by

$$\left[n(f')^{n-1} + 2Gr^* e^{\gamma\theta} f'\right] f'' = (\theta' + \Lambda\phi')e^{\gamma\theta} + \gamma(f')^n\theta', \tag{3.19}$$

$$\theta'' + \frac{1}{2}f\theta' - \varepsilon f' = \varepsilon\left(f'h - \theta' g\right), \tag{3.20}$$

$$\frac{1}{Le}\phi'' + \frac{1}{2}f\phi' + Sr\theta'' = \varepsilon\left(f'k - \phi' g\right). \tag{3.21}$$

The corresponding boundary conditions are

$$\left.\begin{array}{llllll} f(\varepsilon,\eta)=0, & \theta(\varepsilon,\eta)=1-\varepsilon & \phi(\varepsilon,\eta)=1 & \text{at} & \eta=0 \\ f'(\varepsilon,\eta)\to 0, & \theta(\varepsilon,\eta)\to 0 & \phi(\varepsilon,\eta)\to 0 & \text{as} & \eta\to\infty \end{array}\right\}, \tag{3.22}$$

At the third level, we differentiate equations (3.19) - (3.22) with respect to ε and neglect the terms $\dfrac{\partial g}{\partial \varepsilon}$, $\dfrac{\partial h}{\partial \varepsilon}$ and $\dfrac{\partial k}{\partial \varepsilon}$ to get the following set of equations

$$\left[n(f')^{n-1}+2Gr^*e^{\gamma\theta}f'\right]g''+\left[n(n-1)(f')^{n-2}g'+2Gr^*e^{\gamma\theta}(g'+\gamma f'h)\right]f''$$
$$-e^{\gamma\theta}\left[h'+\Lambda k'+\gamma(\theta'+\Lambda\phi')h\right]-\gamma\left[n(f')^{n-1}\theta'\ g'+(f')^n h'\right]=0, \tag{3.23}$$

$$h''+\frac{1}{2}(fh'+3g\theta')-(f'+\varepsilon g')(1+h)+\varepsilon h'g=0, \tag{3.24}$$

$$\frac{1}{Le}k''+\frac{1}{2}(fk'+3g\phi')+Srh''-f'k+\varepsilon(gk'-kg')=0, \tag{3.25}$$

The corresponding boundary conditions are

$$\left.\begin{array}{llllll} g(\varepsilon,\eta)=0, & h(\varepsilon,\eta)=-1, & k(\varepsilon,\eta)=0 & \text{at} & \eta=0 \\ g'(\varepsilon,\eta)\to 0, & h(\varepsilon,\eta)\to 0, & k(\varepsilon,\eta)\to 0 & \text{as} & \eta\to\infty \end{array}\right\}. \tag{3.26}$$

The set of differential equations (3.19) - (3.21), (3.23) - (3.25) together with the boundary conditions (3.22) and (3.26) are solved by means of the SLM. The SLM algorithm starts with the assumption that the functions $f(\eta)$, $\theta(\eta)$, $g(\eta)$ and $h(\eta)$ can be expressed as

$$\left.\begin{array}{ll} f(\eta)=f_i(\eta)+\sum_{m=0}^{i-1}F_m(\eta), & \theta(\eta)=\theta_i(\eta)+\sum_{m=0}^{i-1}\Theta_m(\eta), \\ \phi(\eta)=\phi_i(\eta)+\sum_{m=0}^{i-1}\Phi_m(\eta), & g(\eta)=g_i(\eta)+\sum_{m=0}^{i-1}G_m(\eta), \\ h(\eta)=h_i(\eta)+\sum_{m=0}^{i-1}H_m(\eta), & k(\eta)=k_i(\eta)+\sum_{m=0}^{i-1}K_m(\eta) \end{array}\right\}, \tag{3.27}$$

where f_i, θ_i, ϕ_i, g_i, h_i and k_i are unknown functions and F_m, Θ_m, Φ_m, G_m, H_m and K_m are successive approximations which are obtained by recursively solving the linear part of the equation system that results from substituting firstly equation (3.27) in equations (3.19) - (3.26). The main assumption of the SLM is that f_i, θ_i, ϕ_i, g_i, h_i and k_i become increasingly smaller when i becomes large, that is

$$\lim_{i\to\infty} f_i = \lim_{i\to\infty} \theta_i = \lim_{i\to\infty} \phi_i = \lim_{i\to\infty} g_i = \lim_{i\to\infty} h_i = \lim_{i\to\infty} k_i = 0. \tag{3.28}$$

The initial guesses $F_0(\eta)$, $\Theta_0(\eta)$, $\Phi_0(\eta)$, $G_0(\eta)$, $H_0(\eta)$ and $K_0(\eta)$ which are chosen to satisfy the boundary conditions (3.22) and (3.26) which are taken to be

$$\left.\begin{array}{lll} F_0(\eta) = 1 - e^{-\eta}, & \Theta_0(\eta) = (1-\varepsilon)e^{-\eta} & \Phi_0(\eta) = e^{-\eta}, \\ G_0(\eta) = 1 - e^{-\eta}, & H_0(\eta) = -e^{-\eta} & K_0(\eta) = \eta e^{-\eta}, \end{array}\right\} \tag{3.29}$$

Thus, starting from the initial guesses, the subsequent solutions $F_i(\eta)$, $\Theta_i(\eta)$, $\Phi_i(\eta)$, $G_i(\eta)$, $H_i(\eta)$ and $K_i(\eta)$ $(i \geq 1)$ are obtained by successively solving the linearized form of the equations which are obtained by substituting equation (3.27) in the governing equations (3.19) - (3.26). The linearized equations to be solved are

$$a_{1,i-1}F_i'' \quad + a_{2,i-1}F_i' + a_{3,i-1}\Theta_i' + a_{4,i-1}\Theta_i + a_{5,i-1}\Phi_i' = r_{1,i-1}, \tag{3.30}$$

$$b_{1,i-1}\Theta_i'' \quad + b_{2,i-1}\Theta_i' + b_{3,i-1}F_i' + b_{4,i-1}F_i + b_{5,i-1}H_i + b_{6,i-1}G_i = r_{2,i-1}, \tag{3.31}$$

$$\begin{aligned} c_{1,i-1}\Phi_i'' \quad & + c_{2,i-1}\Phi_i' + c_{3,i-1}F_i' + c_{4,i-1}F_i + c_{5,i-1}\Theta_i'' + c_{6,i-1}K_i + c_{7,i-1}G_i \\ & = r_{3,i-1}, \end{aligned} \tag{3.32}$$

$$\begin{aligned} d_{1,i-1}G_i'' \quad & + d_{2,i-1}G_i' + d_{3,i-1}F_i'' + d_{4,i-1}F_i' + d_{5,i-1}\Theta_i' + d_{6,i-1}\Theta_i + d_{7,i-1}\Phi_i' \\ + d_{8,i-1}H_i' \quad & + d_{9,i-1}H_i + d_{10,i-1}K_i' = r_{4,i-1}, \end{aligned} \tag{3.33}$$

$$\begin{aligned} e_{1,i-1}H_i'' \quad & + e_{2,i-1}H_i' + e_{3,i-1}H_i + e_{4,i-1}F_i' + e_{5,i-1}F_i + e_{6,i-1}\Theta_i' + e_{7,i-1}G_i' \\ + e_{8,i-1}G_i \quad & = r_{5,i-1}, \end{aligned} \tag{3.34}$$

$$l_{1,i-1}K_i'' \quad +l_{2,i-1}K_i' + l_{3,i-1}K_i + l_{4,i-1}F_i' + l_{5,i-1}F_i + l_{6,i-1}H_i'' + l_{7,i-1}\Phi_i'$$
$$+l_{8,i-1}G_i' \quad +l_{9,i-1}G_i = r_{6,i-1}, \tag{3.35}$$

subject to the boundary conditions

$$\left.\begin{aligned} F_i(0) = F_i'(\infty) = \Theta_i(0) = \Theta_i(\infty) = \Phi_i(0) = \Phi_i(\infty) = 0, \\ G_i(0) = G_i'(\infty) = H_i(0) = H_i(\infty) = K_i(0) = K_i(\infty) = 0, \end{aligned}\right\} \tag{3.36}$$

where coefficients $a_{k,i-1}$ $(k = 1, \ldots, 5)$, $b_{k,i-1}$ $(k = 1, \ldots, 6)$, $c_{k,i-1}$ $(k = 1, \ldots, 7)$, $d_{k,i-1}$ $(k = 1, \ldots, 10)$, $e_{k,i-1}$ $(k = 1, \ldots, 8)$, $l_{k,i-1}$ $(k = 1, \ldots, 9)$ and $r_{k,i-1}$ $(k = 1, \ldots, 6)$ depend on F_{i-1}, Θ_{i-1}, Φ_{i-1}, G_{i-1}, H_{i-1}, K_{i-1} and on their derivatives. The solutions F_i, Θ_i, Φ_i, G_i, H_i and K_i for $i \geq 1$ has been found by iteratively solving equations (3.30) - (3.36) and finally after M iterations the solutions $f(\eta)$, $\theta(\eta)$, $g(\eta)$ and $h(\eta)$ can be written as

$$\left.\begin{aligned} f(\eta) \approx \sum_{m=0}^{M} F_m(\eta), \qquad \theta(\eta) \approx \sum_{m=0}^{M} \Theta_m(\eta), \qquad \phi(\eta) \approx \sum_{m=0}^{M} \Phi_m(\eta), \\ g(\eta) \approx \sum_{m=0}^{M} G_m(\eta), \qquad h(\eta) \approx \sum_{m=0}^{M} H_m(\eta), \qquad k(\eta) \approx \sum_{m=0}^{M} K_m(\eta), \end{aligned}\right\} \tag{3.37}$$

where M is the order of SLM approximation. Equations (3.30) - (3.36) are solved using the Chebyshev spectral collocation method. The method uses Chebyshev polynomials defined on the interval $[-1, 1]$. We first transform the domain of solution $[0, \infty)$ into the domain $[-1, 1]$ using the domain truncation technique where the problem is solved in the interval $[0, L]$ instead of $[0, \infty)$ by using the mapping

$$\frac{\eta}{L} = \frac{\xi + 1}{2}, \qquad -1 \leq \xi \leq 1, \tag{3.38}$$

where L is the scaling parameter used to invoke the boundary condition at infinity. We discretize the domain $[-1, 1]$ using the popular Gauss-Lobatto collocation points

given by

$$\xi = \cos\frac{\pi j}{N}, \qquad j = 0, 1, 2, \ldots, N, \tag{3.39}$$

where N is the number of collocation points used. The functions F_i, Θ_i, G_i and H_i for $i \geq 1$ are approximated at the collocation points as follows

$$\left.\begin{aligned} F_i(\xi) &\approx \sum_{k=0}^{N} F_i(\xi_k)T_k(\xi_j), & \Theta_i(\xi) &\approx \sum_{k=0}^{N} \Theta_i(\xi_k)T_k(\xi_j), \\ \Phi_i(\xi) &\approx \sum_{k=0}^{N} \Phi_i(\xi_k)T_k(\xi_j), & G_i(\xi) &\approx \sum_{k=0}^{N} G_i(\xi_k)T_k(\xi_j), \\ H_i(\xi) &\approx \sum_{k=0}^{N} H_i(\xi_k)T_k(\xi_j), & K_i(\xi) &\approx \sum_{k=0}^{N} K_i(\xi_k)T_k(\xi_j), \end{aligned}\right\} \; j = 0, 1, ..., N \tag{3.40}$$

where T_k is the k^{th} Chebyshev polynomial given by

$$T_k(\xi) = \cos\left[k\cos^{-1}(\xi)\right]. \tag{3.41}$$

The derivatives of the variables at the collocation points are represented as

$$\left.\begin{aligned} \frac{d^r F_i}{d\eta^r} &= \sum_{k=0}^{N} \mathbf{D}_{kj}^r F_i(\xi_k), & \frac{d^r \Theta_i}{d\eta^r} &= \sum_{k=0}^{N} \mathbf{D}_{kj}^r \Theta_i(\xi_k), \\ \frac{d^r \Phi_i}{d\eta^r} &= \sum_{k=0}^{N} \mathbf{D}_{kj}^r \Phi_i(\xi_k), & \frac{d^r G_i}{d\eta^r} &= \sum_{k=0}^{N} \mathbf{D}_{kj}^r G_i(\xi_k), \\ \frac{d^r H_i}{d\eta^r} &= \sum_{k=0}^{N} \mathbf{D}_{kj}^r H_i(\xi_k), & \frac{d^r K_i}{d\eta^r} &= \sum_{k=0}^{N} \mathbf{D}_{kj}^r K_i(\xi_k), \end{aligned}\right\} \; j = 0, 1, ..., N \tag{3.42}$$

where r is the order of differentiation and $\mathbf{D} = \frac{2}{L}\mathcal{D}$ with $\mathcal{D}$ being the Chebyshev spectral differentiation matrix whose entries are defined in (1.30). Substituting equations (3.38) - (3.42) into equations (3.30) - (3.36) leads to the matrix equation

$$\mathbf{A}_{i-1}\mathbf{X}_i = \mathbf{R}_{i-1}. \tag{3.43}$$

In equation (3.43), $\mathbf{A}_{i-1}$ is a $(6N+6)\times(6N+6)$ square matrix and $\mathbf{X}_i$ and $\mathbf{R}_{i-1}$ are $(6N+6)\times 1$ column vectors defined by

$$\mathbf{A}_{i-1}=\begin{bmatrix} A_{11} & \cdots & A_{16} \\ \vdots & \ddots & \vdots \\ A_{61} & \cdots & A_{66} \end{bmatrix},\ \mathbf{X}_i=\begin{bmatrix} F_i \\ \Theta_i \\ \Phi_i \\ G_i \\ H_i \\ K_i \end{bmatrix},\ \mathbf{R}_{i-1}=\begin{bmatrix} \mathbf{r}_{1,i-1} \\ \mathbf{r}_{2,i-1} \\ \mathbf{r}_{3,i-1} \\ \mathbf{r}_{4,i-1} \\ \mathbf{r}_{5,i-1} \\ \mathbf{r}_{6,i-1} \end{bmatrix} \tag{3.44}$$

where

$$\begin{aligned}
F_i &= [f_i(\xi_0), f_i(\xi_1), ..., f_i(\xi_{N-1}), f_i(\xi_N)]^T, \\
\Theta_i &= [\theta_i(\xi_0), \theta_i(\xi_1), ..., \theta_i(\xi_{N-1}), \theta_i(\xi_N)]^T, \\
\Phi_i &= [\phi_i(\xi_0), \phi_i(\xi_1), ..., \phi_i(\xi_{N-1}), \phi_i(\xi_N)]^T, \\
G_i &= [g_i(\xi_0), g_i(\xi_1), ..., g_i(\xi_{N-1}), g_i(\xi_N)]^T, \\
H_i &= [h_i(\xi_0), h_i(\xi_1), ..., h_i(\xi_{N-1}), h_i(\xi_N)]^T, \\
K_i &= [k_i(\xi_0), k_i(\xi_1), ..., k_i(\xi_{N-1}), k_i(\xi_N)]^T,
\end{aligned}$$

$$\begin{aligned}
\mathbf{r}_{1,i-1} &= [r_{1,i-1}(\xi_0), r_{1,i-1}(\xi_1), ..., r_{1,i-1}(\xi_{N-1}), r_{1,i-1}(\xi_N)]^T, \\
\mathbf{r}_{2,i-1} &= [r_{2,i-1}(\xi_0), r_{2,i-1}(\xi_1), ..., r_{2,i-1}(\xi_{N-1}), r_{2,i-1}(\xi_N)]^T, \\
\mathbf{r}_{3,i-1} &= [r_{3,i-1}(\xi_0), r_{3,i-1}(\xi_1), ..., r_{3,i-1}(\xi_{N-1}), r_{3,i-1}(\xi_N)]^T, \\
\mathbf{r}_{4,i-1} &= [r_{4,i-1}(\xi_0), r_{4,i-1}(\xi_1), ..., r_{4,i-1}(\xi_{N-1}), r_{4,i-1}(\xi_N)]^T, \\
\mathbf{r}_{5,i-1} &= [r_{5,i-1}(\xi_0), r_{5,i-1}(\xi_1), ..., r_{5,i-1}(\xi_{N-1}), r_{5,i-1}(\xi_N)]^T, \\
\mathbf{r}_{6,i-1} &= [r_{6,i-1}(\xi_0), r_{6,i-1}(\xi_1), ..., r_{6,i-1}(\xi_{N-1}), r_{6,i-1}(\xi_N)]^T,
\end{aligned}$$

$$A_{11} = \mathbf{a}_{1,i-1}\mathbf{D}^2 + \mathbf{a}_{2,i-1}\mathbf{D}, \quad A_{12} = \mathbf{a}_{3,i-1}\mathbf{D} + \mathbf{a}_{4,i-1}\mathbf{I}, \quad A_{13} = \mathbf{a}_{5,i-1}\mathbf{D},$$

$$A_{14} = \mathbf{O}, A_{15} = \mathbf{O}, \quad A_{16} = \mathbf{O}, \quad A_{21} = \mathbf{b}_{4,i-1}\mathbf{D} + \mathbf{b}_{5,i-1}\mathbf{I},$$

$$A_{22} = \mathbf{b}_{1,i-1}\mathbf{D}^2 + \mathbf{b}_{2,i-1}\mathbf{D}, \quad A_{23} = \mathbf{O}, A_{24} = \mathbf{b}_{6,i-1}\mathbf{I}, \quad A_{25} = \mathbf{b}_{5,i-1}\mathbf{I},$$

$$A_{26} = \mathbf{O}, \quad A_{31} = \mathbf{c}_{3,i-1}\mathbf{D} + \mathbf{c}_{4,i-1}\mathbf{I}, \quad A_{32} = \mathbf{c}_{5,i-1}\mathbf{D}^2, A_{33} = \mathbf{c}_{1,i-1}\mathbf{D}^2 + \mathbf{c}_{2,i-1}\mathbf{D},$$

$$A_{34} = \mathbf{c}_{7,i-1}\mathbf{I}, \quad A_{35} = \mathbf{0}, \quad A_{36} = \mathbf{c}_{6,i-1}\mathbf{I}, A_{41} = \mathbf{d}_{3,i-1}\mathbf{D}^2 + \mathbf{d}_{4,i-1}\mathbf{D},$$

$$A_{42} = \mathbf{d}_{5,i-1}\mathbf{D} + \mathbf{d}_{6,i-1}\mathbf{I}, \quad A_{43} = \mathbf{d}_{7,i-1}\mathbf{D}, A_{44} = \mathbf{d}_{1,i-1}\mathbf{D}^2 + \mathbf{d}_{2,i-1}\mathbf{D},$$

$$A_{45} = \mathbf{d}_{8,i-1}\mathbf{D} + \mathbf{d}_{9,i-1}\mathbf{I}, \quad A_{46} = \mathbf{d}_{10,i-1}\mathbf{D}, A_{51} = \mathbf{e}_{4,i-1}\mathbf{D} + \mathbf{e}_{5,i-1}\mathbf{I},$$

$$A_{52} = \mathbf{e}_{6,i-1}\mathbf{D}, \quad A_{53} = \mathbf{0}, \quad A_{54} = \mathbf{e}_{7,i-1}\mathbf{D} + \mathbf{e}_{8,i-1}\mathbf{I},$$

$$A_{55} = \mathbf{e}_{1,i-1}\mathbf{D}^2 + \mathbf{e}_{2,i-1}\mathbf{D} + \mathbf{e}_{3,i-1}\mathbf{I}, \quad A_{56} = \mathbf{0}, \quad A_{61} = \mathbf{l}_{4,i-1}\mathbf{D} + \mathbf{l}_{5,i-1}\mathbf{I},$$

$$A_{62} = \mathbf{0}, A_{63} = \mathbf{l}_{7,i-1}\mathbf{D}, \quad A_{64} = \mathbf{l}_{8,i-1}\mathbf{D} + \mathbf{l}_{9,i-1}\mathbf{I}, \quad A_{65} = \mathbf{l}_{6,i-1}\mathbf{D}^2,$$

$$A_{66} = \mathbf{l}_{1,i-1}\mathbf{D}^2 + \mathbf{l}_{2,i-1}\mathbf{D} + \mathbf{l}_{3,i-1}\mathbf{I}.$$

In the above definitions T stands for transpose, $\mathbf{a}_{k,i-1}$ $(k = 1, \ldots, 5)$, $\mathbf{b}_{k,i-1}$ $(k = 1, \ldots, 6)$, $\mathbf{c}_{k,i-1}$ $(k = 1, \ldots, 7)$, $\mathbf{d}_{k,i-1}$ $(k = 1, \ldots, 10)$, $\mathbf{e}_{k,i-1}$ $(k = 1, \ldots, 8)$, $\mathbf{l}_{k,i-1}$ $(k = 1, \ldots, 9)$ and $\mathbf{r}_{k,i-1}$ $(k = 1, \ldots, 6)$ are diagonal matrices of order $(N+1) \times (N+1)$, $\mathbf{I}$ is an identity matrix of order $(N+1) \times (N+1)$ and $\mathbf{O}$ is zero matrix of order $(N+1) \times (N+1)$. Finally the solution is obtained as

$$\mathbf{X}_i = \mathbf{A}_{i-1}^{-1}\mathbf{R}_{i-1}. \tag{3.45}$$

3.4 Results and discussion

The problem of natural convection in a thermally stratified variable property power-law fluid saturated non-Darcy porous media subject to the Soret effect has been investigated. A local non-similarity method is employed to derive a system of ordinary differential equations (3.19) - (3.26) from the governing partial differential equations

(3.10) - (3.13). The SLM was used to generate the solutions of the boundary value problem defined by equations (3.19) - (3.26). We have taken $L = 15$ and $N = 60$ for the implementation of SLM which gave sufficient accuracy. Further, we restrict ourselves to the following parameter values $0.5 \leq n \leq 1.5$, $0 \leq \gamma \leq 2$, $0 \leq Sr \leq 0.5$ with the fixed values $Gr^* = 1$ and $Le = 1$. To highlight aiding buoyancy condition we take $\Lambda > 0$ while for opposing buoyancy, $\Lambda < 0$.

However, before discussing the results, it is worth noting the following important result in relation to the stratification parameter. We recall that the definition of local stratification parameter is given by

$$\varepsilon = \frac{Ax}{T_w - T_{\infty,0}}$$

The condition $T_w > T_\infty$ corresponds to the usual upward boundary layer flow. It can be shown with the help of equation (3.1) that the inequality $T_w > T_\infty$ is equivalent to $\varepsilon < 1$. However, at some point along the x- axis we may have $T_w < T_\infty$ (i.e., $\varepsilon > 1$) in which case the fluid starts moving downwards. The line $\varepsilon = 1$ corresponds to no-motion and can be regarded as a "stagnation line". This solution behaviour is encountered during computation and the results are shown in Figure 3.2 which shows the axial velocity for different values of the stratification parameter. Clearly, one observes the "stagnation line" corresponding to $\varepsilon = 1$, the usual boundary layer flow for $\varepsilon < 1$ and the reverse flow for $\varepsilon > 1$.

In the following discussion we restrict ourselves to the usual boundary layer behaviour observed in the region $0 \leq \varepsilon < 1$. In order to validate the solution obtained using the SLM we compare the results with the numerical solution obtained using a shooting technique that uses the Runge-Kutta-Fehlberg (RKF45) and Newton-Raphson schemes. A comparison of axial velocity, temperature and concentration profiles at some selected valued of η is given in Table 3.1 (for aiding buoyancy i.e, $\Lambda = 0.1$) and Table 3.2 (for opposing buoyancy i.e, $\Lambda = -0.1$) and two different values

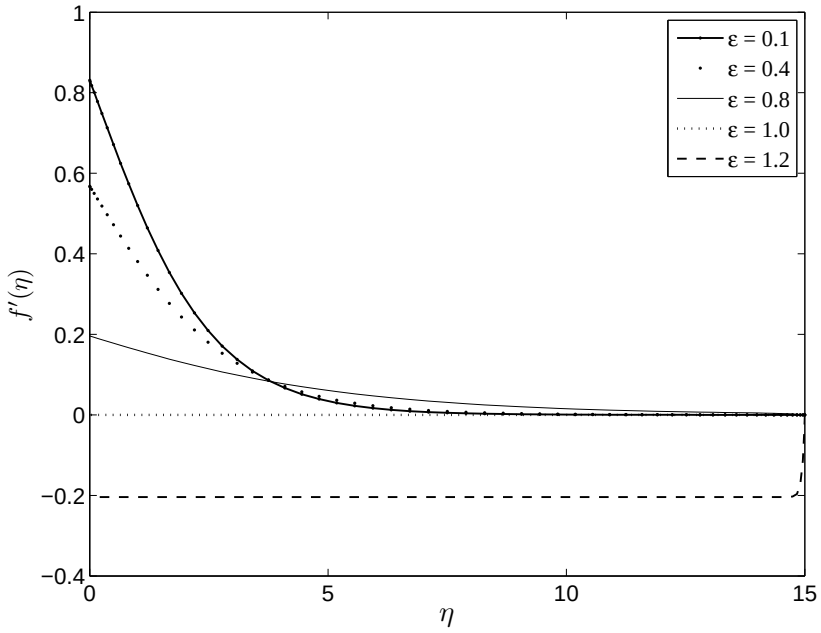

Figure 3.2: Variation of axial velocity profile $f'(Y)$ with ε with $Gr^* = 0.1$, $Le = n = 1$ and $\gamma = Sr = \Lambda = 0$

of n. It is evident that our results are in excellent agreement with those obtained numerically using the shooting technique. Table 3.3 gives a comparison of the present results with those reported in (1993) for the limiting cases $\gamma = Sr = \Lambda = 0$, $n = 1$ and different values of ε and Gr^*. We again observe an excellent agreement between the two sets of results.

The Non-dimensional velocity profile in the non-Darcy medium is plotted for fixed value of γ, Gr^*, Le and Λ for various values of power-law index n, viscous dissipation parameter ε and Soret number Sr in Fig. 3.3. It is interesting to note that the value of velocity $f'(\eta)$ decreases with the viscous dissipation parameter and increases with Soret number when the power-law index n is increasing. The variation of temperature and concentration profiles are displayed through Figures 3.4 - 3.9 for selected values of the parameters in the cases of a pseudoplastic, Newtonian and dilatant fluids. Figures 3.4 and 3.5 show temperature and concentration profiles for different values of n and ε in the case of aiding buoyancy and opposing buoyancy respectively. We observe

Table 3.1: A comparison between the SLM and shooting method results of $f'(\eta)$, $\theta(\eta)$ and $\phi(\eta)$ for different values of n with $Gr^* = 1$, $\gamma = 1$, $Sr = 0.1$, $Le = 1$, $\varepsilon = 0.2$ and $\Lambda = 0.1$

Profile	η	$n = 0.5$		$n = 1$		$n = 1.5$	
		SLM	Shooting	SLM	Shooting	SLM	Shooting
$f'(\eta)$	0.0	0.724114	0.724114	0.750260	0.750260	0.771622	0.771622
	0.1	0.712687	0.712685	0.738753	0.738753	0.760430	0.760429
	1.0	0.530914	0.530912	0.571733	0.571731	0.603845	0.603843
	5.0	0.006263	0.006260	0.039808	0.039804	0.079215	0.079210
$\theta(\eta)$	0.0	0.800000	0.800000	0.800000	0.800000	0.800000	0.800000
	0.1	0.788556	0.788555	0.786239	0.786239	0.784911	0.784910
	1.0	0.606654	0.606652	0.583015	0.583013	0.568953	0.568951
	5.0	0.060521	0.060516	0.035661	0.035657	0.025002	0.024998
$\phi(\eta)$	0.0	1.000000	1.000000	1.000000	1.000000	1.000000	1.000000
	0.1	0.963668	0.963667	0.960592	0.960592	0.958738	0.958737
	1.0	0.659762	0.659760	0.631556	0.631554	0.614962	0.614960
	5.0	0.073136	0.073131	0.043323	0.043320	0.030583	0.030578

that the power-law index n reduces both $\theta(\eta)$ and $\phi(\eta)$. The thermal stratification reduces the thermal boundary layer while increasing concentration boundary layer thickness in the case of aiding buoyancy as can be seen from Figure 3.4. Figure 3.5 shows that the effect of ε on $\theta(\eta)$ and $\phi(\eta)$ in the case of opposing buoyancy is the exact opposite of that observed in the case of aiding buoyancy. The temperature and concentration profiles are given in Figures 3.6 and 3.7 for different values of n and γ for aiding and opposing buoyancy cases respectively. One can easily infer that the variable viscosity parameter γ succeeds in thinning both thermal and concentration boundary layer thicknesses in the case of a pseudoplastic, Newtonian and dilatant fluids for both the aiding and opposing buoyancy cases. We note from equation (3.9) that increasing values of γ tends to reduce the fluid viscosity thereby enhancing momentum boundary layer thickness. Due to increased velocity there is less time

Table 3.2: A comparison between the SLM and shooting method results of $f'(\eta)$, $\theta(\eta)$ and $\phi(\eta)$ for different values of n with $Gr^* = 1$, $\gamma = 1$, $Sr = 0.1$, $Le = 1$, $\varepsilon = 0.2$ and $\Lambda = -0.1$

Profile	η	$n = 0.5$		$n = 1$		$n = 1.5$	
		SLM	Shooting	SLM	Shooting	SLM	Shooting
$f'(\eta)$	0.0	0.599100	0.599100	0.641642	0.641642	0.672453	0.672453
	0.1	0.591234	0.591235	0.633358	0.633358	0.664262	0.664263
	1.0	0.453852	0.453854	0.504500	0.504501	0.541810	0.541813
	5.0	0.008329	0.008333	0.043479	0.043483	0.082115	0.082119
$\theta(\eta)$	0.0	0.800000	0.800000	0.800000	0.800000	0.800000	0.800000
	0.1	0.788980	0.788981	0.786106	0.786106	0.784516	0.784517
	1.0	0.628446	0.628448	0.598062	0.598063	0.580798	0.580800
	5.0	0.087417	0.087422	0.049218	0.049221	0.033640	0.033645
$\phi(\eta)$	0.0	1.000000	1.000000	1.000000	1.000000	1.000000	1.000000
	0.1	0.968022	0.968024	0.964078	0.964078	0.961802	0.961803
	1.0	0.696962	0.696965	0.660575	0.660576	0.640041	0.640043
	5.0	0.104303	0.104307	0.059498	0.059501	0.041139	0.041144

for the heat build-up and this is the reason behind reduced thermal boundary layer thickness. Obviously, when the temperature in the boundary layer is reduced the species concentration tends to decrease. This pattern is observed in both aiding and opposing buoyancy cases. The Soret effect on the temperature and concentration profiles in case of aiding and opposing buoyancy cases is shown in Figures 3.8 and 3.9. The Soret parameter has only a marginal effect on $\theta(\eta)$ in cases but enhances $\phi(\eta)$. It is to be noted that the mass flux created by the temperature gradient gives rise to Soret effect or themophoresis. The thermophoretic force developed due to temperature gradients drives more particles into the boundary layer region thereby increasing the concentration boundary layer. Further, these temperature gradients will not be contributing anything to heat generation leaving the thermal boundary

Table 3.3: Comparison of $f'(0)$ and $\theta'(0)$ for different values of ε and Gr^* when $\gamma = Sr = \Lambda = 0$ and $n = 1$

		$\varepsilon = 0$		$\varepsilon = 0.1$	
Quantity	Gr^*	Singh and Ewari (1993)	Present Results	Singh and Ewari (1993)	Present Results
$f'(0)$	0.4	0.766	0.765564	0.703	0.702562
	1	0.618	0.618034	0.572	0.572381
	4	0.390	0.390388	0.366	0.365535
	6	0.333	0.333333	0.313	0.312829
	10	0.270	0.270156	0.254	0.254138
$-\theta'(0)$	0.4	0.400	0.400144	0.353	0.352629
	1	0.366	0.365770	0.325	0.325165
	4	0.298	0.297849	0.268	0.268117
	6	0.277	0.276813	0.250	0.249921
	10	0.251	0.250793	0.227	0.227147

layers almost unaltered. These qualitative results on the effect of Sr are in agreement with those reported by Kairi and Murthy (2011b).

In figure 3.10 variation of the skin-friction coefficient as a function of Soret number Sr and viscosity parameter γ are shown for different values of power-law index n and viscous dissipation parameter ε with fixed value of Gr^*, Le and Λ. From this figure, a decrease in $f''(0)$ is evident with increasing values of n and ε for all values Sr and γ. In other hand the skin-friction coefficient increases with increasing values Sr and γ for fixed values of n and ε.

The variation of the Nusselt number $Nu_x Ra_x^{-1/2}$ and the Sherwood number $Sh_x Ra_x^{-1/2}$ are shown in Figures 3.11 - 3.16 for selected values of the parameters and power-law index n in aiding and opposing buoyancy cases. Figures 3.11 and 3.12 show heat and mass transfer coefficients as a function of ε for different values of n, Sr and Λ. From

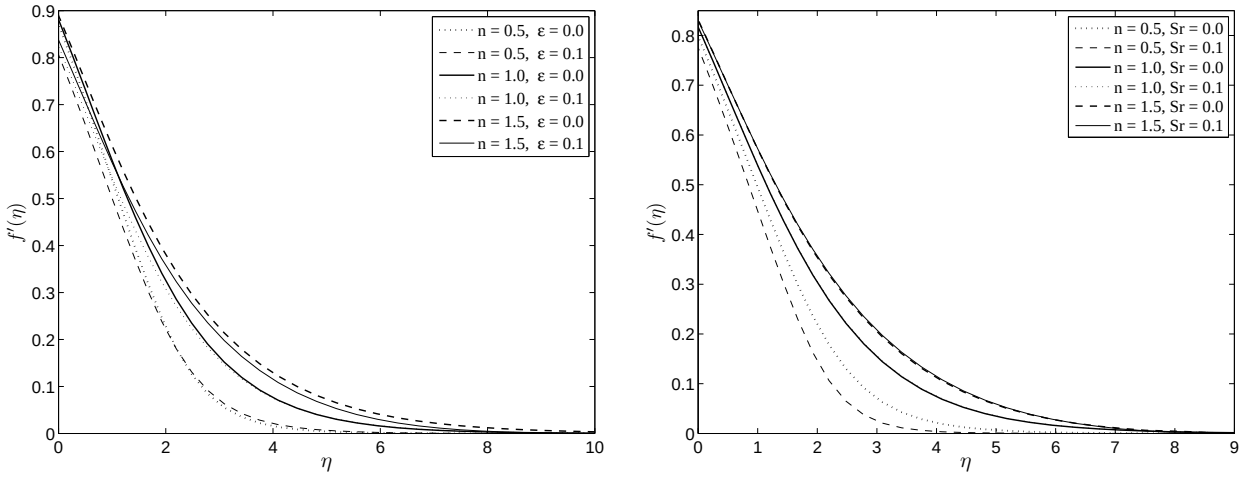

(a) (b)

Figure 3.3: Variation of (a) ε and (b) Sr on $f'(\eta)$ against η varying n when $\gamma = 1, Gr^* = 1, Le = 1$ and $\Lambda = 0.1$.

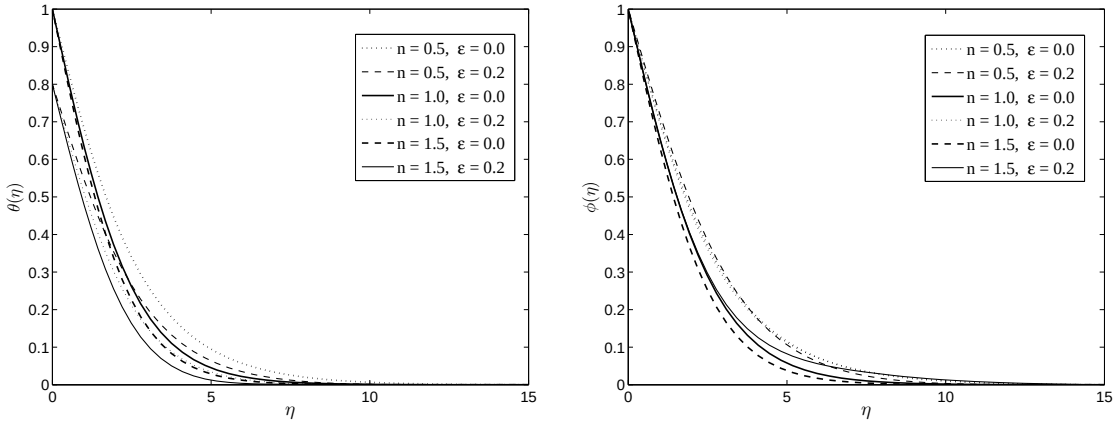

(a) (b)

Figure 3.4: Variation of $\theta(\eta)$ and $\phi(\eta)$ with η for varying ε and n when $\gamma = 1.2$, $Gr^* = 1$, $Sr = 0.1$, $Le = 1$ and $\Lambda = 0.1$

Figure 3.11(a) it is clear that in the aiding buoyancy case, as ε increases $Nu_x Ra_x^{-1/2}$ starts decreasing steadily and also the presence of the Soret parameter enhances heat transfer. In the absence of the Soret effect, increasing ε has the effect of reducing $Sh_x Ra_x^{-1/2}$ while the opposite is true in the presence of the Soret effect. Overall, the Soret number Sr results in the lowering of the mass transfer coefficient. In Figures 3.12(a) and (b), one can identify similar patterns with respect to the thermal stratifi-

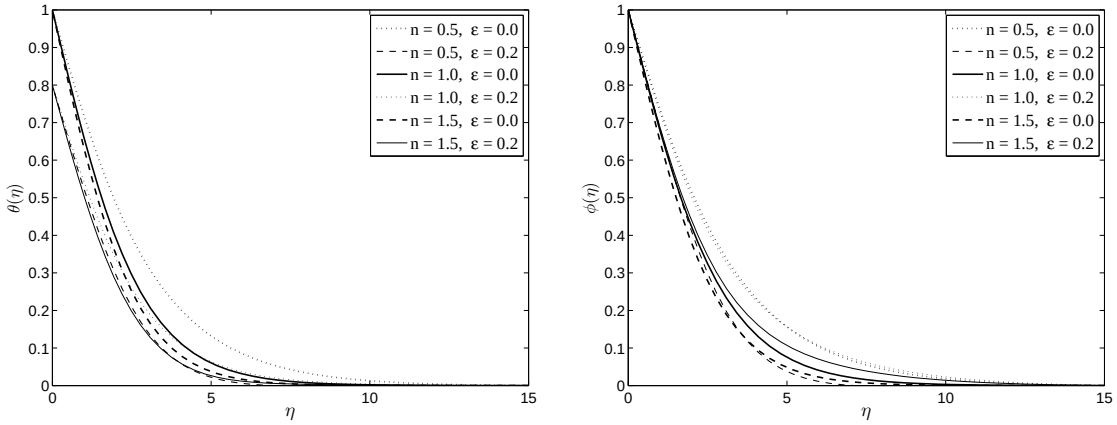

(a) (b)

Figure 3.5: Variation of $\theta(\eta)$ and $\phi(\eta)$ with η for varying ε and n when $\gamma = 1.2$, $Gr^* = 1$, $Sr = 0.1$, $Le = 1$ and $\Lambda = -0.1$

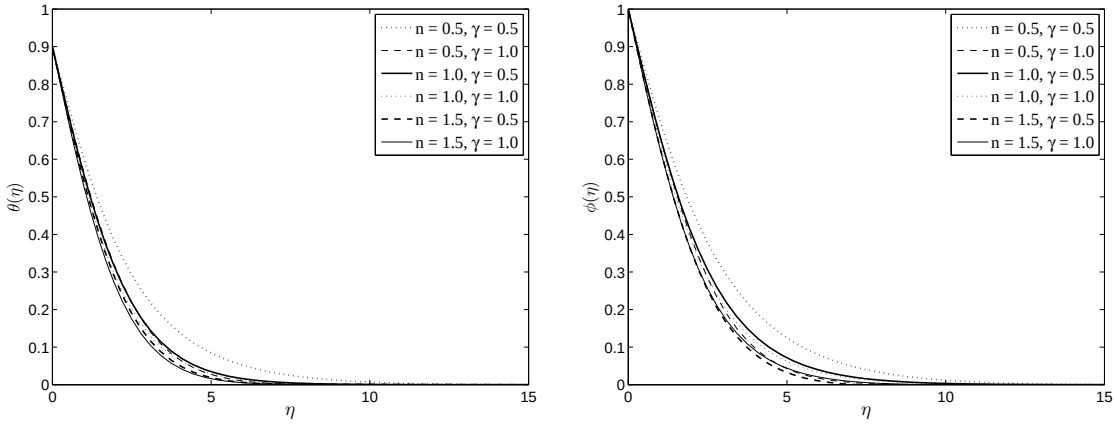

(a) (b)

Figure 3.6: Variation of $\theta(\eta)$ and $\phi(\eta)$ with η for varying γ and n when $\varepsilon = 0.1$, $Gr^* = 1$, $Sr = 0.1$, $Le = 1$ and $\Lambda = 0.1$

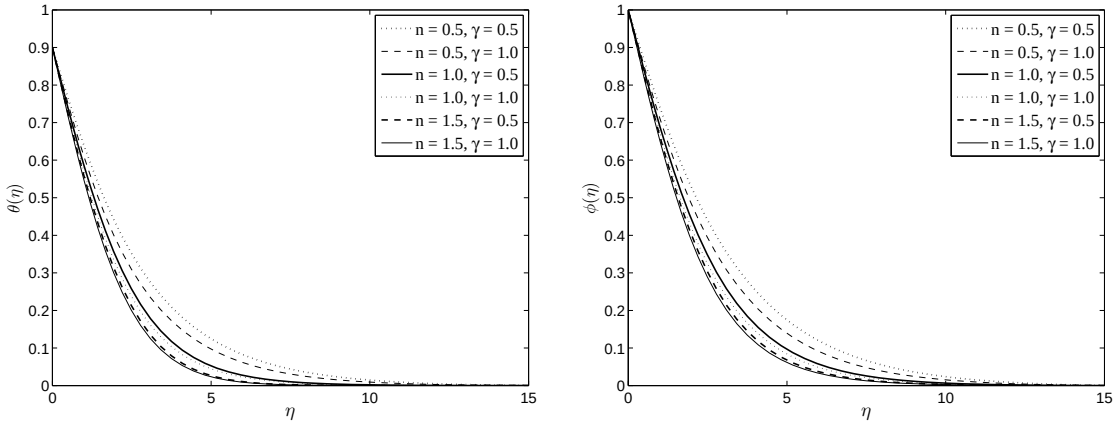

(a) (b)

Figure 3.7: Variation of $\theta(\eta)$ and $\phi(\eta)$ with η for varying γ and n when $\varepsilon = 0.1$, $Gr^* = 1$, $Sr = 0.1$, $Le = 1$ and $\Lambda = -0.1$

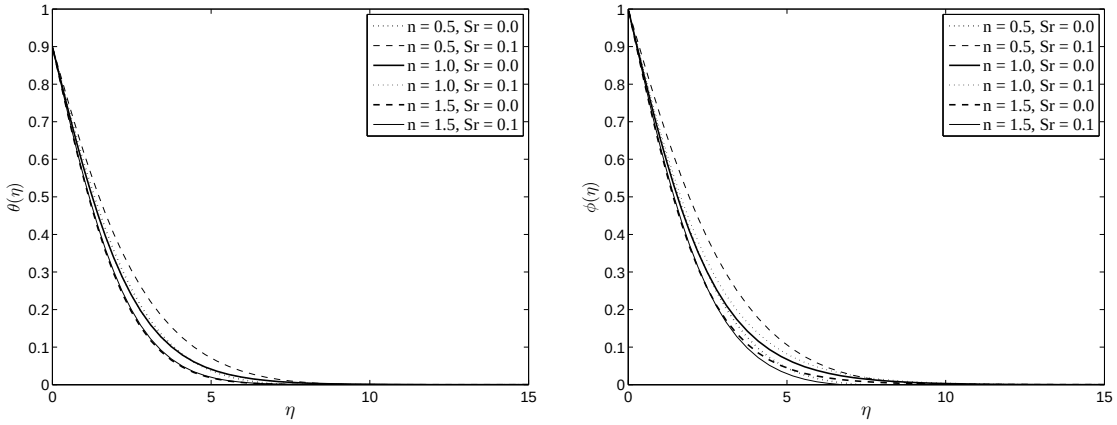

(a) (b)

Figure 3.8: Variation of $\theta(\eta)$ and $\phi(\eta)$ with η for varying Sr and n when $\varepsilon = 0.1$, $\gamma = 1.5$, $Gr^* = 1$, $Le = 1$ and $\Lambda = 0.1$

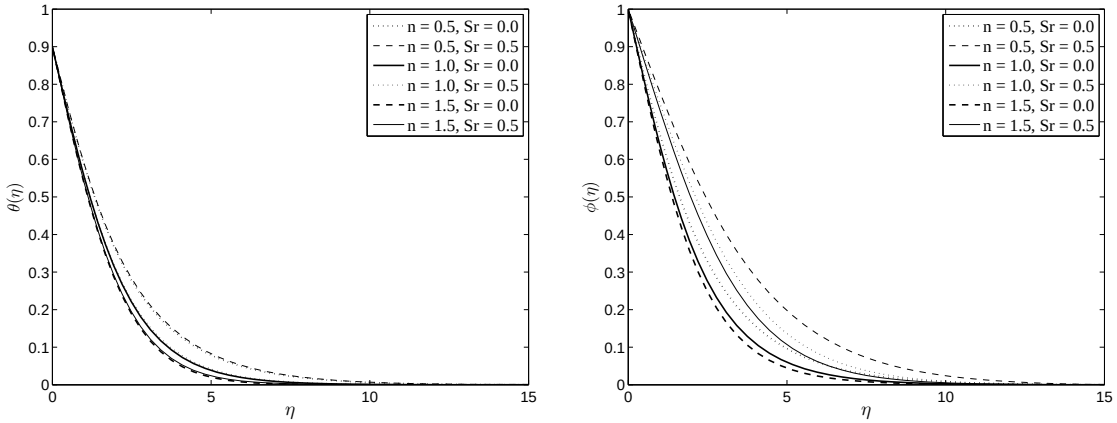

(a) (b)

Figure 3.9: Variation of $\theta(\eta)$ and $\phi(\eta)$ with η for varying Sr and n when $\varepsilon = 0.1$, $\gamma = 1.5$, $Gr^* = 1$, $Le = 1$ and $\Lambda = -0.1$

cation parameter ε. The presence of the Soret effect reduces the heat transfer in this case.

Figures 3.13 and 3.14 depict variations of $Nu_x Ra_x^{-1/2}$ and $Sh_x Ra_x^{-1/2}$ against Sr for different values of n, ε and Λ. It is clear that $Nu_x Ra_x^{-1/2}$ is an increasing function and $Sh_x Ra_x^{-1/2}$ is a decreasing function of Sr. The heat transfer coefficient is lowered by increasing the thermal stratification in the two different flow situations considered. The effect of ε on the mass transfer coefficient subjected to increasing Sr is quite interesting. The stratification parameter ε reduces $Sh_x Ra_x^{-1/2}$ until Sr reaches some value and any further increase in Sr causes ε to enhance $Sh_x Ra_x^{-1/2}$. This situation is true for both aiding and opposing buoyancy cases.

The heat and mass transfer coefficients are shown as a function of variable viscosity parameter γ for different values of n, ε and Λ in Figures 3.15 and 3.16. It is readily seen that γ enhances both heat and mass transfer coefficients for both aiding and opposing buoyancy cases with respect to pseudoplastic, Newtonian and dilatant fluids. Similar behaviour was observed by (2007) and (2011b). The thermal stratification parameter, subjected to a change in the viscosity parameter, reduces heat

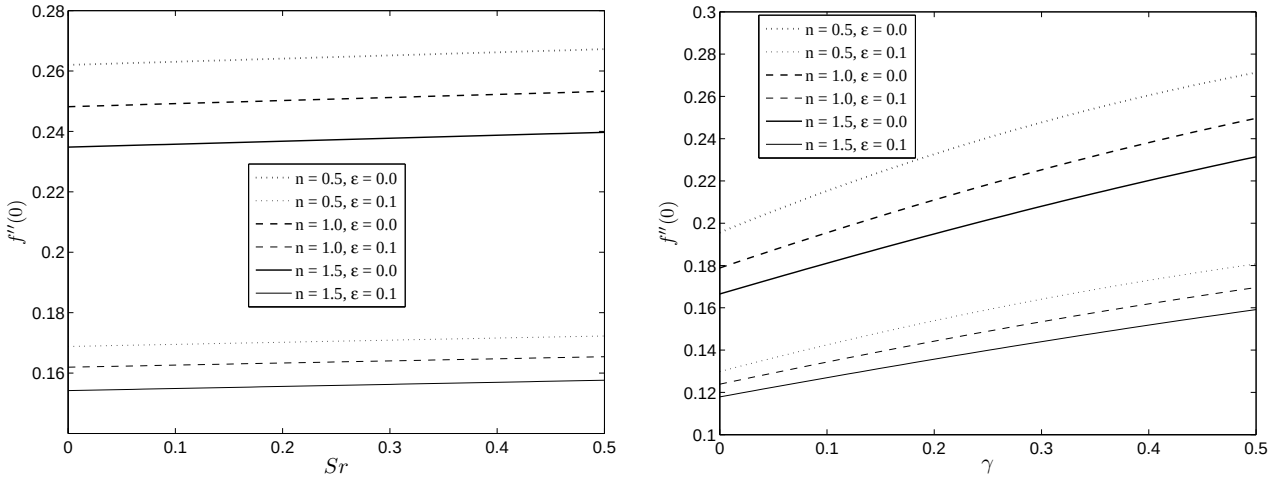

(a) (b)

Figure 3.10: Variation of $f''(0)$ against (a) Sr and (b) γ varying n and ε when $\gamma = 1, Gr^* = 1, Le = 1$ and $\Lambda = 0.1$.

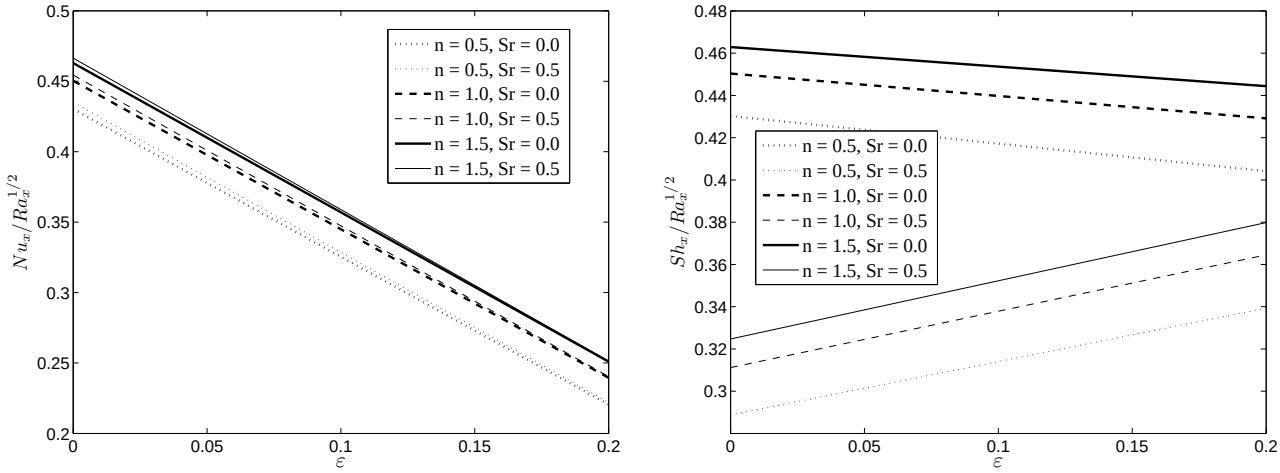

(a) (b)

Figure 3.11: Variation of heat and mass transfer coefficients against ε for varying n and Sr when $\gamma = 1.2$, $Gr^* = 1$, $Le = 1$ and $\Lambda = 0.2$

transfer and enhances mass transfer coefficients.

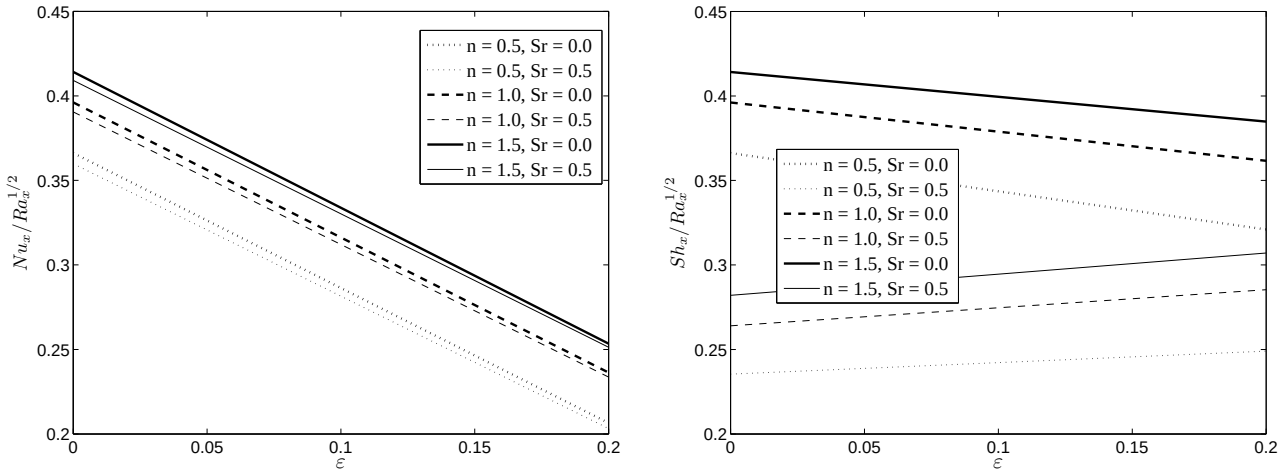

(a) (b)

Figure 3.12: Variation of heat and mass transfer coefficients against ε for varying n and Sr when $\gamma = 1.2$, $Gr^* = 1$, $Le = 1$ and $\Lambda = -0.2$

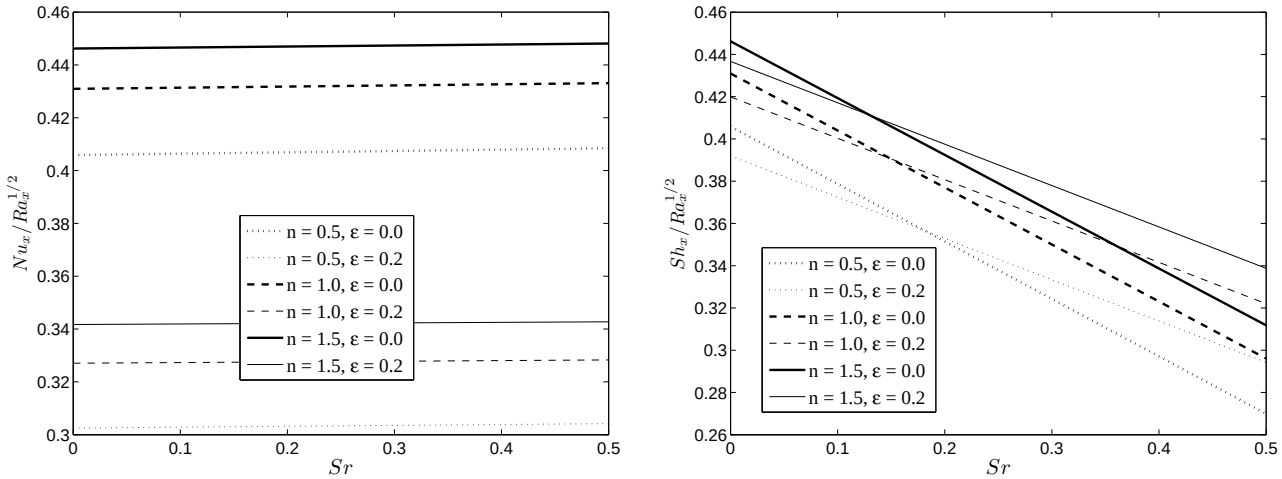

(a) (b)

Figure 3.13: Variation of heat and mass transfer coefficients against Sr for varying ε and n when $\gamma = 1$, $Gr^* = 1$, $Le = 1$ and $\Lambda = 0.1$

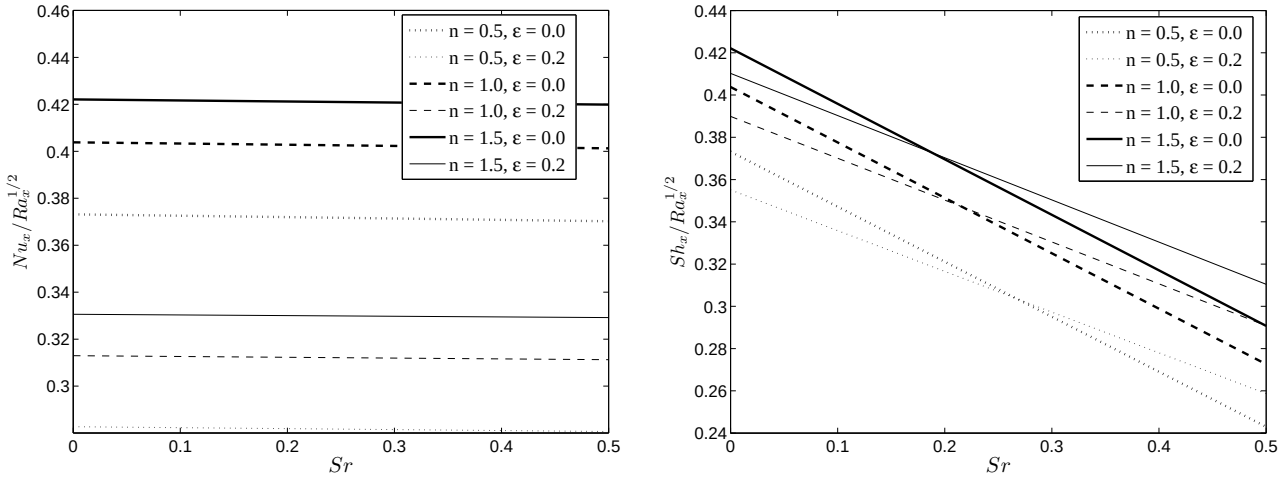

(a) (b)

Figure 3.14: Variation of heat and mass transfer coefficients against Sr for varying ε and n when $\gamma = 1$, $Gr^* = 1$, $Le = 1$ and $\Lambda = -0.1$

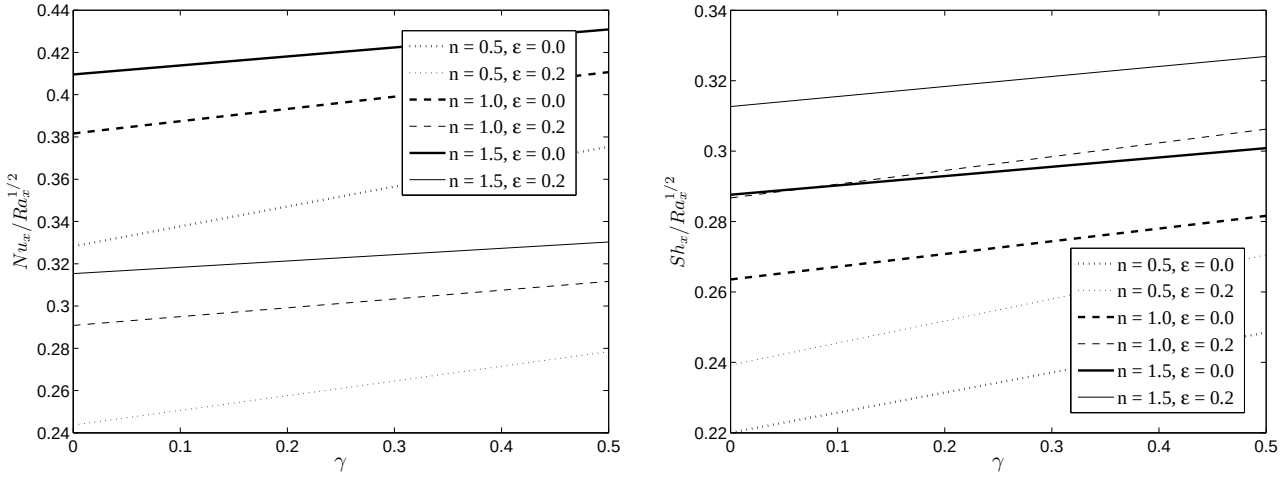

(a) (b)

Figure 3.15: Variation of heat and mass transfer coefficients against γ for varying ε and n when $Sr = 0.5$, $Gr^* = 1$, $Le = 1$ and $\Lambda = 0.1$

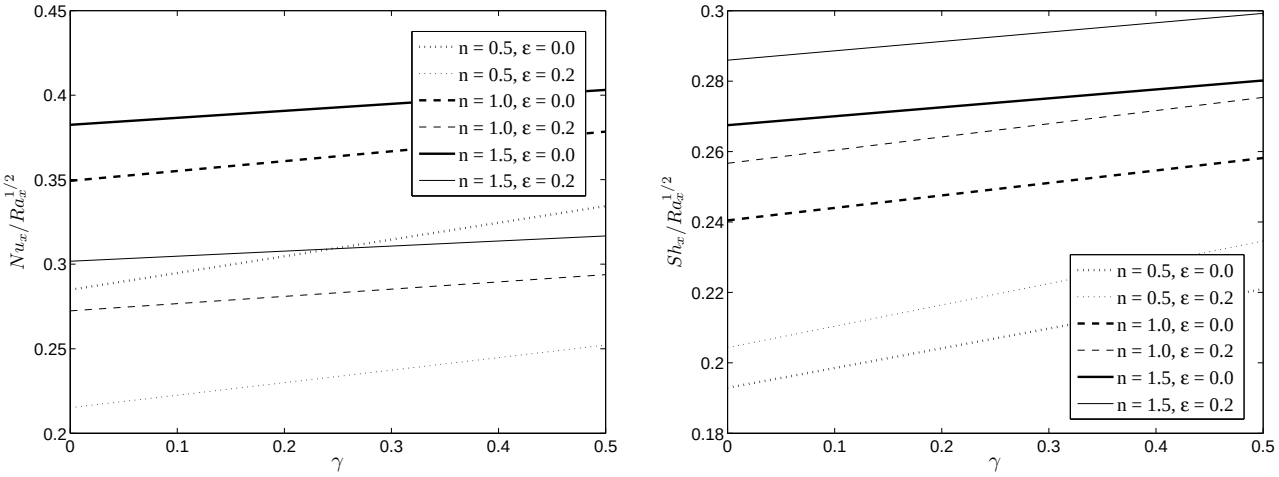

(a) (b)

Figure 3.16: Variation of heat and mass transfer coefficients against γ for varying ε and n when $Sr = 0.5$, $Gr^* = 1$, $Le = 1$ and $\Lambda = -0.1$

3.5 Conclusion

The chapter highlights the Soret effects on the natural convection flow of a variable property non-Newtonian power-law fluid due to a vertical flat plate embedded in a thermally stratified non-Darcy porous medium. The SLM is proven to be an efficient method in handling highly nonlinear coupled boundary value problems arising due to local non-similarity. Temperature and concentration profiles are significantly affected by stratification parameter, Soret number and variable viscosity parameters. The heat and mass transfer coefficients are reduced by the power-law index n in two different flow situations considered. The thermal stratification parameter reduces the Nusselt number but enhances the Sherwood number. The viscosity parameter γ enhances heat and mass transfer coefficients in both cases of $\Lambda > 0$ and $\Lambda < 0$. The Soret number succeeds in enhancing mass transfer coefficient for both $\Lambda > 0$ and $\Lambda < 0$ but reduces the heat transfer coefficient for $\Lambda > 0$ while increasing in the case $\Lambda < 0$.

Chapter 4

Thermal radiation and viscous dissipation effects on mixed convection from a vertical plate in a non-Darcy porous medium*

Abstract

The chapter presents an investigation of the influence of thermal radiation and viscous dissipation on the mixed convective flow due to a vertical plate immersed in a non-Darcy porous medium saturated with a non-Newtonian power-law fluid that exhibits variable viscosity. The Ostwald -de Waele power-law model is used to characterize the non-Newtonian behavior of the fluid. Rosseland approximation is used to describe the radiative heat flux accounted in the energy equation. The governing partial

[0]* Submitted to Acta Mechanica, (2011).

differential equations are transformed into a system of ordinary differential equations and solved numerically using the SLM. The accuracy of the SLM has been tested by comparing the results with those obtained using the shooting technique and with previously published work. The results are analyzed for the effect of various physical parameters such as variable viscosity, thermal radiation, viscous dissipation, mixed convection parameters on dynamics. Skin-friction and heat transfer coefficients are also tabulated for different values of the said parameters.

4.1 Introduction

In recent years, a great deal of interest has been generated in the area of convective heat transfer from a vertical flat plate embedded in a porous medium because of its wide-range of applications in various fields such as thermal insulation, the enhanced recovery of petroleum resource and geophysical flows. The disposal of nuclear waste into the earth's crust or the sea bed is an area of particular interest in the study of convection in a porous medium.

The study of convective heat transfer in a porous medium in non-Newtonian fluids is particularly relevant since a number of industrially important fluids such as molten plastics, polymers, pulps and slurries display non-Newtonian fluid behaviour. Shenoy (1994) presented many interesting applications of non-Newtonian power-law fluids with yield stress on convective heat transport in fluid saturated porous media considering geothermal and oil reservoir engineering applications. A detailed review of Darcy and non-Darcy mixed convection studies can be found in Nield and Bejan (1984).

The natural convection in a non-Newtonian fluid about a horizontal cylinder and sphere and along a vertical plate embedded in a porous medium have been studied

by Chen and Chen (1988a) and Chen and chen (1988b), respectively. The problem of free convection flow of non-Newtonian power-law fluid was studied by Nakayama et al. (1991) for a non-isothermal body of arbitrary shape. The effect of viscous dissipation on a non-Darcy natural convection regime has been considered by Murthy et al. (1997). They observed that a significant decrease in heat transfer can be observed with the inclusion of the viscous dissipation effect.

The effect of viscous dissipation and radiation on the natural convection and heat transfer from vertical flat plate in a non-Darcy porous media saturated with non-Newtonian fluid of variable viscosity has been considered by Kairi et al. (2011a). El-Amin et al. (2003) investigated the influence of viscous dissipation on buoyancy induced flow over a horizontal or a vertical flat plate embedded in a non-Newtonian fluid saturated porous medium. Kumari et al. (2004) studied the non-similar non-Darcy mixed convection flow over a non-isothermal horizontal surface which covers the entire regime of mixed convection flow starting from pure forced convection to pure free convection flow. The effect of variable viscosity on non-Darcy free or mixed convective heat transfer along a vertical surface embedded in a porous medium saturated with a non-Newtonian fluid has been analyzed by Jayanthi et al. (2007). Shenoy (1993) studied the Non-Darcy natural, forced and mixed convection heat transfer in non-Newtonian power-law fluid saturated porous media. Mixed convection flow and heat transfer about an isothermal vertical wall embedded in a fluid saturated porous medium with uniform free stream velocity is considered by Murthy (1998). He analyzed the effects of thermal dispersion and viscous dissipation in both aiding and opposing flows. The problem of mixed convection from a vertical surface embedded in a non-Newtonian power-law fluid saturated non-Darcy porous medium in the presence of melting, radiation and heat generation/absorption effects for aiding and opposing external flows was studied by Chamkha et al. (2010).

The purpose of this chapter is to investigate the effect of viscous dissipation and

the thermal radiation on forced convection from a vertical plate in a non-Darcy porous medium saturated with non-Newtonian fluid possessing variable viscosity property. In particular we model the viscosity variation using Reynolds' law (2004, 2007), which assumes that viscosity decreases exponentially with temperature. We solve the non-linear boundary value problem arising from the non-dimensionalization and local non-similarity method using a novel SLM.

4.2 Basic equations

Consider the steady, laminar, two-dimensional mixed convection boundary layer flow over a semi-infinite vertical flat plate embedded in a non-Darcy porous medium saturated with a non-Newtonian power-law fluid with variable viscosity. A constant free stream velocity U_∞ is assumed. The plate is maintained at a constant temperature T_w and let T_∞ be the ambient temperature. The x-coordinate is measured along the plate from its leading edge and the y-coordinate normal to the plate. Figure 4.1 shows the physical configuration of the problem under consideration. With the usual

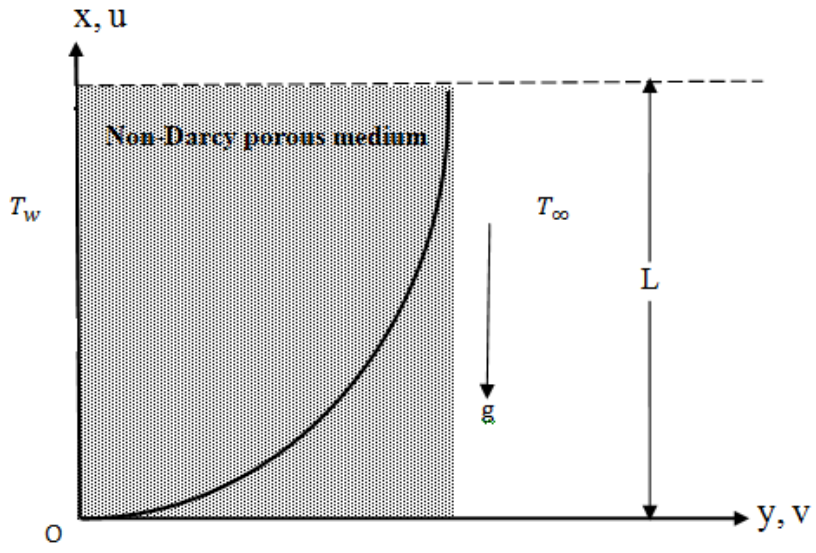

Figure 4.1: Physical model and coordinate system.

boundary layer and Boussinesq approximations, the governing equations, namely the equation of continuity, the non-Darcy flow model and the energy equation for the isotropic and homogeneous porous medium may be written as (see Shenoy 1993);

$$\frac{\partial u}{\partial x}+\frac{\partial v}{\partial y}=0, \tag{4.1}$$

$$\frac{\partial}{\partial y}\left(\frac{\mu}{\rho_\infty K^*}u^n\right)+\frac{\partial}{\partial y}\left(bu^2\right)=\mathrm{g}\beta\frac{\partial T}{\partial y}, \tag{4.2}$$

$$u\frac{\partial T}{\partial x}+v\frac{\partial T}{\partial y}=\alpha\frac{\partial^2 T}{\partial y^2}+\frac{\mu}{\rho_\infty K^* c_p}u\left(u^n+\frac{b\rho_\infty K^*}{\mu}u^2\right)-\frac{1}{\rho_\infty c_p}\frac{\partial q_r}{\partial y}, \tag{4.3}$$

subject to the boundary conditions

$$\left.\begin{aligned} v=0, \quad T=T_w \quad \text{at} \quad y=0, \\ u\to U_\infty, \quad T\to T_\infty \quad \text{as} \quad y\to\infty. \end{aligned}\right\} \tag{4.4}$$

In equations (4.1) - (4.4), u and v are the average velocity components along the x and y directions, respectively, T is the fluid temperature, ρ_∞ is the reference density, g is the acceleration due to gravity, α is the effective thermal diffusivity, β is the coefficient of thermal expansion, c_p is the specific heat at constant pressure, b is the empirical constant associated with the Forchheimer porous inertia term, μ is the consistency index of power law fluid and K^* is the modified permeability of the flow of the non-Newtonian power-law fluid. Here n is the power-law index with $n<1$ representing a pseudoplastic, $n=1$ a Newtonian fluid and $n>1$ a dilatant fluid respectively.

The radiative heat flux term q_r is written using Rosseland approximation (Raptis 1998 and Sparrow 1978) as

$$q_r=-\frac{4\sigma^*}{3k^*}\frac{\partial T^4}{\partial y}, \tag{4.5}$$

where σ^* and k^* are the Stefan-Boltzman constant and the mean absorption coefficient, respectively. The system of non-similar partial differential equations can be

reduced by using the stream function approach

$$u = \frac{\partial \psi}{\partial y} \qquad \text{and} \qquad v = -\frac{\partial \psi}{\partial x}, \tag{4.6}$$

together with the following transformations

$$\eta = \frac{Pe_x^{1/2}}{\chi}\frac{y}{x}, \qquad \psi(\varepsilon,\eta) = \frac{\alpha Pe_x^{1/2}}{\chi} f(\varepsilon,\eta) \qquad \text{and} \qquad \theta(\varepsilon,\eta) = \frac{T - T_\infty}{T_w - T_\infty}, \tag{4.7}$$

where, $\chi^{-1} = 1 + \sqrt{\dfrac{Ra_x}{Pe_x}}$ is mixed convection parameter, $Ra_x = \left(\dfrac{x}{\alpha}\right)\left[\dfrac{\rho_\infty K^* \mathrm{g}\beta(T_w - T_\infty)}{\mu_\infty}\right]^{1/n}$ is the local Rayleigh number and $Pe_x = \dfrac{U_\infty x}{\alpha}$ is the local Peclet number. The fluid viscosity is assumed to obey Reynolds viscosity model (Elbashbeshy 2000 and Massoudi and Phuoc 2004) given by

$$\mu(\theta) = \mu_\infty e^{-\gamma\theta},$$

where γ is the non-dimensional viscosity parameter depending on the nature of the fluid and μ_∞ is the ambient viscosity of the fluid. With the introduction of stream function given in (4.5), the continuity equation (4.1) is automatically satisfied. Now, using the transformations (4.7), the momentum and energy equations, (4.2) and (4.3) respectively, are reduced to the following non-similar equations:

$$\left[n(f')^{n-1} + 2Re^* e^{\gamma\theta} f'\right] f'' = \left[(1-\chi)^{2n} e^{\gamma\theta} + \gamma (f')^n\right] \theta', \tag{4.8}$$

$$\theta'' + \frac{1}{2} f\theta' + \varepsilon e^{-\gamma\theta}(1-\chi)^{-2n}\left(f'^{n+1} + Re^* e^{\gamma\theta} f'^3\right) + \frac{4}{3} R\left[(C_T + \theta)^3 \theta'\right]' = \varepsilon\left(f'\frac{\partial\theta}{\partial\varepsilon} - \theta'\frac{\partial f}{\partial\varepsilon}\right). \tag{4.9}$$

The transformed boundary conditions are

$$\left.\begin{array}{c} f(\varepsilon,\eta) + 2\varepsilon\dfrac{\partial f(\varepsilon,\eta)}{\partial\varepsilon} = 0, \qquad \theta(\varepsilon,\eta) = 1 \qquad \text{at} \qquad \eta = 0, \\ f'(\varepsilon,\eta) \to \chi^2, \qquad\qquad \theta(\varepsilon,\eta) \to 0 \qquad \text{as} \qquad \eta \to \infty, \end{array}\right\} \tag{4.10}$$

where $Re^* = \dfrac{\rho_\infty K^* b}{\mu_\infty}\left(\dfrac{U_\infty}{\chi}\right)^{2-n}$ is the modified Reynolds number, $R = \dfrac{4\sigma^*}{kk^*}(T_w - T_\infty)^3$ is the radiation parameter, $C_T = \dfrac{T_\infty}{T_w - T_\infty}$ is the temperature ratio and $\varepsilon = \dfrac{g\beta x}{c_p}$ is the viscous dissipation parameter. The primes in equations (4.8) - (4.10) represent the differentiation with respect to the variable η. The skin friction and heat transfer coefficients can be respectively obtained from

$$\left.\begin{aligned} \chi^3 Pe_x^{1/2} C_f &= -Pre^{-\gamma} f''(\varepsilon, 0), \\ \chi Pe_x^{-1/2} Nu_x &= -\theta'(\varepsilon, 0), \end{aligned}\right\} \tag{4.11}$$

where $Pr = \dfrac{\nu_\infty}{\alpha}$ is the Prandtl number.

4.3 Method of solution

To solve the system of equations (4.8) and (4.9) subject to the boundary conditions (4.10), we first apply a local similarity and local non-similarity method which has been applied by many investigators (see Minkowycz and Sparrow 1974 and Sparrow and Yu 1971) to solve various non-similarity boundary value problems. For the first level of truncation, the terms accompanied by $\varepsilon\dfrac{\partial}{\partial\varepsilon}$ are assumed to be small. This is particularly true when $\varepsilon \ll 1$. Thus the terms with $\varepsilon\dfrac{\partial}{\partial\varepsilon}$ in equations (4.8) and (4.9) can be neglected to get the following system of equations

$$\left[n(f')^{n-1} + 2Re^* e^{\gamma\theta} f'\right] f'' = \left[(1-\chi)^{2n} e^{\gamma\theta} + \gamma (f')^n\right] \theta', \tag{4.12}$$

$$\theta'' + \frac{1}{2} f\theta' + \varepsilon e^{-\gamma\theta} (1-\chi)^{-2n} \left(f'^{n+1} + Re^* e^{\gamma\theta} f'^3\right) + \frac{4}{3} R\left[(C_T + \theta)^3 \theta'\right]' = 0 \tag{4.13}$$

The corresponding boundary conditions are

$$\left.\begin{aligned} f(\varepsilon,\eta)=0, \qquad \theta(\varepsilon,\eta)=1 \qquad \text{at} \qquad \eta=0, \\ f'(\varepsilon,\eta)\to\chi^2, \qquad \theta(\varepsilon,\eta)\to 0 \qquad \text{as} \qquad \eta\to\infty. \end{aligned}\right\} \tag{4.14}$$

For the second level of truncations, we introduce the variables $g=\dfrac{\partial f}{\partial\varepsilon}$ and $h=\dfrac{\partial\theta}{\partial\varepsilon}$ and recover the neglected terms at the first level of truncation. Thus, the governing equations at the second level are given by

$$\left[n(f')^{n-1}+2Re^*e^{\gamma\theta}f'\right]f''=\left[(1-\chi)^{2n}e^{\gamma\theta}+\gamma(f')^n\right]\theta', \tag{4.15}$$

$$\theta''+\frac{1}{2}f\theta'+\varepsilon e^{-\gamma\theta}(1-\chi)^{-2n}\left(f'^{n+1}+Re^*e^{\gamma\theta}f'^3\right)+\frac{4}{3}R\left[(C_T+\theta)^3\theta'\right]' = \varepsilon\left(f'h-\theta'g\right). \tag{4.16}$$

The corresponding boundary conditions are

$$\left.\begin{aligned} f(\varepsilon,\eta)+2\varepsilon g(\varepsilon,\eta)=0, \qquad \theta(\varepsilon,\eta)=1 \qquad \text{at} \qquad \eta=0, \\ f'(\varepsilon,\eta)\to\chi^2, \qquad \theta(\varepsilon,\eta)\to 0 \qquad \text{as} \qquad \eta\to\infty. \end{aligned}\right\} \tag{4.17}$$

At the third level, we differentiate equations (4.15) - (4.17) with respect to ε and neglect the terms $\dfrac{\partial g}{\partial\varepsilon}$ and $\dfrac{\partial h}{\partial\varepsilon}$ to get the following set of equations

$$\begin{aligned} &\left[n(f')^{n-1}+2Re^*e^{\gamma\theta}f'\right]g''+\left[n(n-1)(f')^{n-2}g'+2Re^*e^{\gamma\theta}(g'+\gamma f'h)\right]f'' \\ &-(1-\chi)^{2n}e^{\gamma\theta}(h'+\gamma\theta'h)-\gamma\left[n(f')^{n-1}\theta'\ g'+(f')^nh'\right]=0, \end{aligned} \tag{4.18}$$

$$\begin{aligned} &\left[1+\frac{4}{3}R(C_T+\theta)^3\right]h''+4R(C_T+\theta)^2h\theta''+8R(C_T+\theta)\theta'[(C_T+\theta)h'+\theta'h] \\ &+(1-\chi)^{-2n}\varepsilon g'\left[3Re^*(f')^2+(n+1)e^{-\gamma\theta}(f')^n)\right]+\varepsilon(h'g-g'h)-f'h \\ &+(1-\chi)^{-2n}\left[Re^*(f')^3+(1-\gamma\varepsilon h)e^{-\gamma\theta}(f')^{n+1}\right]+\frac{1}{2}(fh'+3g\theta')=0. \end{aligned} \tag{4.19}$$

The corresponding boundary conditions are

$$\left.\begin{aligned} g(\varepsilon,\eta)=0, \qquad h(\varepsilon,\eta)=0 \qquad \text{at} \qquad \eta=0, \\ g'(\varepsilon,\eta)\to 0, \qquad h(\varepsilon,\eta)\to 0 \qquad \text{as} \qquad \eta\to\infty. \end{aligned}\right\} \tag{4.20}$$

The set of differential equations (4.15), (4.16), (4.18) and (4.19) together with the boundary conditions (4.17) and (4.20) are solved by means of the (SLM). The SLM algorithm starts with the assumption that the variables $f(\eta)$, $\theta(\eta)$, $g(\eta)$ and $h(\eta)$ can be expressed as

$$\left.\begin{aligned} f(\eta)=f_i(\eta)+\sum_{m=0}^{i-1}F_m(\eta), \qquad \theta(\eta)=\theta_i(\eta)+\sum_{m=0}^{i-1}\Theta_m(\eta), \\ g(\eta)=g_i(\eta)+\sum_{m=0}^{i-1}G_m(\eta), \qquad h(\eta)=h_i(\eta)+\sum_{m=0}^{i-1}H_m(\eta), \end{aligned}\right\} \tag{4.21}$$

where f_i, θ_i, g_i and h_i are unknown functions and F_m, Θ_m, G_m and H_m are successive approximations which are obtained by recursively solving the linear part of the equation system that results from substituting firstly equation (4.21) in equations (4.15) - (4.20). The main assumption of the SLM is that f_i, θ_i, g_i and h_i become increasingly smaller when i becomes large, that is

$$\lim_{i\to\infty} f_i=\lim_{i\to\infty}\theta_i=\lim_{i\to\infty}g_i=\lim_{i\to\infty}h_i=0. \tag{4.22}$$

The initial guesses $F_0(\eta)$, $\Theta_0(\eta)$, $G_0(\eta)$ and $H_0(\eta)$ which are chosen to satisfy the boundary conditions (4.17) and (4.20) which are taken to be

$$\left.\begin{aligned} F_0(\eta)=1+\chi^2\eta-e^{-\eta}, \qquad \Theta_0(\eta)=e^{-\eta} \\ G_0(\eta)=1-\eta e^{-\eta}-e^{-\eta}, \qquad H_0(\eta)=\eta e^{-\eta}. \end{aligned}\right\} \tag{4.23}$$

Thus, starting from the initial guesses, the subsequent solutions F_i, Θ_i, G_i and H_i ($i\geq 1$) are obtained by successively solving the linearised form of the equations which are obtained by substituting equation (4.21) in the governing equations (4.17) - (4.20).

The linearised equations to be solved are

$$a_{1,i-1}F_i'' + a_{2,i-1}F_i' + a_{3,i-1}\Theta_i' + a_{4,i-1}\Theta_i = r_{1,i-1}, \tag{4.24}$$

$$b_{1,i-1}\Theta_i'' + b_{2,i-1}\Theta_i' + b_{3,i-1}\Theta_i + b_{4,i-1}F_i' + b_{5,i-1}F_i + b_{6,i-1}H_i$$
$$+b_{7,i-1}G_i = r_{2,i-1}, \tag{4.25}$$

$$c_{1,i-1}G_i'' + c_{2,i-1}G_i' + c_{3,i-1}F_i'' + c_{4,i-1}F_i' + c_{5,i-1}\Theta_i' + c_{6,i-1}\Theta_i$$
$$+c_{7,i-1}H_i' + c_{8,i-1}H_i = r_{3,i-1}, \tag{4.26}$$

$$d_{1,i-1}H_i'' + d_{2,i-1}H_i' + d_{3,i-1}H_i + d_{4,i-1}F_i' + d_{5,i-1}F_i + d_{6,i-1}\Theta_i''$$
$$+d_{7,i-1}\Theta_i' + d_{8,i-1}\Theta_i + d_{9,i-1}G_i' + d_{10,i-1}G_i = r_{4,i-1}, \tag{4.27}$$

subject to the boundary conditions

$$F_i(0) = F_i'(\infty) = \Theta_i(0) = \Theta_i(\infty) = G_i(0) = G_i'(\infty) = H_i(0) = H_i(\infty) = 0, \tag{4.28}$$

where coefficients $a_{k,i-1}$ $(k = 1, \ldots, 4)$, $b_{k,i-1}$ $(k = 1, \ldots, 7)$, $c_{k,i-1}$ $(k = 1, \ldots, 8)$, $d_{k,i-1}$ $(k = 1, \ldots, 10)$ and $r_{k,i-1}$ $(k = 1, \ldots, 4)$ depend on F_{i-1}, Θ_{i-1}, G_{i-1}, H_{i-1} and on their derivatives.

The solution for F_i, Θ_i, G_i and H_i for $i \geq 1$ has been found by iteratively solving equations (4.24) - (4.28) and finally after M iterations the solutions $f(\eta)$, $\theta(\eta)$, $g(\eta)$ and $h(\eta)$ can be written as

$$\left.\begin{aligned} f(\eta) &\approx \sum_{m=0}^{M} F_m(\eta), \qquad \theta(\eta) \approx \sum_{m=0}^{M} \Theta_m(\eta), \\ g(\eta) &\approx \sum_{m=0}^{M} G_m(\eta), \qquad h(\eta) \approx \sum_{m=0}^{M} H_m(\eta), \end{aligned}\right\} \tag{4.29}$$

where M is termed the order of SLM approximation. Equations (4.24) - (4.28) are solved using the Chebyshev spectral collocation method. The method is based on the Chebyshev polynomials defined on the interval $[-1, 1]$. We first transform the domain

of solution $[0,\infty)$ into the domain $[-1,1]$ using the domain truncation technique where the problem is solved in the interval $[0,L]$ instead of $[0,\infty)$ by using the mapping

$$\frac{\eta}{L}=\frac{\xi+1}{2}, \qquad -1\leq\xi\leq 1, \tag{4.30}$$

where L is the scaling parameter used to invoke the boundary condition at infinity. We discretize the domain $[-1,1]$ using the popular Gauss-Lobatto collocation points given by

$$\xi=\cos\frac{\pi j}{N}, \qquad j=0,1,2,\ldots,N, \tag{4.31}$$

where N is the number of collocation points used. The functions F_i, Θ_i, G_i and H_i for $i\geq 1$ are approximated at the collocation points as follows

$$\left.\begin{aligned} F_i(\xi)&\approx\sum_{k=0}^{N}F_i(\xi_k)T_k(\xi_j),\ \Theta_i(\xi)\approx\sum_{k=0}^{N}\Theta_i(\xi_k)T_k(\xi_j),\\ G_i(\xi)&\approx\sum_{k=0}^{N}G_i(\xi_k)T_k(\xi_j),\ H_i(\xi)\approx\sum_{k=0}^{N}H_i(\xi_k)T_k(\xi_j),\end{aligned}\right\}\ j=0,1,...,N, \tag{4.32}$$

where T_k is the k^{th} Chebyshev polynomial given by

$$T_k(\xi)=\cos\left[k\cos^{-1}(\xi)\right]. \tag{4.33}$$

The derivatives of the variables at the collocation points are represented as

$$\left.\begin{aligned} \frac{d^rF_i}{d\eta^r}&=\sum_{k=0}^{N}\mathbf{D}_{kj}^rF_i(\xi_k),\ \frac{d^r\Theta_i}{d\eta^r}=\sum_{k=0}^{N}\mathbf{D}_{kj}^r\Theta_i(\xi_k),\\ \frac{d^rG_i}{d\eta^r}&=\sum_{k=0}^{N}\mathbf{D}_{kj}^rG_i(\xi_k),\ \frac{d^rH_i}{d\eta^r}=\sum_{k=0}^{N}\mathbf{D}_{kj}^rH_i(\xi_k),\end{aligned}\right\}\quad j=0,1,...,N, \tag{4.34}$$

where r is the order of differentiation and $\mathbf{D}=\frac{2}{L}\mathcal{D}$ with $\mathcal{D}$ being the Chebyshev spectral differentiation matrix whose entries are defined in (1.30) Substituting equations

(4.24) - (4.28) into equations (4.30) - (4.34) leads to the matrix equation

$$\mathbf{A}_{i-1}\mathbf{X}_i = \mathbf{R}_{i-1}. \tag{4.35}$$

In equation (4.35), $\mathbf{A}_{i-1}$ is a $(4N+4)\times(4N+4)$ square matrix and $\mathbf{X}_i$ and $\mathbf{R}_{i-1}$ are $(4N+4)\times 1$ column vectors defined by

$$\mathbf{A}_{i-1} = \begin{bmatrix} A_{11} & A_{12} & A_{13} & A_{14} \\ A_{21} & A_{22} & A_{23} & A_{24} \\ A_{31} & A_{32} & A_{33} & A_{34} \\ A_{41} & A_{42} & A_{43} & A_{44} \end{bmatrix}, \qquad \mathbf{X}_i = \begin{bmatrix} F_i \\ \Theta_i \\ G_i \\ H_i \end{bmatrix}, \qquad \mathbf{R}_{i-1} = \begin{bmatrix} \mathbf{r}_{1,i-1} \\ \mathbf{r}_{2,i-1} \\ \mathbf{r}_{3,i-1} \\ \mathbf{r}_{4,i-1} \end{bmatrix}, \tag{4.36}$$

where

$$\begin{aligned} F_i &= [f_i(\xi_0), f_i(\xi_1), ..., f_i(\xi_{N-1}), f_i(\xi_N)]^T, \\ \Theta_i &= [\theta_i(\xi_0), \theta_i(\xi_1), ..., \theta_i(\xi_{N-1}), \theta_i(\xi_N)]^T, \\ G_i &= [g_i(\xi_0), g_i(\xi_1), ..., g_i(\xi_{N-1}), g_i(\xi_N)]^T, \\ H_i &= [h_i(\xi_0), h_i(\xi_1), ..., h_i(\xi_{N-1}), h_i(\xi_N)]^T, \end{aligned}$$

$$\begin{aligned} \mathbf{r}_{1,i-1} &= [r_{1,i-1}(\xi_0), r_{1,i-1}(\xi_1), ..., r_{1,i-1}(\xi_{N-1}), r_{1,i-1}(\xi_N)]^T, \\ \mathbf{r}_{2,i-1} &= [r_{2,i-1}(\xi_0), r_{2,i-1}(\xi_1), ..., r_{2,i-1}(\xi_{N-1}), r_{2,i-1}(\xi_N)]^T, \\ \mathbf{r}_{3,i-1} &= [r_{3,i-1}(\xi_0), r_{3,i-1}(\xi_1), ..., r_{3,i-1}(\xi_{N-1}), r_{3,i-1}(\xi_N)]^T, \\ \mathbf{r}_{4,i-1} &= [r_{4,i-1}(\xi_0), r_{4,i-1}(\xi_1), ..., r_{4,i-1}(\xi_{N-1}), r_{4,i-1}(\xi_N)]^T, \end{aligned}$$

$$A_{11} = \mathbf{a}_{1,i-1}\mathbf{D}^2 + \mathbf{a}_{2,i-1}\mathbf{D}, \qquad A_{12} = \mathbf{a}_{3,i-1}\mathbf{D} + \mathbf{a}_{4,i-1}\mathbf{I}, \qquad A_{13} = \mathbf{O},$$

$$A_{14} = \mathbf{O}, \qquad A_{21} = \mathbf{b}_{4,i-1}\mathbf{D} + \mathbf{b}_{5,i-1}\mathbf{I}, \qquad A_{22} = \mathbf{b}_{1,i-1}\mathbf{D}^2 + \mathbf{b}_{2,i-1}\mathbf{D} + \mathbf{b}_{3,i-1}\mathbf{I},$$

$$A_{23} = \mathbf{b}_{7,i-1}\mathbf{I}, \qquad A_{24} = \mathbf{b}_{6,i-1}\mathbf{I}, \qquad A_{31} = \mathbf{c}_{3,i-1}\mathbf{D}^2 + \mathbf{c}_{4,i-1}\mathbf{D},$$

$$A_{32} = \mathbf{c}_{5,i-1}\mathbf{D} + \mathbf{c}_{6,i-1}\mathbf{I}, \qquad A_{33} = \mathbf{c}_{1,i-1}\mathbf{D}^2 + \mathbf{c}_{2,i-1}\mathbf{D}, \qquad A_{34} = \mathbf{c}_{7,i-1}\mathbf{D} + \mathbf{c}_{8,i-1}\mathbf{I},$$

$$A_{41} = \mathbf{d}_{4,i-1}\mathbf{D} + \mathbf{d}_{5,i-1}\mathbf{I}, \qquad A_{42} = \mathbf{d}_{6,i-1}\mathbf{D}^2 + \mathbf{d}_{7,i-1}\mathbf{D} + \mathbf{d}_{8,i-1}\mathbf{I},$$

$$A_{43} = \mathbf{d}_{9,i-1}\mathbf{D} + \mathbf{d}_{10,i-1}\mathbf{I}, \qquad A_{44} = \mathbf{d}_{1,i-1}\mathbf{D}^2 + \mathbf{d}_{2,i-1}\mathbf{D} + \mathbf{d}_{3,i-1}\mathbf{I}.$$

In the above definitions T stands for transpose, $\mathbf{a}_{k,i-1}$ $(k = 1, \ldots, 4)$, $\mathbf{b}_{k,i-1}$ $(k = 1, \ldots, 7)$, $\mathbf{c}_{k,i-1}$ $(k = 1, \ldots, 8)$, $\mathbf{d}_{k,i-1}$ $(k = 1, \ldots, 10)$ and $\mathbf{r}_{k,i-1}$ $(k = 1, \ldots, 4)$ are diagonal matrices of order $(N+1) \times (N+1)$, $\mathbf{I}$ is an identity matrix of order $(N+1) \times (N+1)$ and $\mathbf{O}$ is zero matrix of order $(N+1) \times (N+1)$. Finally the solution is obtained as

$$\mathbf{X}_i = \mathbf{A}_{i-1}^{-1}\mathbf{R}_{i-1}. \tag{4.37}$$

4.4 Results and discussion

In this chapter we discuss the results obtained through the solution of the system (4.15) - (4.20). We used the SLM in generating the results presented in this study. We have taken $L = 15$ and $N = 60$ for the implementation of SLM. Further, we restrict ourselves to the following values parameters $0.5 \leq n \leq 1.5$, $0 \leq \varepsilon \leq 0.2$, $0 \leq \gamma \leq 2$, $0 \leq R \leq 2$ and take fixed values $Re^* = 1$, $\chi = 0.5$ and $C_T = 0.1$.

In order to validate the SLM solution procedure we compare the SLM results with the previous studies by Kairi (2011a) and Murthy (1997) and the numerical solution obtained by the shooting technique that uses the Runge-Kutta-Fehlberg (RKF45) and Newton-Raphson schemes. The heat transfer coefficients in the case of a Newtonian fluid in absence of dispersion is shown in Table 4.1. It is evident that our results are

in excellent agreement with those of Kairi (2011a) and Murthy (1997).

Table 4.1: Comparison between some previous studies and present results of heat transfer coefficient $-\theta'(0)$ at different values of ε when $n = 1$, $Re^* = 1$, $\gamma = 0$, $R = 0$, $C_T = 0$, and $\chi = 0$

ε	Murthy (1997)	Kairi (2011a)	4^{th} order SLM	Shooting method
0.0	0.3658	0.3658	0.3658	0.3658
0.01	0.3619	0.3619	0.3619	0.3619
0.1	0.3261	0.3262	0.3262	0.3262

Table 4.2: Effect of dissipation parameter ε on $-f''(0)$ and $-\theta'(0)$ when $R = 0.1$, $C_T = 0.5$, $\chi = 0.5$, $\gamma = 1$ and $Re^* = 1$ for different values of n

Quantity	ε	$n = 0.5$		$n = 1$		$n = 1.5$	
		SLM	Shooting	SLM	Shooting	SLM	Shooting
$-f''(0)$	0.00	0.154934	0.154934	0.089516	0.089516	0.049431	0.049431
	0.05	0.131315	0.131314	0.074797	0.074797	0.040131	0.040131
	0.10	0.106934	0.106933	0.059661	0.059661	0.030597	0.030597
	0.20	0.056021	0.056019	0.028059	0.028058	0.010747	0.010747
$-\theta'(0)$	0.00	0.350818	0.350818	0.296413	0.296413	0.265913	0.265913
	0.05	0.297337	0.297335	0.247675	0.247674	0.215883	0.215882
	0.10	0.242131	0.242129	0.197556	0.197555	0.164595	0.164593
	0.20	0.126849	0.126845	0.092913	0.092910	0.057815	0.057811

The skin-friction and heat transfer coefficients are tabulated in Tables 4.2 - 4.4 for various values of ε, γ and R for the cases of a pseudoplastic, Newtonian and dilatant fluids. We observe from Tables 4.2 and 4.4 that the heat transfer coefficient decreases with increasing values of the viscous dissipation parameter ε and radiation parameter R in the cases of a pseudoplastic, Newtonian and dilatant fluids. These results concur with those reported by Kairi et al. (2011a) and Murthy et al. (1997). The heat transfer coefficient increases with an increase in the variable viscosity parameter γ in cases of

Table 4.3: Effect of variable viscosity parameter γ on $-f''(0)$ and $-\theta'(0)$ when $R = 0.1$, $C_T = 0.5$, $\chi = 0.5$, $\varepsilon = 0.1$ and $Re^* = 1$ for different values of n

Quantity	γ	$n = 0.5$		$n = 1$		$n = 1.5$	
		SLM	Shooting	SLM	Shooting	SLM	Shooting
$-f''(0)$	0.0	0.056144	0.056144	0.023605	0.023605	0.011987	0.011987
	0.5	0.093851	0.093851	0.046221	0.046221	0.023091	0.023091
	1.0	0.106934	0.106933	0.059661	0.059661	0.030597	0.030597
	2.0	0.100208	0.100208	0.061748	0.061748	0.033482	0.033482
$-\theta'(0)$	0.0	0.200838	0.200838	0.170218	0.170218	0.148810	0.148810
	0.5	0.225418	0.225417	0.185401	0.185400	0.157385	0.157384
	1.0	0.242131	0.242130	0.197556	0.197555	0.164595	0.164594
	2.0	0.261356	0.261354	0.213539	0.213537	0.174709	0.174707

pseudoplastic, Newtonian and dilatant fluids as can be seen from Table 4.3. Similar behavior was observed by Jayanthi et al. (2007) and Kairi et al. (2011a).

Table 4.4: Effect radiation parameter R on $-f''(0)$ and $-\theta'(0)$ when $Re^* = 1$, $C_T = 0.5$, $\gamma = 1$, $\varepsilon = 0.1$ and $\chi = 0.5$ for different values of n

Quantity	R	$n = 0.5$		$n = 1$		$n = 1.5$	
		SLM	Shooting	SLM	Shooting	SLM	Shooting
$-f''(0)$	0.0	0.138429	0.138429	0.077319	0.077319	0.039690	0.039690
	0.5	0.064052	0.064052	0.035658	0.035657	0.018257	0.018257
	1.0	0.047218	0.047218	0.026265	0.026264	0.013446	0.013446
	2.0	0.034067	0.034067	0.018951	0.018950	0.009716	0.009716
$-\theta'(0)$	0.0	0.313446	0.313446	0.256026	0.256026	0.213510	0.213510
	0.5	0.145034	0.145033	0.118073	0.118072	0.098211	0.098210
	1.0	0.106917	0.106916	0.086970	0.086969	0.072333	0.072331
	2.0	0.077139	0.077138	0.062751	0.062749	0.052268	0.052265

Table 4.3 shows that the skin-friction coefficient increases with the increase in

the variable viscosity parameter γ in the cases $n = 1$ and $n > 1$ while for $n < 1$ it initially increases and then start decreasing. The viscous dissipation parameter ε and the radiation parameter R have decreasing effect on the skin-friction coefficient for all three kinds of power-law liquids considered. The same is reiterated in Tables 4.2 and 4.4. The overall effect of power-law index is to reduce both skin-friction and heat transfer coefficients as can be seen from Tables 4.2 - 4.4.

The variation of velocity and temperature profiles are displayed through Figures 4.2 - 4.7 for selected values of the parameters in the cases of pseudoplastic, Newtonian and dilatant fluids. Figures 4.2 - 4.3 illustrate the variation of axial velocity $f'(\eta)$ and temperature distribution $\theta(\eta)$ for pseudoplastics, Newtonian and dilatant fluids for with respect to dissipation parameter ε. It is observed from these figures that an increasing in the dissipation parameter ε increases the velocity and temperature distributions for all values of the power-law index n. Similar observations were made by Kairi et al. (2011a).

The effect of variable viscosity parameter γ on the axial velocity distribution and the temperature distribution are projected in Figures 4.4 and 4.5 while the other parameter are fixed. It can be seen that increasing values of γ correspond to increasing the momentum boundary layer thickness for any value of the power-law index n. But the opposite is true in case of temperature distribution as shown in Figure 4.5.

Figures 4.6 and 4.7 highlight the effect of the thermal radiation parameter R for $n = 0.5$, $n = 1$ and $n = 1.5$ on the axial velocity and temperature distributions, respectively. It is evident from these figures that the thermal radiation parameter R has an increasing effect on both axial velocity and temperature distributions for any value of the power-law index n.

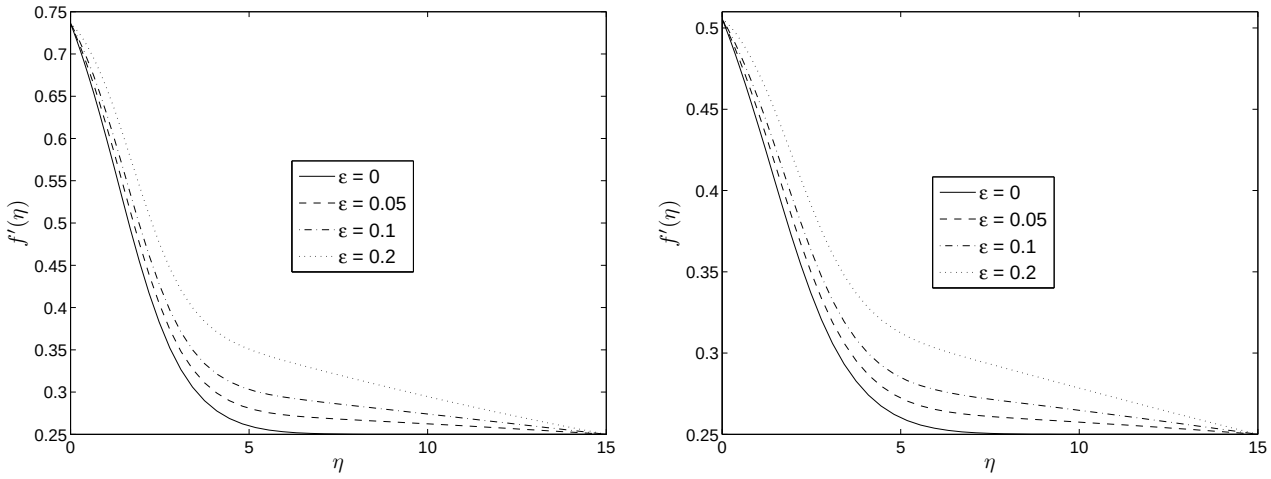

(a)

(b)

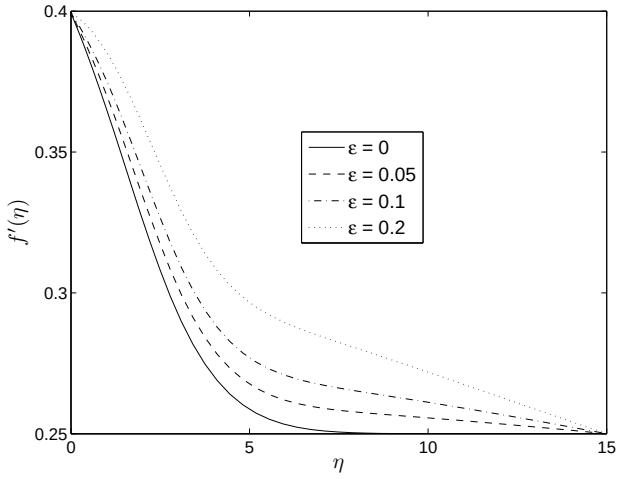

(c)

Figure 4.2: Variation of velocity distribution with η varying ε when $Re^* = 1$, $\gamma = 0.5$, $R = 0.5$, $C_T = 0.1$, and $\chi = 0.5$ for (a) $n = 0.5$ (b) $n = 1$ and (c) $n = 1.5$

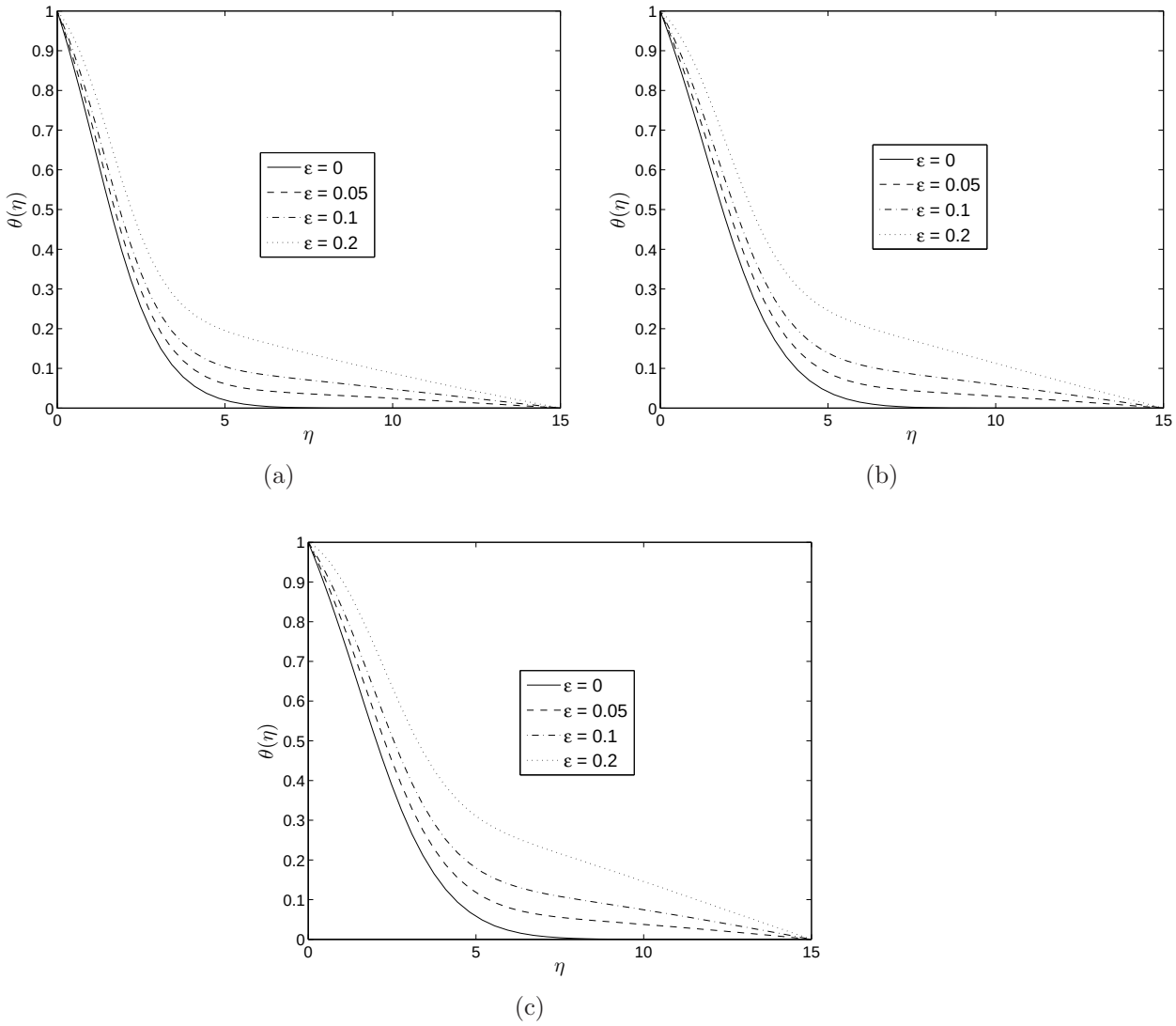

Figure 4.3: Variation of temperature distribution with η varying ε when $Re^* = 1$, $\gamma = 0.5$, $R = 0.5$, $C_T = 0.1$, and $\chi = 0.5$ for (a) $n = 0.5$ (b) $n = 1$ and (c) $n = 1.5$

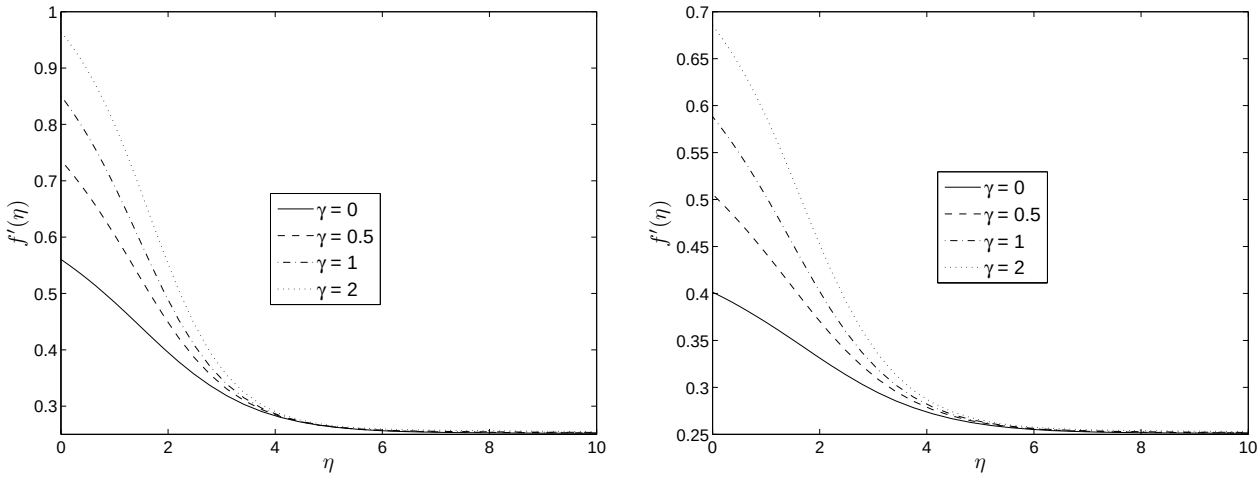

(a) (b)

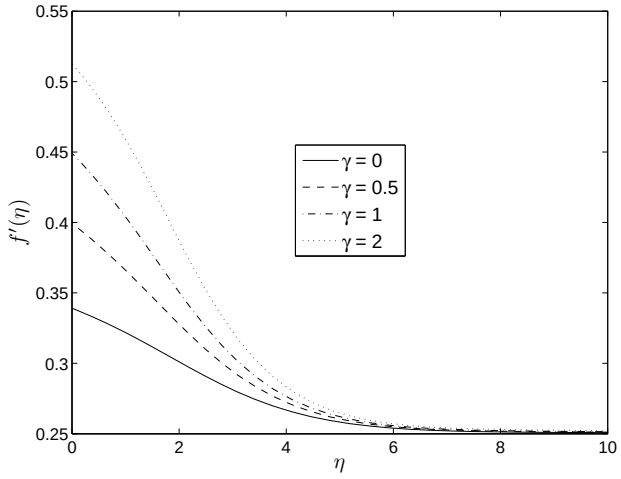

(c)

Figure 4.4: Variation of velocity distribution with η varying γ when $Re^* = 1$, $R = 0.5$, $C_T = 0.1$, $\varepsilon = 0.01$, and $\chi = 0.5$ for (a) $n = 0.5$ (b) $n = 1$ and (c) $n = 1.5$

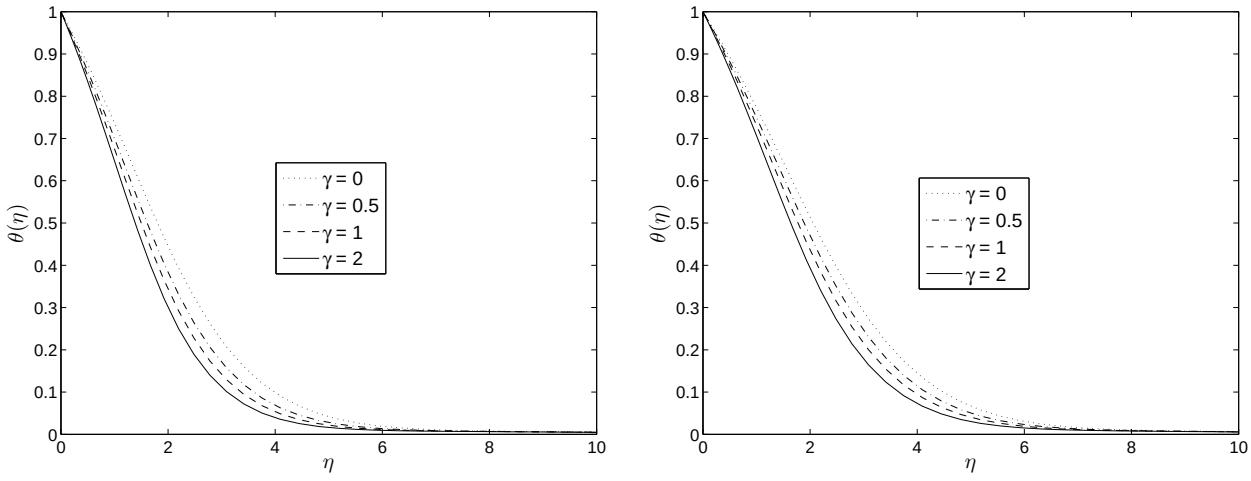

(a) (b)

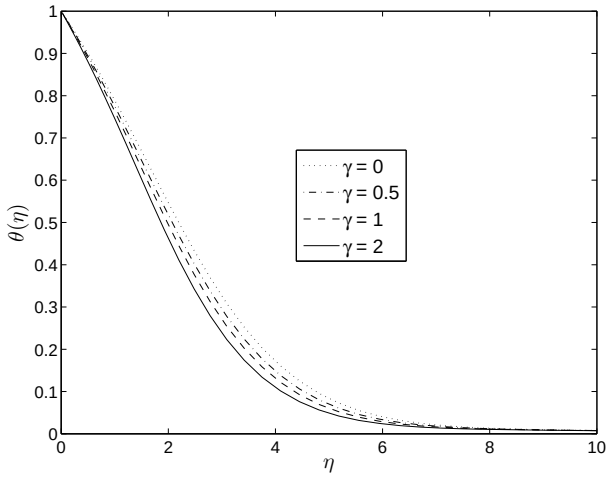

(c)

Figure 4.5: Variation of temperature distribution with η varying γ when $Re^* = 1$, $R = 0.5$, $C_T = 0.1$, $\varepsilon = 0.01$, and $\chi = 0.5$ for (a) $n = 0.5$ (b) $n = 1$ and (c) $n = 1.5$

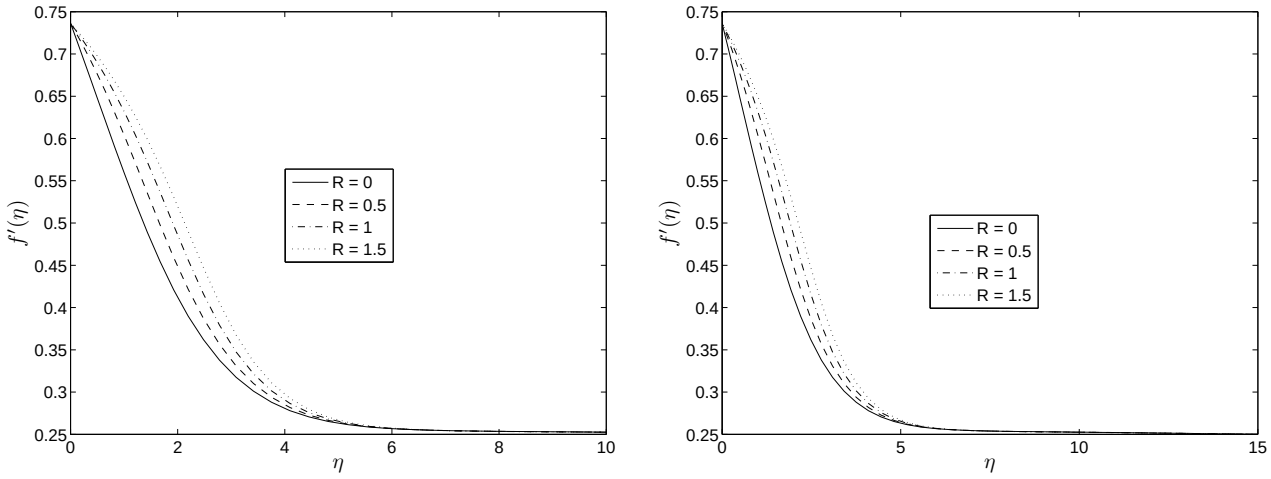

(a)

(b)

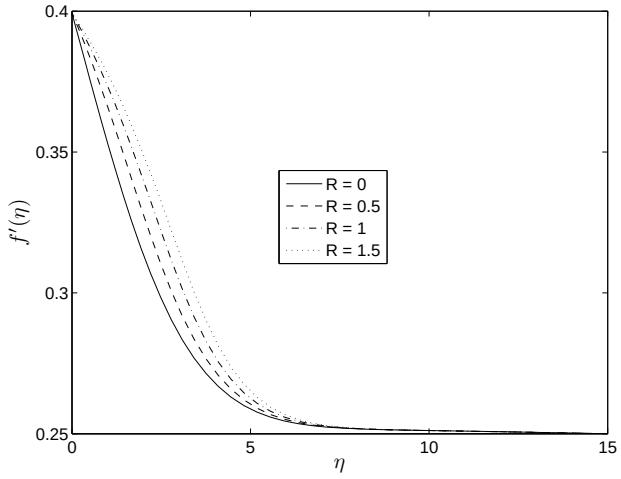

(c)

Figure 4.6: Variation of velocity distribution with η varying R when $Re^* = 1$, $C_T = 0.1$, $\chi = 0.5$, $\varepsilon = 0.01$, and $\gamma = 0.5$ for (a) $n = 0.5$ (b) $n = 1$ and (c) $n = 1.5$

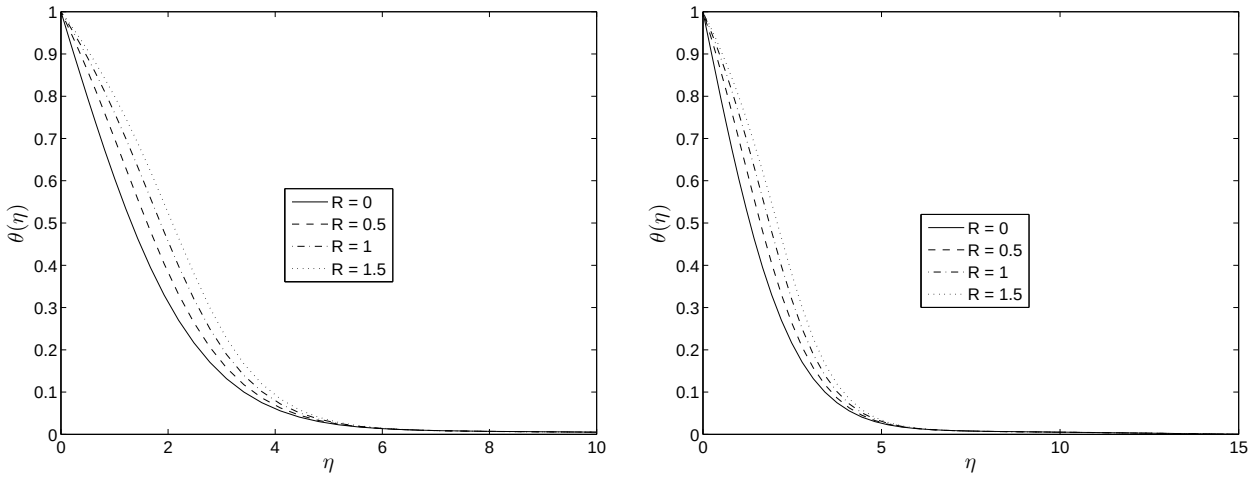

(a)

(b)

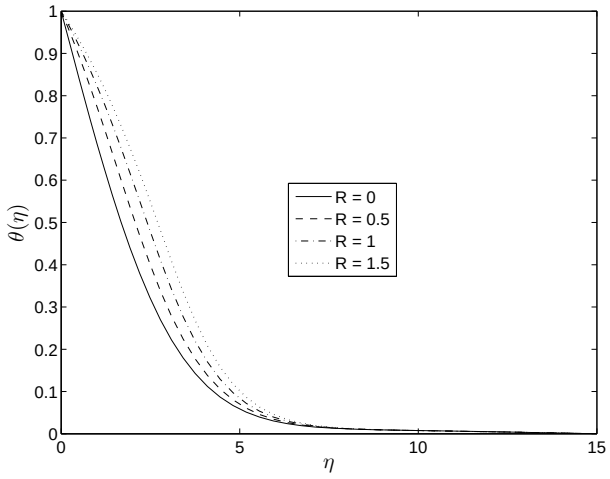

(c)

Figure 4.7: Variation of temperature distribution with η varying R when $Re^* = 1$, $C_T = 0.1$, $\chi = 0.5$, $\varepsilon = 0.01$, and $\gamma = 0.5$ for (a) $n = 0.5$ (b) $n = 1$ and (c) $n = 1.5$

4.5 Conclusion

In this chapter the effects of viscous dissipation, thermal radiation and variable viscosity on the mixed convective flow of a non-Newtonian power-law fluid from a vertical flat plate embedded in a non-Darcy porous medium are addressed. The SLM is proven to be an efficient method in handling highly nonlinear coupled boundary value problems arising due to local non-similarity. Velocity and temperature profiles are significantly affected by viscous dissipation, thermal radiation and variable viscosity parameters. The heat transfer coefficient decreases with increases in the power-law index n, dissipation parameter ε and thermal radiation parameter R while the opposite is true in the case of the viscosity parameter γ.

Chapter 5

On cross-diffusion effects on flow over a vertical surface using a linearisation method*

Abstract

In this chapter we explore the use of a non-perturbation linearisation method to solve the coupled highly nonlinear system of equations due to flow over a vertical surface subject to a magnetic field. The linearisation method is used in combination with an asymptotic expansion technique. The effects of Dufour, Soret and magnetic filed parameters are investigated. The velocity, temperature and concentration distributions as well as the skin-friction, heat and mass transfer coefficients have been obtained and discussed for various physical parametric values. The accuracy of the solutions has been tested using a local nonsimilarity method. The results show that the non-perturbation technique is an accurate numerical algorithm that converges rapidly and

[0]* Boundary Value Problems 2012:25, DOI:10.1186/1687-2770-2012-25, (2012), (available online).

may serve as a viable alternative to finite difference and finite element methods for solving nonlinear boundary value problems.

5.1 Introduction

Convection driven by density variations caused by two different components which have different rates of diffusion plays an important role in fluid dynamics since such flows occur naturally in many physical and engineering processes. Heat and salt in sea water provide perhaps the best known example of double-diffusive convection, Stern (1960). Other examples of double diffusive convection are encountered in diverse applications such as in chemical and petroleum industries, filtration processes, food processing, geophysics and in the modelling of solar ponds and magma chambers. A review of the literature in this subject can be found in Nield and Bejan (1999).

One of the earliest studies of double diffusive convection was by Nield (1968). Baines and Gill (1969) investigated linear stability boundaries while Rudraiah et al. (1982) used the nonlinear perturbation theory to investigate the onset of double diffusive convection in a horizontal porous layer. Poulikakos (1986) presented the linear stability analysis of thermosolutal convection using the Darcy-Brinkman model. Bejan and Khair (1985) presented a multiple scale analysis of heat and mass transfer about a vertical plate embedded in a porous medium. They considered concentration gradients which aid or oppose thermal gradients. Related studies on double diffusive convection have been undertaken by, among others, Lai (1990), Afify (2004) and Makinde and Sibanda (2008).

Investigations by, among others, Eckert and Drake (1972) and Mortimer and Eyring (1980) have provided examples of flows such as in the geosciences, where diffusion-thermo and thermal-diffusion effects are quite significant. Anjalidevi and

Devi (2011) showed that diffusion-thermo and thermal-diffusion effects are significant when density differences exist in the flow regime. In general, Diffusion-thermo and thermal-diffusion effects have been found to be particularly important for intermediate molecular weight gases in binary systems that are often encountered in chemical engineering processes. Theoretical studies of the Soret and Dufour effects on double diffusive convection have been made by many researchers, among them, Kafoussias and Williams (1995), Postelnicu (2004), Mansour et al. (2008), Narayana and Sibanda (2010) and Awad et al. (2010b).

In this chapter we investigate convective heat and mass transfer along a vertical flat plate in the presence of diffusion-thermo, thermal diffusion effects and an external magnetic field. The governing momentum, heat and mass transfer equations are, in general, strongly coupled and highly nonlinear. In this chapter, the coupled set of differential equations that describe convective heat and mass transfer flow along a vertical flat plate in the presence of diffusion-thermo, thermal diffusion effects and an external magnetic field are solved using the successive linearisation method. A non-similarity technique is used to validate the linearisation method.

5.2 Equations of motion

We consider the problem of double diffusive convection along a vertical plate with an external magnetic field imposed along the y-axis. The induced magnetic field is assumed to be negligible. The fluid temperature and solute concentration in the ambient fluid are T_∞, C_∞ and those at the surface are T_w and C_w respectively. The coordinates system and the flow configuration are shown in Figure 5.1. Under the usual boundary layer and Boussinesq approximations the governing equations for a

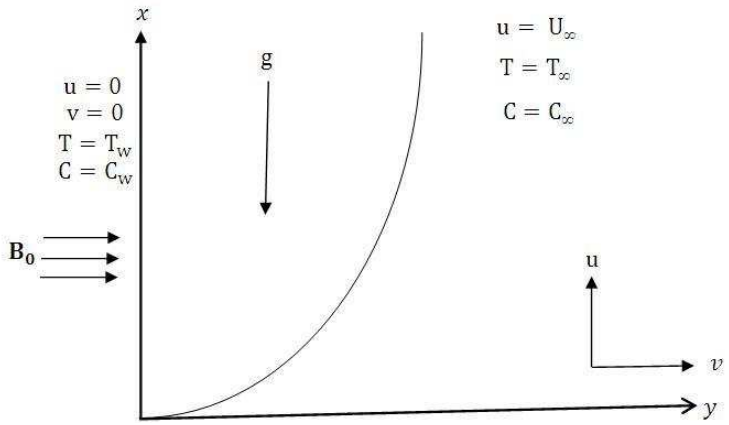

Figure 5.1: Physical model and coordinate system

viscous incompressible fluid may be written as (Kafoussias and Williams 1995);

$$\frac{\partial u}{\partial x} + \frac{\partial v}{\partial y} = 0, \tag{5.1}$$

$$u\frac{\partial u}{\partial x} + v\frac{\partial u}{\partial y} = \nu\frac{\partial^2 u}{\partial y^2} - \frac{\sigma B_0^2}{\rho}u + \mathrm{g}\beta_T(T - T_\infty) + \mathrm{g}\beta_C(C - C_\infty), \tag{5.2}$$

$$u\frac{\partial T}{\partial x} + v\frac{\partial T}{\partial y} = \alpha\frac{\partial^2 T}{\partial y^2} + \frac{D_m k_T}{c_s c_p}\frac{\partial^2 C}{\partial y^2}, \tag{5.3}$$

$$u\frac{\partial C}{\partial x} + v\frac{\partial C}{\partial y} = D_m\frac{\partial^2 C}{\partial y^2} + \frac{D_m k_T}{T_m}\frac{\partial^2 T}{\partial y^2}, \tag{5.4}$$

subject to the boundary conditions

$$u = 0,\ \ v = 0,\ \ T = T_w,\ \ C = C_w \quad \text{on} \quad y = 0, \tag{5.5}$$

$$u = U_\infty,\ \ T = T_\infty,\ \ C = C_\infty \quad \text{when} \quad y \to \infty. \tag{5.6}$$

where u and v are the velocity components along the x- and y- axes respectively, T and C are the fluid temperature and solute concentration across the boundary layer, ν is the kinematic viscosity, ρ is the fluid density, σ is the electrical conductivity, B_0 is the uniform magnetic field, β_T and β_C are the coefficients of thermal and solutal expansions, D_m is the thermal diffusivity, k_T is the thermal diffusion ratio, c_s is the concentration susceptibility, c_p is the fluid specific heat capacity, T_m is the mean fluid

temperature, U_∞ is the free stream velocity and g is the gravitational acceleration.

To satisfy the continuity equation (5.1), we define the stream function ψ in terms of the velocity by

$$u = \frac{\partial \psi}{\partial y} \quad \text{and} \quad v = -\frac{\partial \psi}{\partial x},$$

and introduce the following dimensionless variables

$$\left.\begin{aligned} \xi = \frac{x}{\ell},\ \eta = \left(\frac{U_\infty}{\nu \xi}\right)^{1/2} y,\ \ \psi = (U_\infty \nu \xi)^{1/2} f(\xi, \eta), \\ \theta(\xi, \eta) = \frac{T - T_\infty}{T_w - T_\infty},\ \ \phi(\xi, \eta) = \frac{C - C_\infty}{C_w - C_\infty}, \end{aligned}\right\} \tag{5.7}$$

where, without loss of generality, we take the constant length ℓ to be unity in the subsequent analysis. Using equations (5.7) in (5.2) - (5.4), we get the transformed equations

$$f''' + \frac{1}{2} f f'' - Ha_x f' + Gr_x \theta + Gc_x \phi = \xi \left(f' \frac{\partial f'}{\partial \xi} - f'' \frac{\partial f}{\partial \xi} \right), \tag{5.8}$$

$$\frac{1}{Pr} \theta'' + \frac{1}{2} f \theta' + D_f \phi'' = \xi \left(f' \frac{\partial \theta}{\partial \xi} - \theta' \frac{\partial f}{\partial \xi} \right), \tag{5.9}$$

$$\frac{1}{Sc} \phi'' + \frac{1}{2} f \phi' + S_r \theta'' = \xi \left(f' \frac{\partial \phi}{\partial \xi} - \phi' \frac{\partial f}{\partial \xi} \right), \tag{5.10}$$

with corresponding boundary conditions

$$\left.\begin{aligned} f = 0,\ \ f' = 0,\ \ \theta = 1,\ \ \phi = 1, \quad \text{on} \quad \eta = 0, \\ f' = 1,\ \ \theta = 0,\ \ \phi = 0, \quad \text{when} \quad \eta \to \infty. \end{aligned}\right\} \tag{5.11}$$

The fluid and physical parameters in equations (5.8) - (5.10) are the local thermal and solutal Grashof numbers Gr_x and Gc_x, the local magnetic field parameter Ha_x, the Prandtl number Pr, the Dufour number D_f, the Soret number S_r and the Schmidt

number Sc. These parameters are defined as follows

$$Gr_x = \frac{g\beta_T(T_w - T_\infty)x}{\nu^2}, \quad Gc_x = \frac{g\beta_C(C_w - C_\infty)x}{\nu^2}, \quad Ha_x = \frac{\sigma B_0^2 x}{\rho U_\infty}, \quad Pr = \frac{\nu}{\alpha},$$
$$D_f = \frac{D_m K_T(C_w - C_\infty)}{\alpha C_s C_p(T_w - T_\infty)}, \quad S_r = \frac{K_T D_m(T_w - T_\infty)}{\alpha T_m(C_w - C_\infty)}, \quad Sc = \frac{\nu}{D_m}.$$

The parameters of engineering interest in heat and mass transport problems are the skin friction coefficient C_{fx}, the Nusselt number Nu_x and the Sherwood number Sh_x. These parameters characterize the surface drag, the wall heat and mass transfer rates respectively, and are defined by

$$C_{fx} = \frac{\mu}{\rho U^2}\left(\frac{\partial u}{\partial y}\right)_{y=0} = \frac{f''(\xi,0)}{\sqrt{Re_x}}, \tag{5.12}$$

$$Nu_x = \frac{-x}{T_w - T_\infty}\left(\frac{\partial T}{\partial y}\right)_{y=0} = -\sqrt{Re_x}\,\theta'(\xi,0), \tag{5.13}$$

and

$$Sh_x = \frac{-x}{C_w - C_\infty}\left(\frac{\partial C}{\partial y}\right)_{y=0} = -\sqrt{Re_x}\,\phi'(\xi,0), \tag{5.14}$$

where $Re_x = U_\infty x/\nu$.

5.3 Method of solution

The main challenge in using the linearisation method as described in section 1.5 is how to generalize the method so as to find solutions of partial differential equations of the form (5.8) - (5.10). It is certainly not clear how the method may be applied directly to the terms on the right hand side of equations (5.8) - (5.10). For this reason, equations (5.8) - (5.10) are first simplified and reduced to sets of ordinary differential equations by assuming regular perturbation expansions for f, θ and ϕ in powers of ξ

(which is assumed to be small) as follows

$$\left.\begin{aligned} f = f_{M_1}(\eta,\xi) = \sum_{i=0}^{M_1} \xi^i f_i(\eta), \quad \theta = \theta_{M_1}(\eta,\xi) = \sum_{i=0}^{M_1} \xi^i \theta_i(\eta), \\ \phi = \phi_{M_1}(\eta,\xi) = \textstyle\sum_{i=0}^{M_1} \xi^i \phi_i(\eta) \end{aligned}\right\} \tag{5.15}$$

where M_1 is the order of the approximate solution. Substituting (5.15) into equations (5.8)-(5.10) and equating the coefficients of like powers of ξ, we obtain the zeroth order set of ordinary differential equations

$$f_0''' + \frac{1}{2} f_0 f_0'' - Ha_x f_0' + Gr_x \theta_0 + Gc_x \phi_0 = 0, \tag{5.16}$$

$$\frac{1}{Pr}\theta_0'' + \frac{1}{2} f_0 \theta_0' + D_f \phi_0'' = 0, \tag{5.17}$$

$$\frac{1}{Sc}\phi_0'' + \frac{1}{2} f_0 \phi_0' + S_r \theta_0'' = 0, \tag{5.18}$$

with corresponding boundary conditions

$$\left.\begin{aligned} f_0 = 0,\ f_0' = 0,\ \theta_0 = 1,\ \phi_0 = 1, \quad & \text{at } \eta = 0 \\ f_0' = 1,\ \theta_0 = 0,\ \phi_0 = 0, \quad & \text{as } \eta = \infty. \end{aligned}\right\} \tag{5.19}$$

The $O(\xi^1)$ equations are

$$f_1''' + \frac{1}{2} f_0 f_1'' - (Ha_x + f_0') f_1' + \frac{3}{2} f_0'' f_1 + Gr_x \theta_1 + Gc_x \phi_1 = 0, \tag{5.20}$$

$$\frac{1}{Pr}\theta_1'' + \frac{1}{2} f_0 \theta_1' - f_0' \theta_1 + \frac{3}{2}\theta_0' f_1 + D_f \phi_1'' = 0, \tag{5.21}$$

$$\frac{1}{Sc}\phi_1'' + \frac{1}{2} f_0 \phi_1' - f_0' \phi_1 + \frac{3}{2}\phi_0' f_1 + Sr\,\theta_1'' = 0, \tag{5.22}$$

with boundary conditions

$$\left.\begin{aligned} f_1 = 0,\ f_1' = 0,\ \theta_1 = 0,\ \phi_1 = 0, \quad & \text{at } \eta = 0 \\ f_1' = 0,\ \theta_1 = 0,\ \phi_1 = 0, \quad & \text{as } \eta = \infty. \end{aligned}\right\} \tag{5.23}$$

Finally, the $O(\xi^2)$ equations are

$$f_2''' + \frac{1}{2}f_0 f_2'' - (Ha_x + 2f_0')f_2' + \frac{5}{2}f_0'' f_2 + Gr_x\theta_2 + Gc_x\phi_2 = f_1'f_1' - \frac{3}{2}f_1 f_1'', \quad (5.24)$$

$$\frac{1}{Pr}\theta_2'' + \frac{1}{2}f_0\theta_2' - 2f_0'\theta_2 + \frac{5}{2}\theta_0' f_2 + D_f\phi_2'' = f_1'\theta_1 - \frac{3}{2}f_1\theta_1', \quad (5.25)$$

$$\frac{1}{Sc}\phi_2'' + \frac{1}{2}f_0\phi_2' - 2f_0'\phi_2 + \frac{5}{2}\phi_0' f_2 + Sr\theta_2'' = f_1'\phi_1 - \frac{3}{2}f_1\phi_1'. \quad (5.26)$$

These equations have to be solved subject to boundary conditions

$$\left.\begin{aligned} &f_2 = 0,\ f_2' = 0,\ \theta_2 = 0,\ \phi_2 = 0, && \text{at } \eta = 0 \\ &f_2' = 0,\ \theta_2 = 0,\ \phi_2 = 0, && \text{as } \eta = \infty. \end{aligned}\right\} \quad (5.27)$$

The coupled system of equations (5.16) - (5.18), (5.20) - (5.22) and (5.24) - (5.26) together with the associated boundary conditions (5.19), (5.23) and (5.27), respectively, may be solved independently pairwise one after another. These equations may now be solved using the successive linearisation method in the manner described in (1.5). We begin by solving equations (5.16) - (5.18) with boundary conditions (5.19).

The method is therefore free of the major limitations associated with other perturbation methods. In the SLM algorithm assumption is made that the functions $f_0(\eta)$, $\theta_0(\eta)$ and $\phi_0(\eta)$ may be expressed as

$$\left.\begin{aligned} &f_0(\eta) = F_i(\eta) + \sum_{m=0}^{i-1} F_m(\eta), \qquad \theta_0(\eta) = \Theta_i(\eta) + \sum_{m=0}^{i-1} \Theta_m(\eta), \\ &\phi_0(\eta) = \Phi_i(\eta) + \textstyle\sum_{m=0}^{i-1} \Phi_m(\eta) \end{aligned}\right\}. \quad (5.28)$$

where F_i, Θ_i and Φ_i ($i \geq 1$) are unknown functions and F_m, Θ_m and Φ_m are successive approximations which are obtained by recursively solving the linear part of the system that is obtained from substituting equations (5.28) in (5.16) - (5.18). In choosing the form of the expansions (5.28), prior knowledge of the general nature of the solutions, as is often the case with perturbation methods, is not necessary. Suitable initial

guesses $F_0(\eta)$, $\Theta_0(\eta)$ and $\Phi_0(\eta)$ which are selected to satisfy the boundary conditions (5.19) are

$$F_0(\eta) = \eta + e^{-\eta} - 1, \qquad \Theta_0(\eta) = e^{-\eta}, \qquad \Phi_0(\eta) = e^{-\eta}, \tag{5.29}$$

The subsequent solutions F_i, Θ_i, and Φ_i are obtained by iteratively solving the linearised form of the equations that are obtained by substituting equation (5.28) in the governing equations (5.16) - (5.18). The linearised equations to be solved are

$$F_i''' + a_{1,i-1}F_i'' - Ha_xF_i' + a_{2,i-1}F_i + Gr_x\Theta_i + Gc_x\Phi_i = r_{1,i-1}, \tag{5.30}$$

$$\frac{1}{Pr}\Theta_i'' + b_{1,i-1}\Theta_i' + b_{2,i-1}F_i + D_f\Phi_i'' = r_{2,i-1}, \tag{5.31}$$

$$\frac{1}{Sc}\Phi_i'' + c_{1,i-1}\Phi_i' + c_{2,i-1}F_i + Sr\Theta_i'' = r_{3,i-1}, \tag{5.32}$$

subject to the boundary conditions

$$F_i(0) = F_i'(0) = F_i'(\infty) = \Theta_i(0) = \Theta_i(\infty) = \Phi_i(0) = \Phi_i(\infty), \tag{5.33}$$

where the coefficients parameters $a_{k,i-1}, b_{k,i-1}, c_{k,i-1}, d_{k,i-1}$ and $r_{k,i-1}$ are defined by

$$a_{1,i-1} = \frac{1}{2}\sum_{m=0}^{i-1} F_m, \quad a_{2,i-1} = \frac{1}{2}\sum_{m=0}^{i-1} F_m'', \quad b_{1,i-1} = \frac{1}{2}\sum_{m=0}^{i-1} F_m$$

$$b_{2,i-1} = \frac{1}{2}\sum_{m=0}^{i-1} \Theta_m', \quad c_{1,i-1} = \frac{1}{2}\sum_{m=0}^{i-1} F_m \quad c_{2,i-1} = \frac{1}{2}\sum_{m=0}^{i-1} \Phi_m',$$

$$r_{1,i-1} = Ha_x\sum_{m=0}^{i-1} F_m' - \frac{1}{2}\sum_{m=0}^{i-1} F_m \sum_{m=0}^{i-1} F_m'' - \sum_{m=0}^{i-1} F_m''' - Gr_x\sum_{m=0}^{i-1} \Theta_m - Gc_x\sum_{m=0}^{i-1} \Phi_m,$$

$$r_{2,i-1} = -\frac{1}{Pr}\sum_{m=0}^{i-1} \Theta_m'' - \frac{1}{2}\sum_{m=0}^{i-1} F_m \sum_{m=0}^{i-1} \Theta_m' - D_f\sum_{m=0}^{i-1} \Phi_m'',$$

$$r_{3,i-1} = -\frac{1}{Sc}\sum_{m=0}^{i-1} \Phi_m'' - \frac{1}{2}\sum_{m=0}^{i-1} F_m \sum_{m=0}^{i-1} \Phi_m' - Sr\sum_{m=0}^{i-1} \Phi_m'',$$

Once each solution F_i, Θ_i and Φ_i $(i \geq 1)$, has been found from iteratively solving equations (5.30) - (5.32), the approximate solutions for the system (5.16) - (5.18) are

obtained as

$$f_0(\eta) \approx \sum_{i=0}^{M_2} F_i(\eta), \qquad \theta_0(\eta) \approx \sum_{i=0}^{M_2} \Theta_i(\eta), \qquad \phi_0(\eta) \approx \sum_{i=0}^{M_2} \Phi_i(\eta), \tag{5.34}$$

where M_2 is the order of the SLM approximations. In this work we used the Chebyshev spectral collocation method to solve equations (5.30) - (5.32). The physical region $[0, \infty)$ is first transformed into the spectral domain $[-1, 1]$ using the domain truncation technique in which the problem is solved on the interval $[0, L]$ where L is a scaling parameter used to invoke the boundary condition at infinity. This is achieved by using the mapping

$$\frac{\eta}{L} = \frac{\zeta + 1}{2}, \qquad -1 \leq \zeta \leq 1, \tag{5.35}$$

We discretise the spectral domain $[-1, 1]$ using the Gauss-Lobatto collocation points given by

$$\zeta_j = \cos \frac{\pi j}{N}, \qquad j = 0, 1, .., N, \tag{5.36}$$

where N is the number of collocation points used. The unknown functions F_i, Θ_i and Φ_i are approximated at the collocation points defined by

$$\left.\begin{aligned} F_i(\zeta) &\approx \sum_{k=0}^{N} F_i(\zeta_k) T_k(\zeta_j), \\ \Theta_i(\zeta) &\approx \sum_{k=0}^{N} \Theta_i(\zeta_k) T_k(\zeta_j) \\ \Phi_i(\zeta) &\approx \sum_{k=0}^{N} \Phi_i(\zeta_k) T_k(\zeta_j), \end{aligned}\right\} \qquad j = 0, 1, ..., N \tag{5.37}$$

where T_k is the kth Chebyshev polynomial defined as

$$T_k(\zeta) = \cos\left[k \cos^{-1}(\zeta)\right]. \tag{5.38}$$

The derivatives of the variables at the collocation points are represented as

$$\left.\begin{aligned} F_i^{(r)} &= \sum_{k=0}^{N} \mathbf{D}_{kj}^r F_i(\zeta_k), \\ \Theta_i^{(r)} &= \sum_{k=0}^{N} \mathbf{D}_{kj}^r \Theta_i(\zeta_k), \\ \Phi_i^{(r)} &= \sum_{k=0}^{N} \mathbf{D}_{kj}^r \Phi_i(\zeta_k) \end{aligned}\right\} \qquad j = 0, 1, ..., N \tag{5.39}$$

where r is the order of differentiation and $\mathbf{D} = \frac{2}{L}\mathcal{D}$ with $\mathcal{D}$ being the Chebyshev spectral differentiation matrix whose entries are defined by (1.30). Substituting equations (5.35)-(5.39) into (5.30)-(5.32) gives the following linear system of equations

$$\mathbf{A}_{i-1}\mathbf{X}_i = \mathbf{R}_{i-1} \tag{5.40}$$

subject to the boundary conditions

$$\left.\begin{aligned} F_i(\zeta_0) = \sum_{k=0}^{N} \mathcal{D}_{0k} F_i(\zeta_k) = g_i(\zeta_0) = \Theta_i(\zeta_0) = \Phi_i(\zeta_0) = 0 \\ F_i(\zeta_N) = g_i(\zeta_N) = \Theta_i(\zeta_N) = \Phi_i(\zeta_N) = 0. \end{aligned}\right\} \tag{5.41}$$

Here $\mathbf{A}_{i-1}$ is a $3(N+1) \times 3(N+1)$ square matrix while $\mathbf{X}_i$ and $\mathbf{R}_{i-1}$ are $3(N+1) \times 1$ column vectors defined by

$$\mathbf{A}_{i-1} = \begin{bmatrix} A_{11} & A_{12} & A_{13} \\ A_{21} & A_{22} & A_{23} \\ A_{31} & A_{32} & A_{33} \end{bmatrix}, \qquad \mathbf{X}_i = \begin{bmatrix} \tilde{\mathbf{F}}_i \\ \tilde{\Theta}_i \\ \tilde{\Phi}_i \end{bmatrix}, \qquad \mathbf{R}_{i-1} = \begin{bmatrix} \mathbf{r}_{1,i-1} \\ \mathbf{r}_{2,i-1} \\ \mathbf{r}_{3,i-1} \end{bmatrix} \tag{5.42}$$

where

$$\tilde{\mathbf{F}}_i = [F_i(\zeta_0), F_i(\zeta_1), \cdots, F_i(\zeta_{N-1}), F_i(\zeta_N)]^T, \tag{5.43}$$

$$\tilde{\Theta}_i = [\Theta_i(\zeta_0), \Theta_i(\zeta_1), \cdots, \Theta_i(\zeta_{N-1}), \Theta_i(\zeta_N)]^T, \tag{5.44}$$

$$\tilde{\Phi}_i = [\Phi_i(\zeta_0), \Phi_i(\zeta_1), \cdots, \Phi_i(\zeta_{N-1}), \Phi_i(\zeta_N)]^T, \tag{5.45}$$

$$\mathbf{r}_{1,i-1} = [r_{1,i-1}(\zeta_0), r_{1,i-1}(\zeta_1), \cdots, r_{1,i-1}(\zeta_{N-1}), r_{1,i-1}(\zeta_N)]^T \tag{5.46}$$

$$\mathbf{r}_{2,i-1} = [r_{2,i-1}(\zeta_0), r_{2,i-1}(\zeta_1), \cdots, r_{2,i-1}(\zeta_{N-1}), r_{2,i-1}(\zeta_N)]^T \tag{5.47}$$

$$\mathbf{r}_{3,i-1} = [r_{3,i-1}(\zeta_0), r_{3,i-1}(\zeta_1), \cdots, r_{3,i-1}(\zeta_{N-1}), r_{3,i-1}(\zeta_N)]^T \tag{5.48}$$

and

$$\left.\begin{aligned} &A_{11} = \mathcal{D}^3 + a_{1,i-1}\mathcal{D}^2 - Ha_x\mathcal{D} + [a_{3,i-1}], \;\; A_{12} = [Gr_x], \;\; A_{13} = [Gc_x], \\ &A_{21} = [b_{2,i-1}], \;\; A_{22} = Pr^{-1}\mathcal{D}^2 + b_{1,i-1}\mathcal{D}, \; A_{23} = D_f\mathcal{D}^2 \;\; A_{31} = [c_{2,i-1}], \\ &A_{32} = Sr\mathcal{D}^2, \quad A_{33} = Sc^{-1}\mathcal{D}^2 + c_{1,i-1}\mathcal{D}, \end{aligned}\right\} \tag{5.49}$$

where $[\cdot]$ is a diagonal matrix of size $(N+1)\times(N+1)$ and $a_{k,i-1}, b_{k,i-1}, c_{k,i-1}$ are diagonal matrices of size $(N+1)\times(N+1)$ and T is the transpose. After modifying the matrix system (5.40) to incorporate the boundary conditions (5.41), the solution is obtained as

$$\mathbf{X}_i = \mathbf{A}_{i-1}^{-1}\mathbf{R}_{i-1} \tag{5.50}$$

Equation (5.50) gives a solution of (5.16) - (5.18) for f_0, θ_0 and ϕ_0. The procedure is repeated to obtain the $O(\xi^1)$ and $O(\xi^2)$ solutions using equations (5.20) - (5.22) and (5.24) - (5.26) respectively.

5.4 Results and discussion

In generating the results in this chapter we determined through numerical experimentation that $L = 15$, $N = 40$ and $M_2 = 5$ gave sufficient accuracy for the linearisation method. The value of the Prandtl number used is $Pr = 0.71$ which physically corresponds to air. The Schmidt number used $Sc = 0.22$ is for hydrogen at approximately 25° and one atmospheric pressure (see Afify 2009). In concert with previous related studies, the Dufour and Soret numbers are chosen in such a way that their product is constant, provided the mean temperature T_m is also kept constant.

To determine the accuracy and validate the linearisation method, equations (5.8) - (5.10) were further solved using a local nonsimilarity method (LNSM) developed by Sparrow and his co-workers (1970, 1971). Previous studies have consistently used the Matlab `bvp4c` solver to evaluate the accuracy of the successive linearisation method. However, as with other BVP solvers, the accuracy and convergence of the `bvp4c` algorithm depends on a good initial guess and works better for systems involving few equations (Shampine et al. 2005).

Tables 5.1-5.3 show, firstly the effects of various parameters on the skin-friction and the local heat and mass transfer coefficients at different values of ξ and, secondly, give a sense of the accuracy and convergence rate of the linearisation method. The results from the two methods are in excellent agreement with the second order SLM series giving accuracy of up to five significant figures.

Table 5.1 shows the effect of increasing the magmatic field parameter Ha_x on the local skin friction, heat and mass transfer coefficients. We observe that increasing the magnetic field parameter reduces the local skin friction as well as the heat and mass transfer coefficients. In Table 5.2 we present the effect of the Soret parameter on $f''(0)$, $-\theta'(0)$ and $-\phi'(0)$ which are respectively proportional to the local skin friction

Table 5.1: The effect of the magnetic field parameter Ha_x on $f''(0)$, $\theta'(0)$ and $\phi'(0)$ when $Gr_x = 0.5, Gc_x = 2, D_f = 0.2$ and $Sr = 0.3$.

		$\xi = 0.005$			$\xi = 0.01$		
		SLM results		LNSM	SLM results		LNSM
Profile	Ha_x	$M_2 = 2$	$M_2 = 3$		$M_2 = 2$	$M_2 = 3$	
$f''(0)$	0.0	3.045324	3.045324	3.045324	3.045324	3.045324	3.045324
	0.5	2.299370	2.299370	2.299370	2.299370	2.299370	2.299370
	1.0	1.940291	1.940291	1.940291	1.940291	1.940291	1.940291
	2.0	1.532041	1.532041	1.532041	1.532041	1.532041	1.532041
	2.5	1.404033	1.404033	1.404033	1.404033	1.404033	1.404033
$-\theta'(0)$	0.0	0.513493	0.513493	0.513493	0.513493	0.513493	0.513493
	0.5	0.435640	0.435640	0.435640	0.435640	0.435640	0.435640
	1.0	0.392869	0.392869	0.392869	0.392869	0.392869	0.392869
	2.0	0.335307	0.335307	0.335307	0.335307	0.335307	0.335307
	2.5	0.314405	0.314405	0.314405	0.314405	0.314405	0.314405
$-\phi'(0)$	0.0	0.289548	0.289548	0.289548	0.289548	0.289548	0.289548
	0.5	0.231673	0.231673	0.231673	0.231673	0.231673	0.231673
	1.0	0.202778	0.202778	0.202778	0.202778	0.202778	0.202778
	2.0	0.169217	0.169217	0.169217	0.169217	0.169217	0.169217
	2.5	0.157771	0.157771	0.157771	0.157771	0.157771	0.157771

coefficient, the local Nusselt number and Sherwood number. We observe that $f''(0)$ and $-\theta'(0)$ increase with increases in Sr while $-\phi'(0)$ decreases as Sr increases. These results are confirmed in Table 5.3. Here the Nusselt number increases as the Soret number increases while the opposite trend occurs as the Dufour number increases. The recent study by El-Kabeir (2011) shows that these results may be modified by injection, suction or the presence of a chemical reaction. The influence of the various fluid and physical parameters on the fluid properties is given qualitatively in Figures 5.2 - 5.5. Figures 5.2 - 5.3 illustrate the effect of the magnetic filed parameter on the

Table 5.2: The effect of the Soret parameter Sr on $f''(0)$, $\theta'(0)$ and $\phi'(0)$ when $Gr_x = 0.5, Gc_x = 2$ and $Ha_x = 1$.

		$\xi = 0.005$			$\xi = 0.01$		
		SLM results		LNSM	SLM results		LNSM
Profile	Sr	$M_2 = 2$	$M_2 = 3$		$M_2 = 2$	$M_2 = 3$	
$f''(0)$	0.1	1.933303	1.933303	1.933302	1.933303	1.933303	1.933302
	0.4	1.946426	1.946426	1.946426	1.946426	1.946426	1.946426
	0.6	1.959632	1.959632	1.959632	1.959632	1.959632	1.959632
	1.5	2.023004	2.023004	2.023004	2.023004	2.023004	2.023004
	2.0	2.059313	2.059313	2.059313	2.059313	2.059313	2.059313
$-\theta'(0)$	0.1	0.368159	0.368159	0.368159	0.368159	0.368159	0.368159
	0.4	0.396905	0.396905	0.396905	0.396905	0.396905	0.396905
	0.6	0.402187	0.402187	0.402187	0.402187	0.402187	0.402187
	1.5	0.416430	0.416430	0.416430	0.416430	0.416430	0.416430
	2.0	0.422788	0.422788	0.422788	0.422788	0.422788	0.422788
$-\phi'(0)$	0.1	0.213565	0.213565	0.213565	0.213565	0.213565	0.213565
	0.4	0.197708	0.197708	0.197708	0.197708	0.197708	0.197708
	0.6	0.187601	0.187601	0.187601	0.187601	0.187601	0.187601
	1.5	0.141063	0.141063	0.141063	0.141063	0.141063	0.141063
	2.0	0.114262	0.114262	0.114262	0.114262	0.114262	0.114262

velocity $f'(\eta)$, temperature θ and concentration ϕ profiles within the boundary layer. We observe that, as expected, strengthening the magnetic field slows down the fluid motion due to an increasing drag force which acts against the flow if the magnetic field is applied in the normal direction. We also observe that the magnetic field parameter enhances the temperature and concentration profiles. The effect of broadening both the temperature and concentration distributions is to reduce the wall temperature and concentration gradients thereby reducing the heat and mass transfer rates at the wall.

Table 5.3: Soret and Dufour effects of the skin friction coefficient C_f, Nusselt number Nu and Sherwood number Sh when $Gr_x = 0.5, Gc_x = 2, Sc = 0.22$ and $Ha_x = 0.5$

S_r	D_f	C_f	Nu	Sh
0.1	0.60	1.933303	0.368159	0.213565
0.2	0.30	1.935047	0.386060	0.207941
0.4	0.15	1.946426	0.396905	0.197708
0.6	0.10	1.959632	0.402187	0.187601
1.5	0.04	2.023004	0.416430	0.141063
2.0	0.03	2.059313	0.422788	0.114262

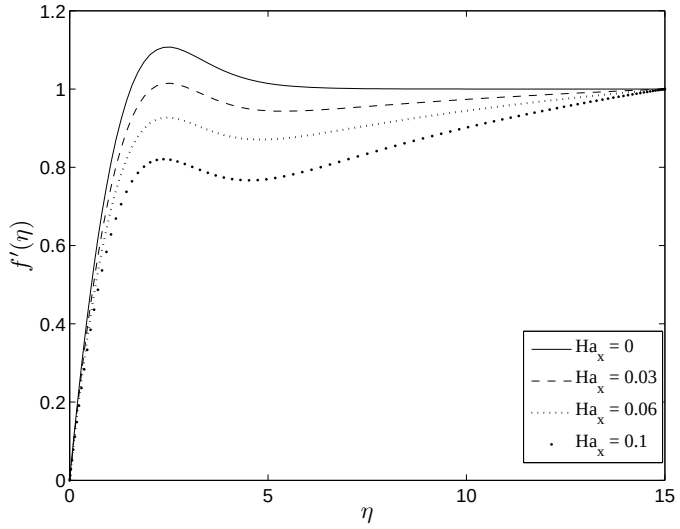

Figure 5.2: Effect of the magmatic field parameter Ha_x on $f'(\eta)$ when $Gr_x = 0.5, Gc_x = 0.1, D_f = 0.2, Sr = 0.3$ and $\xi = 0.01$.

Figure 5.4 shows the effect of increasing the Soret parameter (reducing the Dufour parameter) on the fluid velocity $f'(\eta)$. The fluid velocity is found to increase with the Soret parameter.

The effect of Soret parameter on the temperature within the thermal boundary layer and the solute concentration is shown in Figures 5.5(a) - 5.5(b), respectively. An increase in the Soret effect reduces the temperature within the thermal boundary

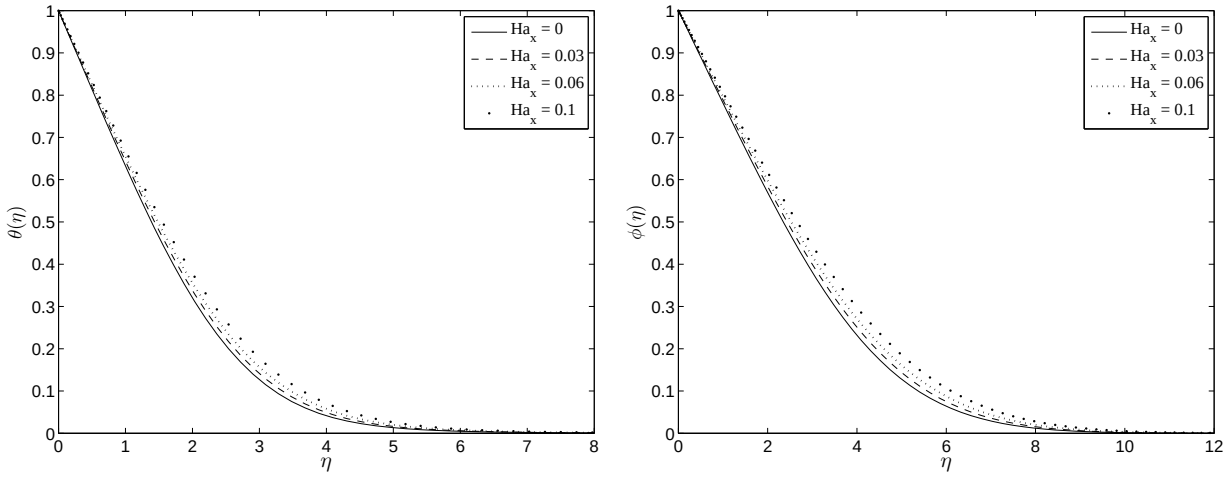

Figure 5.3: Effect of the magmatic field parameter Ha_x on (a) $\theta(\eta)$ and (b) $\phi(\eta)$ when $Gr_x = 0.5, Gc_x = 0.1, D_f = 0.2, Sr = 0.3$ and $\xi = 0.01$.

layer leading to an increase in the temperature gradient at the wall and an increase in heat transfer rate at the wall. On the other hand, increasing the Soret effect increases the concentration distribution which reduces the concentration gradient at the wall. These results are similar to the earlier findings by El-Kaberir (2011) and Alam and Rahman (2006b), although the latter studies were subject to injection/suction.

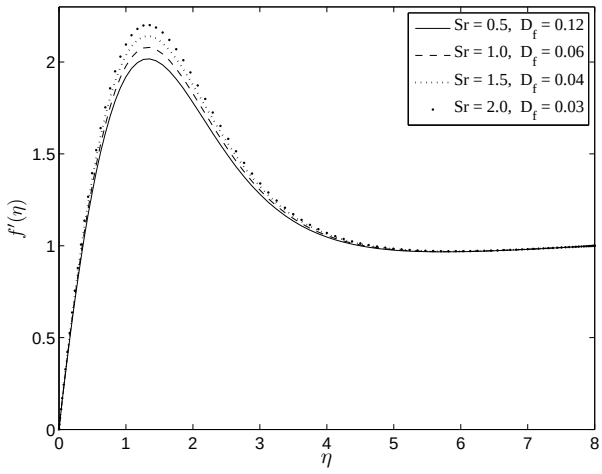

Figure 5.4: Effect of the Soret and Dufour parameters on the velocity $f'(\eta)$ when $Gr_x = 0.5, Gc_x = 2.5, Ha_x = 0.1$ and $\xi = 0.01$.

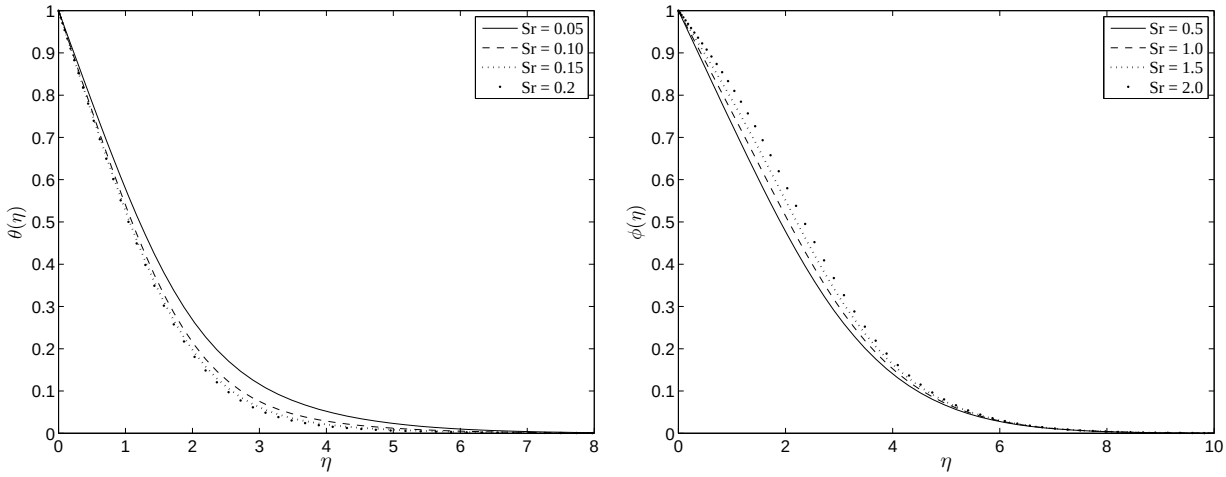

(a) (b)

Figure 5.5: Effect of Soret parameter Sr on (a) $\theta(\eta)$ and (b) $\phi(\eta)$ when $Gr_x = 0.1, Gc_x = 2.5, Ha_x = 0.1$ and $\xi = 0.01$.

5.5 Conclusions

In this chapter we have investigated MHD and cross-diffusion effects on double-diffusive convection from a vertical flat plate in a viscous incompressible fluid. Numerical approximations for the governing equations were found using a combination of a regular perturbation expansion and the successive linearisation method. The solutions were validated by using a local similarity, non-similarity method. We determined the effects of various parameters on the fluid properties as well as on the skin-friction coefficient, the heat and the mass transfer rates. We have shown that the magnetic field parameter enhances the temperature and concentration distributions within the boundary layer. The effect of thermo-diffusion is to reduce the temperature and enhance the velocity and the concentration profiles. The diffusion-thermo effect enhances the velocity and temperature profiles while reducing the concentration distribution. The skin-friction, heat and mass transfer coefficients decrease with an increase in the magnetic field strength. The skin-friction and heat transfer coefficients increase whereas the mass transfer coefficient decreases with increasing Soret

numbers.

Chapter 6

Cross-diffusion, viscous dissipation and radiation effects on an exponentially stretching surface in porous media*

Abstract

In this chapter cross-diffusion convection from an exponentially stretching surface in a fluid saturated porous medium subject to viscous dissipation and radiation effects has been investigated. The governing partial differential equations are transformed into nonlinear ordinary differential equations and solved using a linearisation method. The accuracy and rate of convergence of the solution has been tested using the Matlab `bvp4c` solver. The effects of selected fluid and material parameters on the

[0]* Submitted to published in Mass Transfer Book, InTech - Open Access Publisher, (2011).

velocity, temperature and concentration profiles are determined and discussed. The skin-friction, heat and mass transfer coefficients have been obtained and analyzed for various physical parametric values.

6.1 Introduction

In the last few decades, heat and mass transfer problems on a continuously stretching surface with a given temperature or heat flux distribution, have attracted considerable attention of researchers because of its many applications in industrial and manufacturing processes. Examples of these applications include the drawing of plastic films, glass-fibre and paper production, hot rolling and continuous casting of metals and spinning of fibers. The kinematics of stretching and the simultaneous heating or cooling during such processes play an important role on the structure and quality of the final product.

Sakiadis (1961a,b) was the first to study the boundary layer flow due to a continuous moving solid surface. Subsequently, a huge number of studies dealing with different types of fluids, different forms of stretching velocity and temperature distributions have appeared in the literature. Ali (1995) investigated similarity solutions of laminar boundary-layer equations in a quiescent fluid driven by a stretched sheet subject to fluid suction or injection. Elbashbeshy (2001) extended this problem to a three dimensional exponentially continuous stretching surface. The problem of an exponentially stretching surface with an exponential temperature distribution has been discussed by Magyari and Keller (1999). The problem of mixed convection from an exponentially stretching surface was studied by Partha et al. (2005). They considered the effect of buoyancy and viscous dissipation in the porous medium. They observed that these had a significant effect on the skin friction and the rate of heat transfer. This problem has been extended by Sajid and Hayat (2008) who investigated heat

transfer over an exponentially stretching sheet in the presence of heat radiation. The same problem was solved numerically by Bidin and Nazar (2009) using the Keller-box method. Flow and heat transfer along an exponentially stretching continuous surface with an exponential temperature distribution and an applied magnetic field has been investigated numerically by Al-Odat et al. (2006) while Khan (2006) and Sanjayanand and Khan (2006) investigated heat transfer due to an exponentially stretching sheet in a viscous-elastic fluid.

Thermal-diffusion and diffusion-thermo effects in boundary layer flow due to a vertical stretching surface have been studied by, *inter alia*, Dursunkaya and Worek (1992) while MHD effects, injection/suction, heat radiation, Soret and Dufour effects on the heat and mass transfer on a continuously stretching permeable surface was investigated by El-Aziz (2008). He showed that the Soret and Dufour numbers have a significant influence on the velocity, temperature and concentration distributions.

Srinivasacharya and RamReddy (2011) analyzed the problem of mixed convection in a viscous fluid over an exponentially stretching vertical surface subject to Soret and Dufour effects. Ishak (2011) investigated the effect of radiation on magnetohydrodynamic boundary layer flow of a viscous fluid over an exponentially stretching sheet. Pal (2010) analyzed the effects of magnetic field, viscous dissipation and internal heat generation/absorption on mixed convection heat transfer in the boundary layers on an exponentially stretching continuous surface with an exponential temperature distribution. Loganathan et al. (2011) investigated the effect of a chemical reaction on unsteady free convection flow past a semi-infinite vertical plate with variable viscosity and thermal conductivity. They assumed that the viscosity of the fluid was an exponential function and that the thermal conductivity was a linear function of the temperature. They noted that in the case of variable fluid properties, the results obtained differed significantly from those of constant fluid properties. Javed et al. (2011) investigated the non-similar boundary layer flow over an exponentially stretching con-

tinuous in rotating flow. They observed a reduction in the boundary layer thickness and an enhanced drag force at the surface with increasing fluid rotation.

The aim of the present chapter is to investigate the effects of cross-diffusion, chemical reaction, heat radiation and viscous dissipation on an exponentially stretching surface subject to an external magnetic field. The wall temperature, solute concentration and stretching velocity are assumed to be exponentially increasing functions. The SLM is used to solve the governing coupled non-linear system of equations and we compared the results with the Matlab `bvp4c` numerical routine.

6.2 Problem formulation

Consider a quiescent incompressible conducting fluid of constant ambient temperature T_∞ and concentration C_∞ in a porous medium through which an impermeable vertical sheet is stretched with velocity $u_w(x) = u_0 e^{x/\ell}$, temperature distribution $T_w(x) = T_\infty + T_0 e^{2x/\ell}$ and concentration distribution $C_w(x) = C_\infty + C_0 e^{2x/\ell}$ where C_0, T_0, u_0 and ℓ are positive constants. The x-axis is directed along the continuous stretching surface and the y-axis is normal to the surface. A variable magnetic field $B(x)$ is applied in the y-direction. In addition, heat radiation and cross-diffusion effects are considered to be significant. Figure 6.1 shows the physical configuration of the problem under consideration. The governing boundary-layer equations subject to the

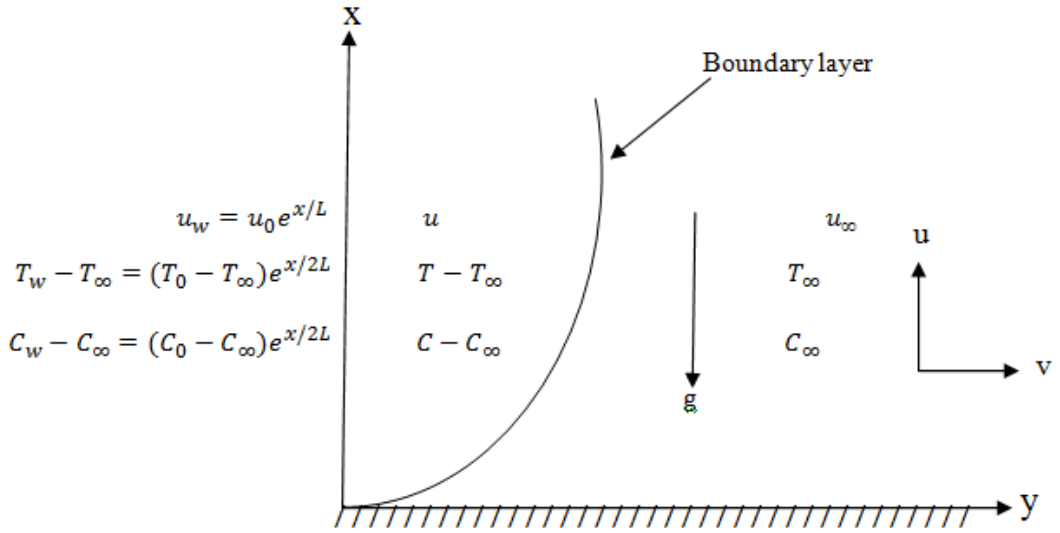

Figure 6.1: Physical model and coordinate system.

Boussinesq approximations are

$$\frac{\partial u}{\partial x} + \frac{\partial v}{\partial y} = 0, \tag{6.1}$$

$$u\frac{\partial u}{\partial x} + v\frac{\partial u}{\partial y} = \nu\frac{\partial^2 u}{\partial y^2} + g\beta_T(T - T_\infty) + g\beta_C(C - C_\infty) - \left(\frac{\nu}{K} + \frac{\sigma B^2}{\rho}\right)u, \tag{6.2}$$

$$u\frac{\partial T}{\partial x} + v\frac{\partial T}{\partial y} = \frac{k}{\rho c_p}\frac{\partial^2 T}{\partial y^2} + \frac{\nu}{c_p}\left(\frac{\partial u}{\partial y}\right)^2 + \frac{D_m K_T}{c_s c_p}\frac{\partial^2 C}{\partial y^2} - \frac{1}{\rho c_p}\frac{\partial q_r}{\partial y}, \tag{6.3}$$

$$u\frac{\partial C}{\partial x} + v\frac{\partial C}{\partial y} = D_m\frac{\partial^2 C}{\partial y^2} + \frac{D_m K_T}{T_m}\frac{\partial^2 T}{\partial y^2} - \gamma(C - C_\infty), \tag{6.4}$$

The boundary conditions are given by

$$\left.\begin{aligned} &u = u_w(x), \quad v = 0, \quad T = T_w(x), \quad C = C_w(x) \quad \text{at} \quad y = 0, \\ &u \to 0, \quad T \to T_\infty, \quad C \to C_\infty \quad \text{as} \quad y \to \infty. \end{aligned}\right\} \tag{6.5}$$

where u and v are the velocity components along the x and y axis, respectively, T and C denote the temperature and concentration, respectively, K is the permeability of the porous medium, ν is the kinematic viscosity, g is the acceleration due to gravity, β_T is the coefficient of thermal expansion, β_C is the coefficient of concentration expansion,

B is the uniform magnetic field, ρ is the liquid density, σ is the electrical conductivity, D_m is the mass diffusivity, c_s is the concentration susceptibility, c_p is the specific heat capacity, T_m is the mean fluid temperature, K_T is the thermal diffusion ratio and γ is the rate of chemical reaction.

The radiative heat flux term q_r is given by the Rosseland approximation (see Raptis 1998 and Sparrow 1971);

$$q_r = -\frac{4\sigma^*}{3k^*}\frac{\partial T^4}{\partial y}, \tag{6.6}$$

where σ^* and k^* are the Stefan-Boltzman constant and the mean absorption coefficient, respectively. We assume that the term T^4 may be expanded in a Taylor series about T_∞ and neglecting higher-order terms to get

$$T^4 \cong 4T_\infty^3 T - 3T_\infty^4, \tag{6.7}$$

Substituting equations (6.6) and (6.7) in equation (6.3) gives

$$u\frac{\partial T}{\partial x} + v\frac{\partial T}{\partial y} = \left(\frac{k}{\rho c_p} + \frac{16\sigma^* T_\infty^3}{3\rho c_p k^*}\right)\frac{\partial^2 T}{\partial y^2} + \frac{\nu}{c_p}\left(\frac{\partial u}{\partial y}\right)^2 + \frac{D_m K_T}{c_s c_p}\frac{\partial^2 C}{\partial y^2}, \tag{6.8}$$

A similarity solutions may be obtained by assuming that the magnetic field term $B(x)$ has the form

$$B(x) = B_0 e^{x/2\ell} \tag{6.9}$$

where B_0 is the constant magnetic field. The system of partial differential equations (6.1) - (6.4) and (6.8) can be simplified further by introducing the stream function ψ where

$$u = \frac{\partial \psi}{\partial y} \qquad \text{and} \qquad v = -\frac{\partial \psi}{\partial x}, \tag{6.10}$$

together with transformations

$$\left.\begin{aligned} &\eta = \frac{y}{L}\sqrt{\frac{Re}{2}}\, e^{x/2\ell}, \qquad \psi = \sqrt{2Re}\nu\, e^{x/2\ell} f(\eta), \\ &T = T_\infty + T_0 e^{2x/\ell}\theta(\eta), \qquad C = C_\infty + C_0 e^{2x/\ell}\phi(\eta) \end{aligned}\right\}. \tag{6.11}$$

Substituting (6.11) into the governing partial differential equations gives

$$f''' + ff'' - 2f'^2 - \left(M + \frac{1}{Re_D}\right) f' + 2\frac{Gr_x}{Re^2}\left(\theta + N_1\phi\right) = 0, \tag{6.12}$$

$$\frac{1}{Pr}\left(1 + \frac{4}{3}R_d\right)\theta'' + f\theta' - 4f'\theta + Gb(f'')^2 + D_f\phi'' = 0, \tag{6.13}$$

$$\frac{1}{Sc}\phi'' + f\phi' - 4f'\phi + Sr\theta'' - 2R\phi = 0. \tag{6.14}$$

The corresponding dimensionless boundary conditions take the form

$$\left.\begin{aligned} &f(\eta) = 0, \quad f'(\eta) = 1, \quad \theta(\eta) = 1 \quad \phi(\eta) = 1 \quad \text{at} \quad \eta = 0 \\ &f'(\eta) \to 0, \quad \theta(\eta) \to 0 \quad \phi(\eta) \to 0 \quad \text{as} \quad \eta \to \infty \end{aligned}\right\} \tag{6.15}$$

where M is the magnetic parameter, Gr_x is the Grashof number, Re is the Reynolds number, N_1 is the buoyancy ratio, Re_D is the Darcy-Reynolds number, Da is the Darcy number, Pr is the Prandtl number, R_d is the thermal radiation parameter, Gb is the viscous dissipation parameter or Gebhart number, D_f is the Dufour number, Sc is the Schmidt number, S_r is the Soret number and R is the chemical reaction rate parameter. These parameters are defined as

$$M = \frac{2\sigma B_0^2\ell}{\rho u_0}, \quad Gr_x = \frac{g\beta_T T_0 \ell^3 e^{2x/\ell}}{\nu^2}, \quad Re = \frac{u_w\ell}{\nu}, \quad N_1 = \frac{\beta_c C_0}{\beta_T T_0}, \tag{6.16}$$

$$Re_D = \frac{2}{ReDa}, \quad Da = \frac{K}{\ell^2}, \quad Pr = \frac{\nu}{\alpha}, \quad R_d = \frac{4\sigma^* T_\infty^3}{kk^*}, \quad Gb = \frac{u_0^2}{c_p T_0}, \tag{6.17}$$

$$D_f = \frac{D_m K_T C_0}{c_s c_p \nu T_0}, \quad Sc = \frac{\nu}{D_m}, \quad S_r = \frac{D_m K_T T_0}{T_m \nu C_0}, \quad R = \frac{\alpha\ell}{u_0}. \tag{6.18}$$

The ratio Gr_x/Re^2 in equation (6.12) is the mixed convection parameter which rep-

resents aiding buoyancy if $Gr_x/Re^2 > 0$ and opposing buoyancy if $Gr_x/Re^2 < 0$. The skin friction coefficient C_{fx}, the Nusselt number Nu_x and the Sherwood Sh_x number are given by

$$C_{fx} = \frac{2\mu}{\rho u_w^2} \left.\frac{\partial u}{\partial y}\right|_{y=0} = \sqrt{\frac{2x}{\ell\, Re_x}}\, f''(0), \tag{6.19}$$

$$Nu_x = -\frac{x}{T_w - T_\infty} \left.\frac{\partial T}{\partial y}\right|_{y=0} = -\sqrt{\frac{xRe_x}{2\ell}}\, \theta'(0) \tag{6.20}$$

$$Sh_x = -\frac{x}{C_w - C_\infty} \left.\frac{\partial C}{\partial y}\right|_{y=0} = -\sqrt{\frac{xRe_x}{2\ell}}\, \phi'(0) \tag{6.21}$$

where $Re_x = xu_w(x)/\nu$ is the local Reynolds number.

6.3 Method of solution

The system of equations (6.12)-(6.14) together with the boundary conditions (6.15) were solved using the SLM which is based on the assumption that the unknown functions $f(\eta)$, $\theta(\eta)$ and $\phi(\eta)$ can be expanded as

$$\left.\begin{aligned} f(\eta) &= f_i(\eta) + \sum_{m=0}^{i-1} F_m(\eta), \qquad \theta(\eta) = \theta_i(\eta) + \sum_{m=0}^{i-1} \Theta_m(\eta), \\ \phi(\eta) &= \phi_i(\eta) + \sum_{m=0}^{i-1} \Phi_m(\eta), \end{aligned}\right\} \tag{6.22}$$

where f_i, θ_i and ϕ_i are unknown functions and F_m, Θ_m and Φ_m $(m \geq 1)$ are successive approximations which are obtained by recursively solving the linear part of the equation system that results from substituting firstly expansions in the governing equations. The main assumption of the SLM is that f_i, θ_i and ϕ_i are very small when i becomes large, then nonlinear terms in f_i, θ_i and ϕ_i and their derivatives are considered to be very small and therefore neglected. The initial guesses $F_0(\eta)$, $\Theta_0(\eta)$

and $\Phi_0(\eta)$ which are chosen to satisfy the boundary condition

$$\left.\begin{array}{llllll} F_0(\eta)=0, & F_0'(\eta)=1, & \Theta_0(\eta)=1 & \Phi_0(\eta)=1 & \text{at} & \eta=0 \\ F_0'(\eta)\to 0, & \Theta_0(\eta)\to 0 & \Phi_0(\eta)\to 0 & \text{as} & \eta\to\infty & \end{array}\right\} \tag{6.23}$$

which are taken to be

$$F_0(\eta)=1-e^{-\eta}, \qquad \Theta_0(\eta)=e^{-\eta}, \qquad \Phi_0(\eta)=e^{-\eta}. \tag{6.24}$$

Thus, starting from the initial guesses, the subsequent solutions F_i, Θ_i and Φ_i $(i\geq 1)$ are obtained by successively solving the linearised form of the equations which are obtained by substituting equation (6.22) in the governing equations. The linearized equations to be solved are

$$F_i'''+a_{1,i-1}F_i''+a_{2,i-1}F_i'+a_{3,i-1}F_i+2\frac{Gr_x}{Re^2}\Theta_i+2\frac{Gr_xN_1}{Re^2}\Phi_i=r_{1,i-1}, \tag{6.25}$$

$$\begin{aligned}&\left(\frac{3+4R_d}{3Pr}\right)\Theta_i''+b_{1,i-1}\Theta_i'+b_{2,i-1}\Theta_i+b_{3,i-1}F_i''+b_{4,i-1}F_i'+b_{5,i-1}F_i\\&+D_f\Phi_i=r_{2,i-1},\end{aligned} \tag{6.26}$$

$$\frac{1}{Sc}\Phi_i''+c_{1,i-1}\Phi_i'+c_{2,i-1}\Phi_i+c_{3,i-1}F_i'+c_{4,i-1}F_i+Sr\Theta_i''=r_{3,i-1}. \tag{6.27}$$

subject to the boundary conditions

$$F_i(0)=F_i'(0)=F_i'(\infty)=\Theta_i(0)=\Theta_i(\infty)=\Phi_i(0)=\Phi_i(\infty)=0, \tag{6.28}$$

where the coefficient parameters are defined as

$$a_{1,i-1} = \sum_{m=0}^{i-1} f'_m, \qquad a_{2,i-1} = -4\sum_{m=0}^{i-1} f'_m - M - \frac{1}{Re_D}, \qquad b_{1,i-1} = \sum_{m=0}^{i-1} f_m,$$
$$b_{2,i-1} = -4\sum_{m=0}^{i-1} f'_m, \qquad b_{3,i-1} = \sum_{m=0}^{i-1} 2Gbf''_m, \qquad b_{4,i-1} = -4\sum_{m=0}^{i-1} \theta_m,$$
$$b_{5,i-1} = \sum_{m=0}^{i-1} \theta'_m, \qquad c_{1,i-1} = \sum_{m=0}^{i-1} f_m, \qquad c_{2,i-1} = -2R - 4\sum_{m=0}^{i-1} f'_m,$$
$$c_{3,i-1} = -4\sum_{m=0}^{i-1} \phi_m \qquad c_{4,i-1} = \sum_{m=0}^{i-1} \phi'_m,$$

and

$$\begin{aligned} r_{1,i-1} = \quad & -\sum_{m=0}^{i-1} f'''_m - \sum_{m=0}^{i-1} f_m \sum_{m=0}^{i-1} f''_m + 2\sum_{m=0}^{i-1} f'^2_m + \left(M + \frac{1}{Re_D}\right)\sum_{m=0}^{i-1} f'_m \\ & -\frac{2Gr_x}{Re^2}\sum_{m=0}^{i-1}(\theta_m + N_1\phi_m) \end{aligned}$$

$$\begin{aligned} r_{2,i-1} = \quad & -\sum_{m=0}^{i-1} \frac{1}{Pr}(\phi''_m + \frac{4R_d}{3Pr}\theta''_m) - \sum_{m=0}^{i-1} f_m \sum_{m=0}^{i-1} \theta'_m + 4\sum_{m=0}^{i-1} f'_m \sum_{m=0}^{i-1} \theta_m \\ & -Gb\sum_{m=0}^{i-1} f''^2_m - D_f \sum_{m=0}^{i-1} \phi''_m \end{aligned}$$

$$r_{3,i-1} = -\frac{1}{Sc}\sum_{m=0}^{i-1} \phi''_m \sum_{m=0}^{i-1} f_m \sum_{m=0}^{i-1} \phi'_m + 4\sum_{m=0}^{i-1} f_m \sum_{m=0}^{i-1} \theta_m - Sr\sum_{m=0}^{i-1} \phi''_m + 2R\sum_{m=0}^{i-1} \phi_m$$

The solution for F_i, Θ_i and Φ_i for $i \geq 1$ has been found by iteratively solving equations (6.25)-(6.27) and finally after M iterations the solutions $f(\eta)$, $\theta(\eta)$ and $\phi(\eta)$ can be written as

$$f(\eta) \approx \sum_{m=0}^{M} F_m(\eta), \qquad \theta(\eta) \approx \sum_{m=0}^{M} \Theta_m(\eta), \qquad \Phi(\eta) \approx \sum_{m=0}^{M} \Phi_m(\eta). \tag{6.29}$$

where M is termed the order of SLM approximation. Equations (6.25)-(6.27) are solved using the Chebyshev spectral collocation method. The method is based on the Chebyshev polynomials defined on the interval $[-1, 1]$. We first transform the domain of solution $[0, \infty)$ into the domain $[-1, 1]$ using the domain truncation technique where the problem is solved in the interval $[0, L]$ where L is a scaling parameter used to invoke the boundary condition at infinity. This is achieved by using the mapping

$$\frac{\eta}{L} = \frac{\xi + 1}{2}, \qquad -1 \leq \xi \leq 1, \tag{6.30}$$

We discretize the domain $[-1, 1]$ using the Gauss-Lobatto collocation points given by

$$\xi = \cos\frac{\pi j}{N}, \qquad j = 0, 1, 2, \ldots, N, \tag{6.31}$$

where N is the number of collocation points used. The functions F_i, Θ_i and Φ_i for $i \geq 1$ are approximated at the collocation points as follows

$$\left.\begin{aligned} &F_i(\xi) \approx \sum_{k=0}^{N} F_i(\xi_k) T_k(\xi_j), \qquad \Theta_i(\xi) \approx \sum_{k=0}^{N} \Theta_i(\xi_k) T_k(\xi_j), \\ &\Phi_i(\xi) \approx \textstyle\sum_{k=0}^{N} \Phi_i(\xi_k) T_k(\xi_j) \end{aligned}\right\} \quad j = 0, 1, \ldots, N, \tag{6.32}$$

where T_k is the k^{th} Chebyshev polynomial given by

$$T_k(\xi) = \cos\left[k \cos^{-1}(\xi)\right]. \tag{6.33}$$

The derivatives of the variables at the collocation points are represented as

$$\left.\begin{aligned} &\frac{d^r F_i}{d\eta^r} = \sum_{k=0}^{N} \mathbf{D}_{kj}^r F_i(\xi_k), \qquad \frac{d^r \Theta_i}{d\eta^r} = \sum_{k=0}^{N} \mathbf{D}_{kj}^r \Theta_i(\xi_k), \\ &\frac{d^r \Phi_i}{d\eta^r} = \sum_{k=0}^{N} \mathbf{D}_{kj}^r \Phi_i(\xi_k) \end{aligned}\right\} \quad j = 0, 1, \ldots, N, \tag{6.34}$$

where r is the order of differentiation and $\mathbf{D} = \frac{2}{L}\mathcal{D}$ with $\mathcal{D}$ being the Chebyshev spectral differentiation matrix whose entries are defined by (1.30). Substituting equations (6.30)-(6.34) into equations (6.25)-(6.27) leads to the matrix equation

$$\mathbf{A}_{i-1}\mathbf{X}_i = \mathbf{R}_{i-1}. \tag{6.35}$$

In equation (6.35), $\mathbf{A}_{i-1}$ is a $(3N+3)\times(3N+3)$ square matrix and $\mathbf{X}_i$ and $\mathbf{R}_{i-1}$ are $(3N+3)\times 1$ column vectors defined by

$$\mathbf{A}_{i-1} = \begin{bmatrix} A_{11} & A_{12} & A_{13} \\ A_{21} & A_{22} & A_{23} \\ A_{31} & A_{32} & A_{33} \end{bmatrix}, \qquad \mathbf{X}_i = \begin{bmatrix} F_i \\ \Theta_i \\ \Phi_i \end{bmatrix}, \qquad \mathbf{R}_{i-1} = \begin{bmatrix} \mathbf{r}_{1,i-1} \\ \mathbf{r}_{2,i-1} \\ \mathbf{r}_{3,i-1} \end{bmatrix}, \tag{6.36}$$

where

$$\begin{aligned} F_i &= [f_i(\xi_0), f_i(\xi_1), ..., f_i(\xi_{N-1}), f_i(\xi_N)]^T, \\ \Theta_i &= [\theta_i(\xi_0), \theta_i(\xi_1), ..., \theta_i(\xi_{N-1}), \theta_i(\xi_N)]^T, \\ \Phi_i &= [\phi_i(\xi_0), \phi_i(\xi_1), ..., \phi_i(\xi_{N-1}), \phi_i(\xi_N)]^T, \end{aligned}$$

$$\begin{aligned} \mathbf{r}_{1,i-1} &= [r_{1,i-1}(\xi_0), r_{1,i-1}(\xi_1), ..., r_{1,i-1}(\xi_{N-1}), r_{1,i-1}(\xi_N)]^T, \\ \mathbf{r}_{2,i-1} &= [r_{2,i-1}(\xi_0), r_{2,i-1}(\xi_1), ..., r_{2,i-1}(\xi_{N-1}), r_{2,i-1}(\xi_N)]^T, \\ \mathbf{r}_{3,i-1} &= [r_{3,i-1}(\xi_0), r_{3,i-1}(\xi_1), ..., r_{3,i-1}(\xi_{N-1}), r_{3,i-1}(\xi_N)]^T, \end{aligned}$$

$$\begin{aligned} &A_{11} = \mathbf{D}^3 + \mathbf{a}_{1,i-1}\mathbf{D}^2 + \mathbf{a}_{2,i-1}\mathbf{D} + \mathbf{a}_{3,i-1}\mathbf{I}, \qquad A_{12} = 2\frac{Gr_x}{Re^2}\mathbf{I}, \qquad A_{13} = 2\frac{Gr_x N_1}{Re^2}\mathbf{I}, \\ &A_{21} = \mathbf{b}_{3,i-1}\mathbf{D}^2 + \mathbf{b}_{4,i-1}\mathbf{D} + \mathbf{b}_{5,i-1}\mathbf{I}, \qquad A_{22} = \left(\frac{3+4R_d}{3Pr}\right)\mathbf{D}^2 + \mathbf{b}_{1,i-1}\mathbf{D} + \mathbf{b}_{2,i-1}\mathbf{I}, \\ &A_{23} = D_f\mathbf{D}^2, \qquad A_{31} = \mathbf{c}_{3,i-1}\mathbf{D} + \mathbf{c}_{4,i-1}\mathbf{I}, \qquad A_{32} = Sr\mathbf{D}^2, \\ &A_{33} = \frac{1}{Sc}\mathbf{D}^2 + \mathbf{c}_{1,i-1}\mathbf{D} + \mathbf{c}_{2,i-1}\mathbf{I}. \end{aligned}$$

In the above definitions T stands for transpose, $\mathbf{a}_{k,i-1}$ $(k = 1, \ldots, 6)$, $\mathbf{b}_{k,i-1}$ $(k = 1, \ldots, 7)$, $\mathbf{c}_{k,i-1}$ $(k = 1, \ldots, 6)$, and $\mathbf{r}_{k,i-1}$ $(k = 1, 2, 3)$ are diagonal matrices of order $(N + 1) \times (N + 1)$, $\mathbf{I}$ is an identity matrix of order $(N + 1) \times (N + 1)$. Finally the solution is obtained as

$$\mathbf{X}_i = \mathbf{A}_{i-1}^{-1}\mathbf{R}_{i-1}. \tag{6.37}$$

6.4 Results and discussion

In generating the results presented here it was determined through numerical experimentation that $L = 15$ and $N = 60$ gave sufficient accuracy for the linearisation method. In addition, the results in this work were obtained for Prandtl number used is $Pr = 0.71$ which physically corresponds to air. The Schmidt number used $Sc = 0.22$ is for hydrogen at approximately 25° and one atmospheric pressure. The Darcy-Reynolds number was fixed at $Re_D = 100$.

Tables 6.1 - 6.7 show, firstly the effects of various parameters on the skin-friction, the local heat and the mass transfer coefficients for different physical parameters values. Secondly, to confirm the accuracy of the linearisation method, these results are compared to those obtained using the Matlab `bvp4c` solver. The results from the two methods are in excellent agreement with the linearisation method converging at the four order with accuracy of up to six decimal places.

The effect of increasing the magnetic filed parameter M on the skin-friction coefficient $f''(0)$, the Nusselt number $-\theta'(0)$ and the Sherwood number $-\phi'(0)$ are given in Table 6.1. Here we find that increasing the magnetic filed parameter leads to reduces Nusselt number and Sherwood number as well as skin friction coefficient in case of aiding buoyancy. These results are to be expected, and are, in fact, similar to those obtained previously by, among others (Ishak 2011 and Ibrahim and Makinde 2010).

Table 6.1: The effect of various values of M on skin-friction, heat and mass transfer coefficients when $Gr/Re^2 = 1,\ Gb = 2,\ R_d = 5,\ D_f = 0.3,\ Sr = 0.2,\ R = 2$ and $N_1 = 0.1$

		SLM results				
	M	1st order	2nd order	3rd order	4th order	`bvp4c`
$f''(0)$	0.0	-0.4814153	-0.4850253	-0.4849715	-0.4849715	-0.4849715
	0.5	-0.6740552	-0.6763684	-0.6763449	-0.6763449	-0.6763449
	1.0	-0.8493782	-0.8508257	-0.8508252	-0.8508252	-0.8508252
	3.0	-1.4360464	-1.4353137	-1.4353164	-1.4353164	-1.4353165
$-\theta'(0)$	0.0	1.1403075	1.0665625	1.0664508	1.0664507	1.0664506
	0.5	0.9901280	0.9608685	0.9608557	0.9608557	0.9608557
	1.0	0.8635520	0.8564487	0.8564359	0.8564359	0.8564359
	3.0	0.4988671	0.4618122	0.4618155	0.4618155	0.4618155
$-\phi'(0)$	0.0	3.4850628	3.4316981	3.4316040	3.4316040	3.4316040
	0.5	3.4646441	3.4269708	3.4269284	3.4269284	3.4269284
	1.0	3.4471832	3.4252628	3.4252469	3.4252469	3.4252469
	3.0	3.3955048	3.4354074	3.4354027	3.4354027	3.4354027

In Table 6.2 an increase in the mixed convection parameter Gr/Re^2 (that is, aiding buoyancy) enhances the skin friction coefficient. This is explained by the fact that an increase in the fluid buoyancy leads to an acceleration of the fluid flow, thus increasing the skin friction coefficient. Similar results were obtained in the past by Srinivasacharya and RamReddy (2011) and Partha et al. (2005). Also, the non-dimensional heat and mass transfer coefficients increase when Gr/Re^2 increases. This is because an increasing in mixed convection parameter, increases the momentum transport in the boundary layer this is leads to carried out more heat and mass species out of the surface, then reducing the thermal and concentration boundary layers thickness and hence increasing the heat and mass transfer rates.

Tables 6.3 and 6.4 show the effects of increasing of radiation parameter R_d and

Table 6.2: The effect of various values of Gr/Re^2 on skin-friction, heat and mass transfer coefficients when $M = 0.5,\ Gb = 0.2,\ R_d = 5,\ D_f = 0.3,\ Sr = 0.2,\ R = 2$ and $N_1 = 0.1$

		SLM results				
	Gr/Re^2	1st order	2nd order	3rd order	4th order	`bvp4c`
$f''(0)$	0.0	-1.4591484	-1.4698210	-1.4698846	-1.4698846	-1.4698846
	0.5	-0.9012908	-0.8997233	-0.8997257	-0.8997257	-0.8997257
	1.0	-0.4050173	-0.3931112	-0.3932958	-0.3932959	-0.3932959
	1.5	0.0553527	0.0821847	0.0812023	0.0811981	0.0811981
$-\theta'(0)$	0.0	0.9642741	0.9380080	0.9372522	0.9372516	0.9372517
	0.5	1.1100348	1.1100992	1.1100977	1.1100977	1.1100977
	1.0	1.2140010	1.2061822	1.2061407	1.2061406	1.2061406
	1.5	1.2971738	1.2750888	1.2748485	1.2748460	1.2748459
$-\phi'(0)$	0.0	3.2852476	3.3276503	3.3277472	3.3277472	3.3277472
	0.5	3.3804463	3.3723007	3.3723035	3.3723035	3.3723035
	1.0	3.4560434	3.4095381	3.4096350	3.4096350	3.4096350
	1.5	3.5209405	3.4435308	3.4438413	3.4438410	3.4438410

chemical reaction parameter R on the skin-friction, the heat and mass transfer rates respectively. The skin-friction coefficient is enhanced by the radiation parameter. It is however reduced by the chemical reaction parameter (Loganathan et al. 2011). Increasing the radiation parameter R_d and chemical reaction parameter R have the same effect on the heat and mass transfer rates, that is, $-\theta'(0)$ decreases while $-\phi'(0)$ is increases. This is because for large values of R_d and R leads to an increased of conduction over the radiation, this is to decrease the buoyancy force and the thicknesses of the thermal and the momentum boundary layers (Salem 2006 and Sajid 2008).

Table 6.5 shows the influence of the viscous dissipation parameter Gb. The skin-friction coefficient and the Sherwood number increase as Gb increases. When viscous

Table 6.3: The effect of various values of R_d on skin-friction, heat and mass transfer coefficients when $M = 0.5,\ Gr/Re^2 = 1,\ Gb = 2,\ D_f = 0.3,\ Sr = 0.2,\ R = 2$ and $N_1 = 0.1$

		SLM results				
	R_d	1st order	2nd order	3rd order	4th order	`bvp4c`
$f''(0)$	0.0	-0.8321942	-0.8296098	-0.8296126	-0.8296126	-0.8296126
	0.1	-0.8265136	-0.8237362	-0.8237399	-0.8237399	-0.8237399
	1.0	-0.7847954	-0.7809951	-0.7810165	-0.7810165	-0.7810165
	5.0	-0.6740552	-0.6763684	-0.6763449	-0.6763449	-0.6763449
$-\theta'(0)$	0.0	1.6073424	1.5812386	1.5812108	1.5812108	1.5812107
	0.1	1.5660595	1.5413761	1.5413484	1.5413484	1.5413483
	1.0	1.3427120	1.3213291	1.3212411	1.3212411	1.3212410
	5.0	0.9901280	0.9608685	0.9608557	0.9608557	0.9608557
$-\phi'(0)$	0.0	3.3194186	3.3140414	3.3140501	3.3140501	3.3140501
	0.1	3.3290532	3.3224223	3.3224330	3.3224330	3.3224330
	1.0	3.3799905	3.3652798	3.3653080	3.3653080	3.3653079
	5.0	3.4646441	3.4269708	3.4269284	3.4269284	3.4269284

dissipation is considered, the temperature of the liquid will be at higher level than the viscous dissipation is neglected. So the value of $\theta'(0)$ is decreased when Gb is increased. Then leads to reduction in the Nusselt number, this is showed in Table 6.5.

The effect of the Soret parameter on the skin-friction, the heat and the mass transfer coefficients is presented in Table 6.6. We observe that $f''(0)$ and $-\theta'(0)$ increase with Sr while $-\phi'(0)$ decreases as Sr increases. This is because, either an increase in temperature difference or a decrease in concentration difference leads to an enhance in the value of the Soret parameter. Hence increasing in this parameter leads to increase in the heat transfer rate and decreases the mass transfer rate, similar findings were reported by Partha et. al (2006).

Table 6.4: The effect of various values of R on skin-friction, heat and mass transfer coefficients when $M = 0.5,\ Gr/Re^2 = 1,\ Gb = 2,\ R_d = 5,\ D_f = 0.3,\ Sr = 0.2$ and $N_1 = 0.1$

		SLM results				
	R	1st order	2nd order	3rd order	4th order	`bvp4c`
$f''(0)$	0.0	-0.6731258	-0.6744797	-0.6744636	-0.6744636	-0.6744636
	0.5	-0.6734801	-0.6753000	-0.6752798	-0.6752798	-0.6752798
	1.0	-0.6737396	-0.6757935	-0.6757718	-0.6757718	-0.6757718
	3.0	-0.6742259	-0.6766852	-0.6766608	-0.6766608	-0.6766608
$-\theta'(0)$	0.0	1.1189720	1.0911185	1.0911318	1.0911318	1.0911318
	0.5	1.0820871	1.0533659	1.0533660	1.0533660	1.0533660
	1.0	1.0488745	1.0198614	1.0198547	1.0198547	1.0198547
	3.0	0.9383805	0.9090094	0.9089938	0.9089938	0.9089938
$-\phi'(0)$	0.0	2.3759654	2.3053444	2.3050605	2.3050605	2.3050605
	0.5	2.6922827	2.6370931	2.6369476	2.6369476	2.6369476
	1.0	2.9735168	2.9263265	2.9262389	2.9262389	2.9262389
	3.0	3.8920543	3.8602613	3.8602362	3.8602362	3.8602362

Table 6.7 shows the effect of the Dufour number on the skin-friction, the heat and the mass transfer coefficients. It seen that as the Dufour parameter increases, the skin-friction coefficient and mass transfer rate are enhanced while the mass transfer rate is reduced. We note that the Soret and Dufour numbers have opposite effects on $-\theta'(0)$ and $-\phi'(0)$. The reason is either decrease in temperature difference or increase in concentration difference leads to an increase in the value of Dufour number and hence to increasing in D_f parameter leads to decrees in the heat transfer rate and increase the mass transfer rate (see Partha et al. 2006).The effect of Soret number on heat and mass rates is the exact opposite of the effect of Dufour number, this is shown in Table 6.6 and Table 6.7.

The effects of the various fluid and physical parameters on the fluid properties

Table 6.5: The effect of various values of Gb on skin-friction, heat and mass transfer coefficients when $M = 0.5,\ Gr/Re^2 = 1,\ R_d = 5,\ D_f = 0.3,\ Sr = 0.2,\ R = 2$ and $N_1 = 0.1$

		SLM results				
	Gb	1st order	2nd order	3rd order	4th order	`bvp4c`
$f''(0)$	0.0	-0.7323337	-0.7305116	-0.7305610	-0.7305610	-0.7305611
	0.5	-0.7163917	-0.7157877	-0.7158090	-0.7158091	-0.7158091
	1.0	-0.7013730	-0.7019055	-0.7019068	-0.7019068	-0.7019068
	2.0	-0.6740552	-0.6763684	-0.6763449	-0.6763449	-0.6763449
$-\theta'(0)$	0.0	1.2009406	1.1944030	1.1944165	1.1944165	1.1944165
	0.5	1.1392509	1.1296026	1.1296021	1.1296021	1.1296021
	1.0	1.0838318	1.0693714	1.0693680	1.0693680	1.0693679
	2.0	0.9901280	0.9608685	0.9608557	0.9608557	0.9608557
$-\phi'(0)$	0.0	3.4146264	3.3843228	3.3843345	3.3843345	3.3843345
	0.5	3.4291011	3.3962484	3.3962534	3.3962534	3.3962534
	1.0	3.4422018	3.4072701	3.4072627	3.4072627	3.4072627
	2.0	3.4646441	3.4269708	3.4269284	3.4269284	3.4269284

are displayed qualitatively in Figures 6.2 - 6.8. Figure 6.2 illustrates the effect of the magnetic parameter M on the velocity, temperature and concentration distributions. We observe that increasing the magnetic filed parameter reduces the velocity. This is because the magnetic field creates Lorentz force which acts against the flow if the magnetic field is applied in the normal direction. We also observe that the magnetic field parameter enhances the temperature and concentration profiles.

Figure 6.3 shows the dimensionless velocity, temperature and concentration profiles for various values of the mixed convection parameter Gr/Re^2 in the case of both aiding flow and opposing flow. We note that when the value of Gr/Re^2 increases, the velocity rise (the velocity is higher for aiding flow and less for opposing flow). The temperature and concentration are reduced as Gr/Re^2 increasing. Same result were

Table 6.6: The effect of various values of Sr on skin-friction, heat and mass transfer coefficients when $M = 0.5,\ Gr/Re^2 = 1,\ Gb = 2,\ R_d = 5,\ D_f = 0.3,\ R = 2$ and $N_1 = 0.1$

		SLM results				
	Sr	1st order	2nd order	3rd order	4th order	`bvp4c`
$f''(0)$	0.0	-0.6742846	-0.6766272	-0.6766046	-0.6766046	-0.6766046
	0.5	-0.6737087	-0.6759780	-0.6759533	-0.6759533	-0.6759533
	1.0	-0.6731258	-0.6753228	-0.6752957	-0.6752958	-0.6752958
	1.5	-0.6725373	-0.6746627	-0.6746334	-0.6746334	-0.6746334
$-\theta'(0)$	0.0	0.9828644	0.9546059	0.9545933	0.9545933	0.9545933
	0.5	1.0016528	0.9707871	0.9707741	0.9707740	0.9707740
	1.0	1.0228265	0.9889532	0.9889398	0.9889398	0.9889397
	1.5	1.0470766	1.0096688	1.0096553	1.0096553	1.0096552
$-\phi'(0)$	0.0	3.5295306	3.4851406	3.4850983	3.4850983	3.4850983
	0.5	3.3620504	3.3352671	3.3352239	3.3352239	3.3352239
	1.0	3.1747048	3.1686539	3.1686069	3.1686069	3.1686069
	1.5	2.9619418	2.9807441	2.9806896	2.9806897	2.9806896

found by Srinivasacharya and RamReddy (2011). Figure 6.4 demonstrates the influence of the thermal radiation parameter R_d on the fluid velocity, temperature and concentration distributions. It is clearly shown in this figure that the velocity and the temperature profiles are increasing with increasing values of R_d but a decreasing in the concentration profile. The non-dimensional fluid velocity, temperature and concentration distributions with effect of the viscous dissipation parameter Gb inside the boundary layer have been shown in Figure 6.5. The thermal boundary layer thickness is increased the with the increasing of Gb while concentration decreases.

In Figures 6.6-6.7 we showed the effect of increasing the Soret Sr and the Dufour D_f parameters on the fluid velocity $f'(\eta)$, temperature $\theta(\eta)$ and concentration $\phi(\eta)$, respectively. The fluid velocity is found to increase with both parameters. An

Table 6.7: The effect of various values of D_f on skin-friction, heat and mass transfer coefficients when $M = 0.5,\ Gr/Re^2 = 1,\ Gb = 2,\ R_d = 5,\ Sr = 0.2,\ R = 2$ and $N_1 = 0.1$

		SLM results				
	D_f	1st order	2nd order	3rd order	4th order	`bvp4c`
$f''(0)$	0.0	-0.7127673	-0.7114335	-0.7114262	-0.7114262	-0.7114262
	0.1	-0.6935377	-0.6939073	-0.6938903	-0.6938903	-0.6938903
	0.3	-0.6543133	-0.6588061	-0.6587812	-0.6587812	-0.6587812
	0.7	-0.5726141	-0.5881245	-0.5881708	-0.5881708	-0.5881708
$-\theta'(0)$	0.0	1.2808105	1.2551495	1.2551551	1.2551551	1.2551551
	0.1	1.1374017	1.1098984	1.1098988	1.1098988	1.1098988
	0.3	0.8388100	0.8078862	0.8078505	0.8078505	0.8078505
	0.7	0.1890478	0.1524654	0.1522122	0.1522122	0.1522121
$-\phi'(0)$	0.0	3.3957339	3.3637967	3.3637968	3.3637968	3.3637968
	0.1	3.4297171	3.3949274	3.3949086	3.3949086	3.3949086
	0.3	3.5005612	3.4599748	3.4599038	3.4599038	3.4599038
	0.7	3.6551802	3.6026815	3.6024423	3.6024423	3.6024423

increase in Sr reduces the temperature distribution while D_f enhances temperature distribution. Albeit that the effect is much more pronounced in the case of Dufour number effect. This may be attributed that the Dufour number is entering directly into heat equation and Soret number does not appear in the heat equation. Thus the effect of Soret number on the temperature distribution is very small. It is also noted that from Figures 6.6 - 6.7, an increase in Sr enhances the concentration distribution while the concentration distribution reduced by increasing in D_f. However, the effect of Soret parameter on temperature and concentration distribution is the exact opposite of the effect of Dufour parameter.

It is noticed that the velocity reduces with increase in the value of chemical reaction parameter R, also as R increasing, the thermal boundary layer thickness

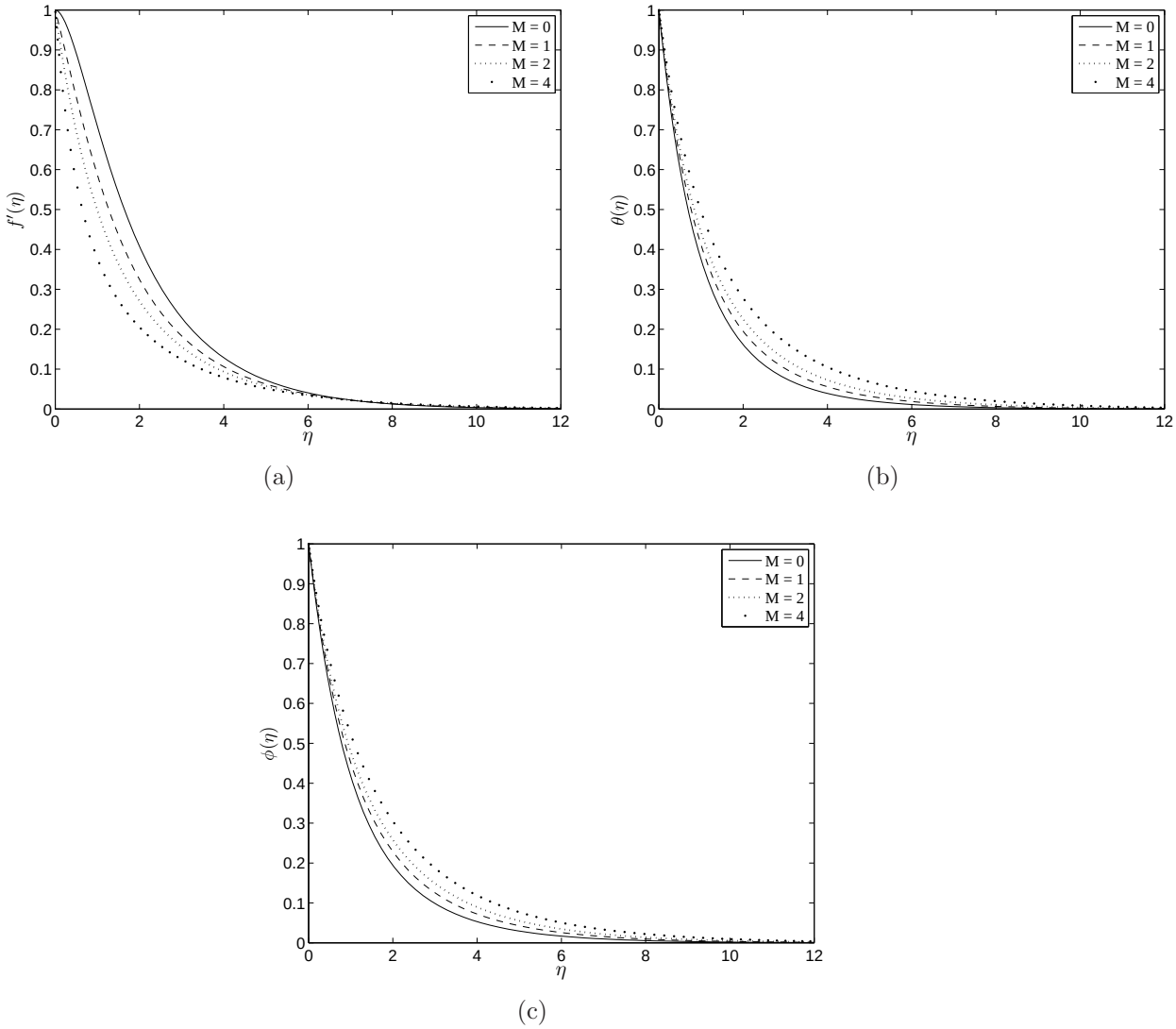

Figure 6.2: Variation of magnetic parameter M on the (a) velocity (b) temperature (c) concentration distributions when $Gr/Re^2 = 1,\ N_1 = 0.5,\ Gb = 0.2,\ R_d = 1,\ D_f = 0.3,\ Sr = 0.2$ and $R = 1$.

enhances while concentration boundary layer thickness which reduces with increase in the chemical reaction parameter R, these are noticed from Figure 6.8.

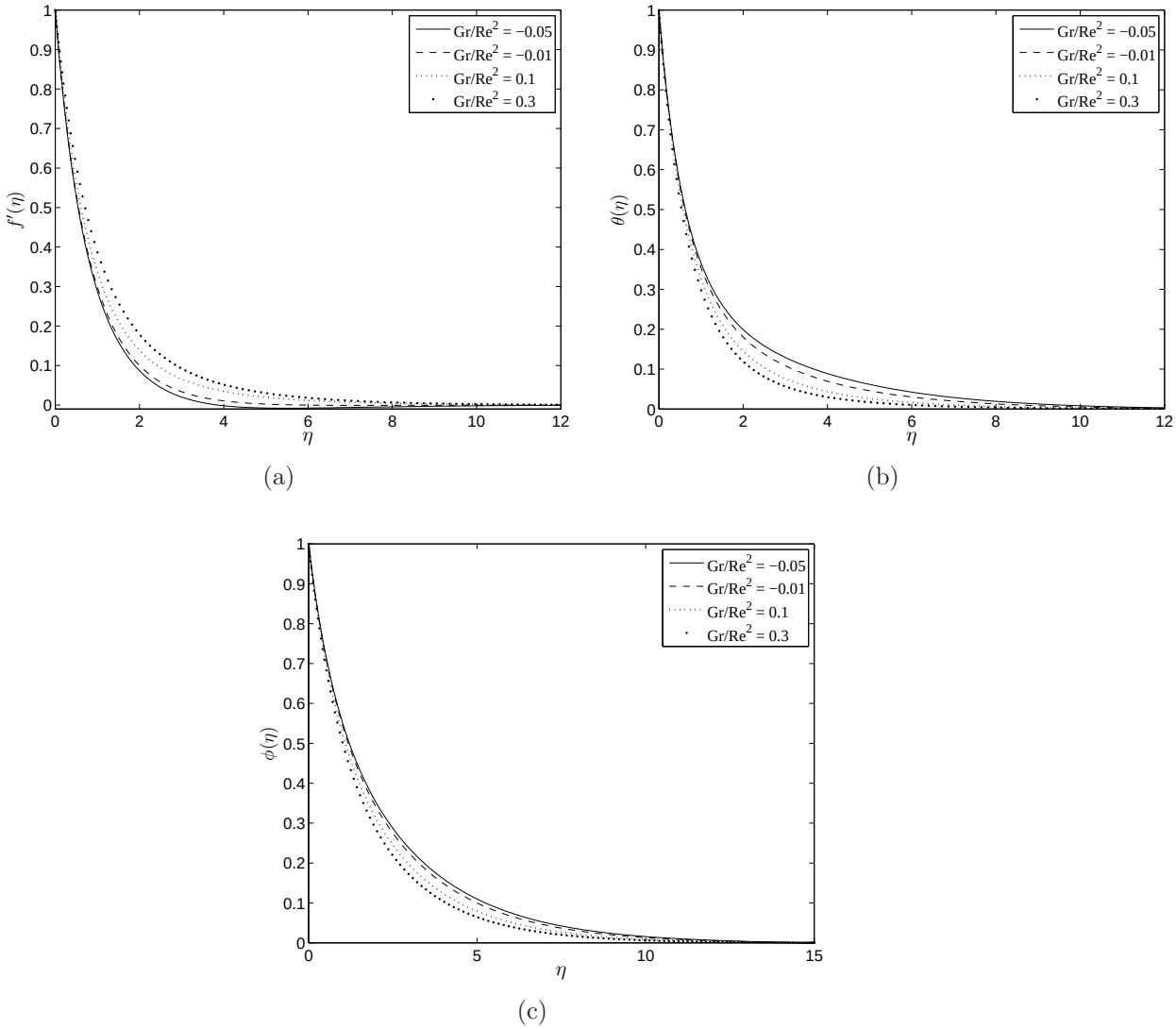

(a) (b)

(c)

Figure 6.3: Variation of mixed convection parameter Gr/Re^2 on the (a) velocity (b) temperature (c) concentration distributions when $M = 1,\ N_1 = 0.1,\ Gb = 1,\ R_d = 4,\ D_f = 0.3,\ Sr = 0.2$ and $R = 0.1$

6.5 Conclusion

In this chapter we have studied the effects of Cross-diffusion and viscous dissipation on heat and mass transfer convection from an exponentially stretching surface in a porous media, we considered the magnetic, radiation and chemical reaction effects. The governing equations were solved using the successive linearisation method. which

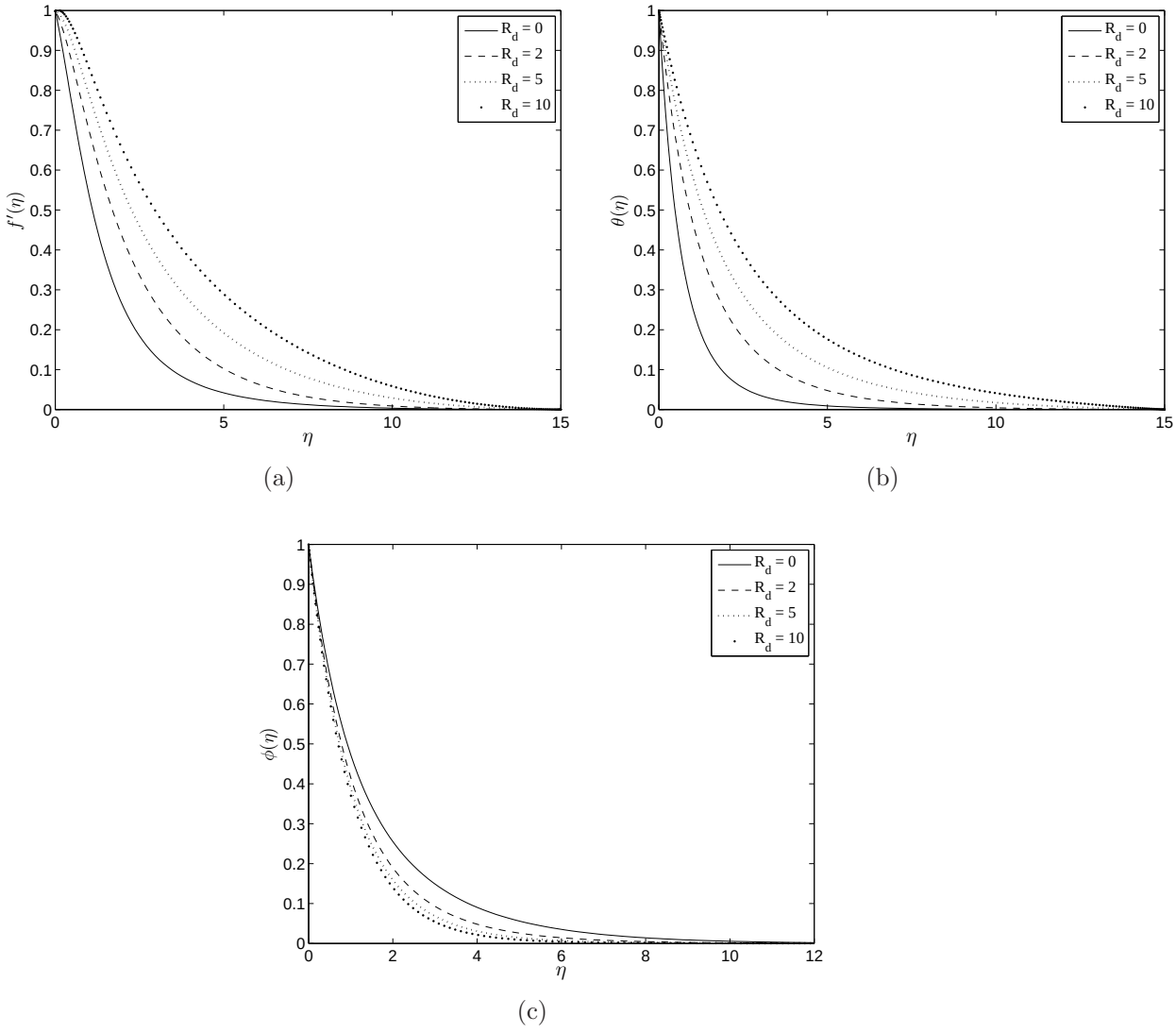

Figure 6.4: Variation of thermal radiation parameter R_d on the (a) velocity (b) temperature (c) concentration distributions when $M = 1,\ N_1 = 0.5,\ Gb = 0.2,\ Gr/Re^2 = 1,\ D_f = 0.3,\ Sr = 0.2$ and $R = 0.1$

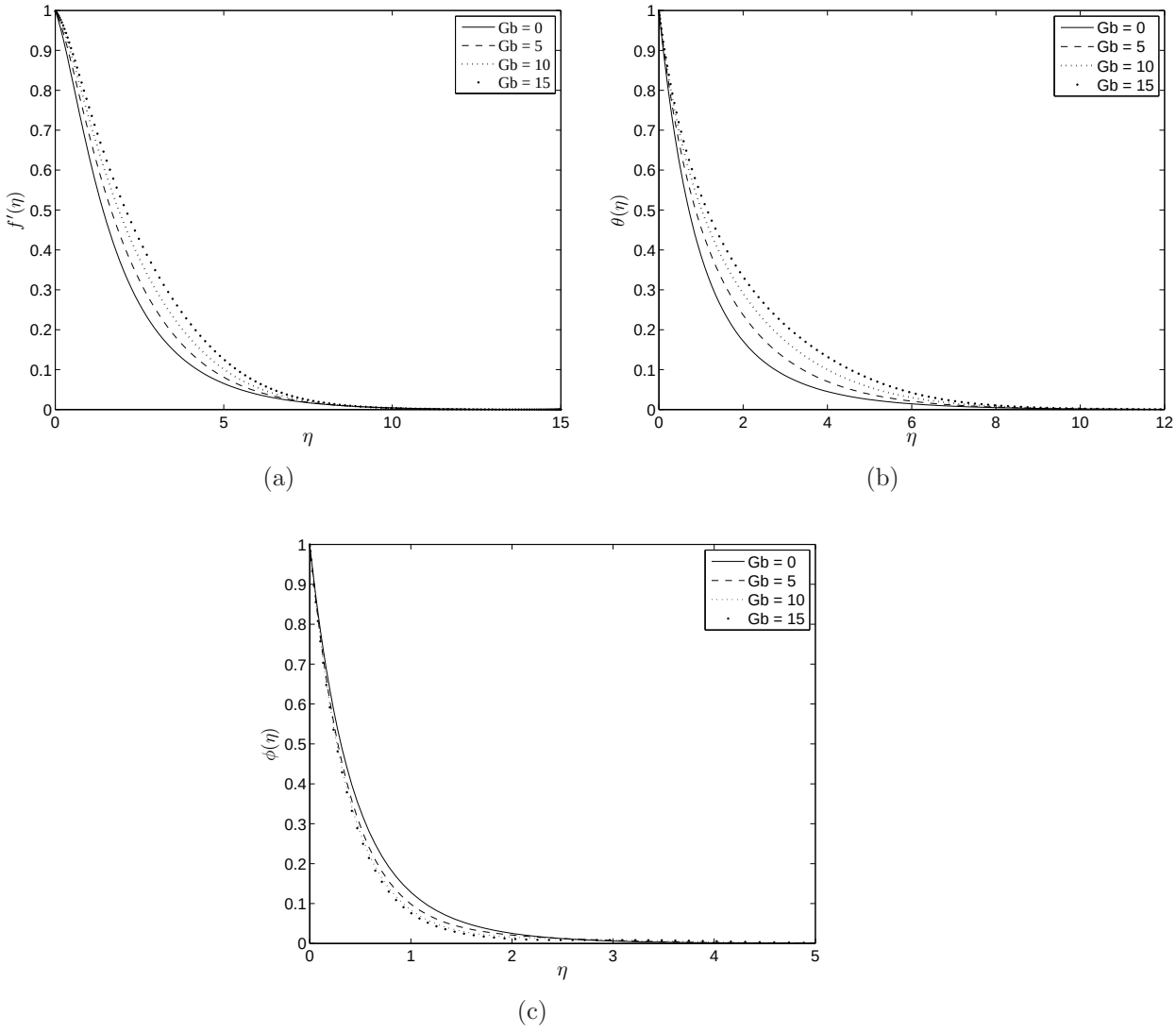

Figure 6.5: Variation of viscous dissipation parameter Gb on the (a) velocity (b) temperature (c) concentration distributions when $M = 1,\ N_1 = 0.5,\ R_d = 1,\ Gr/Re^2 = 1,\ D_f = 0.3,\ Sr = 0.2$ and $R = 0.1$

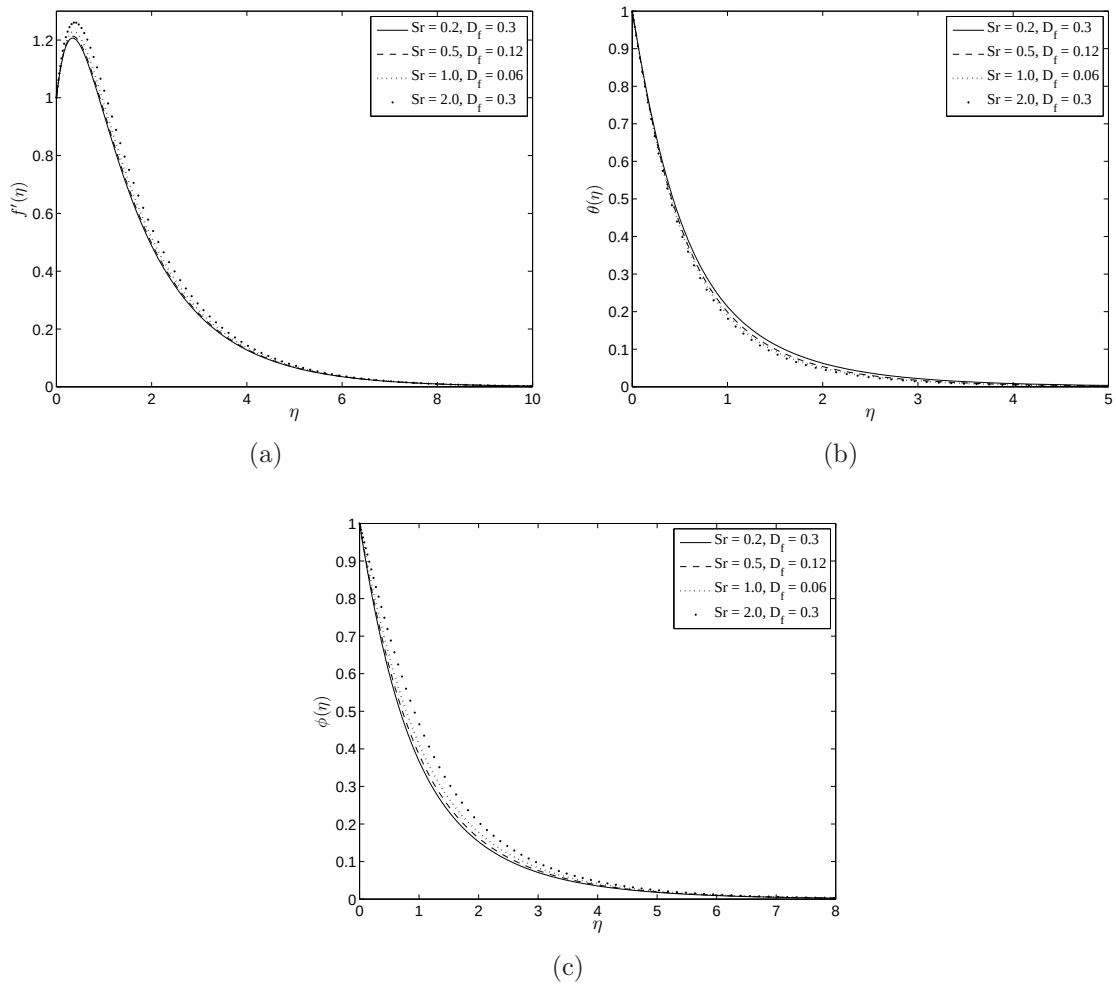

Figure 6.6: Variation of Soret number Sr on the (a) velocity (b) temperature (c) concentration distributions when $M = 1,\ N_1 = 5,\ R_d = 10,\ Gr/Re^2 = 2,\ Gb = 0.5$ and $R = 0.1$

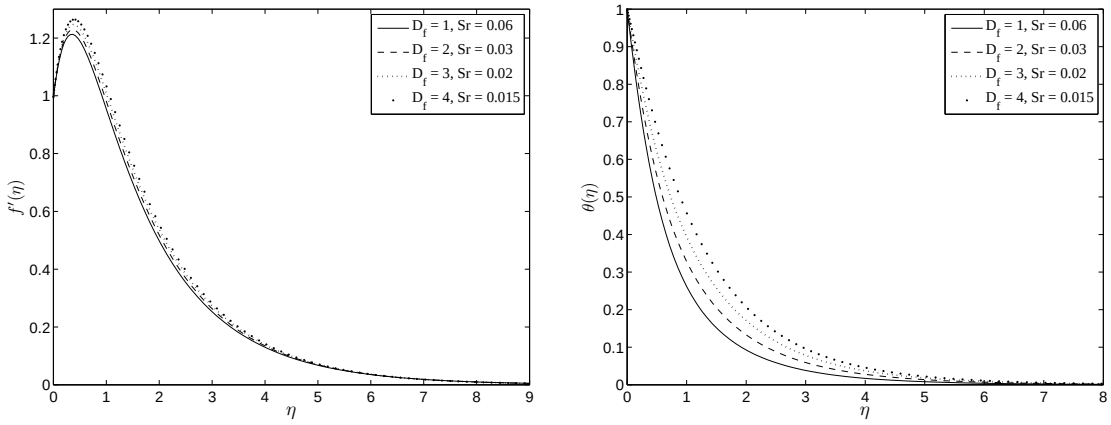

(a)

(b)

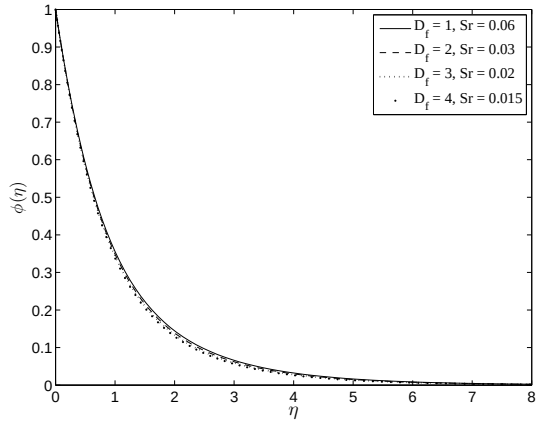

(c)

Figure 6.7: Variation of Dufour number D_f on the (a) velocity (b) temperature (c) concentration distributions when $M = 1,\ N_1 = 5,\ R_d = 10,\ Gr/Re^2 = 2,\ Gb = 2$ and $R = 0.1$

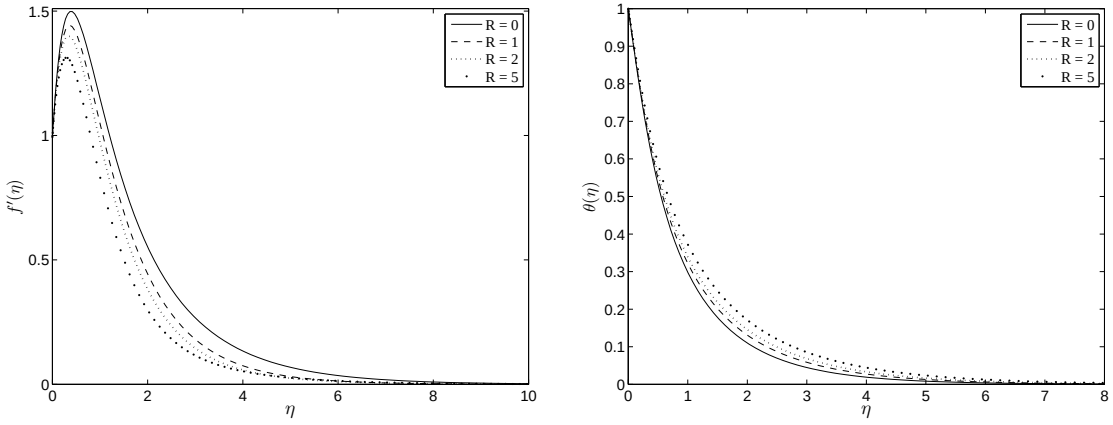

(a)

(b)

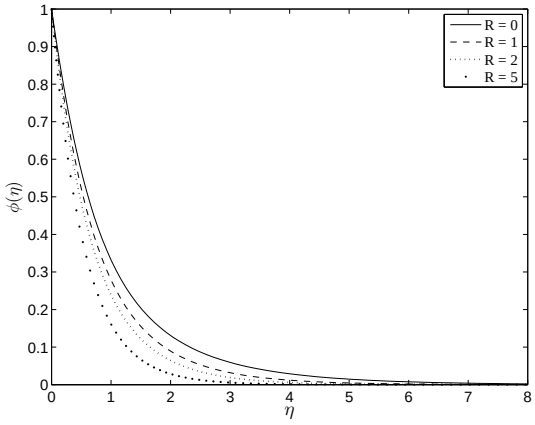

(c)

Figure 6.8: Variation of is chemical reaction parameter R on the (a) velocity (b) temperature (c) concentration distributions when $M = 1,\ N_1 = 2,\ R_d = 0.1,\ Gr/Re^2 = 1,\ Gb = 0.5,\ D_f = 0.3$ and $Sr = 0.2$

has been suggested from a limited number of studies and it gives accurate results with few iterations and it requires shorter times to run the code. Tables and graphs were presented showing the effects of various physical parameters on the fluid properties, the skin-friction coefficient and the heat and the mass transfer rates. It was found that the effect of increasing of the magnetic field parameter is to decelerate the fluid motion while enhancing the temperature and concentration on the dimensionless. It was also observed that the velocity increase with the mixed convection parameter while the temperature and concentration profiles decrease. The effect of Soret number is to reduce the temperature and enhance the velocity and the concentration profiles and an opposite effects occurred by Dufour number on the temperature and concentration distributions. An increase in viscous dissipation and radiation parameters enhances temperature and reduces the concentration distributions.The skin-friction, heat and mass transfer coefficients decrease with an increase in the magnetic field strength. The skin-friction and heat transfer coefficients increase whereas the mass transfer coefficient decreases with increasing Soret number but Dufour number effect is to decrease Nusselt number and increase Sherwood number.

Chapter 7

Conclusion

The overall objectives of this study were to investigate convection and cross-diffusion effects on heat and mass transfer in porous media saturated with Newtonian and non-Newtonian fluids, and to apply a recent hybrid linearization-spectral technique to solve the highly nonlinear and coupled governing equations. We modeled the fluid flows in different flow geometries by systems of partial differential equations. The resulting governing equations for momentum, energy and concentration have been transformed into a system of nonlinear ordinary differential equations by introducing suitable similarity transformations. A successive linearization method has been used to solve the nonlinear differential equation that governs the flow. The accuracy and convergence rate of the obtained solution series have been verified by comparing the results with other numerical methods and with some available results published in the literature. Tabulated and graphical results were presented and discussed showing the effects of different values of cross-diffusion on the velocity, temperature and concentration distributions as well as some physical parameters effects entering into the problem such as the magnetic field, viscous dissipation and thermal radiation parameters. The corresponding local skin-friction, rate of heat and mass transfer

coefficients were also calculated and presented in graphs and tabular form showing the effects of various parameters on them.

The results have shown that the fluid velocity, temperature, and concentration profiles are appreciably influenced by the Soret and Dufour effects, they also play a significant role and should not be neglected. We therefore conclude that cross-diffusion effects have to be considered in the fluid, heat, and mass transfer. We also showed that the magnetic field, viscous dissipation, and radiation parameters have greater effects on the fluid velocity, temperature, and concentration boundary layer thickness. It is also noted that the successive linearization method is valid even for systems of highly nonlinear differential equations. Furthermore, it has great potential for being used in many other related studies involving complicated nonlinear problems in science and engineering, especially in the field of fluid mechanics, which is rich in nonlinear phenomena. We highlight the main findings that have been made in this study.

- Chapter 2:

  In this chapter the effects of Soret and viscous dissipation parameters on natural convection from a vertical plate immersed in a power-law fluid saturated with a non-Darcy porous medium have been investigated. The governing partial differential equations are transformed into a system of ordinary differential equations using a local non-similar method and the model has been solved by the SLM. The results were tested by comparison with the shooting technique. Our discussion showed that:

  (i) Increases in the Soret number leads to decreases in the temperature distribution and increases in the concentration distribution for aiding buoyancy case. Additionally there are increases in both temperature and concentration distributions for opposing buoyancy case.

  (ii) The Nusselt number is enhanced and the Sherwood number is reduced by

increases in the Soret number for aiding buoyancy, and both the Nusselt and Sherwood numbers are reduced by the Soret number for opposing buoyancy.

(iii) Increasing the viscous dissipation parameter increases both heat and mass transfer rates for aiding buoyancy and opposing buoyancy cases.

- Chapter 3:

  The study of the effect of thermal-diffusion on the natural convection from a vertical plate in a thermally stratified porous medium saturated with a non-Newtonian fluid has been investigated in this chapter. We considered the aiding buoyancy and opposing buoyancy flow situations. The following points give an outline of the chapter:

  (i) Temperature and concentration profiles are significantly affected by stratification, Soret and variable viscosity parameters.

  (ii) The Soret number succeeds in enhancing the mass transfer rate for the two different flow situations considered, but reduces the heat transfer rate for aiding buoyancy while increasing it in the case of opposing buoyancy.

  (iii) The heat and mass transfer coefficients are reduced by the power-law index for both aiding buoyancy and opposing buoyancy cases.

  (iv) The Nusselt number reduced the thermal stratification parameter, but enhanced the Sherwood number.

- Chapter 4:

  Discussed in this chapter is the mixed convective flow of a non-Newtonian power-law fluid from a vertical flat plate embedded in a non-Darcy porous medium influenced by viscous dissipation and thermal radiation. The governing partial differential equations are transformed into a system of ordinary differential equations, applying the local similarity and local non-similarity method, with the model being solved with SLM technique. We discussed the three kinds of

power-law fluids (pseudoplastic, Newtonian and dilatant fluids). It was found that:

(i) The viscous dissipation and thermal radiation parameters have increasing effects on both velocity and temperature profiles for all values of the power-law index.

(ii) The skin-friction and heat transfer coefficients are reduced by an increase in the viscous dissipation and thermal radiation parameters.

(iii) When the viscosity parameter increases, the rate of heat transfer increases.

(iv) The power-law index decreases the heat transfer rate.

- Chapter 5:

  In this chapter we have applied the linearization method to the problem of cross-diffusion, double-diffusion and hydromagnetic effects on convection fluid flow over a vertical surface. The linearization method is used in combination with a perturbation expansion method and the accuracy of the solutions has been tested using a local nonsimilarity method. The key results are as follows:

  (i) The comparison between the two methods (SLM and local nonsimilarity methods) showed that there is excellent agreement, while the second order of the SLM series is accurate up to five significant figures.

  (ii) The effect of increasing the Soret number increases the velocity and concentration distributions but decreases the temperature distribution.

  (iii) The Soret number has an increasing effect on skin-friction and heat transfer coefficients and a decreasing effect on the mass transfer coefficient.

  (iv) As the Dufour number increases, the skin-friction and heat transfer coefficients decrease, while the mass transfer coefficient increases.

  (v) The Soret and Dufour numbers have opposite effects on thermal and concentration distributions.

(vi) Increases in magnetic field parameter increases both temperature and concentration profiles and decreases both heat and mass transfer rates.

- Chapter 6:

  We have studied the effects of cross-diffusion on heat and mass transfer convection from an exponentially stretching surface in a porous media. We also considered the magnetic, viscous dissipation and radiation effects. The results are summarized as follows:

  (i) The effect of the Soret number was to decrease the temperature and enhance the velocity and concentration profiles.

  (ii) The thermal boundary layer thickness is increased with the increasing of viscous dissipation parameter while concentration decreases.

  (iii) The skin-friction and heat transfer coefficients increased, whereas the mass transfer coefficient increased with an increasing Soret number. The effect of the Dufour number is to decrease the heat transfer rate and increase the mass transfer rate.

  (iv) The temperature and concentration are reduced while the heat and mass transfer coefficients enhanced as mixed convection parameter increasing.

References

Abbasbandy, S., (2006): The application of the homotopy analysis method to nonlinear equations arising in heat transfer, *Physics Letters A*, **360**, 109–113.

Abbasbandy, S., (2007): Homotopy analysis method for heat radiation equations, *Int. Comm. Heat and Mass Transfer*, **34**, 380–387.

Abreu, C. R. A., M. F. Alfradique, and A. T. Silva, (2007): Boundary layer flows with Dufour and Soret effects: I: Forced and natural convection, *Chem. Eng. Sci.*, **61**, 4282–4289.

Adomian, G., (1989): Nonlinear Stochastic Systems Theory and Applications to Physics, *Kluwer Academic Publishers*.

Adomian, G., (1990): A review of the decomposition method and some recent results for nonlinear equation, *Math. Comput. Modell.*, **13**, 17–43.

Adomian, G. and R. Rach, (1992): Noise terms in decomposition series solution, *Comput. Math. Appl.*, **24**, 61–64.

Adomian, G., (1994): Solving Frontier Problems of Physics: The Decomposition Method, *Kluwer Academic Publishers*.

Afify, A. A., (2004): MHD free convective flow and mass transfer over a stretching sheet with chemical reaction, *Int. J. Heat and Mass Transfer*, **40**, 495–500.

Afify, A. A., (2007): Effects of variable viscosity on non-Darcy MHD free convection along a non-isothermal vertical surface in a thermally stratified porous medium, *Appl. Math. Modell.*, **31**, 1627–1634.

Afify, A. A., (2009): Similarity solution in MHD: Effects of thermal diffusion and diffusion thermo on free convective heat and mass transfer over a stretching surface considering suction or injection, *Comm. Nonlin. Sci. Numer. Simul.*, **14**, 2202–2214.

Alam, M. S., M. M. Rahman, M. A. Maleque, and M. Ferdows, (2006a): Dufour and Soret effects on steady MHD combined free-forced convective and mass transfer flow past a semi-infinite vertical plate, *Thammasat Int. J . Sci. Tech.*, **11**, 1–12.

Alam, M. S. and M. M. Rahman, (2006b): Dufour and Soret effects on mixed convection flow past a vertical porous flat plate with variable suction, *Nonlinear Analysis: Modeling and Control*, **11**, 3–12.

Ali, M. E., (1995): On thermal boundary layer on a power law stretched surface with suction or injection, *Int. J. of Heat and Fluid Flow*, **16**, 280–290.

Al-Odat, M. Q., R.A. Damseh, and T. A. Al-Azab, (2006): Thermal boundary layer on an exponentially stretching continuous surface in the presence of magnetic field effect, *Int. J. Appl. Mech. Eng.*, **11**, 289–299.

Altevogt, A. S., D. E. Rolston, and S. Whitaker, (2003): New equations for binary gas transport in porous media, Part 1: Equation development, *Advances in Water Resources*, **26**, 695 –715.

Anjalidevi, S. P. and R. U. Devi, (2011): Soret and Dufour effects on MHD slip flow with thermal radiation over a porous rotating infnite disk, *Comm. Nonlin. Sci.*, **16**, 1917–1930.

Anwar Beg, O., J. Zueco, and H. S. Takha, (2008): Laminar free convection from a continuously-moving vertical surface in thermally-stratified non-Darcian high-

porosity medium: Network numerical study, *Int. Comm. Heat and Mass Transfer*, **35**, 810–816.

Aris, R., (1975): The Mathematical Theory of Diffusion and Reaction in Permeable Catalyst, *Volume I, Clarendon Press, Oxford*.

Awad, F. G. and P. Sibanda, (2010a): Dufour and Soret effects on heat and mass transfer in a micropolar fluid in a horizontal channel,, *WSEAS Transactions on Heat and Mass Transfer*, **5**, 165–177.

Awad, F. G., P. Sibanda, and S. S. Motsa, (2010b): On the linear stability analysis of a Maxwell fluid with double-diffusive convection, *Appl. Math. Modell.*, **34**, 3509–3517.

Awad, F. G., P. Sibanda, M. Narayana, and S. S. Motsa, (2011a): Convection from a semi-finite plate in a fluid saturated porous medium with cross-diffusion and radiative heat transfer, *Int. J. of the Physical Sci.*, **6**, 4910–4923.

Awad, F. G., P. Sibanda., S. S. Motsa, and O. D. Makinde, (2011b): Convection from an inverted cone in a porous medium with cross-diffusion effects, *Computers and Mathematics with Applications*, **61**, 1431–1441.

Awrejcewicz, J., I. V. Andrianov, and L. I. Manevitch, (1998): Asymptotic approaches in Nonlinear Dynamics, *Springer-Verlag, Berlin*.

Baehr, H. D. and K. Stephan, (1998): Heat and Mass Transfer, *Springer-Verlag, Berlin*.

Baines, P. G and A. E. Gill, (1969): On thermohaline convection with linear gradients, *J. Fluid Mech.*, **37**, 289–306.

Bashier, E. B. M. and K. C. Patidar, (2011a): A novel fitted operator finite difference method for a singularly perturbed delay parabolic partial differential equation, *Appl. Math. and Comput.*, **217**, 4728–4739.

Bashier, E. B. M. and K. C. Patidar, (2011b): A fitted numerical method for a system of partial delay differential equations, *Computers and Mathematics with Applications*, **61**, 1475–1492.

Bashier, E. B. M. and K. C. Patidar, (2011c): A second-order fitted operator finite difference method for a singularly perturbed delay parabolic partial differential equation, *J. Difference Equations and Applications*, **17**, 779–794.

Bear, J., (1972): Dynamics of Fluids in Porous Media, *Dover Publications, New York*.

Bejan, A., (1984): Convection Heat Transfer, *John Wiley and Sons, New York*.

Bejan, A. and K. R. Khair, (1985): Heat and mass transfer by natural convection in porous medium, *Int. J. Heat and Mass Transfer*, **28**, 909–918.

Bellman, R. E. and R. E. Kalaba, (1965): Quasilinearization and Nonlinear Boundary-Value Problems, *Elsevier, New York*.

Bhadauria, B. S., (2007): Double diffusive convection in a porous medium with modulated temperature on the boundaries, *Transport Porous Media*, **70**, 191–211.

Bhadauria, B. S. and A. K. Srivastava, (2010): Magneto-double diffusive convection in an electrically conducting-fluid-saturated porous medium with temperature modulation of the boundaries, *Int. J. Heat and Mass Transfer*, **53**, 2530–2538.

Bidin, B. and R. Nazar, (2009): Numerical solution of the boundary layer flow over an exponentially stretching sheet with thermal radiation, *Euro J. Sci. Res.*, **33**, 710–717.

Boyd, J. P., (2003): Chebyshev polynomial expansions for simultaneous approximation of two branches of a function with application to the one-dimensional Bratu equation, *Appl. Math. Comput.*, **142**, 189–200.

Bridge, J. S. and R. V. Demicco, (2008): Earth Surface Processes, Landforms and Sediment Deposits, *Cambridge University Press*.

Brinkman, H. C., (1947a): A calculation of the viscous force exerted by a flowing fluid on a dense swarm of particles, *Appl. Sci. Res.*, **A1**, 27–34.

Brinkman, H. C., (1947b): On the permeability of media consisting of closely packed porous particles, *Appl. Sci. Res.*, **A1**, 81–86.

Bruschke, M. V. and S. G. Advani, (1990): A finite element/control volume approach to mold filling in anisotropic porous media, *Polymer Composities*, **11**, 398–405.

Canuto, C., M. Y Hussaini, A. Quarteroni, and T. A. Zang, (1988): Spectral Methods in Fluid Dynamics, *Springer-Verlag, Berlin*.

Chamkha, A. J., (1997a): Hydromagnetic natural convection from an isothermal inclined surface adjacent to a thermally stratified porous medium, *Int. J. Eng. Sci.*, **35**, 975–986.

Chamkha, A. J., (1997b): MHD-free convection from a vertical plate embedded in a thermally stratified porous medium with Hall effects, *Appl. Math. Modell.*, **21**, 603–609.

Chamkha, A. J. and A. A. Khaled, (1999): Non-similar hydromagnetic simultaneous heat and mass transfer by mixed convection from a vertical plate embedded in a uniform porous medium, *Numerical Heat Transfer Part A: Applications*, **36**, 327–344.

Chamkha, A. J., E. S. E. Ahmed, and A. S. Aloraier, (2010): Melting and radiation effects on mixed convection from a vertical surface embedded in a non-Newtonian fluid saturated non-Darcy porous medium for aiding and opposing eternal flows, *Int. J. Phys. Sci.*, **5**, 1212–1224.

Chen, H. T. and C. K. Chen, (1988a): Natural convection of a non-Newtonian fluid about a horizontal cylinder and sphere in a porous medium, *Int. Comm. Heat and Mass Transfer*, **15**, 605–614.

Chen, H. T. and C. K. Chen, (1988b): Natural convection of non-Newtonian fluids along a vertical plate embedded in a porous medium, *ASME J. Heat Transfer*, **110**, 257–260.

Chen, A. H. and J. H. Horng, (1999): Natural convection from a vertical cylinder in a thermally stratified porous medium, *Int. J. Heat and Mass Transfer*, **34**, 423–428.

Chen, Z. and R. Ewing, (2002): Fluid Flow and Transport in Porous Media, *Mathematical and Numerical Treatment, AMS*.

Cheng, P. and W. J. Minkowycz, (1977a): Free convection about a vertical flat plate embedded in a porous medium with application to heat transfer from a dike, *J. Geophys. Res.*, **82**, 2040–2044.

Cheng, P., (1977b): Combined free and forced convection flow about inclined surfaces in porous media, *Int. J. Heat and Mass transfer*, **20**, 807–814.

Cheng, C. Y., (2000): Natural convection heat and mass transfer near a vertical wavy surface with constant wall temperature and concentration in a porous medium, *Int. Comm. in Heat and Mass Transfer*, **27**, 1143–1154.

Cheng, C. Y., (2006): Natural convection heat and mass transfer of non-Newtonian power law fluids with yield stress in porous media from a vertical plate with variable wall heat and mass fluxes, *Int. Comm. in Heat and Mass Transfer*, **33**, 1156–1164.

Cheng, C. Y., (2008): Double-diffusive natural convection along a vertical wavy truncated cone in non-Newtonian fluid saturated porous media with thermal and mass stratification, *Int. Comm. in Heat and Mass Transfer*, **35**, 985–990.

Cheng, C. Y., (2009): Soret and Dufour effects on natural convection heat and mass transfer from a vertical cone in a porous medium, *Int. Comm. in Heat and Mass Transfer*, **36**, 1020–1024.

Cheng, C. Y., (2011): Soret and Dufour effects on free convection boundary layers of non-Newtonian power law fluids with yield stress in porous media over a verti-

cal plate with variable wall heat and mass fluxes, *Int. Comm. in Heat and Mass Transfer*, **38**, 615–619.

Choi, S. U. S., (1995): Enhancing thermal conductivity of fluids with nanoparticles. In development and applications of non-Newtonian flows, *ASME, New York*, **66**, 99–105.

Choi, S. U. S., (2009): Nanofluids: From vision to reality through research, *J. Heat Transfer*, **131**, 0331061–0331069.

Christopher, R. H. and S. Middleman, (1965): Power law fluid flow through a packed tube, *Industrial and Engineering Chemistry Fundamentals*, **4**, 422–426.

Conte, S. D. and C. De. Boor, (1981): Elementary Numerical Analysis, *McGraw-Hill*.

Darcy, H., (1856): Les Fontaines publiques de la ville de Dijon, *Paris Victor Dalmont*.

Das, S. K., S. U. S. Choi, and H. E. Patel, (2006): Heat transfer in nanofluidsa review, *Heat Transfer Eng.*, **27**, 3–19.

Dharmadhikari, R. V. and D. D. Kale, (1985): Flow of non-Newtonian fluids through porous media, *Chem. Eng. Sci.*, **40**, 527–529.

Dinarvand, S. and M. M. Rashidi, (2010): A reliable treatment of a homotopy analysis method for two-dimensional viscous flow in arectangular domain bounded by two moving porous walls, *Nonlin. Anal. Real World Appl.*, **11**, 1502–1512.

Domairry, D. G., A. Mohsenzadeh, and M. Famouri, (2009): The application of homotopy analysis method to solve nonlinear differential equation governing Jeffery-Hamel flow, *Comm. Nonlin. Sci. Numer. Simul.*, **14**, 85–95.

Don, W. S. and A. Solomonoff, (1995): Accuracy and speed in computing the Chebyshev collocation derivative, *SIAM J. Sci. Comput.*, **16**, 1253–1268.

Dursunkaya, Z. G. and W. M. Worek, (1992): Diffusion-thermo and thermal diffusion effects in transient and steady natural convection from a vertical surface, *Int. J. Heat and Mass Transfer*, **53**, 2060–2065.

Eckeret, E. R. G. and R.M. Drake, (1972): Analysis of Heat and Mass Transfer, *McGraw-Hill*.

El-Amin, M. F., M. A. El-Hakiem, and M. A. Mansour, (2003): Effects of viscous dissipation on a power-law fluid over plate embedded in a porous medium, *Int. J. Heat and Mass Transfer*, **39**, 807–813.

El-Aziz, M. A., (2008): Thermal-diffusion and diffusion-thermo effects on combined heat mass transfer by hydromagnetic three-dimensional free convection over a permeable stretching surface with radiation, *Physics Letters A*, **372**, 263–272.

Elbashbeshy, E. M. A., (2000): Free convection flow with variable viscosity and thermal diffusivity along a vertical plate in the presence of the magnetic field, *Int. J. of Eng. Sci.*, **38**, 207–213.

Elbashbeshy, E. M. A., (2001): Heat transfer over an exponentially stretching continuous surface with suction, *Archive of Mechanics*, **53**, 643–651.

Elder, J. W., (1966): Steady free convection in a porous medium heated from below, *J. Fluid Mech.*, **27**, 29–48.

El-Hakiem, M. A., (2001): Combined convection in non-Newtonian fluids along a nonisothermal vertical plate in a porous medium with lateral mass flux, *Int. J. Heat and Mass Transfer*, **37**, 379–385.

El-Kabeir, S. M. M., (2011): Soret and Dufour effects on heat and mass transfer by mixed convection over a vertical surface saturated porous medium with temperature dependent viscosity, *Int. J. Numer. Meth. Fluids*, DOI:10.1002/fld.2655.

Ergun, S., (1952): Flow through Packed Columns, *Chem. Eng. Progress*, **48**, 89–94.

Erickson, L. E., L. T. Fan, and V. G. Fox, (1966): Heat and mass transfer on a moving continuous flat plate with suction or injection, *Int. Eng. Chem.*, **5**, 19–25.

Forchheimer, P., (1901): Wasserbewegung durch Boden, *Zeitschrift des Vereines Deutscher Ingenieure*, **45**, 1736–1741 and 1781–1788.

Gaikwad, S. N., M. S. Malashetty, and K. R. Prasad, (2007): An analytical study of linear and non-linear double diffusive convection with Soret and Dufour effects in couple stress fluid, *International Journal of Non-Linear Mechanics*, **42**, 903–913.

Gebhart, B., (1962): Effects of viscous dissipation in natural convection, *J. of Fluid Mech.*, **14**, 225–235.

Gebhart, B. and J. MoUendorf, (1969): Viscous dissipation in external natural convection flows, *J. of Fluid Mech.*, **38**, 97–107.

Geetha, P. and M. B. K. Moorthy, (2001): Viscous dissipation effect on steady free convection and mass transfer flow past a Semi-infinite flat plate, *J. of Compu. Sci.*, **7**, 1113–1118.

Grosan, T. and I. Pop, (2001): Free convection over a vertical flat plate with a variable wall temperature and internal heat generation in a porous medium saturated with a non-Newtonian fluid, *Technische Mechanik*, **4**, 23–30.

Gupta, P. S. and A. S. Gupta, (1977): Heat and mass transfer on a stretching sheet with suction and blowing, *The Canadian J. of Chem. Eng.*, **55**, 744–746.

Guttamann, A. J., (1989): Asymptotic analysis of power series expansions, *Academic Press, New York*, **13**, 1–234.

Hayat, T. and M. Sajid, (2007a): Homotopy analysis of MHD boundary layer flow of an upper-convected Maxwell fluid, *Int. J. Eng. Sci.*, **45**, 393–401.

Hayat, T., Z. Abbas, M. Sajid, and S. Asghar, (2007b): The influence of thermal radiation on MHD flow of a second grade fluid, *Int. J. Heat and Mass Transfer*, **50**, 931–941.

He, J. H., (1999): Homotopy perturbation technique, *Comput. Meth. Appl. Mech. Eng.*, **178**, 257–262.

He, J. H., (2003a): A simple perturbation approach to Blasius equation, *Appl. Math. Comput.*, **140**, 217–222.

He, J. H., (2003b): Homotopy perturbation method: a new nonlinear analytical technique, *Appl. Math. Comput.*, **135**, 73–79.

He, J. H., (2004): Comparison of homotopy perturbation method and homotopy analysis method, *Appl. Math. Comput.*, **156**, 527–539.

He, J. H., (2005): Application of homotopy perturbation method to nonlinear wave equations, *Chaos, Solitons and Fractals*, **26**, 695–700.

He, J. H., (2006): Homotopy perturbation method for solving boundary value problems, *Physics Letters A*, **350**, 87–88.

Hong, J. T.,Y. Yamada, and C.L. Tien, (1987): Effect of non-Darcian and nonuniform porosity on vertical plate natural convection in porousmedium, *Int. J. Heat and Mass Transfer*, **109**, 356–362.

Horton, C. W. and F. T. Roger, (1945): Convection currents in a porous medium, *J. Appl. Phys.*, **16**, 367–370.

Hung, C. I. and C. B. Chen, (1997): Non-Darcy free convection in a thermally stratified porous medium along a vertical plate with variable heat flux, *Int. J. Heat and Mass Transfer*, **33**, 101–107.

Hung, C. I., C. H. Chen, and C. B. Chen, (1999): Non-Darcy free convection along a nonisothermal vertical surface in a thermally stratified porous medium, *Int. J. Eng. Sci.*, **37**, 477–495.

Hung, J. S., R.Tsai, K. H. Hung, and C. H. Hung, (2011): Thermal-diffusion and diffusion-thermo effects on natural convection along an inclined stretching surface in a porous medium with chemical reaction, *Chem. Eng. Comm.*, **198**, 453–473.

Ibrahim, S. Y. and O. M. Makinde, (2010): Chemically reacting MHD boundary layer flow of heat and mass transfer past a moving vertical plate with suction, *Scientific Research and Essay*, **5**, 2875–2882.

Ingham, D. B. and I. Pop, (1998): Transport Phenomena in Porous Medium, *Pergamon Press, Oxford*.

Irmay, S., (1958): On the theoretical derivation of Darcy and Forchheimer formulas, *J. Geophys. Res.*, **39**, 702–707.

Ishak, A., R. Nazar and, I. Pop, (2008): Mixed convection boundary layer flow over a vertical surface embedded in a thermally stratified porous medium, *Physics Letters A*, **372**, 2355–2358.

Ishak, A., (2011): MHD boundary layer flow due to an exponentially stretching sheet with radiation effect, *Sains Malaysiana*, **40**, 391–395.

Jaluria, Y., (1980): Natural Convection Heat and Mass Transfer, *Pregamon Press, Oxford*.

Javed, T., M. Sajid, Z. Abbas, and N. Ali, (2011): Non-similar solution for rotating flow over an exponentially stretching surface, *Int. J. of Numer. Meth. Heat and Fluid Flow*, **21**, 903–908.

Jayanthi, S. and M. Kumari, (2007): Effect of variable viscosity on non-Darcy free or mixed convection flow on a vertical surface in a non-Newtonian fluid saturated porous medium, *Appl. Math. Comput.*, **186**, 1643–1659.

Jumah, R. Y. and A.S. Mujumdar, (2000): Free convection heat and mass transfer of non- Newtonian power law fluids with yield stress from a vertical plate in saturated porous media, *Int. Comm. Heat and Mass Transfer*, **27**, 485 –494.

Jumah, R. Y., F. A. Banat, and F. A. Al-Rub, (2001): Darcy-Forchheimer mixed convection heat and mass transfer in fluid saturated porous media, *J. Numer. Meth. for Heat and Fluid Flow*, **11**, 600–618.

Kafoussias, N. G. and E. W. Williams, (1995): Thermal-diffusion and diffusion thermo effects on mixed free-forced convective and mass transfer boundary layer flow with temperature dependent viscosity, *Int. J. Eng. Sci.*, **33**, 1369–1384.

Kairi, R. R. and P.V.S.N. Murthy, (2009a): Free convection in a thermally stratified non-darcy porous medium saturated with a non-Newtonian fluid, *Int. J. Fluid Mech. Res.*, **36**, 414–423.

Kairi, R. R. and P. V. S. N. Murthy, (2009b): Effect of melting and thermo-diffusion on natural convection heat mass transfer in a Non-Newtonian fluid saturated Non-Darcy porous medium, *The Open Transport Phenomena Journal*, **1**, 7–14.

Kairi, R. R., P. V. S. N. Murthy, and C. O. Ng, (2011a): Effect of viscous dissipation on natural convection in a non-Darcy porous medium saturated with non-Newtonian fluid of variable viscosity, *The Open Transport Phenomena Journal*, **3**, 1–8.

Kairi, R. R. and P.V.S.N. Murthy, (2011b): Effect of viscous dissipation on natural convection heat and mass transfer from vertical cone in a non-Newtonian fluid saturated non-Darcy porous medium, *Appl. Math. Comput.*, **217**, 8100–8114.

Kaviany, M., (1995): Principles of Heat Transfer in Porous Media, *Springer, 2nd Edition.*

Khan, S. K., (2006): Boundary layer viscoelastic fluid flow over an exponentially stretching sheet, *Int. J. of Appl. Mech. Eng.*, **11**, 321–335.

Kim, J., Y. T. Kang, and C. K. Choi, (2007): Soret and Dufour effects on convective instabilities in binary nanofluids for absorption application, *Int. J. of Refrigeration*, **30**, 323–328.

Kothandaraman, C. P., (2006): Fundamentals of Heat and Mass Transfer, *New Age International Publishers, New Delhi.*

Kumari, M. and G. Nath, (2004): Non-Darcy mixed convection in power-law fluids along a non-isothermal horizontal surface in a porous medium, *Int. J. Eng. Sci.*, **42**, 353–369.

Lage, J. L., (1998): The Fundamental Theory of Flow Through Permeable Media: From Darcy to Turbulence, *In Transport Phenomena in Porous Media (eds. D.B. Ingham and I. Pop). Pergamon, Oxford.*

Lai, F. C., (1990): Coupled heat and mass transfer by natural convection from a horizontal line source in saturated porous medium, *Int. Comm. Heat and Mass Transfer*, **17**, 489–499.

Lapwood, E. R., (1948): Convection of a fluid in a porous medium, *Proc. Cambridge Philos Soc.*, **44**, 508–521.

Laurait, G. and E. Nat Prasad, (1987): Convection in a vertical porous cavity a numerical study for Brinkmannextended Darcy formulation, *J. Heat Transfer*, **11**, 295–320.

Lee, S., S. U. S. Choi, S. Li and, J. A. Eastman, (1999): Measuring thermal conductivity of fluids containing oxide nanoparticles, *J. Heat Transfer*, **121**, 280–289.

Lehr, J. H. and J. K. Lehr, (2000): Standard Handbook of Enviromental Science, Health and Technology, *McGraw-Hill.*

Li, M. C., Y. W. Tian, and Y. C. Zhai, (2006): Soret and Dufour effects in strongly endothermic chemical reaction system of porous media, *Transactions of Nonferrous Metals Society of China*, **16**, 1200–1204.

Liao, S. J., (1992): The Proposed Homotopy Analysis Technique for the Solution of Nonlinear Problems, *PhD Thesis, Shanghai Jiao Tong University.*

Liao, S. J., (2003): Beyond Perturbation: Introduction to Homotopy Analysis Method, *Chapman and Hall/CRC Press.*

Liao, S. J., (2006): An analytic solution of unsteady boundary-layer flows caused by an impulsively stretching plate, *Comm. Nonlin. Sci. Numer. Simul.*, **11**, 326–339.

Liao, S. J. and Y. Tan, (2007): A general approach to obtain series solutions of nonlinear differential equations, *Studies in Applied Mathematics*, **119**, 297–355.

Liao, S. J., (2009): Notes on the homotopy analysis method: Some definitions and theories, *Comm. Nonlin. Sci. Numer. Simul.*, **14**, 983–997.

Lipscombe, T. C., (2010): Comment on application of the homotopy method for analytical solution of non-Newtonian channel flows, *Physica Scripta*, **81**, 37001.

Liu, C. S., (2010): The essence of the homotopy analysis method, *Appl. Math. Comput.*, **216**, 1299 –1303.

Lloyd, J. R. and E. M. Sparrow, (1970): Combined forced and free convection flow on vertical surfaces, *Int. J. Heat and Mass Transfer*, **13**, 434–448.

Loganathan, P., D. Iranian, and P. Ganesan, (2011): Effects of chemical reaction on unsteady free convection and mass transfer flow past a vertical plate with variable viscosity and thermal conductivity, *Euro J. Sci. Res.*, **59**, 403–416.

Lubuma, J. and K. C. Patidar, (2006): Uniformly convergent non-standard finite difference methods for self-adjoint singular perturbation problems, *J. Comput. Appl. Math.*, **191**, 228–238.

Lyapunov, A. M., (1992): General Problem on Stability of Motion, *Taylor and Francis, London.*

Magyari, E. and B. Keller, (1999): Heat and mass transfer in the boundary layers on an exponentially stretching continuous surface, *J. Phys. D: Appl. Phys*, **32**, 577–585.

Magyari, E., I. Pop and B. Keller, (2006): Unsteady free convection along an infinite vertical flat plate embedded in a stably stratified fluid-saturated porous medium, *Transport in Porous Media*, **62**, 233–249.

Mahmoud, M. A. A., (2009): Thermal radiation effect on unsteady MHD free convection flow past a vertical plate with temperature-dependent viscosity, *The Canadian J. of Chem. Eng.*, **87**, 47–52.

Makinde, O. D. and P. Sibanda, (2008): MHD mixed-convective flow and heat and mass transfer past a vertical plate in a porous medium with constant wall suction, *J. of Heat Transfer-Transactions of ASME*, **130**, 1–8.

Makinde, O. D., (2009): On MHD boundary-layer flow and mass transfer past a vertical plate in a porous medium with constant heat flux, *Int. J. of Numer. Meth. for Heat and Fluid Flow*, **19**, 546–554.

Makinde, O. D. and A. Aziz, (2010): MHD mixed convection from a vertical plate embedded in a porous medium with a convective boundary condition, *Int. J. of Therm. Sci.*, **49**, 1813–1820.

Makinde, O. D., (2011a): MHD mixed-convection interaction with thermal radiation and nth order chemical reaction past a vertical porous plate embedded in a porous medium, *Chem. Eng. Comm.*, **198**, 590–608.

Makinde, O. D., (2011b): On MHD mixed convection with Soret and dufour effects past a vertical plate embedded in a porous medium, *Latin American Applied Research*, **41**, 63–68.

Makinde, O. D. and P. O. Olanrewaju, (2011c): Unsteady mixed convection with Soret and Dufour effects past a porous palte moving through a binary mixture of chemically reacting fluid, *Chemical Engineering Communications*, **198(7)**, 920–938.

Makukula, Z. G. and S. S. Motsa, (2010a): On new solutions for heat transfer in a visco-elastic fluid between parallel plates, *Int. J. of Math. Models and Meth. in Appl. Sci.*, **4**, 221–230.

Makukula, Z. G., S. S. Motsa, and P. Sibanda, (2010b): On a new solution for the viscoelastic squeezing flow between two parallel plates, *J. of Adv. Research in Appl. Math.*, **2**, 31–38.

Makukula, Z. G., P. Sibanda,. and S. S. Motsa, (2010c): A Note on the solution of the Von Karman equations using series and Chebyshev spectral methods, *Boundary Value Problems*, Article ID 471793, DOI:10.1155/2010/471793.

Makukula, Z. G., P. Sibanda, and S.S. Motsa, (2010d): A novel numerical technique for two-dimensional laminar flow between two moving porous walls, *Math. Problems in Eng.*, Article ID 528956, DOI:10.1155/2010/528956.

Mandelzweig, V. B., (1999): Quasilinearization method and its verification on exactly solvable models in quantum mechanics, *J. Math. Phys.*, **40**, 62–66.

Mandelzweig, V. B. and F. Tabakin, (2001): Quasilinearization pproach to nonlinear problems in physics with application to nonlinear ODE's, *Comput. Phys. Comm.*, **141**, 268–281.

Mansour, M. A., N.F. El-Anssary, and A. M. Aly, (2008): Effects of chemical reaction and thermal stratification on MHD free convective heat and mass transfer over a vertical stretching surface embedded in a porous media considering Soret and Dufour numbers, *J. Chem. Eng.*, **145**, 340–345.

Maria, N., (2011): Free convective heat and mass transfer induced by a constant heat and mass fluxes vertical wavy wall in a non-Darcy double stratified porous medium, *Int. J. Heat and Mass Transfer*, **54**, 2310–2318.

Marpu, D. R., (1995): Forchheimer and Brinkman extended Darcy flow model on natural convection in a vertical cylindrical porous annulus, *Acta Mechanica*, **109**, 41–48.

Massoudi, M. and T. X. Phuoc, (2004): Flow of a generalized second grade non-Newtonian fluid with variable viscosity, *Continuum Mechanics Thermodynamics*, **16**, 529–538.

McNabb, A., (1965): On convection in a porous medium, *Proc. 2nd Australasian Conf. Hydraulics and Fluid Mech., University of Auckland*, C161–C171.

Minkowycz, W. J. and E. M. Sparrow, (1974): Local non-similar solution for natural convection on a vertical cylinder, *J. Heat Transfer*, **96**, 178–183.

Mojtabi, A. and M. C. Charrier-Mojtabi, (2005): Double Diffusive Convection in Porous Media, *Handbook of Porous Media*.

Mortimer, R. G. and H. Eyring, (1980): Elementary transition state theory of the Soret and Dufour effects, *In Proc. Natl. Acad. Sci.*, **77**, 1728–1731.

Motsa, S. S. and P. Sibanda, (2005): Investigation of compliancy effects on the inviscid instability in fluid flow over a flat plate with heat transfer, *Int. J. Numer. Meth. for Heat and fluid flow*, **15** 504–516.

Motsa, S. S., (2008): On the onset of convection in a porous layer in the presence of Dufour and Soret effects, *SAMSA J. of Pure and Appl. Math.*, **3**, 58–65.

Motsa, S. S. and P. Sibanda, (2010a): A new algorithm for solving singular IVPs of Lane-Emden type, *Proceedings of the 4th International Conference on Applied Mathematics, Simulation and Modelling. NAUN International Conferences, Corfu Island, Greece*, 176–180.

Motsa, S. S., P. Sibanda, and S. Shateyi, (2010b): A new spectral-homotopy analysis method for solving a nonlinear second order BVP, *Comm. Nonlin. Sci. Numer. Simul.*, **15**, 2293–2302.

Motsa, S. S., P. Sibanda, F. G. Awad F. G. and S. Shateyi, (2010c): A new spectral-homotopy analysis method for the MHD Jeffery-Hamel problem, *Computers and Fluids*, **39**, 1219–1225.

Motsa, S. S. and S. Shateyi, (2010d): A New approach for the solution of three-dimensional magnetohydrodynamic rotating flow over a shrinking sheet, *Math. Problems in Eng.*, Article ID 586340, DOI:10.1155/2010/586340.

Motsa, S. S., G. T. Marewo, P. Sibanda, and S. Shateyi, (2011a): An improved spectral homotopy analysis method for solving boundary layer problems, *Boundary Value Problems*, **2011:3**, DOI:10.1186/1687–2770–2011–3.

Motsa, S. S. and P. Sibanda, (2011b): An efficient numerical method for solving Falkner-Skan boundary layer flows, *Int. J. Numer. Meth. Fluids*, DOI: 10.1002/fld.2570.

Munyakazi, B. J. and K. C. Patidar, (2008): On Richardson extrapolation for fitted operator finite difference methods, *Appl. Math. and Comput.*, **201**, 465–480.

Munyakazi, J. B. and K. C. Patidar, (2010): Higher order numerical methods for singularly perturbed elliptic problems, *Neural, Parallel and Scientific Computations Archive*, **18**, 75–88.

Murthy, P. V. S. N. and P. Singh, (1997): Effect of viscous dissipation on a non-Darcy natural convection regime, *Int. J. Heat and Mass Transfer*, **40**, 1251–1260.

Murthy, P. V. S. N., (1998): Thermal dispersion and viscous dissipation effects on non-Darcy mixed convection in a fluid saturated porous medium, *Int. J. Heat and Mass Transfer*, **33**, 295–300.

Murthy, P. V. S. N., D. Srinivasacharya, and P.V.S.S.S.R. Krishna, (2004): Effect of double stratification on free convection in a Darcian porous medium, *J. Heat Transfer*, **126**, 297–300.

Nakayama, A. and H. Koyama, (1987a): An integral method for free convection from a vertical heated surface in a thermally stratified porous medium, *Wärme-und Stoffübertragung*, **21**, 297–300.

Nakayama, A. and H. Koyama, (1987b): Effect of thermal stratification on free convection within a porous medium, *J. Thermophysics Heat Transfer*, **1**, 282–285.

Nakayama, A. and I. Pop, (1989): Free convection over a nonisothermal body in a porous medium with viscous dissipation, *Int. Comm. in Heat and Mass Transfer*, **16**, 173–180.

Nakayama, A. and H. Koyama, (1991): Bouyancy induced flow of non-Newtonian fluids over a non-isothermal body of arbitrary shape in a fluid saturated porous medium, *Appl. Sci. Res.*, **48**, 55–70.

Nakayama, A. and I. Pop, (1991): A unified similarity transformation for free, forced and mixed convection in Darcy and non-Darcy porous media, *Int. J. Heat and Mass Transfer*, **34**, 357–67.

Nakayama, A., (1995): PC-Aided Numerical Heat Transfer and Convective Flow, *CRC Press, Boca Raton.*

Narayana, P. A. L. and P. V. S. N. Murthy, (2006): Free convective heat and mass transfer in a doubly stratified non-Darcy porous medium, *J. Heat Transfer*, **128**, 1204–1212.

Narayana, P. A. L. and P. V. S. N. Murthy, (2007): Soret and Dufour effects on free convection heat and mass transfer in a doubly stratified Darcy porous medium, *J. of Porous Media*, **10**, 613–624.

Narayana, P. A. L. and P. V. S. N. Murthy, (2008): Soret and Dufour effects on free convection heat and mass transfer from a horizontal flat plate in a Darcy porous medium, *Int. J. Heat Tansfer*, **130**, 1–5.

Narayana, P. A. L., P. V. S. N Murthy, P. V. S. S. S. R. Krishna, and A. Postelnicu, (2009): Free convective heat and mass transfer in a doubly stratified porous medium saturated with a power-law fluid, *Int. J. Fluid Mech. Res.*, **36**, 524–537.

Narayana, P. A. L. and P. Sibanda, (2010): Soret and Dufour effects on free convection along a vertical wavy surface in a fluid saturated Darcy porous medium, *Int. J. Heat and Mass Transfer*, **53**, 3030–3034.

Nield, D. A., (1968): Onset of thermohaline convection in a porous medium, *Water Resources Research*, **4**, 553–560.

Nield, D. A. and A. Bejan, (1984): Convection in Porous Media, *Springer-Verlag, New York*.

Nield, D. A. and A. Bejan, (1999): Convection in Porous Media, *Springer-Verlag, New York*.

Olanrewaju, P. O. and O. D. Makinde, (2011): Effects of thermal diffusion and diffusion thermo on chemically reacting MHD boundary layer flow of heat and mass transfer past a moving vertical plate with suction/injection, *Arabian Journal of Science and Engineering*, **36**, 1607–1619.

Pal, D., (2010): Mixed convection heat transfer in the boundary layers on an exponentially stretching surface with magnetic field, *Appl. Math. Comm.*, **217**, 2356–2369.

Pal, D. and H. Mondal, (2011): Effects of Soret, Dufour, chemical reaction and thermal radiation on MHD non-Darcy unsteady mixed convective heat and mass transfer over a stretching sheet, *Comm. Nonlin. Sci. Numer. Simul.*, **16**, 1942–1958.

Palani, G. and U. Srikanth, (2009): MHD flow past a semi-infinite vertical plate with mass transfer, *Nonlinear Analysis: Modelling and Control*, **14**, 345–356.

Parand, K., M. Shanini, and M. Dehghan, (2010a): Solution of a laminar boundary layer flow via a numerical method, *Comm. Nonlin. Sci. Numer. Simul.*, **5**, 360–367.

Parand, K., M. Ghasemi, S. Rezazadeh, A. Peiravi, A. Ghorbanpour, and A. T. golpaygani, (2010b): Quasilinearization approach for solving volterra's population model, *Appl. Comput. Math.*, **9**, 95–103.

Partha, M. K., P. V. S. N. Murthy, and G. P. Rajasekhar, (2005): Effect of viscous dissipation on the mixed convection heat transfer from an exponentially stretching surface, *Int. J. Heat and Mass Transfer*, **41**, 360–366.

Partha, M. K., P. V. S. N. Murthy, and G. P. Raja Sekhar, (2006): Soret and Dufour effects in a non- Darcy porous medium, *J. Heat Transfer*, **128**, 605–610.

Patidar, K. C., (2005): High order fitted operator numerical method for self-adjoint singular perturbation problems, *Appl. Math. Comput.*, **171**, 547–566.

Pop, I. and D. B. Ingham, (2001): Convection Heat Transfer: Mathematical and Computational Modelling of Viscous Fluid and Porous Media, *Pergamon Press, Oxford.*

Postelnicu, A., (2004): Influence of a magnetic field on heat and mass transfer by natural convection from vertical surfaces in porous media considering Soret and Dufour effects, *Int. J. Heat and Mass Transfer*, **47**, 1467–1472.

Postelnicu, A., (2007): Influence of chemical reaction on heat and mass transfer by natural convection from vertical surfaces in porous media considering Soret and Dufour effects, *Int. J. Heat and Mass Transfer*, **43**, 595–602.

Poulikakos, D. and A. Bejan, (1985): The departure from Darcy flow in natural convection in a vertical porous layer, *Phys. Fluids*, **28**, 3477–3484.

Poulikakos, D., (1986): Double diffusive convection in a horizontally sparsely packed porous layer, *Int. Comm. Heat and Mass Transfer*, **13**, 587–598.

Prasad, V. and A. Tuntomo, (1987): Inertia effects on natural convection in a vertical porous cavity, *Numer. Heat Transfer*, **11**, 295–320.

Putra, N., W. Roetzel, and S. K. Das, (2003): Natural convection of nanofluids, *Int. J. Heat and Mass Transfer*, **39**, 775–784.

Rajagopal, K. R., T. Y. Na, and A.S. Gupta, (1984): Flow of a viscoelastic fluid over a stretching sheet, *Rheologica Acta*, **23** 213–215.

Ralston, A. and P. Rabinowitz, (1988): A First Course in Numerical Analysis, *McGraw-Hill.*

Ranganathan, P. and R. Viskanta, (1984): Mixed convection boundary-layer flow along a vertical wall in saturated porous medium, *Numer. Heat Transfer*, **7**, 305–317.

Raptis, A., (1998): Radiation and free convection flow through a porous medium, *In. Comm. Heat and Mass Transfer*, **25**, 289–295.

Rastogi, S. K. and D. Poulikakos, (1995): Double-diffusion from a vertical surface in a porous region saturated with a non-Newtonian fluid, *Int. J. Heat and Mass Transfer*, **38**, 935 - 946.

Rathore, M. M. and R. Kapuno, (2010): Engineering Heat Transfer, *Jones and Bartllet, Ontario, Canada*.

Reddy, M. G and N. B. Reddy, (2010): Radiation and mass transfer effects on unsteady MHD free convection flow past a vertical porous plate with viscous dissipation, *Int. J. of Appl. Math. and Mech.*, **6**, 96–110.

Rees, D. A. S. and I. Pop, (1994): A note on a free convection along a vertical wavy surface in a porous medium, *ASME J. of Heat Transfer*, **115**, 505–508.

Rees, D. A. S. and I. Pop, (1998): Free convection boundary-layer flow of a micropolar fluid from a vertical flat plate, *IMA J. Appl. Math.*, **61**, 179–197.

Rudraiah, N., P. K. Srimani, and R. Friedrich, (1982): Finite amplitude convection in a two component fluid saturated porous layer, *Int. J. Heat and Mass Transfer*, **25**, 715–722.

Rudramoorthy, R. and K. Mayilsamy, (2004): Heat and Mass Transfer, *Pearson Education*.

Sajid, M. and T. Hayat, (2008): Influence of thermal radiation on the boundary layer flow due to an exponentially stretching sheet, *Int. Comm. Heat and Mass Transfer*, **35**, 347–356.

Sakiadis, B. C., (1961a): Boundary-layer behavior on continuous solid surfaces: I. Boundary-layer equations for two-dimensional and axisymmetric flow, *AIChE Journal*, **7**, 26–28.

Sakiadis, B. C., (1961b): Boundary-layer behavior on continuous solid surfaces: II. The boundary layer on a continuous flat surface, *AIChE Journal*, **7**, 226–227.

Salem, A. M., (2006): Coupled heat and mass transfer in Darcy-Forchheimer mixed convection from a vertical flat plate embedded in a fluid-saturated porous medium under the effects of radiation and viscous dissipation, *J. of the Korean Phy. Society*, **48**, 409–413.

Sanjayanand, E. and S. K. Khan, (2006): On heat and mass transfer in a viscoelastic boundary layer flow over an exponentially stretching sheet, *Int. J. of Therm. Sci.*, **45**, 221–225.

Sawhney, G. S., (2010): Heat and Mass Transfer, *I K International Publishing House*.

Seddeek, M. A., A. A. Darwish, and M. S. Abdelmeguid, (2007): Effect of chemical reaction and variable viscosity on hydromagnetic mixed convection heat and mass transfer for Hiemenz flow through porous media with radiation, *Comm. Nonlin. Sci. and Numer. Simul.*, **12**, 195–213.

Sen, A. K., (1987): Natural convection in a shallow porous cavity - The Brinkman model, *Int. J. Heat and Mass Transfer*, **30**, 855–868.

Shampine, L. F., R. Ketzscher, and S. A. Forth, (2005): Using AD to solve BVPs in Matlab, *ACM Transactions on Mathematical Software*, **31**, 195–213.

Shateyi, S. and S.S. Motsa, (2010a): Variable viscosity on magnetohydrodynamic fluid flow and heat transfer over an unsteady stretching surface with hall effect, *Boundary Value Problems*, Article ID 257568, DOI:10.1155/2010/257568.

Shateyi, S., S. S. Motsa, and P. Sibanda, (2010b): The effects of thermal radiation, Hall currents, Soret, and Dufour on MHD flow by mixed convection over

a vertical surface in porous media, *Math. Problems in Eng.*, Article ID 627475, DOI:10.1155/2010/627475.

Shateyi, S., S. S. Motsa, and P. Sibanda, (2010c): Homotopy analysis of heat and mass transfer boundary layer flow through a non-porous channel with chemical reaction and heat generation, *The Canadian J. of Chem. Eng.*, **88**, 975 982.

Shenoy, A. V., (1993): Darcy-Forchheimer natural, forced and mixed convection heat transfer in non-Newtonian power-law fluidsaturated porous media, *Transport in Porous Media*, **11**, 219–241.

Shenoy, A. V., (1994): Non-Newtonian fluid heat transfer in porous media, *Adv. Heat Transfer*, **24**, 101–190.

Sibanda, P. and O. D. Makinde, (2010): On MHD flow and heat transfer past a rotating disk in porous medium with Ohmic heating and viscous dissipation, *Int. J. Nume. Meth. for Heat and Fluid Flow*, **20**, 269–285.

Sibanda, P., S. S. Motsa, and Z. G. Makukula, (2012): A spectral-homotopy analysis method for heat transfer flow of a third grade fluid between parallel plates, *In. J. of Numer. Meth. for Heat and fluid Flow*, **22**, 4–23.

Singh, P. and K. Sharma, (1990): Integral method to free convection in thermally stratified porous medium, *Acta Mechanica*, **83**, 157–163.

Singh, P. and K. Ewari, (1993): Non-Darcy free convection from vertical surfaces in thermally stratified porous media, *Int. J. Eng. Sci.*, **31**, 69–73.

Singh, P. and Queeny, (1997): Free convection heat and mass transfer along a vertical surface in a porous medium, *Acta Mechanica*, **123**, 69–93.

Singh, P. K., P. V. Harikrishna, T. Sundararajan, and S. K. Das, (2011): Experimental and numerical investigation into the heat transfer study of nanofluids in microchannel, *J. Heat Transfer*, **133**, 121701.

Sparrow, E. M., H. Quack, and C. J. Boerner, (1970): Local non-similarity boundary layer solutions, *J. AIAA*, **83**, 1936–1942.

Sparrow, E. M. and H. S. Yu, (1971): Local non-similarity thermal boundary layer solutions, *J. Heat Transfer*, **93**, 328–334.

Sparrow, E. M. and R. D. Cess, (1978): Radiation Heat Transfer, *McGraw-Hill*.

Srinivasacharya, D. and Ch. RamReddy, (2010): Heat and mass transfer by natural convection in a doubly stratified non-Darcy micropolar fluid, *Int. Comm. Heat and Mass Transfer*, **37**, 873–880.

Srinivasacharya, D. and Ch. RamReddy, (2011): Soret and Dufour Effects on mixed convection from an exponentially stretching surface, *Int. J. of Nonlin. Sci.*, **12**, 60–68.

Stern, M. E., (1960): The salt fountain and thermohaline convection, *Tellus*, **12**, 172–175.

Sulochana, C., N. Gururaj, and S. Devika, (2011): Finite element analysis of thermo-diffusion effect on convection heta and amass thrnasfer through a porous medium in circular annulus, *Int. J. of Appl. Math and Mech.*, **7**, 80–101.

Takhar, H. S. and I. Pop, (1987): Free convection from a vertical flat plate to a thermally stratified Darcian flow, *Mech. Res. Comm.*, **14**, 81–86.

Takhar, H. S., A. J. Chamkha, and G. Nath, (2001): Natural convection flow from a continuously moving vertical surface immersed in a thermally stratified medium, *Int. J. Heat and Mass Transfer*, **38**, 17–24.

Takhar, H. S., A. J. Chamkha, and G. Nath, (2002): Natural convection on a vertical cylinder embedded in a thermally stratified high-porosity medium, *Int. J. Therm. Sci.*, **41**, 83–93.

Tewari, K. and P. Singh, (1992): Natuaral convection in a thermally stratified fluid saturated porous medium, *Int. J. Eng. Sci.*, **30**, 1003–1007.

Thirumaleshwar, M., (2006): Fundamentals of Heat and Mass Transfer, *Dorling Kindersley, India.*

Tong, T. W. and E. Subramanian, (1985): A boundary layer analysis for natural convection in porous enclosure use of the Brinkman extended Darcy flow model, *Int. J. Heat and Mass Transfer*, **28**, 563–571.

Tourigny, Y. and P. G. Drazin, (2000): The asymptotic behaviour of algebraic approximants, *Proc. Roy. Soc. Lond. A*, **456**, 1117 –11 37.

Trefethen, L. N., (2000): Spectral Methods in MATLAB, *SIAM.*

Trevisan, O. V. and A. Bejan, (1990): Combined heat and mass transfer by natural convection in a porous medium, *Adv. Heat Transfer*, **20**, 315–352.

Tsai, R. and J. S. Huang, (2009): Numerical study of Soret and Dufour effects on heat and mass transfer from natural convection flow over a vertical porous medium with variable wall heat fluxes, *Computational Materials Science*, **47**, 23–30.

Vafai, K., (2005): Handbook of Porous Media, *Second Edition, CRC Press.*

Venkanna, B. K., (2010): Fundamentals of Heat and Mass Transfer, *Prentice-Hall of India Pvt. Ltd.*.

Wang, X. and A. S. Mujumdar, (2007): Heat transfer characteristics of nanofluids: a review, *Int. J. Therm. Sci.*, **46**, 1–19.

Wazwaz, A. M., (2005): Adomians decomposition method for a reliable treatment of the Bratu-type equations, *Appl. Math.Comput.*, **166**, 652–663.

Wen, D. and Y. Ding, (2006): Natural convective heat transfer of suspensions of titanium dioxide nanoparticles (nanofluids), *IEEE Transactions On Nanotechnology*, **5**, 220–227.

Wooding, R. A., (1957): Steady state free thermal convection of liquid in a saturated permeable medium, *J. Fluid Mech.*, **2**, 273–285.

Wooding, R. A., (1963): Convection in a saturated porous medium at large Rayleigh number or Peclet number, *J. Fluid Mech.*, **15**, 527–544.

Yang, C. and S. J. Liao, (2006): On the explicit purely analytic solution of Von Karman swirling viscous flow, *Comm. Nonlin. Sci. Numer. Simul.*, **11**, 83–93.